ULVA-MICROBIAL INTERACTIONS LINKED TO THE ENVIRONMENT: VARIATION AND ACCLIMATION

Luna van der Loos

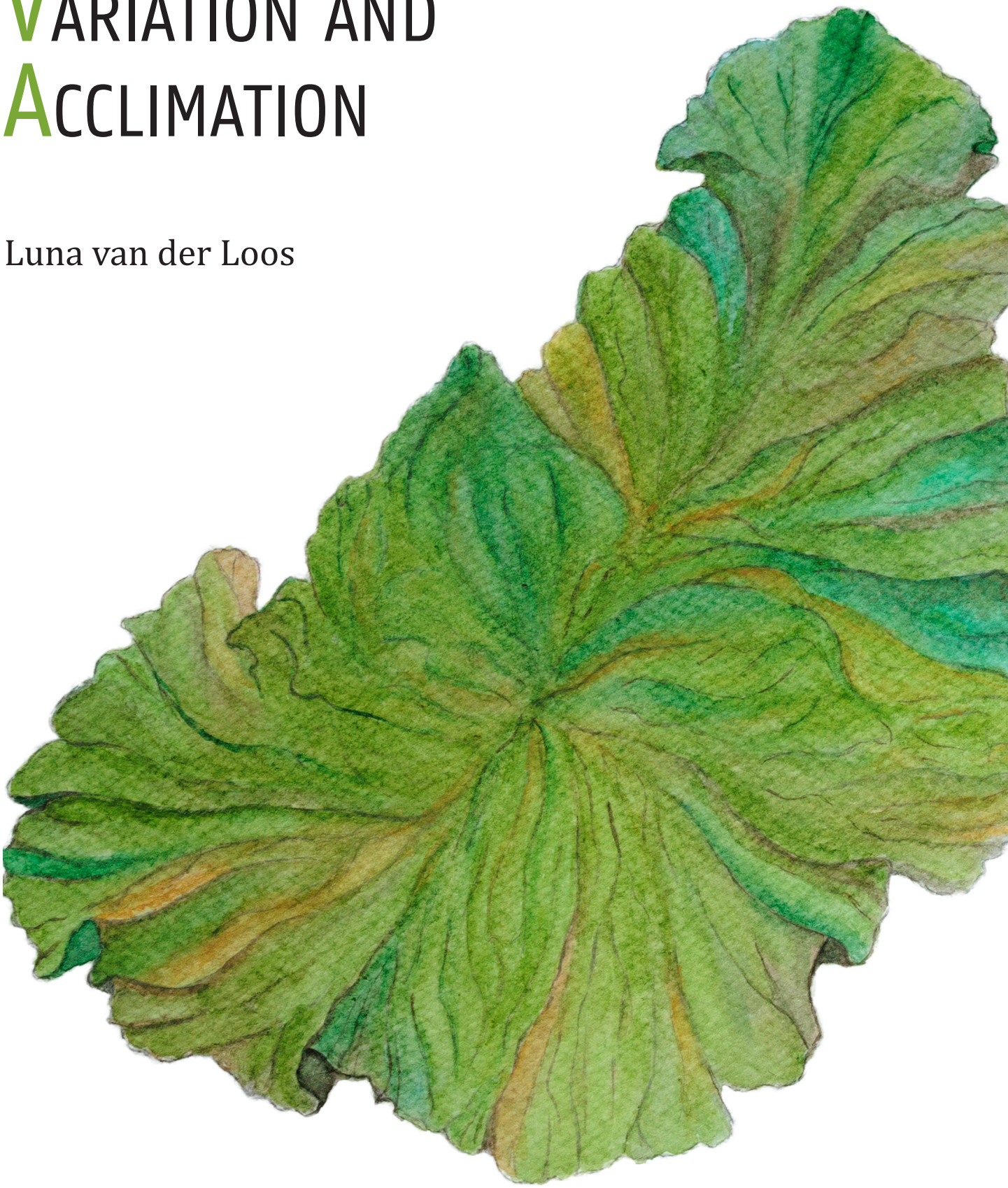

Ulva-microbial interactions Linked to the environment: Variation and Acclimation

Luna van der Loos

Promotors:
Prof. Dr. Olivier De Clerck
Prof. Dr. Anne Willems
Prof. Dr. Frederik Leliaert

Thesis submitted in fulfilment of the requirements for the degree of Doctor (PhD) of Science – Biology

Faculty of Sciences
Ghent University
Belgium
January 2024

UNIVERSITEIT GENT
FACULTY OF SCIENCES
RESEARCH GROUP PHYCOLOGY
fwo

Cover art: watercolour sketch based on "*Ulva latissima* – Breed watervlies" (Flora Batava VIII, 1844)
By Luna van der Loos
2024

Examination committee

Prof. Dr. Koen Sabbe (chair)
Department of Biology, Ghent University, Belgium

Dr. Jonas Blomme
Department of Plant Biotechnology and Bioinformatics, Ghent University, Belgium
VIB-UGent Center for Plant Systems Biology, Ghent, Belgium

Prof. Dr. Sofie Goormachtig
Department of Plant Biotechnology and Bioinformatics, Ghent University, Belgium

Prof. Dr. Tom Defoirdt
Department of Biotechnology, Ghent University, Belgium

Prof. Dr. Ellen Decaestecker
Department of Biology, KU Leuven, Belgium

Dr. Simon Dittami
Station Biologique de Roscoff, Sorbonne Université, France

This research was financially supported by FWO (PhD Fellowship fundamental research 3F020119) and the Research Group Phycology (Ghent University).

Contents

Acknowledgements

Writing a thesis and doing research is like a symbiosis: it would not be possible without a lot of other associates. First of all, the people most closely involved with the research project: Olivier De Clerck, Anne Willems, and Frederik Leliaert. Thank you for being excellent promotors and finding the balance between letting me experiment on my own and give advice when needed. Sophie Steinhagen, thank you for starting the best collaboration I could have wished for. I think we can safely conclude that my thesis would have looked completely different without you. I hope we keep collaborating on all things *Ulva*!

I owe my love of nature to both of my parents. Thank you for pointing out all the plants, birds, and shells during the many family hikes. I would like to thank my dad especially for always answering my many, many 'why' questions when I was a kid (patiently, most of the time) and the encouragement to keep asking questions. My grandparents and mom I want to thank especially for sharing their love for Brittany with me. The family summer holidays left ample time to explore the wonderful worlds of rocky pools. Without the countless hours spent catching crabs and playing with my Barbie doll between *Ascophyllum nodosum*, I might never have discovered seaweeds at all. Of course, a big thank you to Maya, the best little sister. Who else would have stayed with me while hiking and snorkelling — holding my fins, holding my butterfly net, holding my buckets with seaweeds? (My apologies for all the hours you were seen in the company of someone wearing Teva sandals).

Throughout all of this, I have so many more people to be thankful of: my aunts and cousins for all their support during fun times and hard times. My diving buddies at G.B.D. Calamari (Iris Menger, Tim Kauling, Lukas Verboom especially) for sharing their enthusiasm for the underwater world and teaching me how to dive slowly to see more. My friends at Kakapo and fellow Dodos — I'm glad we keep ecology from extinction (are we still buying that island, by the way?). The Owlbears for going on epic adventures together. Karlijn Doorenspleet for being my microbiome buddy. Merel Bakker for being one of those special friends you may not see very often, but who always feels near. Reindert Nijland for introducing me to Nanopore sequencing (and supplying flow cells when I was inadvertently out of stock). Bert Hoeksema for taking me on my first taxonomic expedition in the Caribbean so many years ago and trusting I would be able to take on the macroalgae, as well as guiding me in my first academic writings. Frank Perk, Mart Karremans, and Mick Otten for freely sharing their knowledge of seaweeds in the Netherlands and starting (as well as finishing!) the daunting task to write a field guide together with me. Wouter Engelbart, Miek Zwamborn, Herman van den Muijsenberg, Ellen Schoenmakers, Willem Brandenburg for the conversations in which the beauty of seaweeds was highlighted from all directions. Everyone at the lab, especially Soria Delva, Willem Stock, Eliane Zakka, Sofie Peeters, and Quinten Bafort for sharing an office with me. Sofie D'hondt for all her molecular expertise and help throughout my entire PhD — but just as much for the fun conversations while doing lab work.

Wiebe — of course. What can I say? Thank you for sharing the love of your life with me (your canoe) and safely steering us over all the beautiful rivers and lakes. I'm so glad I asked you about kelp all these years ago.

And last but never least, thank you, mama. Thank you for teaching me so much more than doing a PhD ever could. I am happy you were there at the start of this journey and I can only wish you could have seen the end.

" 'Could we just assume for the moment that I have neglected my seaweed studies in recent years?', said the Patrician.
Really? Oh, the loss is entirely yours, I assure you."

– Terry Pratchett, in: Discworld #21, Jingo

Chapter 1.
General introduction

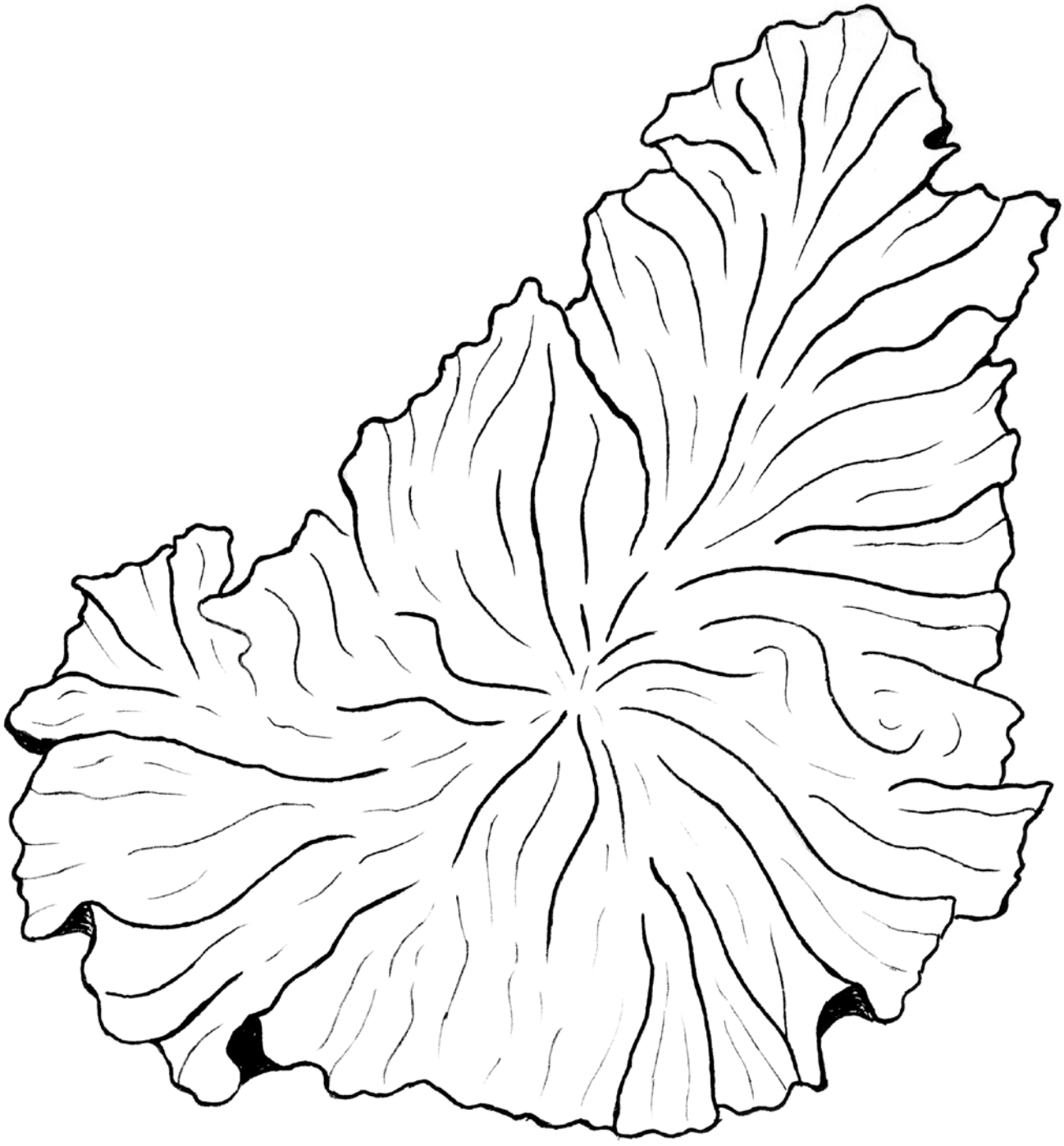

Chapter 1. General introduction

1.1 Seaweeds

Seaweeds, also known as marine macroalgae, are a diverse group of photosynthetic organisms that grow in aquatic environments. Despite their name, seaweeds are not plants. They belong to several different groups of algae, which are evolutionary diverse and distinct from true plants. Seaweeds can be classified into three main groups based on their pigmentation: red algae (Rhodophyta), brown algae (Phaeophyceae), and green algae (Chlorophyta).

Marine macroalgae play a vital role as foundation species and ecosystem engineers in coastal ecosystems around the world. They provide food, shelter, and habitat for higher trophic levels and are responsible for a major part of the total primary productivity (Tuya et al. 2008, Pessarrodona et al. 2022). In addition, they provide essential ecosystem services, including nutrient cycling, coastal protection, oxygenation, and carbon sequestration (Hurd et al. 2022, Cotas et al. 2023). From an economic perspective, seaweeds can be used as sustainable biomass feedstocks for the food and biotech industries, and play a role in integrated aquaculture systems and bioremediation (Bolton et al. 2016, Duarte et al. 2021, Kotta et al. 2022).

Worldwide, more than 11,000 species of macroalgae can be found and a large proportion of the biodiversity likely remains undescribed (Appeltans et al. 2012, Stiger-Pouvreau and Zubia 2020). One of the most common and most ubiquitous groups of species are the green seaweeds belonging to the genus *Ulva*. *Ulva* species occur worldwide from tropic to arctic ecosystems, and their high tolerance to environmental variables such as light, salinity, and temperature allows them to thrive in diverse habitats (Mantri et al. 2020). *Ulva* species have been proposed as model organism for various research areas, including the study of morphological development, host–bacterial interactions, and aquaculture (Wichard et al. 2015, Blomme et al. 2023, Buck and Shpigel 2023). *Ulva* is therefore the perfect candidate for this PhD thesis.

1.2 The genus *Ulva*

1.2.1 Morphology and taxonomy

The genus *Ulva* (Chlorophyta, Ulvophyceae, Ulvales, *Ulvaceae*) was erected by the Swedish botanist Carolus Linnaeus in 1753 in his *Species Plantarum.* In this work, Linnaeus described nine species in the genus *Ulva*, of which the names *U. compressa*, *U. intestinalis*, *U. lactuca* (later assigned as the generitype of the genus *Ulva*), and *U. linza* are still in use today. Linnaeus' morphological descriptions included terms such as "tubulosa simplex" (simple tubes), "tubulosa ramosa" (branched tubes), "membranacea" (membranous), and "fronde oblonga" (oblong blades) (Linnaeus 1753). To the present day, *Ulva* species are commonly called sea lettuces or gut weeds due to these typical shapes. In the nineteenth century, the genus *Ulva* was split into several genera, including *Enteromorpha* Link, *Monostroma* Thuret, and *Ulvaria* Ruptecht (Mantri et al. 2020). In general, the genus *Ulva* included the blade-like thalli composed of two cell layers, whereas *Enteromorpha* comprised the branched or unbranched monostromatic tubes (Fig. 1.01) (Tran et al. 2022). The genus name *Enteromorpha* had been in use for almost 200 years, until Hayden et al. (2003) used molecular methods to show that *Enteromorpha* and *Ulva* were not distinct genera after all. Indeed, there are several *Ulva* species that display both foliose and tubular morphologies. *Ulva compressa*, for example, occurs as attached, branched tubes in the North Sea, while in the lower saline regions of the Baltic Sea and estuaries like the Westerschelde (the Netherlands) and Olhão (Portugal), it takes the form of unattached, foliose thalli (Steinhagen et al. 2019b).

Currently, over a 100 taxonomically accepted *Ulva* species are listed in AlgaeBase (Guiry and Guiry 2023). These species display a tremendous amount of morphological variation and cryptic diversity (Fig. 1.02) (Steinhagen et al. 2023). Morphological identifications of *Ulva* species are based on characteristics such as colour, texture, the presence of perforations, cell size, chloroplast shape, the number of pyrenoids, etc., but these characteristics are far from reliable. Not only is there a lot of morphological variation *within* species, there are also a lot of overlapping characteristics *between* species. In addition, *Ulvaceae* morphology overlaps with foliose and tubular species from other families (e.g., *Kornmanniaceae*, *Monostromataceae*; Fig. 1.02). Consequently, *Ulva* species are extremely difficult to identify based on morphology. In the recent 20 years, molecular work has significantly improved our understanding of *Ulva* diversity (Text box 1) (see e.g., Hughey et al. 2019, 2020, 2021). Yet, there is still considerable confusion, as DNA analyses can only provide a correct identification if based on a solid reference database. After sequencing the lectotype material of *Ulva rigida*, for example, it was discovered that every sequence deposited under that name in public databases was incorrect. Instead, the majority of those sequences were identical to the lectotype of *Ulva lacinulata* (Hughey et al. 2021). This shows that a better characterisation of type material through gene sequencing is necessary to avoid the continued misapplication of names.

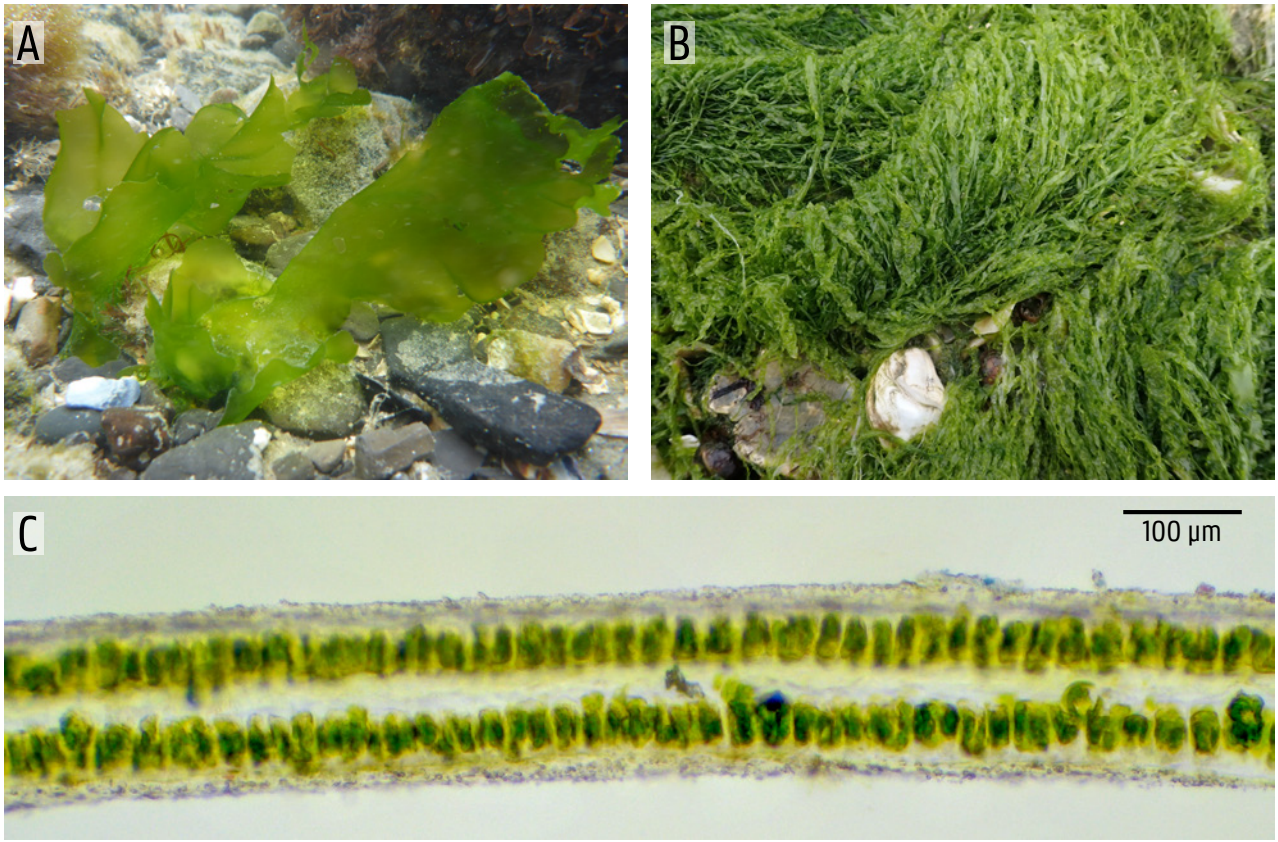

FIGURE 1.01 Morphology of *Ulva*. (A) A typical foliose *Ulva*, (B) A typical tubular *Ulva* (previously *Enteromorpha*), (C) Cross-section of bistromatic blade (picture by Mart Karremans).

FIGURE 1.02 Overview of the morphological variation that can be found in Ulvales. A) *Blidingia minima*, B) *Blidingia minima*, C) *Ulva australis*, D) *Kornmannia leptoderma*, E) *Ulva* sp. 4, F) mix of *Ulva prolifera* and *Blidingia marginata*, G) *Ulva australis*, H) *Ulva flexuosa* subsp. *pilifera*, I) *Ulva compressa*, J) *Ulva compressa*, K) *Ulva linza*, L) *Ulva intestinalis*, M) *Ulva torta*, and N) *Ulva* sp. 4.

Text box 1 Sequencing techniques

Over the past few decades, advancements in sequencing techniques and cost reductions have greatly enhanced the accessibility of DNA sequencing. From the first-ever completion of the human genome sequencing in 2003 after 13 years of dedicated effort, we have progressed to the point where new technologies can now sequence a human genome in a matter of hours. The work in this thesis heavily relies on molecular methods. Both for the identification of *Ulva* species (which are hard to distinguish based on morphology only) and the characterisation of microbes (which are rather small and therefore hard to study based on morphology as well), these molecular methods are extremely useful. Here, we provide a summary of the sequencing techniques used in this thesis.

Genetic information is present in all living organisms, and the entirety of this genetic data is referred to as a genome. The human genome for example is approximately 3.1 Gbp (gigabasepair) in size (Collins et al. 2003), while the *Ulva* genome is considerably smaller at around 100 Mbp (De Clerck et al. 2018). A typical bacterial genome measures around 5 Mbp (but can vary from 0.1 Mbp to 15 Mbp) (Land et al. 2015), and viral genomes can be as small as 1–2 kbp (Rosario et al. 2017).

Traditional sequencing methods are generally limited to sequencing shorter fragments of DNA. Sanger sequencing, which was developed in 1977, for example sequences DNA fragments that are about 300 to 1,000 bp in length (Pervez et al. 2022). For taxonomic purposes, it is not always necessary to sequence an entire genome. Instead, specific segments (markers) of the genome are targeted using primers and amplified by PCR (Polymerase Chain Reaction) before sequencing. A good DNA barcoding marker is taxonomically informative (i.e., it needs to be able to differentiate between species) and at the same time should be conserved enough for primers to be able to bind to the DNA of all the targeted species (Carugati et al. 2015). In green seaweeds, we often use the plastid markers *tuf*A (a 600 bp fragment of a gene that encodes the elongation factor Tu) or *rbc*L (a 1,400 bp fragment of a gene that encodes ribulose 1,5-biphosphate carboxylase) (Manhart 1994, Vieira et al. 2016). For the taxonomic identification of bacteria, the 16S rRNA gene is used (a 1,600 bp fragment) (Park and Won 2018). In each case, the obtained sequence is compared to a reference database for taxonomic identification.

Sanger sequencing is only suitable for samples containing a single species (e.g., a single *Ulva* strain or a single bacterial isolate). However, when dealing with samples containing a mixture of various species, like the entire bacterial community associated with an *Ulva* thallus, alternative methods are needed. One of the most widely adopted next-generation sequencing (NGS) techniques for this purpose is Illumina sequencing technology. Illumina sequencing employs a sequencing-by-synthesis approach and enables high-throughput parallel sequencing. This results in reads with high read accuracy (>99.9%) but with relatively short read lengths (150–300 bp) (Pervez et al. 2022). More recently, Oxford Nanopore Technologies (a third-generation sequencing technology) has gained popularity. This technique relies on nanopores and detects changes in the ionic current, allowing for significantly longer reads, with the current record standing at a single read of 4 Mb. Although the initial read accuracy was relatively low, recent reports indicate a raw read accuracy exceeding 99% (Wang et al. 2021). Both of these sequencing methods can be applied to amplicon sequencing, where specific DNA marker products are sequenced after amplification, or they can be employed for metagenomic sequencing and whole-genome sequencing purposes. Whole-genome sequencing aims to analyse the whole genome of a single species, while metagenomic sequencing focuses on analysing genetic material from a complex mixture of organisms, such as a microbial community or environmental sample. In both cases, the genomes are assembled by identifying overlapping regions between DNA reads to create a contiguous representation of the organism's genome. Comprehensive genome analysis extends beyond mere taxonomic classification, enabling the exploration of functional gene groups, including functions like carbohydrate metabolism, cofactors and vitamins metabolism, and the synthesis of secondary metabolites (Kanehisa et al. 2008). Metagenomic sequencing of an *Ulva*-associated bacterial community for example gives an overview of the functional potential of this community.

In this thesis, Sanger sequencing was used for the identification of *Ulva* species (Chapter 2, 4, 5, and 7). Oxford Nanopore long-read sequencing was used for the taxonomic composition of bacterial communities based on 16S amplicons (Chapter 2, 3, and 4) and for whole-genome sequencing of bacterial isolates (Chapter 6). Finally, metagenomic and metatranscriptomic (RNA-based) sequencing with Illumina technology were used for the functional profiling of bacterial and viral communities (Chapter 5 and 7).

1.2.2 Life cycle and reproduction

Ulva has an isomorphic biphasic life cycle, meaning that it has two multicellular phases that are morphologically indistinguishable (Fig. 1.03). During sexual reproduction, the haploid gametophytes produce haploid biflagellate gametes through mitosis. When gametes of different mating types are fused, a zygote is formed. The zygote develops into a diploid sporophyte and these in turn produce haploid quadri-flagellate zoospores through meiosis that develop into gametophytes. Asexual reproduction can also occur at every stage. Unfused gametes, for example, can regrow into gametophytes (Balar and Mantri 2020).

The reproductive cycle of *Ulva* is affected by several abiotic factors (including temperature, light, and desiccation), as well as biotic factors (including tissue age, algal–bacterial interactions, and the concentration of swarming inhibitors) (Kalita and Tytlianov 2003, Gao et al. 2017, Balar and Mantri 2020). The life cycle of the lab strains of *Ulva compressa* [in the literature often mentioned under its synonym *Ulva mutabilis*] has been exceptionally well studied (Stratmann et al. 1996, Wichard and Oertel 2010). Gametogenesis or sporogenesis can be induced by fragmentation of the thalli and washing the small fragments to remove sporulation inhibitors SI-1 and SI-2 from the medium. After 36 hours, the vegetative cells start to convert into gametangia or sporangia. On the morning of the third day after induction, the release of the gametes or zoospores can be triggered by light and the removal of swarming inhibitor SWI from the medium. Similar methods have been demonstrated for *Ulva linza* (Vesty et al. 2015). With *Ulva fenestrata* cultures, gametogenesis or sporogenesis is often induced by punching discs from older parts of the thalli (similar to the fragmentation method, but with larger fragments). Fertile parts, which are often visible after 5–7 days, are exposed to a desiccation shock and rehydrated in fresh medium, after which the reproductive cells are released (Steinhagen et al. 2021b).

Both *Ulva* gametes and zoospores are phototactic during their motile phase, swimming either towards the light or in the opposite direction (Haxo and Clendenning 1953). This phototactic behaviour plays an important role both in the mass-collection of reproductive cells for aquaculture and in obtaining bacteria-free individuals (see section 1.5.2) (Spoerner et al. 2012, Steinhagen et al. 2021b).

1.3 *Ulva* and the environment

The ubiquitous distribution of *Ulva* is not without reason: *Ulva* species are known to be highly tolerant to changing environmental conditions and can be found in a wide range of habitats (Beer 2022). These plastic species have the ability to combine rapid growth during optimal conditions with high persistence and survival during stress periods (Vermaat and Sand-Jensen 1987). Although a high abundance of *Ulva* is usually associated with shallow water and eutrophic conditions (Ho 1981, Lavery et al. 1991, Anderson et al. 1996), *Ulva* has been reported from the supralittoral zone down to 85 m depth (Spalding et al. 2016). Studies on *Ulva lactuca* collected in Denmark [with the recent taxonomic advances, this is more likely to be *Ulva fenestrata*] showed that the minimum light requirements for growth and photosynthesis were as low as 2.5 µmol photons m^{-2} s^{-1}, which corresponded to only 0.5% of the surface light of Danish water in Summer (Sand-Jensen 1988). *Ulva* species have even been reported to survive over 40 days in the dark whilst maintaining chlorophyll content and low growth rates if supplied with external glucose and acetate (Markager and Sand-Jensen 1990). Optimal irradiance for the northern hemisphere *Ulva fenestrata* reportedly ranges between 55–100 µmol photons m^{-2} s^{-1} (Sand-Jensen 1988, Toth et al. 2020). Growth saturation irradiance for several strains from the Yellow Sea is frequently higher, e.g., 136 µmol photons m^{-2} s^{-1} in *Ulva linza* (Kim et al. 2011), and 200 µmol photons m^{-2} s^{-1} in *Ulva prolifera* (Luo et al. 2012). However, the effect of irradiance on *Ulva* performance often depends on other parameters, such as nutrient concentrations, temperature, and salinity (Xiao et al. 2016).

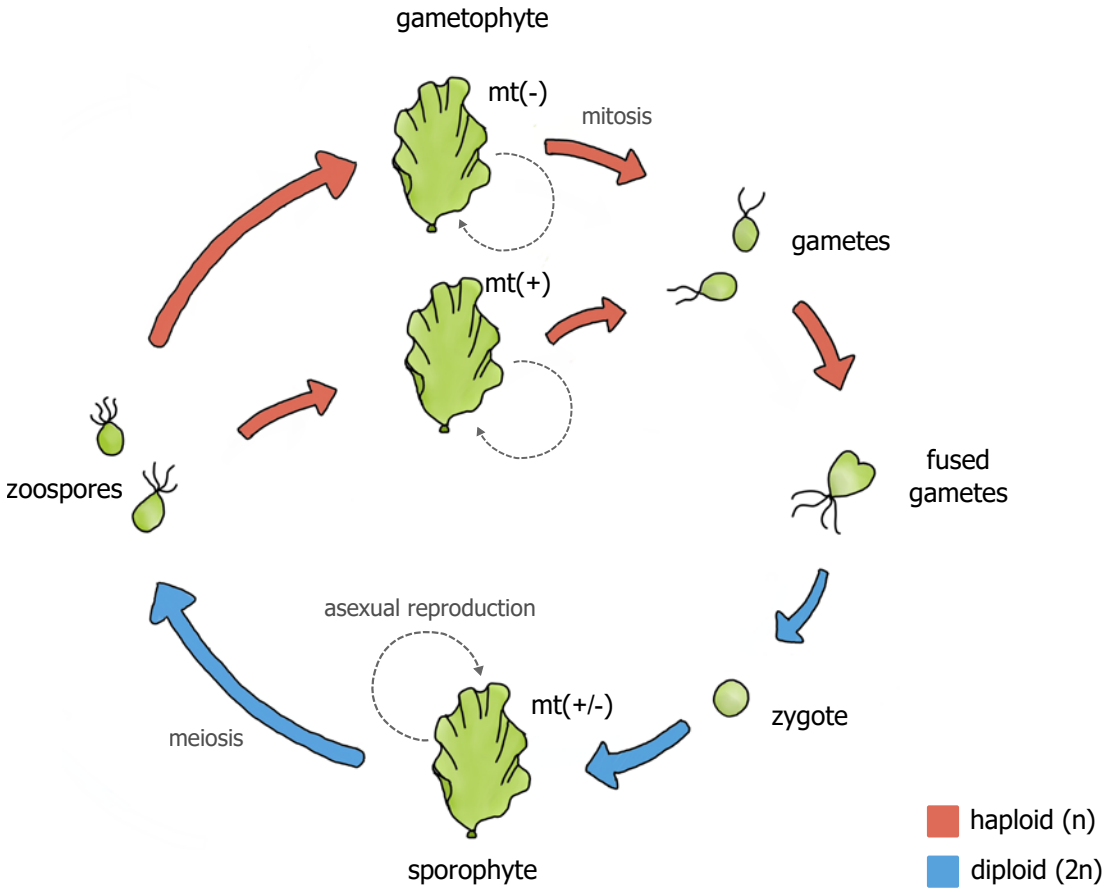

FIGURE 1.03 Typical *Ulva* life cycle. *Ulva* species alternate between gametophytic (haploid) and sporophytic (diploid) life phases. Mating types are indicated by (+) and (-). Asexual reproduction can also occur (indicated by dashed arrows).

Salinity is a major driver of biodiversity and species composition of invertebrate (Boulton et al. 2007), microbial (Lozupone and Knight 2007), and macroalgal communities (Snoeijs 1999). Interestingly, *Ulva* is one of the only genera in the green lineage that includes both freshwater and marine species (Rybak 2018, Mantri et al. 2020). *Ulva* species can be found across the entire salinity spectrum, and while a few species grow exclusively in freshwater (salinity < 0.5 PSU), e.g. *Ulva limnetica* (described from Japan) (Ichihara et al. 2009) and *Ulva shanxiensis* (described from China) (Chen et al. 2015), the majority of the species occurs in marine or brackish habitats (salinity 0.5–45 PSU). Many *Ulva* species are very tolerant to fluctuating salinity conditions. *Ulva intestinalis* and *Ulva linza*, for example, can be found from 3 PSU to 34 PSU, spanning the entire Atlantic Ocean–Baltic Sea salinity gradient (Steinhagen et al. 2023). More surprisingly, experimental work on *U. limnetica* showed that this freshwater species can survive in water with a salinity ranging from 0 to 30 PSU (Ichihara et al. 2013), indicating that this species has not lost its acclimation potential. The acclimation mechanisms of *Ulva* to fluctuating salinity are not well understood. Transcriptomic studies showed that genes related to photosynthesis and glycolysis pathways (e.g., malate dehydrogenase, soluble starch synthase, and chloroplast ascorbate peroxidase genes) are upregulated in lower salinity conditions, as well as processes related to ion transportation and osmolytes metabolism (Ichihara et al. 2011, Xing et al. 2021). Under hypersaline conditions, *Ulva* rapidly accumulate the organic osmolyte proline (Kakinuma et al. 2006) and is known to upregulate antioxidant enzymes (Sung et al. 2009). A deeper understanding of these mechanisms will help us understand why *Ulva* has such a remarkable tolerance.

Light, temperature, nutrients, and salinity collectively affect *Ulva* abundance. In coastal ecosystems, *Ulva* is an important food source for herbivores (Green and Fong 2016, Storero et al. 2022). However, *Ulva* species are also notorious for developing extensive blooms, known as green tides (Fig. 1.04) (Fletcher 1996, Ye et al. 2011). The sudden beaching of huge masses of algae poses significant ecological and economic hazards. In Brittany (France), for example, each year over 100,000 m^3 of landed algae smother the coast, resulting in an estimated cost of €2.4 million for cleaning and disposal (Charlier et al. 2007, 2008). In China, the largest green tides have covered ~1/8 of the area of the Yellow Sea, and more than 1.44 million tons of algae have reportedly landed in Qingdao during the year 2021 (Chen et al. 2022). The decomposition of these huge amounts of beached green algae causes extreme anoxic conditions and the release of gaseous sulphur compounds, resulting in sulphide poisoning and reduced biodiversity (Ye et al. 2011, Wan et al. 2017). Green tide events happen with increasing frequency and scale worldwide (Li et al. 2021, Ren et al. 2022). Eutrophication is attributed a major causal role in the development of green tides and contributes to the observed increasing occurrences (Smetacek and Zingone 2013, Xing et al. 2015). In addition, the interplay of sea surface temperature, precipitation, irradiance, and the availability of "seed" material from neighbouring aquaculture can trigger a green tide event as well as influence the scale of the triggered event (D. Li et al. 2022). Due to the complex interactions of environmental triggers, preventing and mitigating green tides will be no small undertaking.

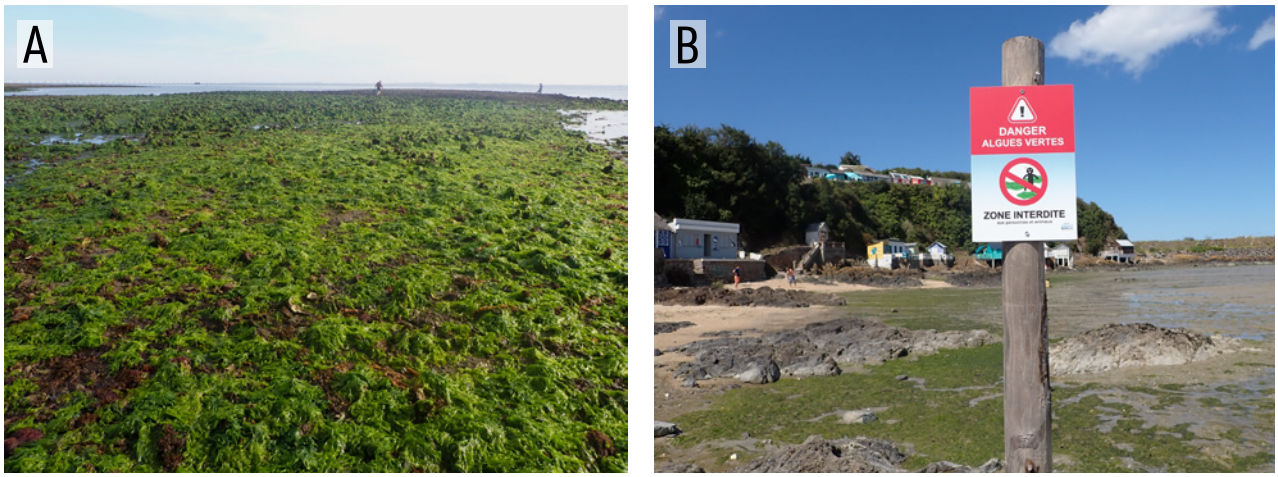

FIGURE 1.04 *Ulva* species are notorious for their role in the occurrence of green tides. A) Large masses of washed-up seaweeds in the Netherlands. B) Forbidden trespassing sign at a beach in Brittany warning against the fumes of rotting green algae.

1.4 Cultivating *Ulva*

The seaweed cultivation industry is currently undergoing exponential growth, driven by the search for alternative sustainable food sources and other valuable products. Seaweed production accounts for ~51% of the total global mariculture production, amounting to nearly 35 million tonnes in volume and a value of 14.7 billion USD in 2019 (Duarte et al. 2021, Cottier-Cook et al. 2022). The majority of the cultivated biomass consists of only a few genera: *Saccharina* and *Undaria* (brown seaweeds), and *Kappaphycus*/*Eucheuma*, *Gracilaria* and *Porphyra* (red seaweeds) (Cai et al. 2021). Cultivation of green seaweeds (e.g., *Monostroma* in Japan) is small and currently contributes merely 0.05% of the total biomass production. Nevertheless, cultivation of *Ulva* is also gaining attention (Bolton et al. 2016, Steinhagen et al. 2022b, Buck and Shpigel 2023, Harsha Mohan et al. 2023). *Ulva*

grows fast, even under high stocking densities, and its tolerance to environmental conditions makes it relatively easy to grow (Al-Hafedh et al. 2015, Steinhagen et al. 2022b). It can be cultivated both out at sea and in land-based systems (Steinhagen et al. 2021b). In addition, *Ulva* has the potential to be used as biofilter in Integrated Multi-Trophic Aquaculture systems, as *Ulva* is generally very efficient in absorbing and removing nitrogen (Copertino et al. 2009, Nederlof et al. 2022). To establish a commercially viable *Ulva* aquaculture industry, various methods for large-scale biomass cultivation are currently being developed.

1.5 *Ulva* as an own ecosystem

[This part of the introduction has been adapted from L.M. van der Loos, B.K. Eriksson & J. Falcão Salles. 2019. The macroalgal holobiont in a changing sea. *Trends in Microbiology.* 27:635–650]

1.5.1 The seaweed holobiont: a functional unity

Seawater contains vast numbers of microorganisms, with up to 10^7 viruses, 10^6 bacteria, and 10^3 microalgae per mL (Cole 1982). Many of these microbes form biofilms on a range of eukaryotic organisms, such as corals, sponges, and macroalgae. The microbial communities associated with different hosts contain a diverse assembly of organisms (including archaea, bacteria, fungi, microalgae, protozoa, and viruses), but differ markedly from the assemblages in seawater (Longford et al. 2007). In fact, together the host and the associated microbes are increasingly regarded by some authors as a functional unity called holobiont [for authoritative reviews on the holobiont concept and evolutionary perspective, see Bordenstein and Theis (2015), McFall-Ngai et al. (2013), Rosenberg and Zilber-Rosenberg (2016), and Agler et al. (2016)]. This single ecological unit is a complex entity with highly specialized symbiotic interactions that are regarded to be important in the functioning of all organisms involved (Barott et al. 2011).

Microbes often play a crucial part in macroalgal health, functioning, and development during the host's various life cycle stages (Wahl et al. 2012, Egan et al. 2013). The interactions between macroalgae and the microbiota are extremely diverse. Ranging from mutualistic, to commensal and parasitic, the microbiota can be fundamental or detrimental to the functioning of the host (Egan et al. 2013). The interplay of macroalgae with their microbial component affects — among others — nutrient exchange, defence mechanism, morphology, reproduction, and settlement (Brock and Clyne 1984, Goecke et al. 2010, Bengtsson et al. 2011). The algal surface is a habitat that is ideal for the growth of the microbiota, as it is rich in organic carbon, oxygen, and nutrients (Brock and Clyne 1984, Goecke et al. 2010, Bengtsson et al. 2011, Lage and Graça 2016). In turn, the microbiota, for example heterotrophic bacteria and nitrogen fixing cyanobacteria, may provide the algal host with CO_2, nitrogen, and vitamins (Croft et al. 2006, Egan et al. 2013, Hollants et al. 2013b). However, the functioning of the holobiont extends far beyond exchanging key nutrients.

Microbial communities form a biofilm on the host, which acts as both a physical and a physiological barrier between the host and the environment (Wahl et al. 2010, 2012). This barrier can modulate the availability of resources for the host, having an 'insulating' effect. The insulating effect can also be positive, as the biofilm can protect the host against toxins, heavy metals, and ultraviolet radiation, by adsorption or even transforming the toxins to less harmful compounds (Riquelme et al. 1997, Goecke et al. 2010, Wahl et al. 2012). Microbes are an important factor in the early phases of macroalgal life-history as well. The amount of bacteria in the biofilm on surfaces (e.g., rocks) has a positive effect on the number of zoospores settling on the substrate (Joint et al. 2000), as does the age of the biofilm (Patel et al. 2003), thus facilitating the successful colonisation of new sur-

faces by macroalgae and the formation of new holobionts (Goecke et al. 2010). In addition, the release of spores can be influenced by biofilms due to the secretion of secondary metabolites that act as a cue (Weinberger et al. 2007, Singh et al. 2011). Finally, the biofilm has an important chemical function. Certain algae-associated bacteria may play a part in the host defence strategies against unwanted microbes and biofouling by outcompeting other bacteria. They can for instance secrete antifouling chemicals and antibiotics, thus maintaining the health of the host (Goecke et al. 2010).

1.5.2 *Ulva*, its microbiome, and morphogenesis

Ulva in particular is a model organism for the study of morphological development and host–bacterial interactions (Wichard et al. 2015). *Ulva* relies on its bacterial symbionts for morphogenesis, and in the absence of appropriate bacteria merely grows as a loose callus-like aggregate of cells with malformed cell walls (Fig. 1.05) (Provasoli 1958, Marshall et al. 2006, Spoerner et al. 2012). Only when exposed to certain bacterial strains, complete morphogenesis is observed. In laboratory experiments, establishing morphogenesis is usually mediated by exposing *Ulva* to a specific *Roseovarius* sp. strain MS2 and a *Maribacter* sp. strain MS6 (Spoerner et al. 2012, Weiss et al. 2017), but several other bacteria also have the capacity to induce morphogenesis (Grueneberg et al. 2016). These bacteria release waterborne morphogens (morphogenetic compounds) that induce blade cell division and thallus elongation (MS2 activity), or rhizoid formation and cell wall development (MS6 activity) (Weiss et al. 2017). To date, only the compound released by MS6 activity strains — thallusin — has been identified (Matsuo et al. 2005, Alsufyani et al. 2020). Bacteria that exhibit MS2 activity include, amongst others, *Paracoccus*, *Sulfitobacter*, and *Halomonas* strains, while bacteria that exhibit MS6 activity include several *Maribacter* and *Zobellia* strains (Grueneberg et al. 2016, Wichard 2023). In addition, two strains, an *Algoriphagus* sp. and a *Polaribacter* sp., exhibit the capability of independently triggering complete morphogenesis without requiring the presence of complementary strains (Grueneberg et al. 2016).

In its natural environment, *Ulva* harbours a microbial biodiversity that extends far beyond the well-studied morphogenesis-inducing bacteria, with reported bacterial operational taxonomic units (OTUs) ranging from 224 to 413 per sample (Roth-Schulze et al. 2018). The majority of these microbes inhabit the surface of *Ulva* thalli (Gemin et al. 2019), given *Ulva*'s relatively simple morphology of being only 1–2 cell layers thick, although a few endophytic bacteria have been identified as well (Deutsch et al. 2023). Interestingly, *Ulva*'s reproductive cells do not appear to inherit bacteria from their parents (i.e., no vertical transmission), as demonstrated by the absence of bacteria on freshly released spores (Syukur et al. 2023). This indicates that *Ulva* gametes and spores rely on horizontal acquisition of their symbionts from the environment. Thus, the environment has a large potential to influence the composition of *Ulva*-associated microbial communities. On the other hand, studies thus far have shown that the taxonomic composition of the *Ulva* microbiome is highly variable across individuals (Tujula et al. 2010, Burke et al. 2011b, Roth-Schulze et al. 2018), suggesting that neutral or stochastic processes likely play a role in driving microbial community structure. The question remains to what extent *Ulva* can "garden" its own microbiome, for example by attracting beneficial microbes and deterring unwanted colonisers from the environmental source pool (Saha and Weinberger 2019).

The availability of truly axenic gametes and zoospores was an important element in advancing the understanding of the symbiotic interactions within the *Ulva* holobiont. Obtaining strictly axenic cultures proves to be challenging for many macroalgal species. Conventional methods, such as antibiotic treatments and sonication (disruption based on sound waves), are effective in eliminating the majority of biofilm, but typically leave behind a residual population of bacteria. Spoerner et al. (2012) were able to effectively obtain axenic *Ulva* cultures

by leveraging the gamete's phototactic behaviour. Due to the gametes' strong attraction to light and their high swimming speed, they can be harvested separately from their accompanying bacteria by passing them through glass pipettes equipped with a light source at the tips. The presence of axenic cultures enables researchers to assess the impact of individual bacteria on *Ulva* growth, physiology, and biochemical composition. For ecological relevance, however, it is equally important to understand how the holobiont as a whole responds to alterations in the microbial community and environmental changes.

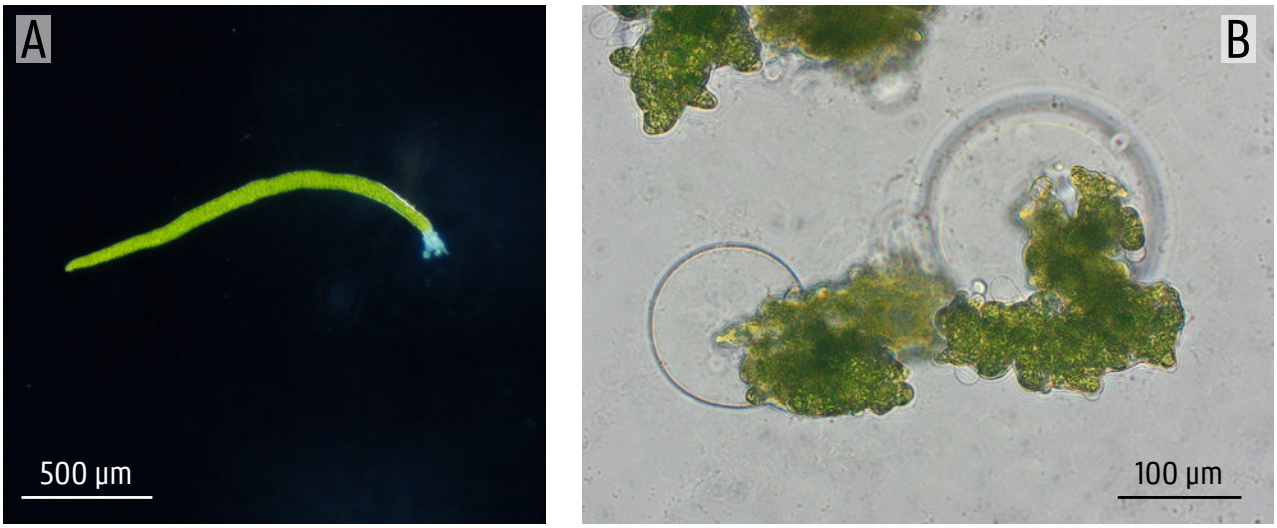

FIGURE 1.05 A) Normal development of *Ulva* germlings (2-week-old culture), with rhizoids and cell walls. B) Axenic *Ulva* culture. Note the malgrowth in the absence of bacteria and the colourless protrusions.

1.5.3 Changing communities in changing environments

Without their associated microbiota, macroalgae cannot function optimally. However, microbes can also induce diseases, especially under changing environmental conditions, such as increasing seawater temperatures and ocean acidification (Egan et al. 2014, Kumar et al. 2016). Here, environmental stressors alter the microbial communities and disturb the symbiotic relation, which results in holobiont break-up (De Fouw et al. 2016, Egan and Gardiner 2016). With the cascading effects of a holobiont break-up and dysbiosis, the results of these changing conditions may be more severe than predicted. However, we also know that interactions between species may shift from negative to positive during increasing amounts of stress (Menge and Sutherland 1987). Thus, an increasing positive importance of mutualisms, facilitative interactions and cooperative behaviour, may also provide holobionts with additional resilience to changing conditions (stress gradient hypothesis; sensu Maestre et al. 2009). In the context of environmental changes, especially those human-induced, the holobiont concept becomes increasingly important.

Environmental change interacts with the holobiont on three basic levels (summarised in Fig. 1.06): (i) direct effect on microbiota; (ii) direct effect on host physiology; and (iii) direct effect on host–microbiota interactions. For example, shifting of environmental conditions expected under climate change scenarios might lead to fluctuations in the microbial composition in the seawater column (Hengst et al. 2010, Krause et al. 2012, Minich and Dinsdale 2015). This will in turn affect the microbial community that can colonise the host and the functional traits associated with those (e.g., microbial communities might shift in terms of absolute abundance, relative abundances, and species richness, ultimately resulting in different functional guilds). Environmental

change may also have a modifying effect on the interactions between host and microbes, as microbial communities with a different functional potential affect the host differently, and vice versa a host with a changed physiology provides a different kind of niche to microbes. For example, an environmentally induced shift towards an epiphytic community with a higher abundance of pathogenic microbes (Mensch et al. 2016, Minich et al. 2018), may subsequently be detrimental to the host. In turn, reduced photosynthetic activity due to a decreased pH, and thus a lower production of oxygen by the algal host (Nunes et al. 2016), could potentially lead to the algal surface being an unfavourable habitat for aerobic bacteria. These are just two of many hypothetical examples that could be given of how climate change can have a transforming effect on host–microbe interactions, and this illustrates the complexity of studying the response of the holobiont to changing environments.

Several studies have shown that the bacterial communities associated with macroalgae change under the influence of temperature (Webster et al. 2011, Saha et al. 2014, Mensch et al. 2020), ocean acidification (Qiu et al. 2019a, Barakat et al. 2021), and salinity (Stratil et al. 2014, Dittami et al. 2016). Such environmentally-induced alterations of the microbial communities have been observed both in terms of taxonomic composition (based on 16S rRNA gene sequencing; Text box 1) and functional gene composition (based on metagenomic sequencing; Text box 1). In *Ulva fasciata*, for example, increased pCO_2 levels induced a shift from a *Halomonas*-dominated bacterial community to a *Vibrio*-dominated community (Barakat et al. 2021). Microbial communities of calcified rhodoliths along an environmental gradient in the Great Amazon Reef System contained more genes related to iron acquisition and photosynthesis in the southern region of this gradient, whereas the microbial communities in the central and northern area were enriched in respiration and sulphur metabolism, concordant with higher nutrient concentrations in these areas (Calegario et al. 2020). Conversely, rholodith-microbial communities remained stable under elevated pCO_2 conditions (Cavalcanti et al. 2018). The ocean acidification treatment did not negatively affect calcium carbonate biomass of the host, suggesting that a stable microbiome is important for host resilience.

The question remains whether microbial communities can help their macroalgal host acclimate — or even adapt — to short-term and long-term changes in the environment and what mechanisms are involved in these interactions. Deciphering the complex interactions between the environment and all the components that together form the macroalgal holobiont will require a mix of laboratory and field experiments, as well as descriptive and manipulative studies. Due to the large amounts of interactions between the environment, the host, and the bacterial communities, it will be very complex to clearly establish causality. However, understanding the mechanisms through which the environment interacts with the holobiont and the magnitude of importance of each component will be essential in understanding the effects of environmental change.

1.6 Research objectives and thesis outline

The general objective of this PhD thesis is to assess how the *Ulva* holobiont acclimates to environmental change. As argued before, *Ulva* is an excellent candidate for seaweed holobiont research. Not only is *Ulva* a model system to study algal–bacterial interactions, its widespread distribution, growing importance in aquaculture, and the availability of a reference genome also make it a highly relevant choice.

To address the general objective, we used a combination of different techniques, including 16S rRNA sequencing, metagenomic sequencing, and whole-genome sequencing (for an overview of sequencing techniques, see Text box 1), and we conducted both field studies and manipulative laboratory experiments. To provide a comprehensive overview of the *Ulva* microbiome, we studied natural populations as well as cultivated strains, and aimed to characterise not only bacteria, but understudied components of the holobiont as well.

This thesis contains six research chapters (chapter 2–7):

- **Chapter 2** describes a pipeline to monitor *Ulva*-associated bacterial communities using long-read Oxford Nanopore sequencing.
- **Chapter 3** analyses seasonal fluctuations and succession patterns in the bacterial communities of natural *Ulva* populations and cultivated *Ulva*.
- **Chapter 4** characterises the taxonomic composition of the *Ulva* microbiome across a natural and stable salinity gradient in the Baltic Sea.
- **Chapter 5**, using the same Atlantic–Baltic Sea salinity gradient, explores how the functional potential of the bacterial communities changes using metagenomic techniques.
- **Chapter 6** tests whether bacteria isolated from high and low salinity environments can affect *Ulva* growth under varying salinity conditions using laboratory experiments.
- **Chapter 7** explores the *Ulva* microbiome beyond bacteria and characterises novel viruses associated with healthy and bleached *Ulva*.

To conclude, **Chapter 8** provides a comprehensive overview of the findings of this thesis, integrating the results from the individual research chapters and delving into future perspectives within in a broader context.

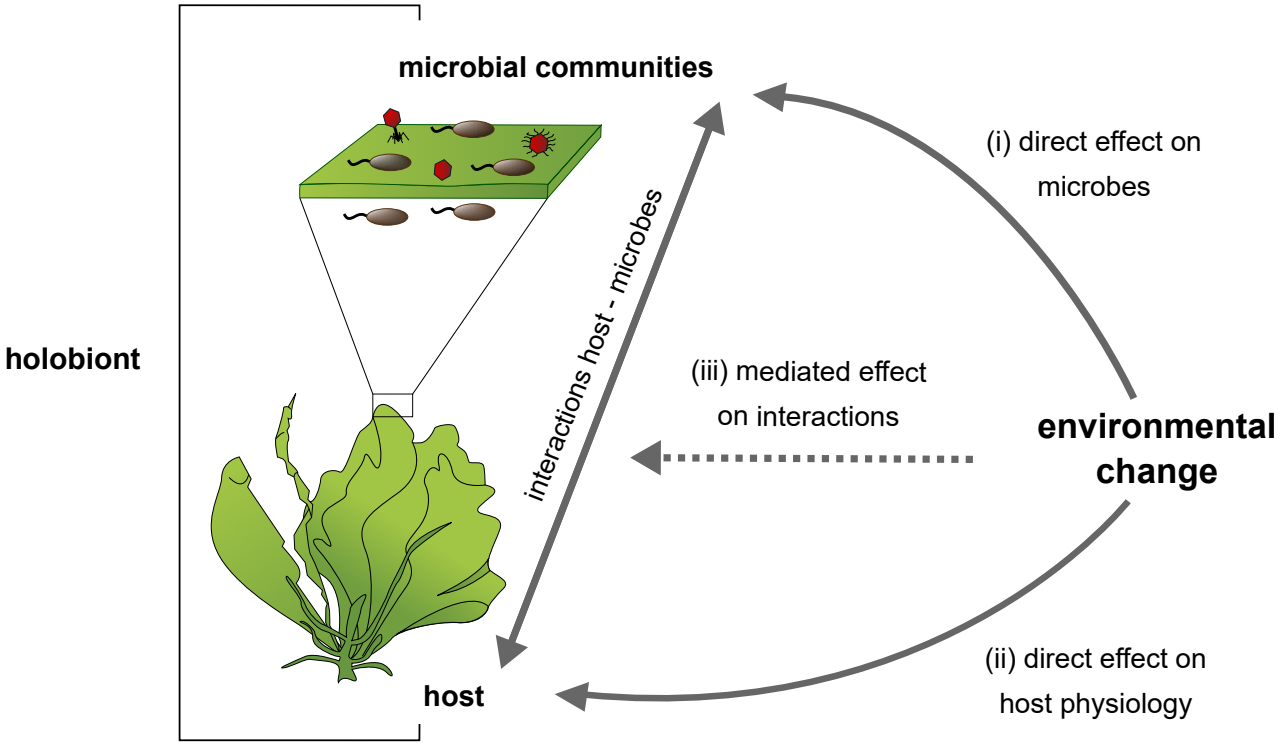

FIGURE 1.06 Overview of the interactions between the host, the microbial community, and environmental change. Environmental change (e.g., stressors or changes in environmental conditions) will separately have an effect on (i) the microbes associated with the host and (ii) the host itself, causing changes in host physiology and microbial community traits. This will affect the interactions between the host and the microbial communities (iii) and thus the outcome of the symbiotic relation.

“She makes the sound the sea makes, knee-deep in the North Sea”

– Alt J, in: Dissolve Me (An Awesome Wave)

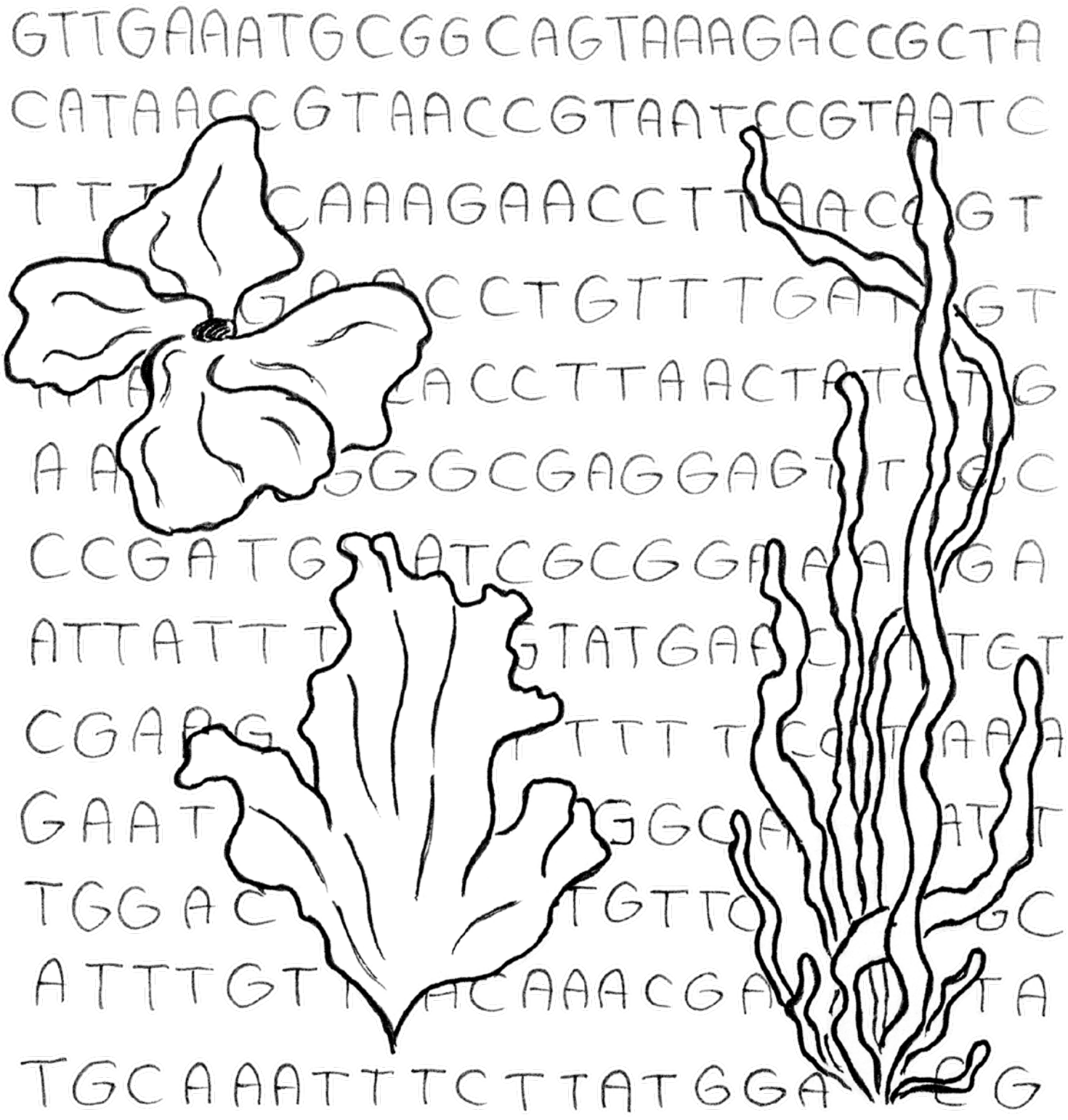
GTTGAAAATGCGGCAGTAAAGACCGCTA
CATAACCGTAACCGTAATCCGTAATC
TTT CAAAGAACCTTAACCGT
ACCTGTTTGATTGT
CACCTTAACTATCTG
AAGGGCGAGGAGTTTGC
CCGATG ATCGCGGGAAAAGA
ATTATTT GTATGAACATGT
CGAAG TTTTTCGTAAA
GAAT GGCATATT
TGGAC TGTTCGC
ATTTGT ACAAACGATA
TGCAAATTTCTTATGGAG

Chapter 2. Characterising algal microbiomes using long-read Nanopore sequencing

This chapter has been published as:
L.M. van der Loos[1,2], S. D'hondt[1], A. Willems[2] & O. De Clerck[1]. 2021. Characterizing algal microbiomes using long-read Nanopore sequencing. *Algal Research*. 59:102456.

[1] Phycology Research Group, Department of Biology, Ghent University, Ghent, Belgium
[2] Laboratory of Microbiology, Department Biochemistry and Microbiology, Ghent University, Ghent, Belgium

Abstract

Microbes are vitally important for seaweed growth, functioning, and reproduction, and are likely to have a big impact on aquaculture. Algae-associated bacteria, however, remain mostly unmonitored in aquaculture. Here, we studied the microbiomes of *Ulva australis* and *Ulva lacinulata*, three natural populations and an aquaculture set-up, based on full-length 16S rRNA gene sequences. The microbiome of cultivated *Ulva* was pronouncedly different from natural populations, and was specifically associated with higher relative abundances of known growth-promoting bacteria *Sulfitobacter* and *Roseobacter*. On a smaller scale, there were species-specific differences as well. In general, *Ulva*-associated communities were highly distinct from environmental seawater and sediment reference samples. We demonstrated a workflow generating full-length 16S rRNA sequences in real-time using Oxford Nanopore sequencing. We compared 3 different reference databases to assign taxonomy with Kraken2 (SILVA, Greengenes and NCBI). In addition, we used Nanopore's cloud-based EPI2ME workflow for comparison. All four methods yielded comparable results in terms of relative abundances on phylum and order level, but differed widely in alpha diversity indices at genus level. Using the NCBI 16S database, especially in combination with the EPI2ME workflow, resulted in a high proportion of false identifications of cyanobacteria due to chloroplast contamination. Based on our results, we recommend assigning taxonomy of Nanopore-derived long-reads with Kraken2 and the SILVA database in seaweed–microbiome studies. The protocols used in this study provide results within 24 hours and may be applicable for rapid microbial surveys in aquaculture.

2.1 Introduction

Recent decades saw a spectacular growth of coastal and onshore aquaculture as a sustainable alternative to food and feed procurement. Seaweed aquaculture in particular has grown faster than any other marine food production sector in the last 20 years (FAO 2020). Seaweeds, however, would not be able to attain proper growth without microbial partners that colonise their surfaces, rhizoids, and in some cases also the cytoplasm itself. Both the microorganisms (including archaea, bacteria, fungi, microalgae, protists, and viruses) and their interactions are extremely diverse, ranging from mutualistic to parasitic. Many of the microbes play a crucial role during the host's various life cycle stages, affecting nutrient exchange, defence mechanisms, morphology, reproduction, and settlement (Weinberger et al. 2007, Goecke et al. 2010, Bengtsson et al. 2011, Wahl et al. 2012, Egan et al. 2013, van der Loos et al. 2019).

A species that is particularly amenable for aquaculture is *Ulva* (Bolton et al. 2016). *Ulva* is relatively easy to grow and can be integrated in multi-trophic land-based systems where it removes excessive nutrients (bioremediation), while the biomass can serve as a direct feed component for co-cultivated animals or be processed as a sustainable biomass feedstock for the food and biotech industries (Neori et al. 2004, Alsufyani et al. 2014, Bikker et al. 2016, Reisky et al. 2019). The *Ulva* thallus is relatively simple, being a blade that is two-cells thick or a tube that is one-cell thick. These morphologies, however, are only established in the presence of appropriate bacterial communities (Spoerner et al. 2012). In axenic culture conditions (cultured in the absence of microbes), *Ulva* grows as a loose callus-like aggregate of cells with malformed cell walls. Only when exposed to certain bacterial strains, complete morphogenesis is observed. In laboratory experiments, establishing morphogenesis is usually mediated by exposing *Ulva* to a specific *Roseovarius* and a *Maribacter* strain (Wichard et al. 2015), but several other bacteria also have the capacity to induce morphogenesis (Grueneberg et al. 2016, Ghaderiardakani et al. 2017). Apart from morphology, these bacteria can also promote *Ulva* growth (Gemin et al. 2019), stimulate settlement of zoospores (Joint et al. 2002, Marshall et al. 2006), and alter the biochemical composition (Polikovsky et al. 2020). For example, certain growth-promoting bacterial isolates have been shown

to singly increase *Ulva* growth by 81% (Gemin et al. 2019), increase glucose and glycerol content, and alter the rhamnose/xylose/glucuronic acid ratio (Polikovsky et al. 2020). It is clear that the impact of bacteria on host physiology can have cascading effects on biomass production and biomass quality in aquaculture. It is therefore important to compare the *Ulva*-associated microbiome in wild and aquaculture populations from an economic perspective as well.

Contrary to fed aquaculture species (e.g. finfish, molluscs, shrimp), in seaweed aquaculture the associated microbiomes are not routinely screened (Bentzon-Tilia et al. 2016, Rajeev et al. 2021). Microbe-monitoring in aquaculture is often targeted toward specific pathogens (e.g., *Aeromonas* and *Vibrio* strains) and is traditionally performed using culture techniques on agar plates (Ganesh et al. 2010). Although culturing bacteria and subsequent identification with Sanger sequencing or MALDI-TOF MS is a highly specific method, it does not provide information on the non-cultivable fraction of the microbiome. Other approaches to assess microbial diversity and communities in aquaculture include flow cytometry (Props et al. 2016) and high-throughput sequencing technologies based on marker genes (Infante-Villamil et al. 2021). Especially high-throughput sequencing, however, has been a labour-intensive and time-consuming method, but this has changed with the recent development of the MinION sequencer by Oxford Nanopore Technologies (ONT), enabling real time long read sequencing (Santos et al. 2020).

Oxford Nanopore sequencing technology directly detects nucleotides based on ionic current shifts that occur as the nucleotides of a single DNA strand pass through a protein nanopore (Jain et al. 2016). This allows for the sequencing of long stretches of DNA, including full-length amplicons of the16S rRNA gene, which is universally used as a marker in taxonomic profiling of prokaryotic species (Santos et al. 2020). A MinION flow cell contains up to 512 nanopore channels and typically produces between 10–30 Gb sequence data. Reads obtained from this hand-sized device (which is simply plugged into a computer) can be basecalled and analysed in real time (Mitsuhashi et al. 2017). Apart from the speed of sequencing and the length of the reads, other advantages include portability (allowing in situ sequencing at remote locations), low costs, and user friendliness [1]. A current trade-off is the relatively low read accuracy compared to other platforms that employ sequencing-by-synthesis such as Illumina technology. Modal raw read accuracy of ONT is currently >97% (Oxford Nanopore Technologies 2021), but is constantly improving due to both enhanced flow cell chemistry and improved basecalling algorithms (Deamer et al. 2016, Karst et al. 2021). Despite lower read accuracy, using the full 16S rRNA gene (~1,500–1,600 bp) has been shown to result in greater taxonomic resolution of microbial communities compared to the use of high-accuracy, partial 16S rDNA fragments (~100–500 bp) (Johnson et al. 2019, Nygaard et al. 2020, Kerkhof 2021). The potential to use MinION derived 16S rDNA reads has been demonstrated in recent studies focusing on, amongst others, coral microbiomes (Carradec et al. 2020, Wijgerde et al. 2020), seawater communities (Curren et al. 2019), mouse gut microbiota (Shin et al. 2016), and building-dust microbiomes (Nygaard et al. 2020). Concerning macroalgae, ONT has only been employed in a single publication in which the hologenome of the green alga *Caulerpa ashmeadii* was characterised using metagenomics (Sauvage et al. 2019).

Few bioinformatics tools and protocols are available for the processing of 16S rDNA Nanopore sequences, especially compared to the number of tools available for the processing of Illumina short-read sequencing technologies (Santos et al. 2020). Existing tools that were specifically designed for shorter, high accuracy reads are in many cases not suitable to analyse long reads with lower accuracy, due to the larger number of errors that accumulate in longer reads. Nanopore's own cloud-based tool EPI2ME is very user friendly and provides end-to-end data analysis service. However, users can only modify initial parameters (including read length and quality) while other parameters are set by default. The FASTQ 16S workflow, for example, assigns taxonomy using BLAST and the standard NCBI 16S database (with >77% identity and >30 coverage as default settings,

although these parameters can also be adjusted in the latest EPI2ME 16S workflow release). Results are visible as a web report and can be downloaded as CSV file. In seaweed microbiome analyses, chloroplast contamination may pose an additional problem. Due to the cyanobacterial origin of the chloroplast, universal 16S rDNA primers may lead to amplification of plastid DNA, resulting in >90% chloroplast-derived reads in some samples (Thomas et al. 2019). To be able to distinguish between real cyanobacteria and plastid sequences, the reference database is of enormous importance. As the EPI2ME platform only works with the NCBI database, other classifier tools such as Kraken2 (Lu and Salzberg 2020), Centrifuge (D. Kim et al. 2016), and Minimap2 (Li 2018) need to be utilised in order to use other traditional and curated 16S rDNA databases, including SILVA (Quast et al. 2013) and Greengenes (DeSantis et al. 2006).

Here, we studied the diversity of bacteria associated with *Ulva australis* and *Ulva lacinulata* in natural and aquaculture populations as a test case to demonstrate a workflow to screen algal-associated bacteria using Oxford Nanopore MinION sequencing technology covering the whole 16S rRNA region. In addition, we compare three different 16S rDNA reference databases to assign taxonomy: SILVA, Greengenes and NCBI, as well as Nanopore's EPI2ME tool.

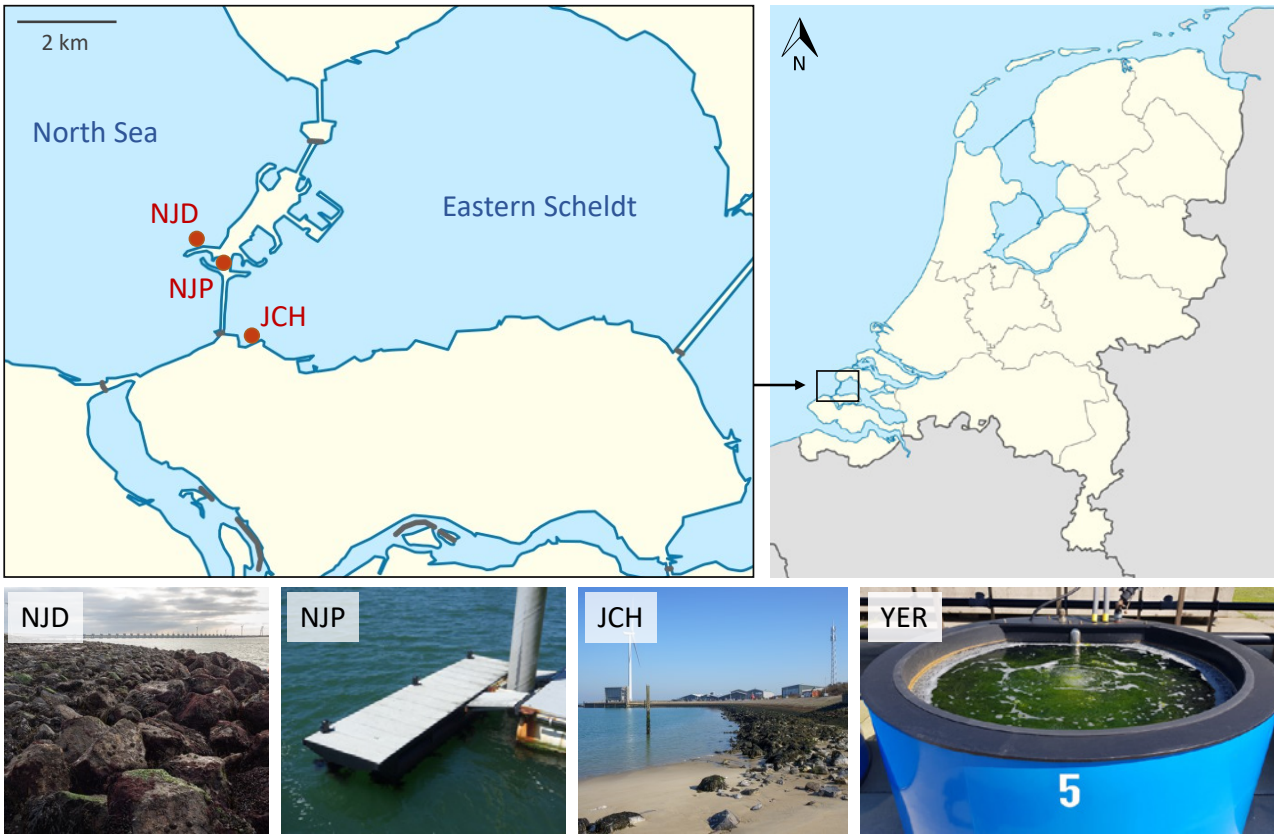

FIGURE 2.01 Map showing sample sites in Zeeland, the Netherlands. The three sample sites included an exposed, rocky shore (NJD), a floating pontoon (NJP), and a sedimentary bay (JCH). Additional samples were received from aquaculture facilities (YER; not on the map). (Map modified from Lencer (2011). Photo credits (left to right): Mick Otten, Frank Perk, Luna van der Loos, Lander Blommaert (NIOZ).

2.2 Materials and methods

2.2.1 Sampling

Ulva individuals were collected in February 2020 at three neighbouring localities in the Netherlands: 1) an exposed rocky shore on the North Sea coast of the storm surge barrier Neeltje Jans (NJD; 51°37'22.0"N, 3°40'15.9"E), 2) a floating pontoon in a sheltered bay on the North Sea coast (NJP; 51°37'05.1"N, 3°40'55.4"E), and 3) rocky substrate in the sedimentary, sheltered bay Jacobahaven in the Eastern Scheldt Delta (JCH; 51°35'52.4"N, 3°41'05.0"E) (Fig. 2.01; Electronic Supplementary Materials S2.01). At each site, five *Ulva* individuals were collected, as well as seawater samples (n = 3, ~500 mL per sample) and sediment samples if possible (n = 3, ~2 mL per sample) as environmental references. All samples were collected at low tide and immediately transported on ice to the laboratory (approximately 1 hour drive). From each *Ulva* individual, a tissue sample (1 cm^2) and a swab sample (by rubbing a cotton swab for 30 seconds on the tissue) were processed for microbiome analyses. Seawater was filtered on a MF-Millipore MCE membrane filter with 0.22 µm pore size. All samples were preserved at –80 °C. All *Ulva* specimens were identified using the *tuf*A and/or *rbc*L DNA barcoding marker, and included *U. australis* and *U. lacinulata* (see Electronic Supplementary Materials S2.01 for NCBI accession numbers). Species were identified according to the latest taxonomic revisions by Hughey et al. (2021).

In addition to natural *Ulva* populations, we included six samples from algal aquaculture facilities at the Royal Netherlands Institute for Sea Research, located in Yerseke (YER). These samples included two strains that originated from Jacobahaven (*Ulva australis*) and the Wadden Island Texel (*Ulva lacinulata*), but had been in culture for over one year. The land-based aquaculture facilities receive sediment-filtered seawater from the Eastern Scheldt.

2.2.2 DNA extraction, PCR amplification, and sequencing

Microbial DNA was extracted with the Qiagen PowerSoil kit following the manufacturer's protocol, from a total of 53 samples (including a negative extraction control and the ATCC microbial standard MSA-1002 as positive control). The full length 16S rRNA gene was amplified by PCR using the following primers: 27F_BCtail-FW (TTTCTGTTGGTGCTGATATTGC_AGAGTTTGATCMTGGCTCAG) and 1492R_BCtail-RV (ACTTGCCTGTCGCTCTATCTTC_CGGTTACCTTGTTACGACTT), each containing a 5′ extension allowing for subsequent barcoding by PCR. 16S rDNA amplification PCRs, including two negative PCR controls, were performed using the Phire Tissue direct PCR Master Mix (Thermo Fisher) with the following thermal profile: 3 min at 98 °C, 30 cycles of 8 s at 98 °C; 8 s at 60 °C; 30 s at 72 °C, final extension of 3 min at 72 °C. Amplicons for each sample were barcoded using the Oxford Nanopore "PCR Barcoding Expansion Pack 1–96 (EXP-PBC096)", and subsequently pooled in equimolar ratios and purified using Agencourt AMPure XP beads. The final library was prepared with the ligation-based sequencing kit SQK-LSK109 according to manufacturer's protocol (Oxford Nanopore Technologies), and sequenced on a MinION with an R9.4.1 flow cell for 48 hours. Bases were called with Nanopore's command line-based tool Guppy, resulting in a total of 3,407,210 reads. See Fig. 2.02 for an overview of the methodological pipeline. The sequences are archived at SRA (accession number PRJNA742225).

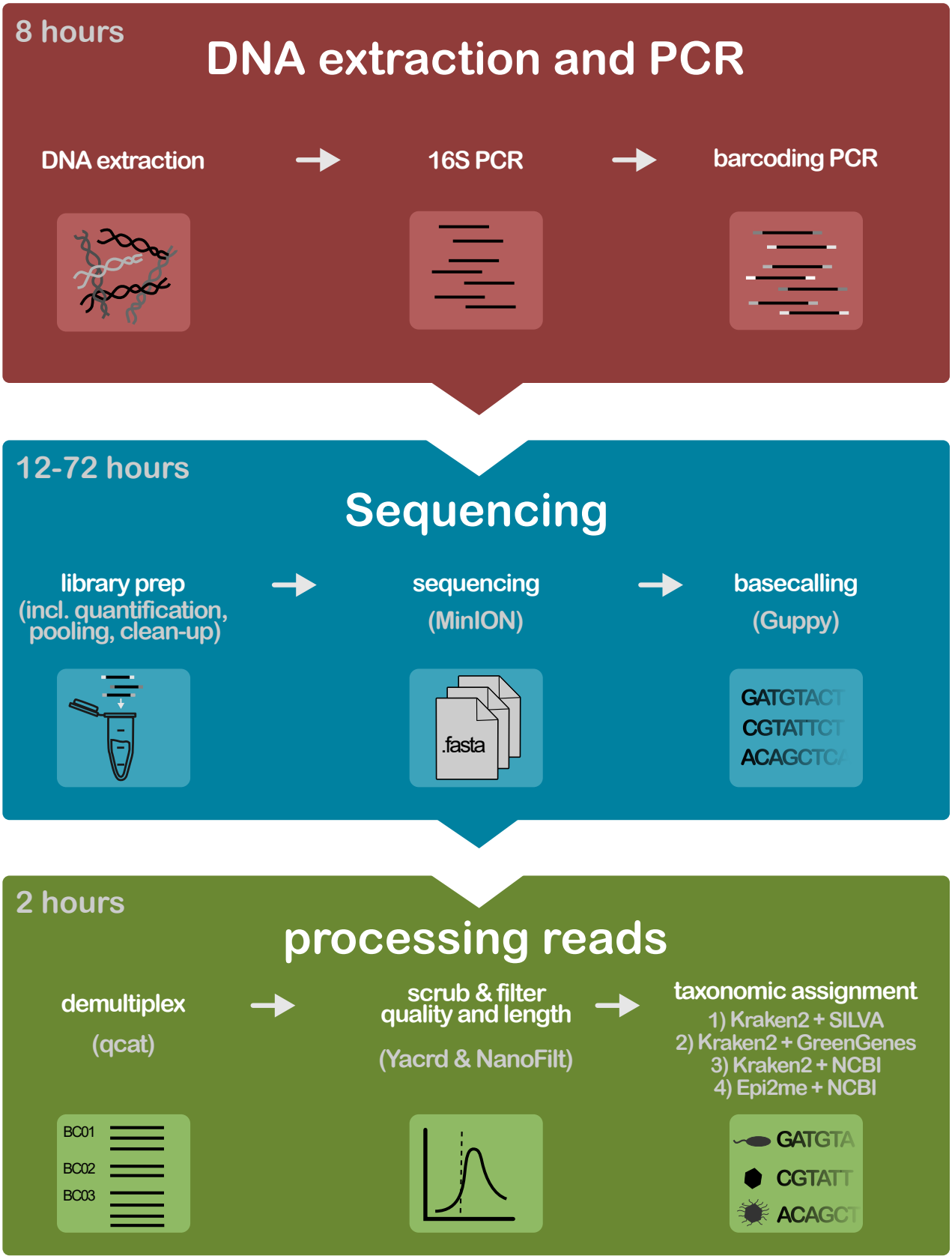

FIGURE 2.02 Pipeline for characterising the seaweed associated microbiome with Oxford Nanopore Technologies.

2.2.3 Read processing, taxonomic assignment, and statistical analyses

Data quality and length were visually inspected with NanoPlot (De Coster et al. 2018) and data were demultiplexed with qcat (ONT, https://github.com/nanoporetech/qcat). Chimeric reads were removed with Yacrd (Marijon et al. 2020) and the remaining reads were filtered on length (1,000–2,000 bp) and quality (Q-score >8) with NanoFilt (De Coster et al. 2018). The resulting 2,611,265 high-quality reads were used to assign taxonomy at genus level in four different ways: 1) Kraken2 in combination with the SILVA 16S database (138.1 release) (Quast et al. 2013, Lu and Salzberg 2020), 2) Kraken2 in combination with the Greengenes 16S database (13.5 release) (DeSantis et al. 2006), 3) Kraken2 in combination with the NCBI 16S database (Agarwala et al. 2018), and 4) Nanopore's cloud-based platform EPI2ME that uses the NCBI 16S database (version 2020.03.11, Metrichor, Oxford, UK; https://EPI2ME.nanoporetech.com)[2]. In the graphs in this manuscript, we use the most recent phylum nomenclature as implemented in the SILVA database. After taxonomic assignment, all chloroplast reads and unidentified reads were removed from the dataset. One sample (swab sample, NJD) was discarded due to contamination. In addition, rare taxa not seen more than two times in at least 10% of the samples were discarded. This protects against OTUs with small mean and trivially large coefficient of variation. As chloroplast removal resulted in reduced read count in tissue samples (varying from only 0.1% to 87.8% loss of reads), DESeq2 was used to normalize read count for sequencing depth (Love et al. 2014).

To assess differences in beta diversity (between-sample diversity) with sample site and sample type, Bray-Curtis dissimilarities were calculated (Bray and Curtis 1957). Metrics were visualised with a Principal Coordinates Analysis (PCoA) plot and compared in a permutational analysis of variance (PERMANOVA) with 9,999 permutations. All data conformed to the underlying assumptions of PERMANOVA, with multivariate spread being equal among groups (similar to homogeneity of variances in an ANOVA) (Anderson 2017). Genera that showed significant differences in abundance between sample types and sample sites were determined using the DESeq2 package (Love et al. 2014) with Benjamini-Hochberg corrected p-values. Data visualisation and statistical tests were performed using the vegan (Oksanen et al. 2020), ggplot2 (Wickham 2016), and phyloseq (McMurdie and Holmes 2013) packages in R.

The full bioinformatics pipeline for each of the four taxonomic assignment methods was validated with the use of a positive control (ATCC microbial standard MSA-1002) (Fig. S2.01). The script, detailing system requirements and specific command line execution from raw reads to taxonomic assignment, is provided in the Electronic Supplementary Materials S2.02.

2.3 Results

2.3.1 Comparing reference databases: alpha diversity

The largest richness (number of identified genera) was found with Kraken2 in combination with the NCBI database (a total of 1,177 genera across all samples, of which 886 associated with *Ulva* samples), followed by SILVA (626 genera, of which 463 in *Ulva* samples), and Greengenes (367 genera, of which 289 in *Ulva* samples). EPI2ME in combination with NCBI found the lowest diversity (265 genera, of which 202 associated with *Ulva*). Based on the validation with the positive control, Kraken2+NCBI may have overestimated the diversity. The ATCC microbial standard MSA-1002 contains 18 genera and while 5 taxa that should have been identified were missing using Kraken2+NCBI, 10 additional taxa were assigned that are not part of the positive control (Fig. S2.01). Using EPI2ME+NCBI and Kraken2+Greengenes, 3 genera were missing, and, respectively 2 and 6 additional taxa were found (Fig. S2.01). Kraken2+SILVA is the only method that did not report any additional taxa,

but 2 genera (*Bifidobacterium* and *Schaalia*) were missing (Fig. S2.01). The genera *Bifidobacterium* and *Schaalia*, which should have been assigned in the positive control, were assigned a few reads each using all four different taxonomic assignment methods, but were removed from the dataset during the filtering of rare taxa.

2.3.2 Comparing reference databases: relative abundance

According to all databases included in this study, the highest average relative abundance of bacteria associated with *Ulva* samples (swab and tissue samples) belonged to the phyla Proteobacteria, Bacteroidota, and Deinococcota (Fig. S2.02). In general, Greengenes classified fewer reads to Actinobacteriota compared to SILVA and NCBI, and EPI2ME classified fewer Deinococcota and Firmicutes compared to Kraken2. Seawater and sediment samples contained mostly Proteobacteria and smaller fractions of Bacteroidota as well.

At order level, *Ulva* samples contained a relatively higher percentage of Chromatiales (mainly due to the presence of *Granulosicoccus*), Flavobacteriales, Saprospirales, and Thiotrichales compared to seawater and sediment samples (Fig. 2.03). Seawater and sediment on the contrary contained more Campylobacterales, Pseudomonadales, and Pelagibacterales. Aquaculture samples (YER) contained a very high relative abundance of Rhodobacterales compared to natural *Ulva* populations. The results based on the SILVA and NCBI databases are comparable. Greengenes classified fewer reads to Chromatiales in the *Ulva* samples and no reads to Pelagibacterales in seawater samples.

SILVA assigned 9.9% of all total reads to chloroplasts, and Greengenes 9.8%. The majority of the chloroplast reads (83%) was found in tissue samples and represented host contamination. A smaller percentage included microalgae. Using the NCBI database, not a single read was identified as chloroplast. Instead, 2.4–23.7% of the reads in tissue samples were classified as Cyanobacteria (Fig. S2.02). Both Kraken2 and EPI2ME therefore showed a relatively high abundance of Cyanobacteria (and specifically Oscillatoriales at order level; Fig. 2.03) in tissue samples when using the NCBI 16S database.

2.3.3 The *Ulva* microbiome and environmental microbiome

The following results describing the environmental and *Ulva* microbiome were based on taxonomic assignments with Kraken2+SILVA. A principal coordinates analysis (PCoA) based on Bray-Curtis distances showed a clear distinction in microbial community composition (genus level) between sediment samples, seawater samples, and *Ulva* samples (Fig. 2.04; $p < 0.01$ for all comparisons, PERMANOVA and Permutative Tukey). Whilst microbial community composition of the environmental samples (seawater and sediment) displayed high similarity within sample site ($p > 0.05$, Permutative Tukey), microbial communities associated with *Ulva* showed more variation, especially between sample sites. Post-hoc tests revealed that bacterial communities from *Ulva* sampled at NJD and JCH (both intertidal areas, but a rocky shore versus a sedimentary bay, respectively) were highly similar ($p > 0.05$, Permutative Tukey), but differed significantly from NJP (floating pontoons) and YER (aquaculture samples). Communities also differed between NJP and YER ($p < 0.01$, Permutative Tukey). In addition, the two *Ulva* species collected (*Ulva australis* and *U. lacinulata*) harboured marginally different microbial communities ($p = 0.03$, Permutative Tukey). Swab and tissue samples from the same individual were statistically similar ($p > 0.05$, Permutative Tukey, corrected for repeated measures).

DESeq2 identified 152 OTUs that differed in abundance between *Ulva* samples and sediment ($p < 0.01$, Benjamini-Hochberg corrected), of which 122 OTUs were more abundant in sediment and 30 more abundantly associated with *Ulva*. Between *Ulva* and seawater communities, 218 OTUs were differentially abundant

($p < 0.01$, Benjamini-Hochberg corrected). Of these, 144 OTUs were more abundant in seawater and 72 in *Ulva* samples. OTUs assigned to unidentified genera of the Clade Ia (Pelagibacterales), the SUP05 cluster (Pseudomonadales), and the OM43 clade (Burkholderiales) were most abundant in seawater, whereas *Woeseia*, *Sulfurovum*, and *Sulfurimonas* were characteristic for sediment communities (Fig. 2.05). *Granulosicoccus* was typically associated with *Ulva* communities. Other abundant components of the *Ulva* microbiome that were not found in environmental samples included *Truepera*, *Postechiella*, *Flavobacterium*, and *Algitalea*. The aquaculture samples contained especially high relative abundances *Sulfitobacter* (4.1–14.1%, compared to 1.3% in natural population samples) (Fig. 2.05). In addition, the cultivated *Ulva lacinulata* strain contained high relative abundances of *Roseobacter* (8.1–10.5%, compared to an average of 0.009% in non-cultivated *Ulva*) and *Methylotenera* (2.92–3.8%, compared to 0.01% in natural populations) (Fig. 2.04).

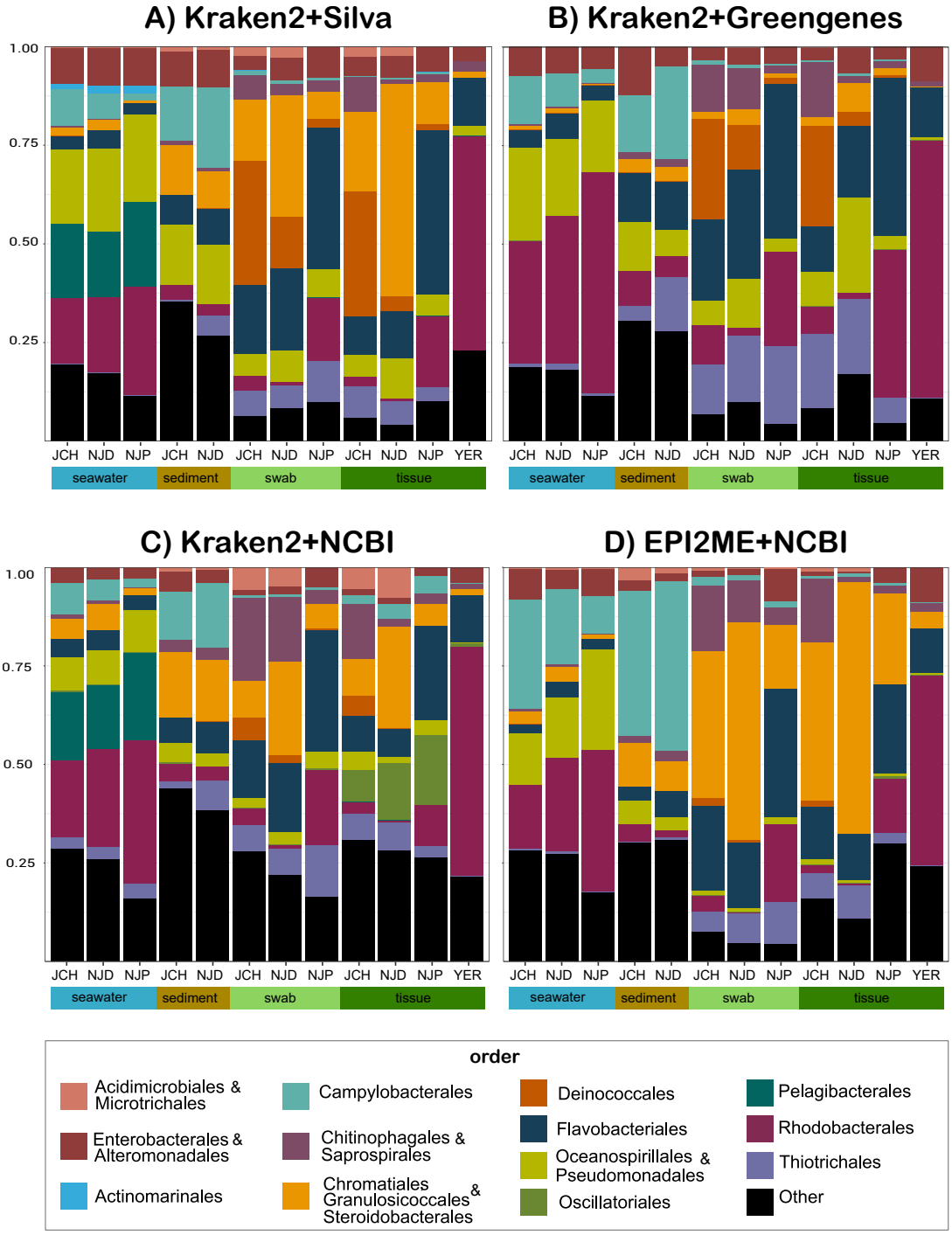

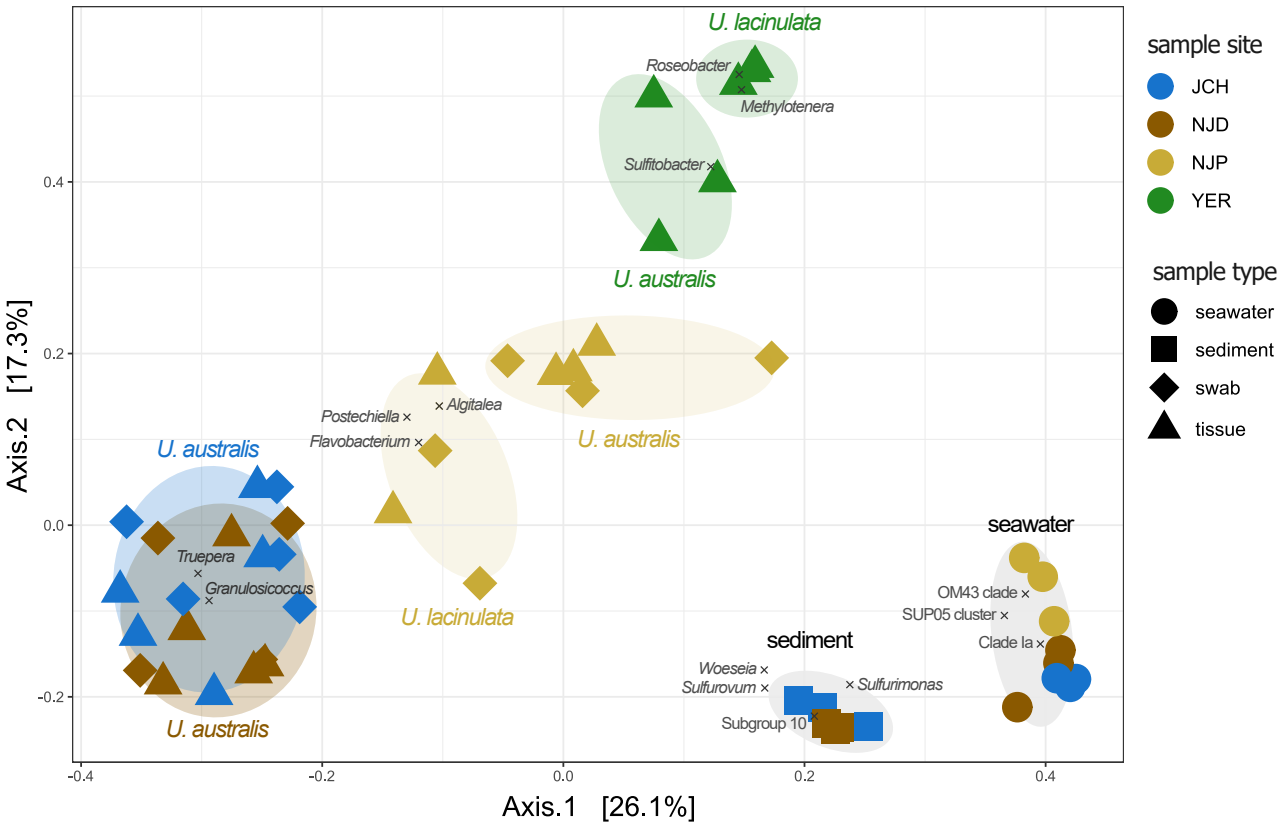

FIGURE 2.04 PCoA plot of the microbial communities (genus level, Bray-Curtis dissimilarities) associated with seawater, sediment, and *Ulva* samples (swab and tissue). Taxonomic assignment was based on KRAKEN2+SILVA. Symbols represent sample type and colours represent sample site. For *Ulva* samples, species identifications using the *tuf*A barcoding marker are labelled (samples belonging to the same *Ulva* species within one sample site are marked with oval shapes). The 15 most differentially abundant genera (identified with DESEQ2) have been projected a posteriori as weighted averages (labelled with a grey cross).

◀ **FIGURE 2.03 (left page)** A comparison of average relative abundance (order level) for each sample type (seawater, sediment, swab, tissue) and sample site (JCH, NJD, NJP, YER). Panel A) KRAKEN2+SILVA, B) KRAKEN2 +Greengenes, C) KRAKEN2+NCBI, and D) EPI2ME+NCBI. The 13 most abundant orders are shown in different colours, all other orders are grouped together (black bars). In this plot, we used the most recent phylum nomenclature as implemented in the SILVA database. As some genera are placed in different orders depending on the database, we have grouped several orders (e.g. Chromatiales, Granulosicoccales, and Steroidobacterales) for comparability and readability of this plot.

2.4 Discussion

2.4.1 Sequencing the seaweed microbiome with Oxford Nanopore Technologies

This study showed long-reads obtained with the MinION device are a promising and time-efficient tool to characterise the seaweed microbiome. The short time span from sample to sequences, coupled with the ability to perform all work in remote locations, allows for very flexible screening. However, the use of Nanopore's cloud-based EPI2ME service is currently not suitable for the analysis of seaweed microbes, as it allows no control over the removal of host-derived chloroplasts. In addition, analyses based on EPI2ME resulted in lower retrieved diversity compared to Kraken2. As Kraken2 in combination with the NCBI database resulted in an overestimation of the diversity, and the Greengenes database has not been updated since 2013, we obtained the best results using Kraken2 in combination with the SILVA database. We therefore recommend using Kraken2 with the SILVA database for seaweed-microbiome studies. In addition, as chloroplast contamination makes up a large proportion of reads in tissue samples, and we found no significant differences in microbial composition between swab and tissue samples, we recommend to use swabs in the future to characterise the seaweed microbiome. In other species, for example for siphonous green seaweeds, in which endophytic bacteria play an important role (e.g., *Bryopsis*; Hollants et al. 2011, 2013b), this is likely not possible. One solution is to design new primer combinations that minimize chloroplast contamination (Thomas et al. 2019); these primers, however, have as of yet only been developed for partial fragments of the 16S rRNA gene. For Nanopore sequencing, to circumvent the problem of host-contamination in those samples where using tissue is necessary, real-time selective sequencing may be a solution.

Adaptive sampling, recently developed by ONT and known as ReadUntil, allows users to enrich target strands of interest (e.g., specific endophytic bacteria) and selectively reject individuals strands that are of no interest (e.g., host chloroplasts) in real-time by mapping the reads to a reference dataset during the sequencing process (Payne et al. 2020). This way, every single pore in the MinION flow cell can eject the strand it is sequencing if it is identified as a molecule of no interest, and start sequencing a new strand instead. When a strand is rejected, the motor on the read is removed such that it will not attach to other pores anymore. ReadUntil works best with longer reads, as a MinION flow cell can sequence at 450 bp/s and it takes typically <1 second to reject a read. Rejecting long reads in an early stage is therefore more effective. A disadvantage of adaptive sequencing is the decreased overall yield per flow cell. The reduced yield can partly be attributed to the fact that pores are empty more often if they reject a high number of reads, but pores may also have a higher chance of getting blocked when ejecting reads. In addition, most adaptive sampling methods require basecalling and this in turns requires computational power. For the basecalling to keep up with the flow cell's sequencing real time, a computer with GPUs is necessary. However, UNCALLED has recently been published as an alternative mapper and, instead of basecalling, relies on matching nanopore current signals to reference sequences. UNCALLED can therefore be used on computers containing CPUs only (Kovaka et al. 2020). This is another example on how MinION sequencing may benefit seaweed microbial research in future studies.

2.4.2 Variability of the *Ulva* microbiome

Whilst the replicates from, respectively, sediment and seawater samples were highly similar, the *Ulva* microbiome showed considerably more variation. This high variation is in accordance with other *Ulva* microbial results based on different sequencing techniques, such as Roche pyrosequencing and Illumina technologies (Burke et al. 2011b, Roth-Schulze et al. 2018, Comba González et al. 2021).

Part of the microbial communities' variability in this study could be explained by differences between sample sites, which in turn are likely caused by environmental factors. Interestingly, the *Ulva* specimens collected at the two intertidal sites (NJD and JCH) harbour very similar microbial communities, whereas the artificial sites that are not influenced by tidal differences (site NJP; floating pontoons, and site YER; aquaculture facilities) are different. The intertidal zone is a stressful environment and may amongst others influence the biodiversity of the microbiome through higher competition at reduced levels of disturbance (Brodie et al. 2016). When sampling 38 sympatric macroalgal species along an intertidal transect, Lemay et al. (2020) found that samples collected from different tidal heights clustered consistently together for most species. In *Ulva,* however, there was a lack of consistency and samples from the low and mid tidal regions were not highly similar. Environmental effects caused by tidal actions may thus play a strong role in the variability and composition of the *Ulva* microbiome.

Within sampling sites, there also seems to be variation in the microbial composition associated with different *Ulva* species. The aquaculture facilities, for example, contained mixed cultures of *Ulva australis* and *Ulva lacinulata* (Fig. 2.04), which formed two separate clusters within the PCoA plot, and a similar pattern is observed in the cluster with samples collected at NJP. *Ulva* species are morphologically very similar. Differences in microbial communities caused by host phylogeny may therefore be related to heterogeneity in the thalli on a micro-scale or to differences in biochemical composition. Recent studies showed that microbial diversity and composition differ between anatomical regions in the thalli of *Laminaria* (Ihua et al. 2020, Lemay et al. 2021), *Taonia* (Paix et al. 2020), and *Fucus* (Lemay et al. 2021). In general, a 'maturation-gradient' was observed in these brown macroalgae, with the older regions supporting higher alpha diversity. Morphological complexity was found to play a major role in epibiotic diversity as well (Lemay et al. 2020). These brown macroalgae, however, show considerably more differentiation in thallus structure (holdfast, stipe, meristem, blade, etc.) than the typical *Ulva* thallus. In this study, all *Ulva* samples were collected from the margins of the blade. Future studies can show whether distinct microbial communities may be associated with different regions of the *Ulva* thalli as well, and how much microbial variation is typically contained within a single blade.

Whether host phylogeny or habitat matters more in determining microbial communities has been a much studied topic. Several studies (e.g., Lachnit et al. 2009, Nylund et al. 2010, Bondoso et al. 2014) showed microbial communities are predominantly influenced by host phylogeny, as the microbiome can be highly species-specific across different habitats, whereas coexisting different species of macroalgae clearly harbour distinct communities. However, these findings are likely scale-dependent and studies often investigated several evolutionary different algal species belonging to the Rhodophyta, Chlorophyta, and Phaeophyceae, which makes the differences between species more pronounced. Closely related host species often share more similar microbiomes (Lachnit et al. 2009). When comparing closely related species, such as the different *Ulva* species in this study, the high variability among individuals and the environmental influence may become more evident. In our study, between-site effects appear to be more important than between-species effects, as *U. lacinulata* collected at NJP is more similar to *U. australis* from NJP than to *U. lacinulata* collected at the aquaculture facilities, and *U. australis* collected at NJD and JCH form a separate cluster from *U. australis* collected at NJP and YER, despite the very short geographical distances between sample sites in this study.

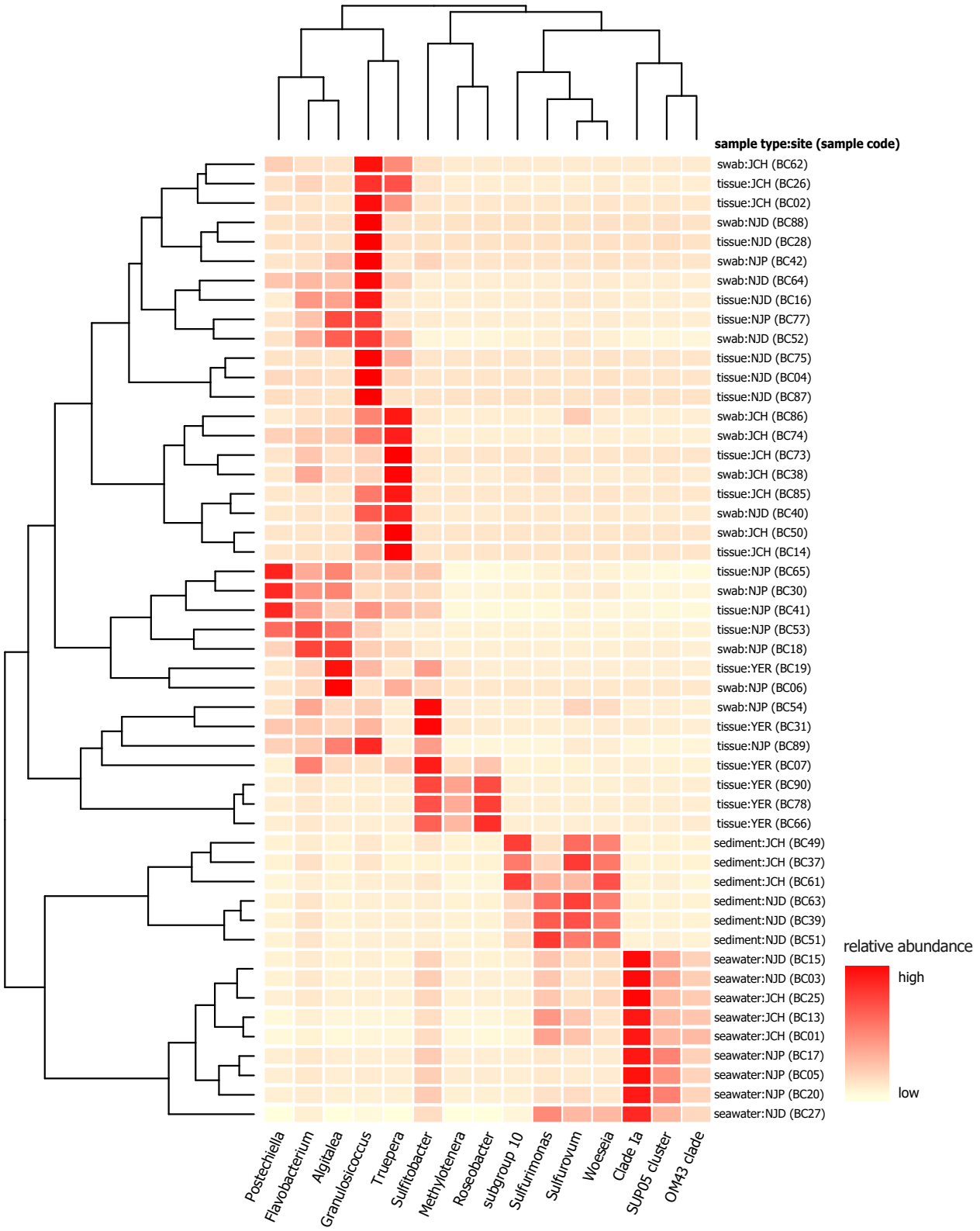

FIGURE 2.05 Heatmap of the 15 most differentially abundant genera identified by mapping 16S rRNA gene amplicons sequenced on a Nanopore MinION against the SILVA reference database. The clustering order of both samples (rows) and microbial taxa (columns) was based on Bray-Curtis distances.

2.4.3 Defining a core microbiome

Defining a core microbiome of a specific seaweed species has been the goal of many sequencing studies. For *Ulva*, it is generally thought that the taxonomic composition is too variable to describe a core community (Burke et al. 2011b, Roth-Schulze et al. 2018). Instead, a functional core of enriched genes can be identified (Burke et al. 2011a, Roth-Schulze et al. 2018). However, certain similarities in microbial taxa reported to be typically associated with *Ulva* can be identified across different studies, despite large spatial distances between sample sites. Roth-Schulze et al. (2018), for example, showed that the genus *Granulosicoccus*, as well as the families *Flavobacteriaceae* and *Rhodobacteraceae*, were highly abundant in both *Ulva australis*, *Ulva rigida* [possibly *U. lacinulata* following the latest taxonomical revisions by Hughey et al. (2021)], and *Ulva ohnoi* collected in Australia and Spain. In another study, Comba González et al. (2021) identified a high relative abundance of *Algitalea* (5%), *Granolusicoccus* (4.9%), *Aquimarina* (4.5), *Litorimonas* (4%), and *Truepera* (4%) associated with *Ulva lactuca* from the Colombian Caribbean. In addition, these taxa showed little temporal fluctuations in relative abundance during a two-year sampling campaign. The same taxa were found to be enriched in *Ulva* samples collected in the Netherlands during this study. Nevertheless, functional composition analyses are essential to reveal the effect of the associated bacteria on host performance. Nanopore's MinION has been used in several metagenomic studies, e.g., in characterising glacier microbiota (Edwards et al. 2016), pathogens in river water (Hamner et al. 2019), and the human gut microbiome (Maghini et al. 2021), indicating the potential use of the MinION for future seaweed metagenomic studies.

2.4.4 The microbiome of cultivated versus natural *Ulva*

The microbiome associated with cultivated *Ulva* is distinctly different from the microbiome associated with natural *Ulva* populations in our study. The *Ulva* microbiome has rarely been studied in aquacultural settings. An exception is a study located at an integrated fish and *Ulva* farm, in which the macroalgae receive lagoon water that has first entered the nutrient rich fish tanks (Ghaderiardakani et al. 2019). In the latter study, Ghaderiardakani et al. showed that the abundance of bacteria that are known to induce morphogenesis in *Ulva* (e.g., *Maribacter*, *Roseobacter*, *Roseovarius*, and *Sulfitobacter*) was enriched in the algae-tanks compared to control lagoon water and water from the tanks containing the fish. These findings support the hypothesis that *Ulva* 'garden' their own beneficial microbiota (Califano et al. 2020, Saha et al. 2020a), for example using surface metabolites and chemoattractants such as dimethylsulfoniopropionate (Kessler et al. 2018). As the bacteria are present in low abundance in the natural lagoon water, the lagoon would act as a reservoir for these growth-promoting bacteria and as such contribute to the large biomass production in the *Ulva* farm. Our results similarly showed that cultivated *Ulva* (which received sediment-filtered water from the Eastern Scheldt) were associated with increased levels of growth-promoting bacteria such as *Sulfitobacter* and *Roseobacter*, compared to natural *Ulva* populations (Fig. 2.05). The microbial-gardening hypothesis, however, does not explain why cultivated *Ulva* would 'garden' more growth-promoting bacteria than natural *Ulva* populations. An alternative hypothesis could be that cultivated *Ulva* samples have a higher abundance of growth-promoting bacteria simply because unhealthy *Ulva* cultures (lacking growth-promoting bacteria) are discarded or removed from the culture tanks.

2.5 Conclusions and perspective

In this study we showed that the MinION is a useful tool in bacterial screening of both cultivated and natural seaweed populations. From an aquaculture-perspective, it is interesting that the microbiome of cultivated *Ulva* is very different from naturally occurring *Ulva*. As it becomes more evident that the microbiome is of utmost importance for growth and functioning of seaweeds (van der Loos et al. 2019, Menaa et al. 2020), many questions are raised on how the presence or absence of certain components of the microbiome may affect growth, reproduction, resilience, and biochemical composition of cultivated *Ulva* and if these can be manipulated. Land-based, closed-system *Ulva* cultivation set-ups that use artificial seawater (instead of natural seawater that contains a reservoir of beneficial bacteria) may benefit from adding growth-promoting bacteria. 'Microbiome engineering' — the manipulation of the microbiome of cultivated crops by inoculating certain microbes — is increasingly gaining in popularity in land-based agriculture (Timmusk et al. 2017, Qiu et al. 2019b, Berg et al. 2021) and preformulated microbial-based fertilisers are even available (e.g., ExploGrow™). In-depth studies on the interactions between microbes and seaweeds may also result in the development of ecological 'biofertilisers' for seaweeds. The development of a rapid and cost-effective screening using MinION will most likely contribute to the implementation of microbial monitoring in *Ulva* cultivation.

Acknowledgements

We thank Lander Blommaert (NIOZ) for supplying the *Ulva* aquaculture samples and Reindert Nijland for his help with MinION-related questions. The research leading to the results presented in this publication was carried out with infrastructure funded by the FWO PhD Fellowship fundamental research (3F020119) and the EMBRC Belgium – FWO project GOH3817N.

Author contributions

L.M.L.: Conceptualization, Methodology, Software, Investigation, Writing – original draft, Visualisation. **S.D.:** Methodology, Investigation, Resources. **A.W.:** Conceptualization, Writing – review & editing, Supervision. **O.D.C.:** Conceptualization, Writing – review & editing, Supervision, Funding acquisition.

Data availability statement

Raw sequence reads and metadata are deposited at SRA (BioProject PRJNA742225). Supplementary data to this article can be found online at https://doi.org/10.1016/j.algal.2021.102456.

Notes

[1] Amplicon sequencing can be performed using both Illumina sequencing and Oxford Nanopore Technologies. These sequencing technologies differ significantly in the following key aspects: 1) sequencing read length, 2) raw read accuracy, 3) speed of results, and 4) costs. Nanopore sequencing easily accommodates full-length amplicon sequencing of the 16S rRNA gene (1,600 bp), while Illumina sequencing typically yields amplicons of up to ~300 bp, often targeting the V1–V2 region of the 16S rRNA gene. On the other hand, Illumina raw read accuracy boasts higher raw read accuracy at 99.9% compared to Nanopore's >97%. Sequencing read length and raw read accuracy in turn affect taxonomic resolution. Previous research showed that the taxonomic resolution of Nanopore-derived data is higher due to the larger read length, despite the lower accuracy (Johnson et al. 2019, Nygaard et al. 2020). Also note that Nanopore's raw read accuracy has currently (February 2024) increased to 99.5% since the publication of this chapter in 2021.

Furthermore, Nanopore sequencing is time-efficient and cost-efficient. Many research groups can afford their own MinION sequencing device with starter costs of 1,900 EUR (including all consumables necessary for the first sequencing run), whereas an Illumina MiSeq incurs a minimum cost ten times higher at 19,000 EUR. In-house sequencing with Nanopore eliminates the need to outsource DNA to companies, facilitating faster troubleshooting in the laboratory. Additionally, the calculated costs for 16S metabarcoding are less than 9 EUR per sample for Nanopore sequencing (including barcoding, library prep, and sequencing) compared to 39 EUR per sample for Illumina sequencing (including barcoding, library prep, and sequencing on a MiSeq), based on quotations from 2020.

[2] An extensive and well-curated reference database is essential for correct taxonomic identifications. However, many microorganisms found in marine environments are poorly characterised and remain undescribed. This raises the question: how do we cope with the unidentified majority? High-accuracy Illumina sequencing offers a solution by enabling analyses at the level of amplicon sequence variants (ASVs). Even when taxonomic assignments are not feasible, ASVs provide a means of differentiation. In contrast, ASVs are generally not utilised with Nanopore data due to the lower accuracy of the reads. Instead, analyses with consensus sequences serve as an alternative approach with Nanopore data. Various tools are available for generating consensus sequences, including Medaka (Oxford Nanopore Technologies Ltd. 2018) and Racon (Vaser et al. 2017), as well as pipelines such as Decona (Doorenspleet et al. 2021) and Amplicon_sorter (Vierstraete and Braeckman 2022).

Supplementary Figures

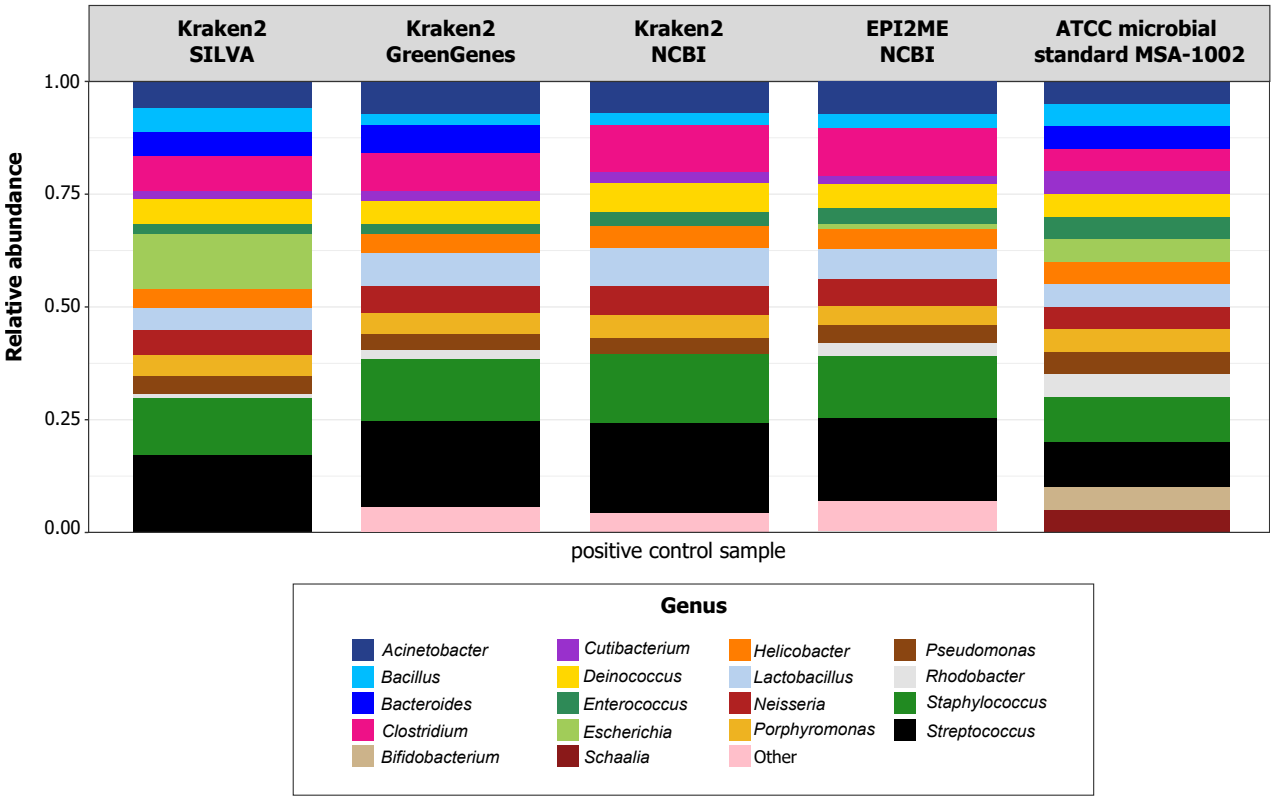

FIGURE S2.01 Relative abundance barplot of the positive control sample. Each column shows the relative abundance of the genera that were found using the four different taxonomic assignment methods (Kraken2+SILVA, Kraken2 +Greengenes, Kraken2+NCBI, and EPI2ME+NCBI.) with the bioinformatical pipeline used in this paper. The column on the far right shows the true composition of the ATCC microbial standard MSA-1002.

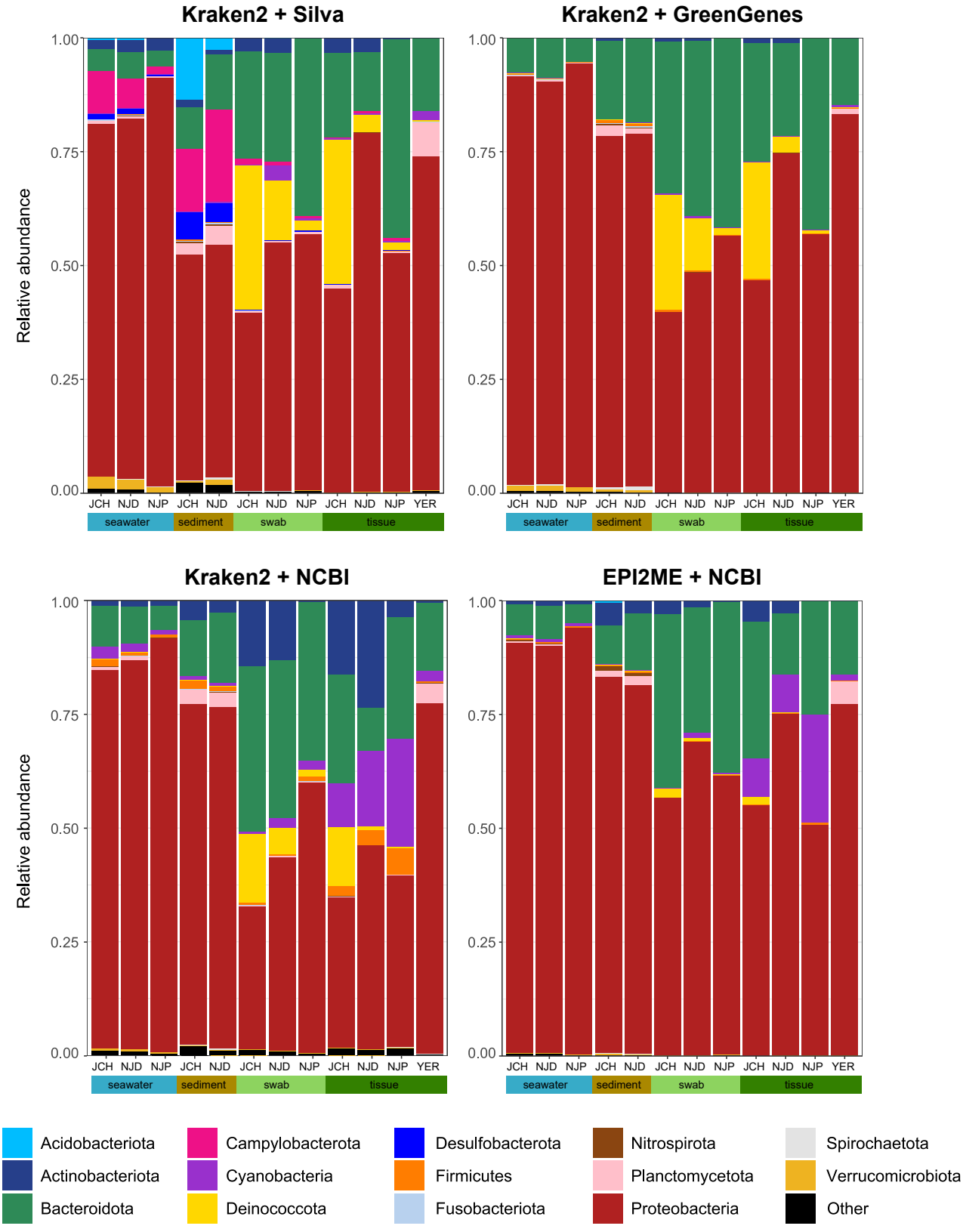

FIGURE S2.02 A comparison of average relative abundance (phylum level) for each sample type (seawater, sediment, swab, tissue) and sample site (JCH, NJD, NJP, YER). Separate plots are shown for the four different taxonomic assignment methods (KRAKEN2+SILVA, KRAKEN2+Greengenes, KRAKEN2+NCBI, and EPI2ME+NCBI). The 14 most abundant phyla are shown in different colours, all other phyla are grouped together (black bars).

"Er zijn geen bomen op de grote zee"

– Vasalis, in: Misthoorn in de herfst

Chapter 3.
The cultivated sea lettuce (*Ulva*) microbiome: Successional and seasonal dynamics

Luna M. van der Loos, Cynthia De Wilde, Anne Willems, Olivier De Clerck, Sophie Steinhagen

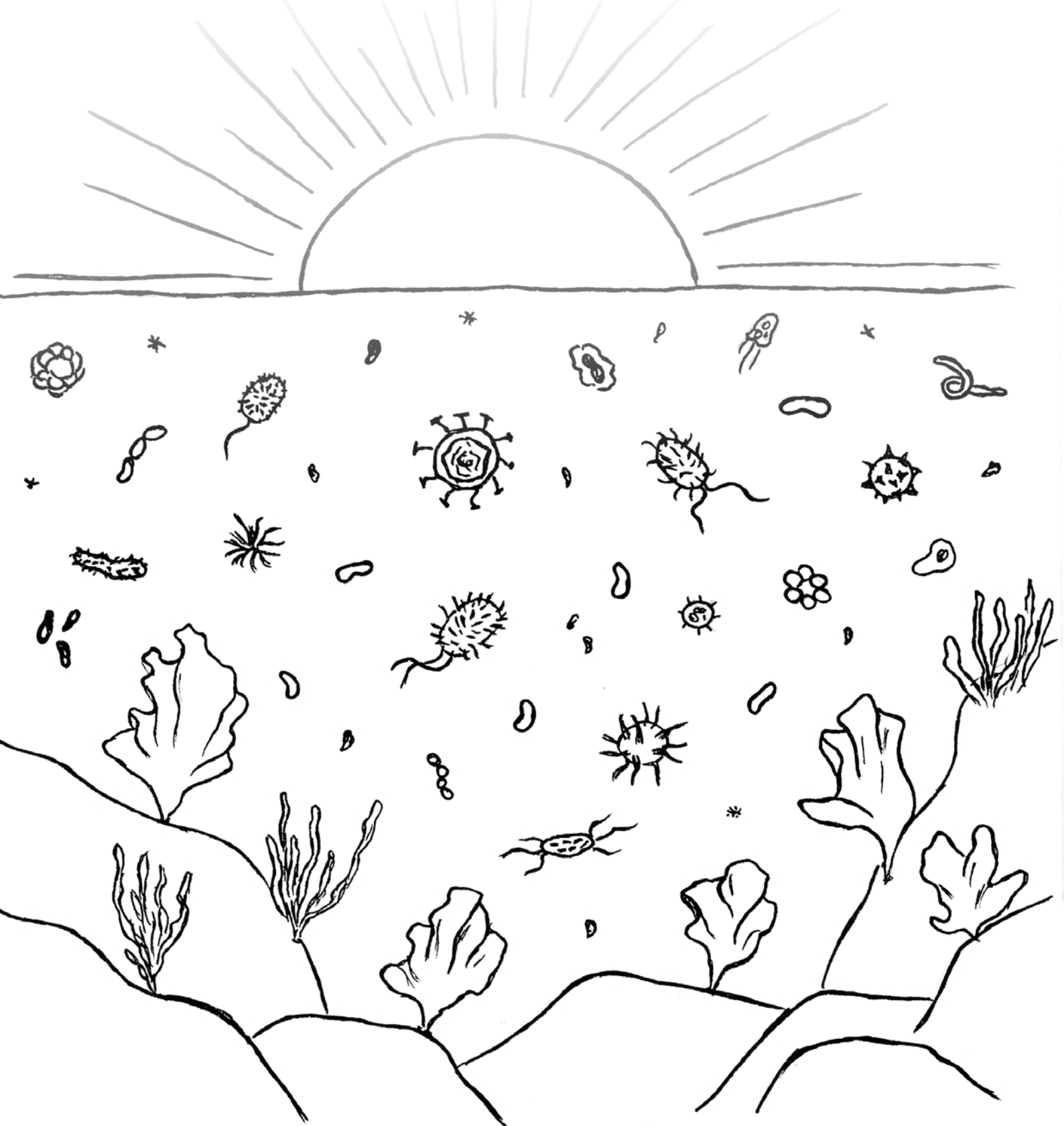

Chapter 3. The cultivated sea lettuce (*Ulva*) microbiome: Successional and seasonal dynamics

This chapter has been published as:
L.M. van der Loos[1,2], C. De Wilde[1], A. Willems[2], O. De Clerck[1] & S. Steinhagen[3]. The cultivated sea lettuce (*Ulva*) microbiome: Successional and seasonal dynamics. *Aquaculture* 585: 740692.

[1] Phycology Research Group, Department of Biology, Ghent University, Ghent, Belgium
[2] Laboratory of Microbiology, Department Biochemistry and Microbiology, Ghent University, Ghent, Belgium
[3] Department of Marine Sciences-Tjärnö, University of Gothenburg, SE-452 96 Strömstad, Sweden

Abstract

The seaweed production industry is rapidly expanding worldwide. The green seaweed *Ulva* is increasingly recognised as an excellent sustainable feedstock, due to its high growth rates, its wide tolerance to environmental conditions, and its potential in bioremediation and integrated multi-trophic aquaculture. Seaweed associated microbes could play an important role in the optimisation of the *Ulva*-crop-system, by increasing host growth, changing biochemical composition, and fending off pathogens that cause disease. In order to be successfully implemented, however, microbiota manipulation requires fundamental knowledge on the successional dynamics of the cultivated *Ulva* microbiome. In this study, we monitored the dynamics of *Ulva*-associated bacterial communities over a time-period of eleven months, from the nursery phase and outplanting in the field up to the harvest. We compared microbial dynamics in land-based tanks and an offshore seafarm, as well as natural populations of *Ulva fenestrata* and *Ulva linza*. Our results showed that *Ulva* hatchlings in the nursery phase harboured a distinct microbiome compared to outplanted *Ulva*. The hatchling communities were dominated by 1–3 genera, several of which have been identified as growth-promoting bacteria before (e.g., *Sulfitobacter*, *Algitalea*). In addition, we found that the nursery conditions played a larger role in the microbiome composition than host specificity, suggesting that the nursery environment is a crucial microbial source pool. The bacterial composition underwent a swift transformation following outplanting, differing significantly from the nursery samples within only seven days. Our results demonstrated that the bacterial communities in the nursery phase remain susceptible to newly introduced microbiota. Controlled nursery conditions could therefore provide the ideal opportunity for microbiota manipulation, but the acquired microbes might not endure the transition to open-water conditions.

3.1 Introduction

The seaweed aquaculture sector is currently experiencing a rapid and global expansion, with a global value amounting to 14.7 billion USD (US Dollar) (Cottier-Cook et al. 2022). Seaweed is increasingly viewed as an important and sustainable feedstock for a wide range of applications. Currently, Europe's increasing demand for macroalgae is met primarily through imports from Asia, predominantly sourced from China and Indonesia, which together produce 90% of the world's algae (Mendes et al. 2022, Zhang et al. 2022). At present, Europe's contribution to the global seaweed production stands at 0.8%. Out of this, approximately 96% of seaweeds are obtained by harvesting natural resources, while less than 4% of the European seaweed biomass is derived from cultivation (Zhang et al. 2022). However, the European Union (EU) has identified seaweed aquaculture as an important contribution to serve the future nutrition that can contribute to a green transition which has been reflected in the EU´s "Farm to Fork" and "Green Deal" strategies. In response to the sustainability objectives set by the United Nations (UN General Assembly, 2015), the European Union is addressing the urgent need for sustainable seaweed biomass through aquaculture that holds the potential to be transformed into nourishing food, renewable materials, and innovative biomolecules (Duarte et al. 2021).

Especially the green seaweed *Ulva* — widely known as sea lettuces or gut weeds — receives increasing attention by the aquaculture sector due to its compelling traits (Buchholz et al. 2012, Lawton et al. 2013, Bolton et al. 2016, Steinhagen et al. 2021b, 2022b, 2022a). The genus *Ulva* stands out because it possesses a combination of valuable characteristics, such as a ubiquitous distribution across different regions (Hayden et al. 2003, Tran et al. 2022, Steinhagen et al. 2023), a wide environmental acclimatisation potential, and resistance to changing abiotic factors (Steinhagen et al. 2019b, Cardoso et al. 2023). In addition, *Ulva* exhibits high growth rates (Lawton et al. 2013, Sebök et al. 2019, Stedt et al. 2022) and can thrive easily under high stocking

densities (Mata et al. 2010, Al-Hafedh et al. 2015). This makes *Ulva* an excellent sustainable future resource and many recent studies have focused on optimisation of its cultivation potential (Bolton et al. 2009, Carl et al. 2014, Califano et al. 2020, Lawton et al. 2021, Steinhagen et al. 2021b, 2022b, 2022a, Cardoso et al. 2023) and the sustainable exploitation of its high-value compounds (Reisky et al. 2019, Olsson et al. 2020b, Toth et al. 2020, Wahlström et al. 2020b, Trigo et al. 2021).

To support an industrially viable *Ulva* aquaculture industry, different methods for the large-scale cultivation of biomass are being developed. Cultivation of *Ulva* spp. in Europe has previously primarily taken place in coastal near-shore areas using on-shore tanks, and basin- or pond infrastructures (e.g., Hiraoka and Oka 2008, Buchholz et al. 2012, Lubsch and Timmermans 2018, Sebök et al. 2019, Califano et al. 2020). However, there is a growing focus on developing methodologies for large-scale offshore cultivation of European strains (Steinhagen et al. 2021b, 2022a, 2022b).

With the increasing demand for *Ulva* biomass, optimisation of the *Ulva*-crop-system is becoming of higher value. A key topic under discussion revolves around the role of *Ulva* as a holobiont, as the performance of *Ulva* is intricately linked to its synergistic and symbiotic microbiome (Wichard 2015, 2023, Alsufyani et al. 2020). *Ulva* depends on its associated bacteria for morphological development (Wichard 2015), but bacteria have also been shown to increase growth (Gemin et al. 2019, H. Wang et al. 2022), and have an effect on biochemical composition of the tissue (Polikovsky et al. 2020).

Plant growth-promoting microorganisms (PGPMs) — acting as biofertilisers, biostimulants, and biocontrol agents — have been shown to enhance crop production in terrestrial plants [e.g., in tomato (Guo et al. 2004), rice (Ashrafuzzaman et al. 2009), and cucumber (Kang et al. 2015)]. Similar to PGPMs in agriculture, seaweed beneficial microorganisms (SBMs) can promote seaweed growth or provide protection against diseases in an aquaculture setting (Li et al. 2023). Microbiota manipulation (i.e., altering the members or functions of a microbial community) in a commercial setting, however, is not always successful, likely due to prevention of colonisation of the new microbes by the existing microbial community (Ke et al. 2021, Wichard 2023). *Ulva*-associated bacterial communities have been studied in both natural ecosystems (Roth-Schulze et al. 2018, Comba González et al. 2021, van der Loos et al. 2022) and in aquaculture (Ghaderiardakani et al. 2019, Califano et al. 2020, van der Loos et al. 2021). Little is known, however, about seasonal and successional patterns in microbial communities associated with aging *Ulva* tissue, especially within a cultivation setting.

Understanding *Ulva*-microbial dynamics is key to successful microbiota manipulation and microbe leveraging in aquaculture. In this study, we compare 1) *Ulva fenestrata* growth, fertility, and the associated bacterial composition over time in a land-based system under different nutrient conditions, and 2) seasonal fluctuations in the bacterial community of an *Ulva fenestrata* natural population, and cultivated *U. fenestrata* and *U. linza* in an offshore seafarm.

3.2 Materials and methods

3.2.1 Experimental design land-based system: nutrient experiment

To assess the effect of nutrients on *Ulva* growth, fertility, and bacterial communities, *Ulva fenestrata* was cultivated in a land-based flow-through system situated within a greenhouse at the Tjärnö Marine Laboratory, University of Gothenburg, Sweden (58°52′36.4″ N, 11°6′42.84″ E). The aquaculture set-up consisted of nine 45 L tanks that continuously received 45 µm filtered natural seawater pumped from 45 m depth with a salinity of 33 PSU using a flow-through system (10–14 L h^{-1}). The tanks were exposed to three different nutrient condi-

tions: 1) filtered seawater from the nearby Kosterfjord (control; SW), 2) seawater enriched with 1x Provasoli´s Enriched Seawater (1x PES) (Provasoli 1968) (see Supplementary Materials & Methods S3.01 for details regarding the composition of the medium), and 3) seawater enriched with 3x elevated PES (3x PES). Each nutrient treatment was replicated in three tanks. The PES medium was added twice a week to the respective treatment tanks by pausing the flow-through system for 60 minutes in all tanks. Permanent water motion was provided by aeration.

Ulva fenestrata was cultivated in the land-based system for a duration of 32 weeks (8 April–17 November 2020), simulating a standard cultivation period (Steinhagen et al. 2021b, 2022a). A week before the start of the experiment, the seaweeds were acclimated to the culture conditions in the greenhouse by adding 140 g *Ulva* tissue to every tank. At the start of the experiment, the biomass in each tank was standardized to 250 g. Throughout the experiment, the biomass was consistently cut down to 250 g at the start of every week to exclude any density-dependent effects. The replicate in tank 8 (3x PES) was stopped earlier, after week 20, due to extreme fouling of diatoms.

Each week, the *Ulva fenestrata* wet weight biomass and the percentage of fertile tissue were measured following a standardized protocol. The seaweed biomass was taken from the tanks, excess water was removed with a salad spinner (spinning 20x), and the wet weight biomass was subsequently determined by a lab scale. Fertility was assessed by taking photos of five randomly selected individuals which were then analysed for fertile thallus tissue in ImageJ (Schneider et al. 2012) following the protocol described by Steinhagen et al. (2021b, 2022a). In addition, a swab sample and tissue sample (1–2 cm^2) were taken for microbial analyses and stored at –80 °C. In total, 99 measurements and samples were processed in both the SW treatment and the PES treatment (3 replicates per week, plus 3 acclimation samples), and 87 measurements and samples were processed in the 3x PES treatment (3 replicates per week in week 1–20, 2 replicates per week in week 21–32, plus 3 acclimation samples) (Electronic Supplementary Table S3.01; Fig. 3.01).

3.2.2 Sample collection offshore seafarm and natural populations

To assess the seasonal and species-specific host effect on the microbiome alteration of two economically and ecologically relevant Northern Hemisphere *Ulva* species, both natural populations and offshore cultivated biomass of *U. fenestrata* and *U. linza* were investigated.

Mature gametophytic material of *U. fenestrata* and *U. linza* was taken from long-term cultivation stocks located at the Tjärnö Marine Laboratory, University of Gothenburg, Sweden (58°52′36.4″ N, 11°6′42.84″ E). Fertility was induced by mincing the material and removal of sporulation and swarming inhibitors following the protocol described by Steinhagen et al. (2021b). Subsequently, the density of swarmers was calculated with the help of a hemocytometer and gamete solutions of both *U. fenestrata* and *U. linza* were diluted to 10,000 gametes mL^{-1} respectively before being further used. The collection, concentration, and application of immobilized gametes on PVC seedling spools that were coiled with nylon cord (ø = 1–2 mm) followed the process described in detail by Steinhagen et al. (2021b). The inoculated spools were submersed in 14 L aquaria supplied with sterile filtered (0.2 µm + UV, 9 L h^{-1}) seawater at an average irradiance of 90–110 µmol m^{-2} s^{-1} under a 12:12 h L:D light regime (light source: OSRAM Lumilux Cool daylight L 58W/865). The settled gametes were allowed to grow in the seedling nursery for six weeks between August to October 2021 in a temperature-controlled room (10 °C). Water changes and growth medium addition of Provasoli Enriched Seawater (PES) were conducted once per week following the concentration specifications of Provasoli (1968). To minimize potential diatom growth, 1 mg L^{-1} GeO_2 was added to the aquaria. After a six-week seedling nursery period, the juvenile thalli were deployed in

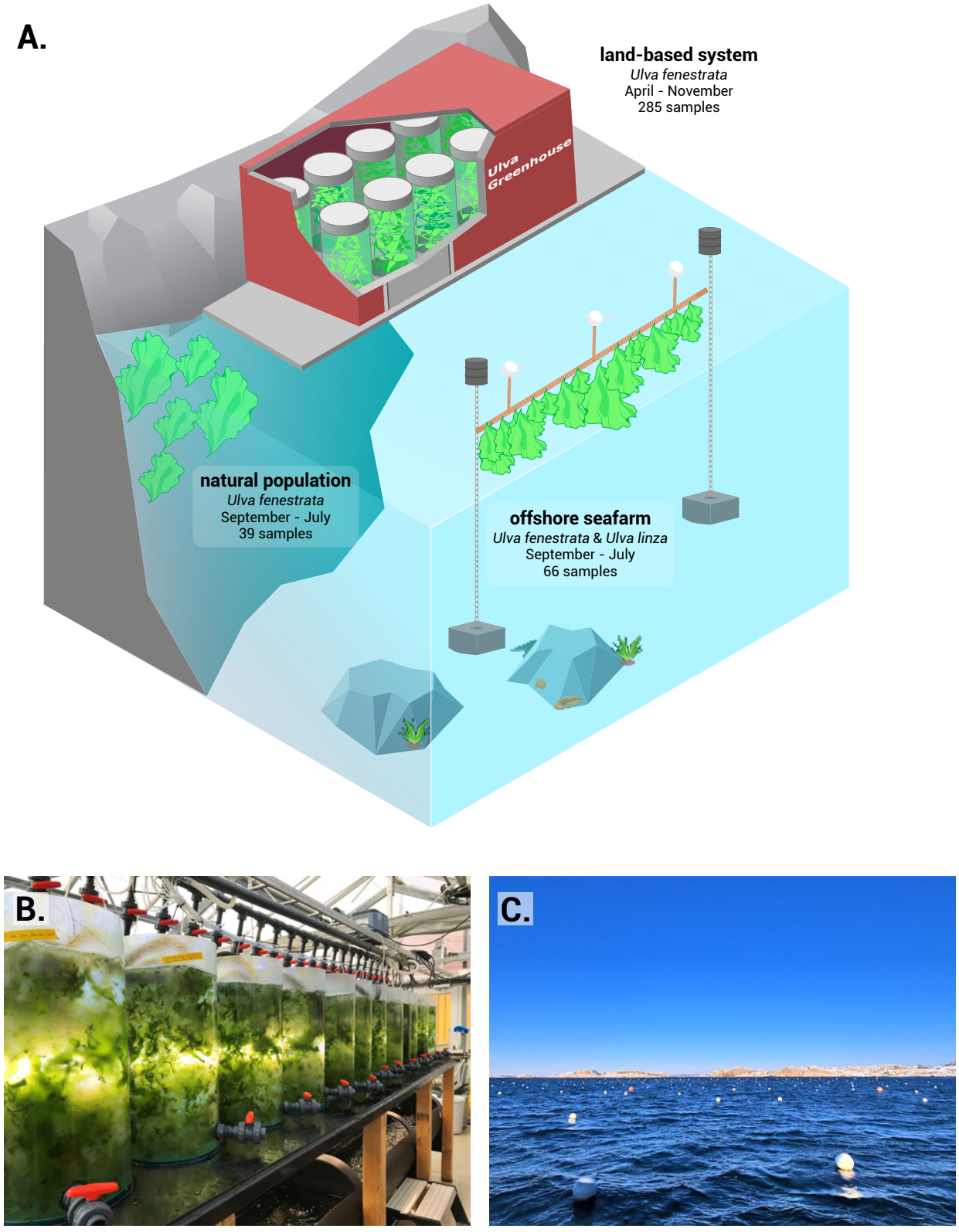

FIGURE 3.01 A) Experimental overview (showing the number of samples collected within the land-based system, natural populations, and the offshore seafarm), B) Land-based cultivation set-up at the Tjärnö Marine Laboratory (Sweden), C) Offshore seafarm in the Koster archipelago (Sweden).

an offshore seafarm (2 ha á 100 × 200 m) located in the Koster archipelago (Skagerrak), Sweden (58°51′54.6″ N, 11°4′5.32″ E) (for details on the seafarm infrastructure see Steinhagen et al. 2021b). The nylon cords maintaining the juvenile thalli of *U. fenestrata* and *U. linza* were transferred to the offshore infrastructure on 21 September 2021 and 18 October 2021, respectively. Cultivation of *U. fenestrata* took place from September 2021 to July 2022, whereas *U. linza* was cultivated from October 2021 to March 2022.

Microbial swab samples (n = 3) were taken before the transplant of the seedlings to the seafarm, one week after the seedlings transplant, and then subsequently every month (see Electronic Supplementary Table S3.02 for exact sampling dates). For collection of microbiome swab samples, sterilised disposable gloves and sterilised equipment were used throughout the sampling procedure to minimize contamination. Before microbiome collection, each individual was rinsed with ~30–50 ml sterile water to remove dirt, subsequently a cotton swab sample for microbiome analyses was generated by rubbing for 30 s on the thallus tissue. The samples were stored on ice until being transferred to −80 °C in the laboratory. A total of 36 samples were collected for *U. fenestrata* and 30 samples for *U. linza*. In addition to the microbial samples from cultivated *U. fenestrata*, the microbiomes of natural populations of *U. fenestrata* within a vicinity of < 5 km of the seafarm were monthly investigated as well (a total of 39 samples) (see Electronic Supplementary Table S3.02; Fig. 3.01).

3.2.3 Molecular characterisation and bioinformatics

The bacterial communities were characterised following the methods in van der Loos et al. (2021, 2022). Total microbial DNA was extracted using the QIAamp DNA mini kit (Qiagen) following the manufacturer's protocol. A bead beating step was included before lysis using zirconium oxide beads (RETCH Mixer mill MM400) for 5 minutes at 30 Hz. The full-length 16S rRNA gene was amplified using the primers 27F_BCtail-FW (TTTCTG TTGGTGCTGATATTGC_AGAGTTTGATCMTGGCTCAG) and 1492R_BCtail-RV (ACTTGCCTGTCGCTCTATCTTC_CGGTTACCTTGTTACGACTT), each containing a 5' extension enabling barcoding in subsequent PCR steps. 16S rDNA PCRs were performed using the Phire Tissue direct PCR Master Mix (Thermo Fisher) and amplicons for each sample were barcoded using the Oxford Nanopore PCR Barcoding Expansion Pack 1–96 (EXP-PBC096). The final libraries were prepared with the ligation-based sequencing kit SQK-LSK109 according to the manufacturer's protocol (Oxford Nanopore Technologies). The libraries were subsequently sequenced on a MinION (with R9.4.1 flow cells, Oxford Nanopore Technologies) for 72 h each.

The land-based nutrient experiment included 285 samples, as well as ten negative extraction samples, four negative PCR controls, and four positive controls (ATCC microbial standard MSA-1002). The seasonality effects study included 105 samples, as well as two negative PCR controls, and two positive controls (ATCC microbial standard MSA-1002). In addition, one randomly chosen sample (sample #148 for the land-based study and sample #60 for the seasonality study) was included in every sequencing run to verify comparability. See Electronic Supplementary Table S3.01 for an overview of all the samples included in the land-based nutrient experiment, and Electronic Supplementary Table S3.02 for an overview of samples included in the seasonality study.

The resulting raw FAST5 reads were basecalled and demultiplexed with Guppy (version 5.0.7, sup model, Oxford Nanopore Technologies). Data quality and length were visually inspected with NanoPlot (De Coster et al. 2018). Subsequently, high-quality reads were obtained using chimaera removal with Yacrd (Marijon et al. 2020), and by filtering the data set on quality (Q-score >8) and length (1,000–2,000 bp) with NanoFilt (De

Coster et al. 2018). The resulting 31,468,650 (land-based nutrient experiment) and 13,995,801 (seasonality study) high-quality reads were used to assign taxonomy at the genus level with Kraken2 in combination with the SILVA 16S database (138.1 release) (Quast et al. 2013, Lu and Salzberg 2020).

After taxonomic assignment, all chloroplast reads (7% of the high-quality reads) were removed from the data set. In addition, rare taxa were discarded (optimal settings were based on the positive controls and retained operational taxonomic units [OTUs] that were found more than 70 times in at least 20% of the samples) to protect against OTUs with small mean and trivially large coefficients of variation. Finally, DESeq2 was used to account for sequencing depth with a variance stabilising transformation (Love et al. 2014). The sequences are archived at SRA (BioProject PRJNA994710).

3.2.4 Statistical analyses

The effect of nutrients and time on *Ulva* growth and fertility was tested using a linear mixed-effects model with the R packages lme4 (Bates et al. 2015) and lmerTest (Kuznetsova et al., 2017). Differences in bacterial alpha diversity (calculated as the observed genus richness) with succession through time and nutrients were assessed using a generalised linear mixed model based on a negative binomial family (in which random variation between the individual tanks was included as random effect to account for repeated measures) (Bates et al. 2015). Bacterial community composition was visualised with an Non-metric Multidimensional Scaling (NMDS) ordination and Bray-Curtis dissimilarities (Bray and Curtis 1957). A permutational analysis of variance (PERMANOVA) with 9,999 permutations was used with the R-package vegan to test the effect of nutrients and succession through time on bacterial communities (Anderson 2017, Oksanen et al. 2020). Pairwise differences were calculated with the R-package pairwiseAdonis (Martinez Arbizu 2020). The percentage of variation in the abundance of bacterial genera explained by the measured variables was calculated with the R-packages variancePartition (Hoffman and Schadt 2016) and Dream (Hoffman and Roussos 2021). In the land-based aquaculture dataset, a linear mixed-effects model was used (in which random variation between the individual tanks was included as random effect to account for repeated measures). In the seasonality study, a linear model was used. All statistical tests were performed in R (R Core Team 2020) and data were visualised using the ggplot2 (Wickham 2016), metacoder (Foster et al. 2017), and phyloseq (McMurdie and Holmes 2013) packages.

3.3 Results

3.3.1 *Ulva fenestrata* growth and fertility in land-based nutrient experiment

Ulva biomass gradually decreased throughout the experiment (F-value = 63.4, p-value < 0.0001, Linear mixed-effects model) from on average 27.8% in week 1 to –15.7% in week 32 across all tanks (Fig. 3.02A, Fig. S3.01). The percentage of fertile thalli showed a quadratic curve: it increased from week 1 to week 16, and decreased from week 16 to week 32 after spore release (F-value = 1.1, p = 0.30, Linear mixed-effects model with quadratic term) (Fig. 3.02B). The nutrient treatment did not affect growth (F-value = 0.2 , p = 0.82, Linear mixed-effects model) (Fig. 3.02A, Fig. S3.01), but the percentage of fertile tissue was higher in the PES and 3x PES treatments compared to the SW treatment (3x PES > PES > SW, F-value = 3.04, p = 0.049, Linear mixed-effects model with quadratic term) (Fig. 3.02B; Fig. S3.02).

44

3.3.2 Changes in *Ulva*-associated bacterial communities over time

Ulva-associated bacterial community composition in the land-based aquaculture experiment was not affected by nutrient treatment (pseudo-F = 1.85, p = 0.99, PERMANOVA), but was significantly different over time (pseudo-F = 31.69, p = 0.0001, PERMANOVA; Fig. 3.02C, Fig. S3.03). All pairwise contrasts between weeks 0–8 versus week 8–16 versus week 16–24 and versus week 24–32 were significant ($p < 0.001$ for all comparisons, pairwise Adonis test) (Fig. 3.03). However, the changes in bacterial community composition were more pronounced during the first 16 weeks (Fig. 3.03). Both succession over time and random differences between the individual tanks explained a considerable part of the variation in the abundance of bacterial genera, while the effect of nutrients was negligible (Fig. 3.04A). Succession over time explained on average 16% (ranging from 0.002%–80%) of the variation in abundance of the individual bacterial genera (Fig. 3.04A). Random variation between tanks explained on average 10% of the variation in bacterial abundance (ranging from 0–41%) (Fig. 3.04A). On the contrary, nutrient treatments explained on average only 0.01% in bacterial abundance (ranging from 0–2%).

During the initial weeks of *Ulva fenestrata* growth in the land-based nutrient experiment, the following eight bacterial families were most abundant: the *Phormidesmiaceae*, *Microtrichaceae*, *Micavibrionaceae*, *Sphingomonadaceae*, *Hyphomonadaceae*, *Colwelliaceae*, *Nitrincolaceae*, and *Saccharospirillaceae*. On the contrary, the families *Pirellula*ceae, *Bdellovibrionaceae*, *Bacteriovoracaceae*, *Rhizobiaceae*, *Trueperaceae*, *Rubritaleaceae*, and the order Synechococcales were more abundant after the first eight weeks of the experiment.

The *Granulosicoccaceae* were most abundant during week 8–16, and the *Arenicellaceae* were mostly absent during week 16–24. More specifically, *Fuerstiella* (69% of the variation in abundance explained by time), an uncultured *Microtrichaceae* (46% of the variation explained), and *Silicimonas* (27% of the variation explained) were most abundant at the start of the experiment, but decreased in abundance after the first 8 weeks (Fig. 3.05). *Mesorhizobium* (29% of the variation in abundance explained by time) was abundant at the start of the experiment, decreased during week 5–10, and peaked again around week 25 (Fig. 3.05). *Sulfitobacter* (22% of the variation in abundance explained by time) was highly abundant throughout the experiment, but most abundant during week 5. *Pseudahrensia* (63% of the variation in abundance explained by time), *Rubidimonas* (34% variation explained), *Truepera* (35% variation explained), and an uncultured *Rhizobiaceae* (61% variation explained) were virtually absent during the initial 12 weeks and became more abundant towards the end of the experiment (Fig. 3.05).

NMDS plots likewise showed a fluctuation with seasons of *Ulva*-associated bacterial communities in the natural population and offshore seafarms (Fig. 3.06). Bacterial communities differed with time (in months) in the natural population of *U. fenestrata* (pseudo-F = 4.6, p = 0.001; PERMANOVA), the *U. fenestrata* offshore seafarm (pseudo-F = 2.3, p = 0.02; PERMANOVA), and the *U. linza* offshore seafarm (pseudo-F = 5.1, $p < 0.0001$; PERMANOVA). Seasonal fluctuation explained between 20–84% of the variation in abundance of the bacterial genera in the natural population, between 28–95% in the *U. fenestrata* offshore seafarm, and between 19–76% in the *U. linza* offshore seafarm. For example, an uncultured *Saprospiraceae* was abundant throughout the year in the natural population, but in both the offshore seafarms only abundant in October–January. During February–May, *Granulosicoccus* abundance peaked in the *U. fenestrata* natural population and seafarm, whereas an uncultured *Rhodobacteraceae* was mainly abundant in June–July. The OM27 clade was present in relatively low abundances, but completely absent from Jan–April. In general, the families *Micavibrionaceae* and *Phormidesmiaceae* were mainly present from Sep–Nov and peaked again during June–July. The *Rhodobacteraceae* were highly abundant throughout the year, with a peak throughout Oct–Dec and in June–July. The *Granulosicocceae* were especially abundant in March–May and the *Flavobacteriaceae* during Dec–May.

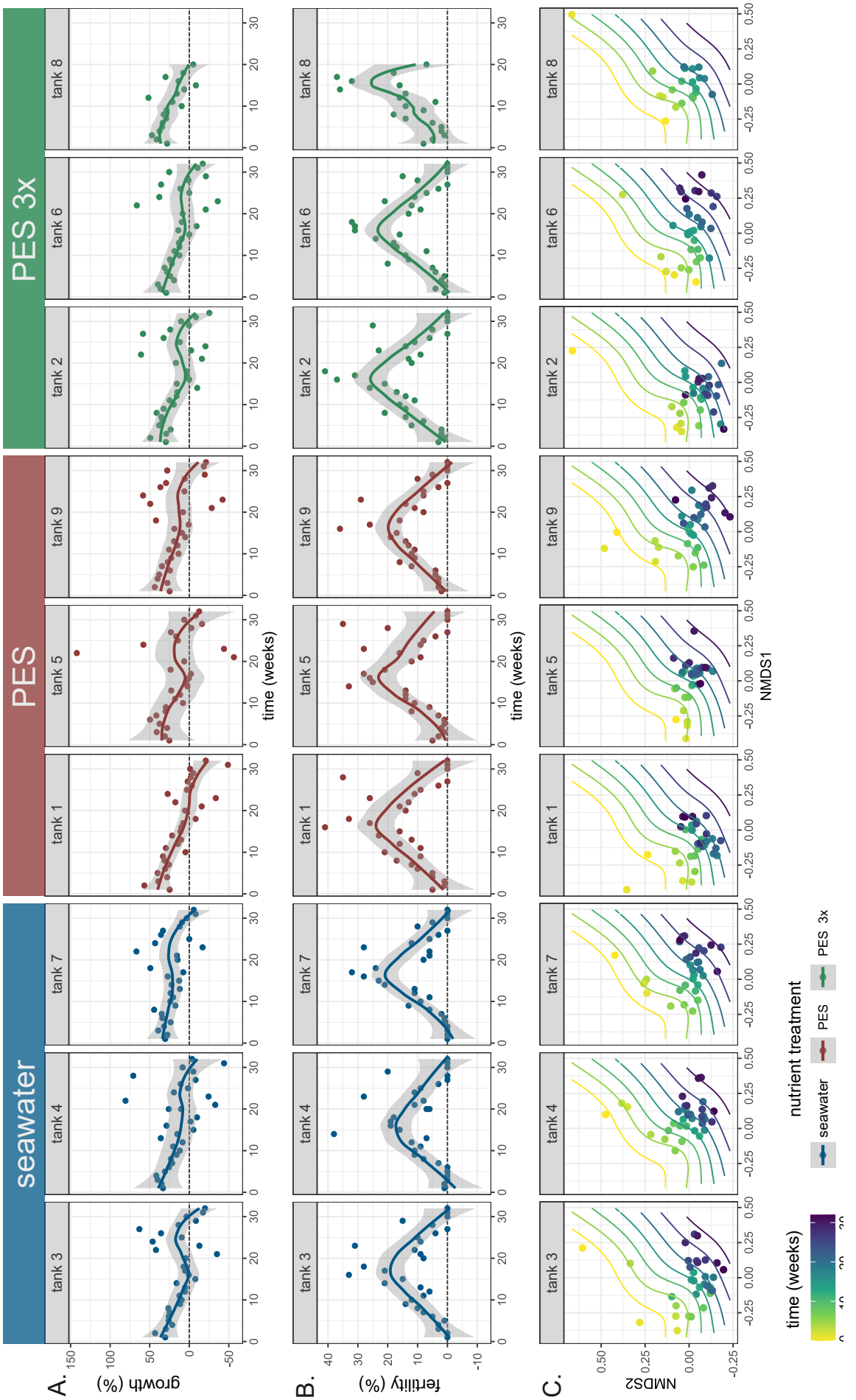
seawater
PES
PES 3x
tank 3
tank 4
tank 7
tank 1
tank 5
tank 9
tank 2
tank 6
tank 8
A.
growth (%)
B.
fertility (%)
C.
NMDS2
NMDS1
time (weeks)
nutrient treatment
seawater
PES
PES 3x
time (weeks)

◀ **FIGURE 3.02 (left page)** *Ulva fenestrata* growth (%, panel A), fertility (%, panel B) and bacterial community composition (NMDS ordination, panel C) in a land-based aquaculture set-up (which consisted of nine experimental tanks) throughout a period of 32 weeks. Colour indicates nutrient treatment in the growth and fertility plots (blue = SW, red = 1x PES, green = 3x PES). Colour indicates time in weeks in the NMDS plots. Curves in panel A and B were fitted with Local Polynomial Regression Fitting (LOESS) using the R package GGPLOT2. Shaded areas represent the 0.95 confidence interval.

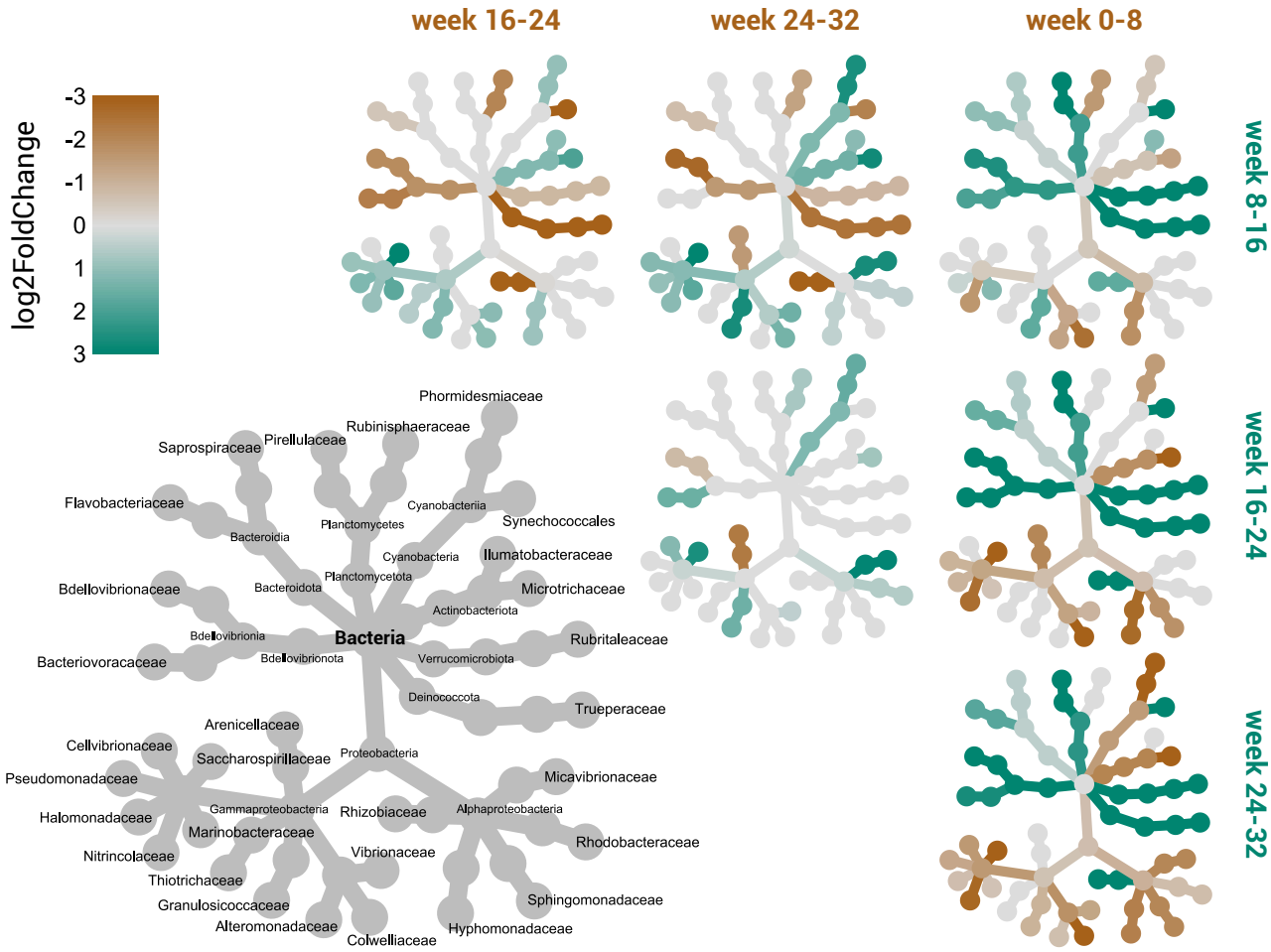

FIGURE 3.03 Pairwise comparisons of phylogenetic heat trees depicting the bacterial families associated with Ulva fenestrata in a land-based aquaculture set-up (which consisted of nine experimental tanks) throughout a period of 32 weeks. The larger, grey tree on the lower left functions as a taxonomic key for the smaller unlabelled trees. The smaller trees provide contrasts between the cultivation weeks (week 0–8 versus week 8–16 versus week 16–24 versus week 24–32). The colour (brown to green) of the nodes and edges corresponds to the log2FoldChange (only significant differences are coloured, $p < 0.05$, Benjamini–Hochberg corrected). Taxa coloured brown were enriched in the cultivation period in columns, whereas taxa coloured green were enriched in the cultivation period in rows. For example, the *Phormidesmiaceae*, *Microtrichaceae*, and *Colwelliaceae* were enriched in the first 8 weeks (brown) compared to the rest of the experimental period (green).

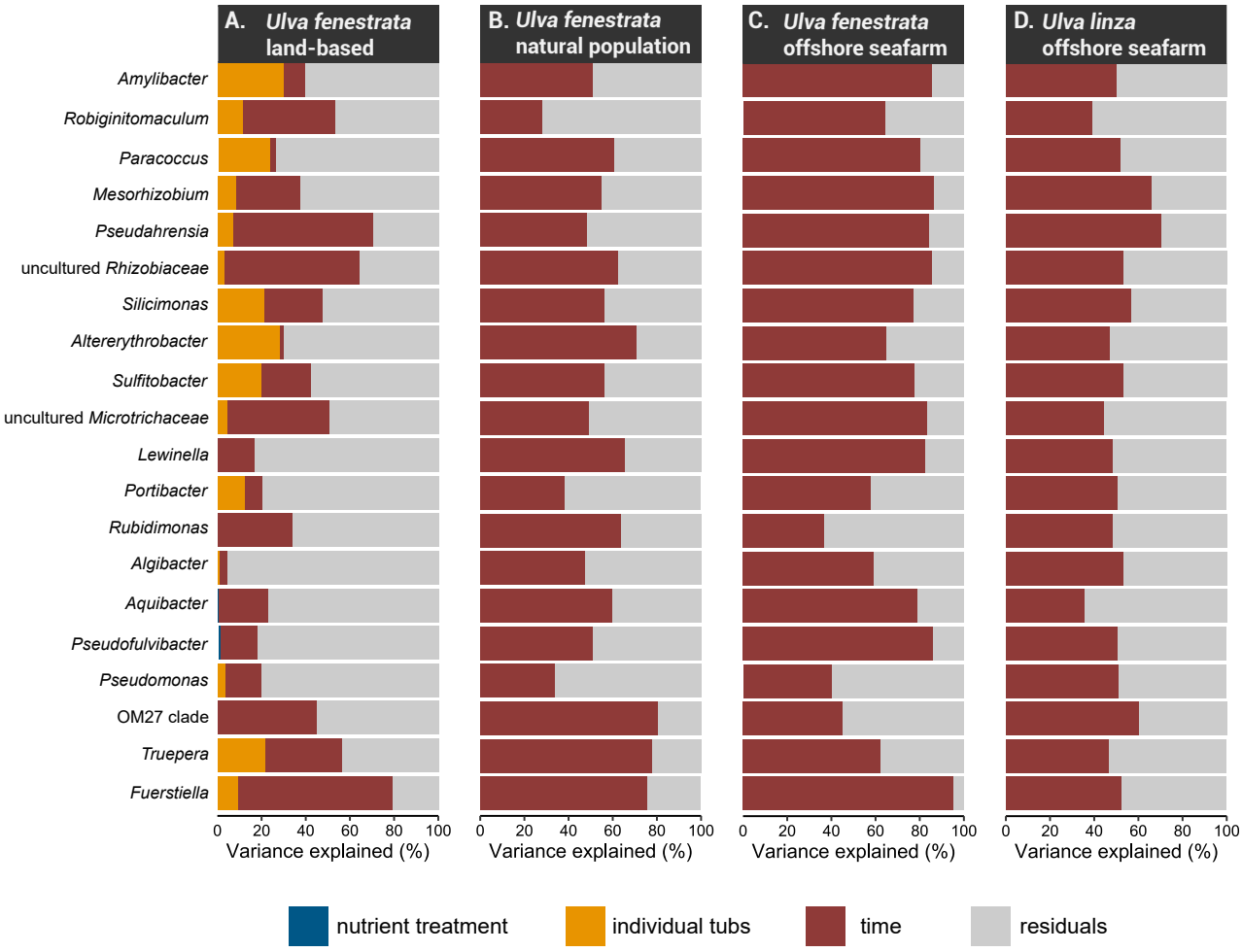

FIGURE 3.04 Variance partitioning plots, showing the amount of variance in abundance of *Ulva*-associated bacterial genera explained (%) by time, nutrients (land-based aquaculture only), and the variation between the individual culture tanks (land-based aquaculture only). A) *Ulva fenestrata* land-based aquaculture facilities; B) *Ulva fenestrata* offshore seafarm; C) *Ulva fenestrata* natural population; and D) *Ulva linza* offshore seafarm. Only the 20 genera explaining most of the variation are shown here.

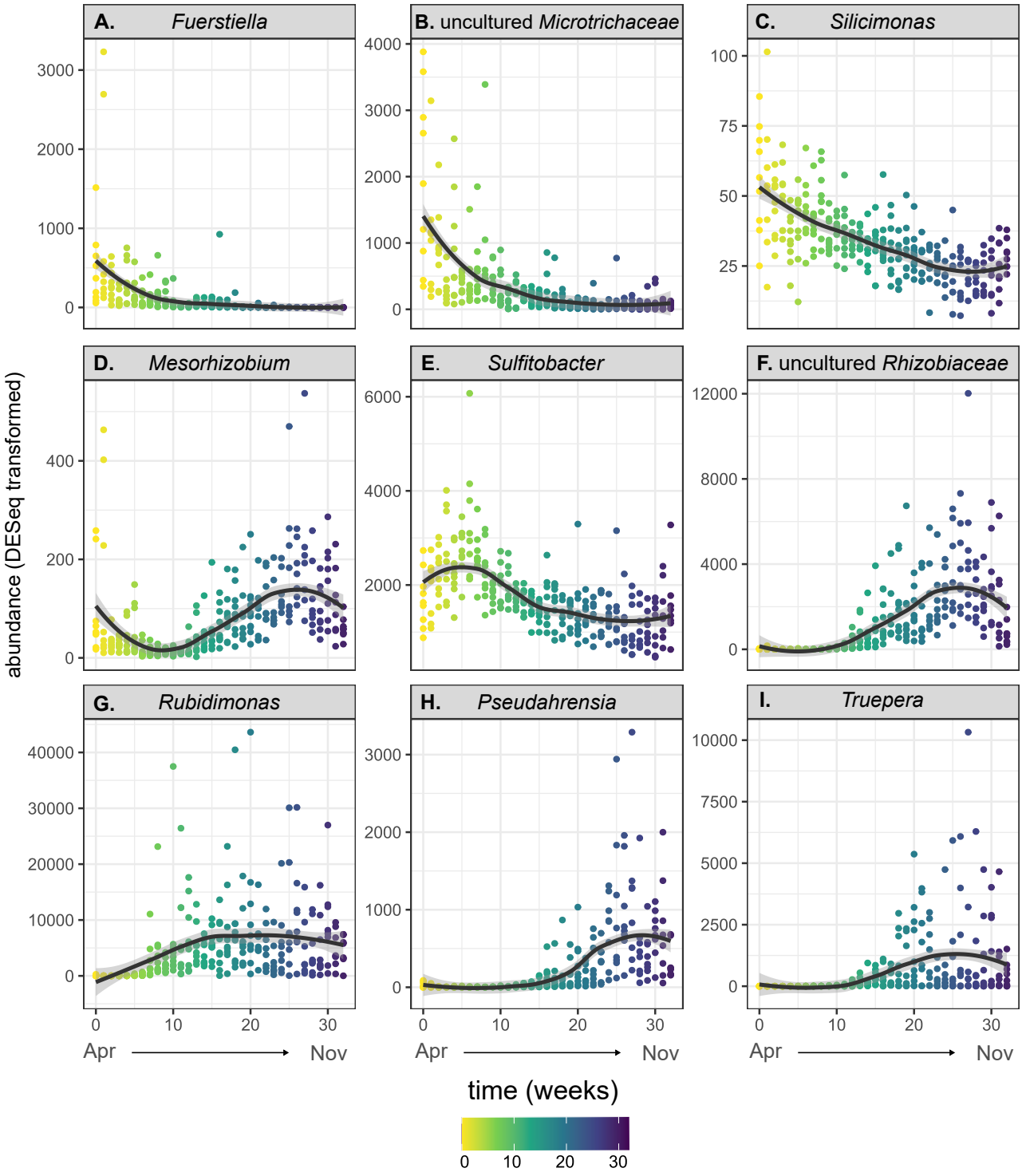

FIGURE 3.05 Abundance (DESeq transformed read counts) of nine bacterial taxa over time (in weeks) throughout April–November in the *Ulva fenestrata* land–based aquaculture system. A) *Fuerstiella*, B) uncultured *Microtrichaceae*, C) *Silicimonas*, D) *Mesorhizobium*, E) *Sulfitobacter*, F) uncultured *Rhizobiaceae*, G) *Rubidimonas*, H) *Pseudahrensia*, and I) *Truepera*. These taxa were selected as examples based on the high amount of variation in abundance explained by succession through time. Curves were fitted with Local Polynomial Regression Fitting (LOESS) using the R package GGPLOT2. Shaded areas represent the 0.95 confidence interval.

3.3.3 From acclimation to aquaculture

The bacterial communities associated with the *Ulva* nursery culture during the acclimation phase (i.e., the samples collected before the *Ulva* thalli were relocated to either the land-based flow-through system or to the offshore seafarms) were very different from the rest of the samples (Fig. 3.02C, Fig. 3.06). This contrast became evident within the span of a single week. For example, the *Ulva fenestrata* seedling samples from the hatchery were collected on 21 September 2021 right before they were transferred to the offshore location and the first samples in the seafarm were collected on 28 September 2021. Although these sampling occasions were merely 7 days apart, their bacterial community composition exhibited substantial dissimilarity (Fig. 3.06B).

Bacterial communities in the acclimation phase were dominated by *Algitalea*, *Flavobacterium*, *Sulfitobacter*, and *Pseudomonas*. The culture stock (thalli 10–15 cm in width) that was moved to the land-based flow-through system, for example, contained especially high relative abundances of *Algitalea* (on average 29% compared to 0% throughout week 1–32) and *Flavobacterium* (12% in the culture stock versus 2% throughout the experiment) (Fig. 3.07A). The *U. fenestrata* hatchlings that were moved to the offshore seafarm typically contained high relative abundances of *Sulfitobacter* (on average 12% compared to 2% throughout Sep–July in the seafarm) and *Pseudomonas* (23% versus 2.1% throughout Sep–July in the seafarm) (Fig. 3.07B). Bacterial communities of *Ulva linza* hatchlings were likewise dominated by *Sulfitobacter* (8.2% in hatchlings versus 0.9% in the seafarm) and *Pseudomonas* (25.6% hatchlings versus 1.2% in seafarm) (Fig. 3.07C). *Algitalea*, *Flavobacterium*, *Sulfitobacter*, and *Pseudomonas* were present in the natural *U. fenestrata* population as well, but only in very low abundance (ranging from 0.4–2.0% relative abundance). See Electronic Supplementary Table S3.03 for an overview of the relative abundance of each bacterial taxon in the collected samples.

The acclimation phase in the hatchery was also characterised by the absence of certain bacteria. An uncultured *Saprospiraceae*, for example, was nearly absent in the microbial communities of the acclimation culture stock and hatchlings, but very common in the land-based flow-through system (up to 60% relative abundance in the final weeks of the experiment), in the natural *U. fenestrata* population (up to 60% relative abundance in June), in the *U. fenestrata* seafarm (up to 80% relative abundance in May/June), and in the *U. linza* seafarm (up to 65% relative abundance in November) (Fig. 3.07). Similar patterns, albeit less extreme, were observed for *Granulosicoccus* and *Leucothrix*. In general, the observed alpha diversity was lower during the nursery stage and during week 1 of the experiment (on average 97 genera) compared to the rest of the experiment (on average 110 genera) ($p = 0.02$; negative binomial model) (Fig. S3.04).

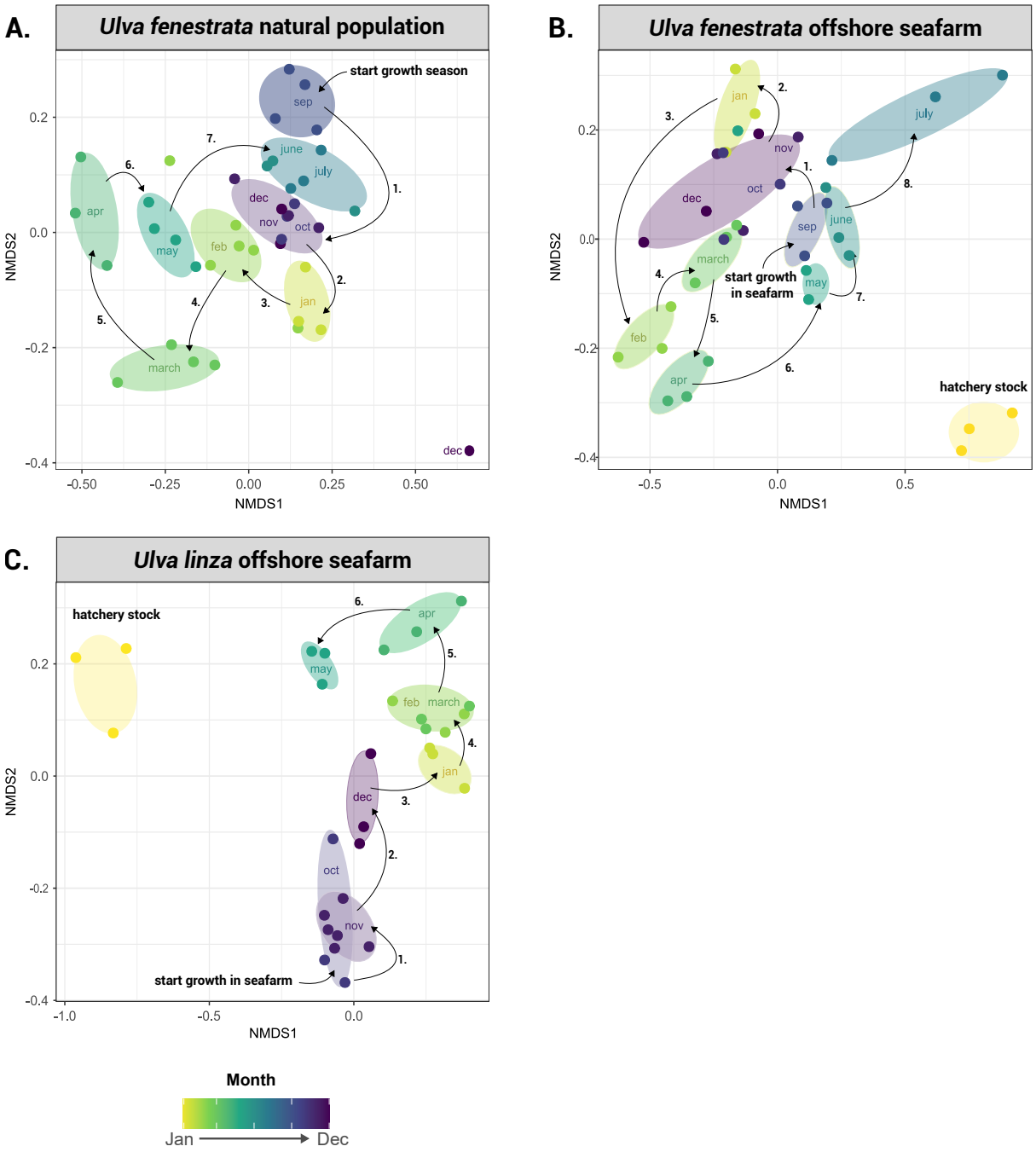

FIGURE 3.06 NMDS ordination of the microbial communities (genus level, Bray-Curtis dissimilarities) associated with *Ulva* throughout September–July in A) natural population of *U. fenestrata*, B) *U. fenestrata* offshore seafarm, and C) *U. linza* offshore seafarm. Taxonomic assignment was based on the SILVA rRNA database. Colours represent sample month. The acclimation samples (seedlings from the hatchery stock) have been indicated in bright yellow.

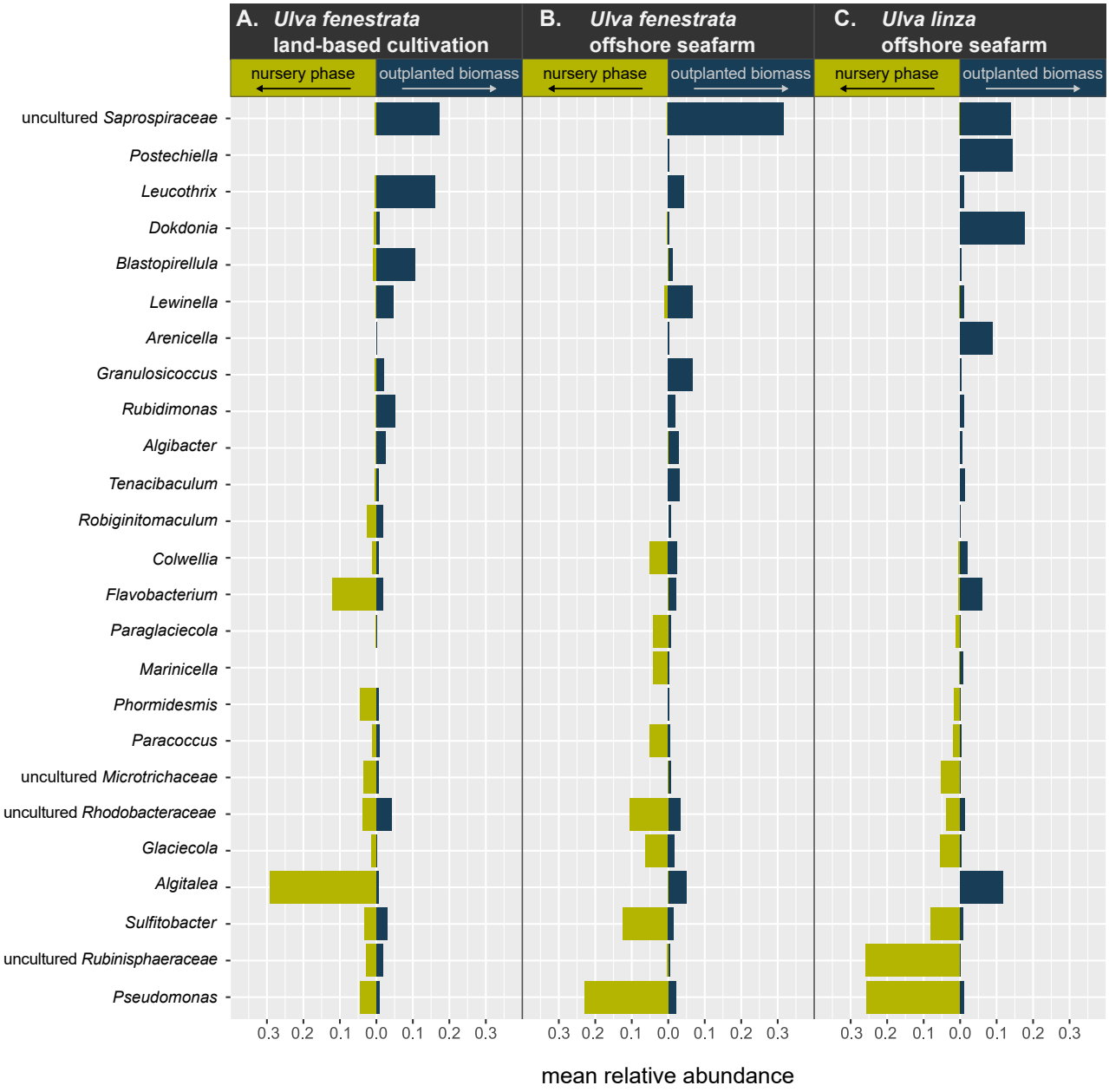

FIGURE 3.07 The mean relative abundance of bacterial taxa during the nursery phase (light green) and during the outplanted phase (dark blue), in the A) *Ulva fenestrata* land-based aquaculture facilities; B) *Ulva fenestrata* offshore seafarm; and C) *Ulva linza* offshore seafarm. Data are shown for the 25 most abundant bacterial genera.

3.4 Discussion

Microbiota manipulation or microbiome engineering could play an important role in sustainable and cost-effective seaweed cultivation, by supporting increased yield of biomass and desired bioactive compounds, as well as supporting disease control and seaweed fitness (Ke et al. 2021, Li et al. 2023). However, manipulation of microbiota requires fundamental knowledge on the dynamics of natural seaweed-associated bacterial communities, and the development of methods to increase the successful colonisation of seaweed beneficial microorganisms on the host. Identifying which bacteria are naturally part of the seaweed bacteriome [see e.g., Bolinches et al. (1988), Comba González et al. (2021), van der Loos et al. (2021)], understanding community assembly dynamics [including its resistance and resilience, see e.g., Nemergut et al. (2013), Coyte et al. (2021)], and deciphering what factors influence host–microbe interactions [see e.g., Witherden et al. (2017), Gilbert and Lynch (2019), van der Loos et al. (2019)] are key to the development of such methods. In addition, this fundamental knowledge is necessary in order to discover potential new SBMs (Li et al. 2023).

Our results demonstrated that *Ulva*-associated bacterial communities are far from static, but are constantly changing. These successional patterns are likely caused by an interplay of seasonal changes in environmental factors, such as irradiance, dissolved inorganic nitrogen, and seawater temperature, as well as the physiological state of the seaweed host (Roleda and Hurd 2019, Juhmani et al. 2020, Jansen et al. 2022). Temporal variation has been observed before in bacterial communities associated with, e.g., *Ulva lactuca* in the Caribbean Sea (Comba González et al. 2021), *Ulva rigida* in Spain (Bolinches et al. 1988), and *Ulva intestinalis* in Germany (Lachnit et al. 2011). In Sweden, natural *Ulva* populations typically start to develop at the end of Summer (September–October) with very reduced growth during Winter, while blooming throughout Spring until early Summer. When the seawater temperatures start to increase, the *Ulva* thalli tend to overgrow with epiphytes and decay. Offshore cultivation therefore generally takes place from September–June. As *Ulva* growth follows seasonal patterns (Steinhagen et al. 2021b, 2022a), the effect of the environmental variables versus the age of *Ulva* thalli on bacterial communities is hard to separate.

Older seaweed tissue has experienced a higher exposure to microbes, both in terms of bacterial abundance and diversity. Perennial and annual kelp species, for example, support different bacterial communities (Lemay et al. 2018), and the older apices of the kelp blades host a distinct and more abundant microbial biofilm than the younger tissue at the meristematic base (Ramírez-Puebla et al. 2022, Burgunter-Delamare et al. 2023). *Ulva*, which does not grow from a localised meristem, exhibits less variation across its blade, but more variation over time (Lemay et al. 2020). Bacterial communities associated with older seaweeds have had more time to establish, which over time could result in less dynamic bacterial communities. Indeed, in our land-based cultivation set-up, the bacterial community changed more pronounced during the first 16 weeks of the cultivation period than during the last 16 weeks. Similarly, *Ulva* growth was generally higher in the first 16 weeks of the experiment, and decreased after fertility reached a peak around week 16. This highlights the need for rejuvenation of culture stocks to maintain high yield.

We also showed that both *Ulva fenestrata* and *Ulva linza* hatchlings in the nursery stage harboured a very distinct bacterial composition compared to thalli grown in land-based tanks and offshore lines. Bacterial communities in the nursery stage were often dominated by 1–3 genera with very high relative abundance (mainly *Algitalea*, *Flavobacterium*, and *Sulfitobacter*). Several of these have been identified as growth promoting bacteria in previous studies (Amin et al. 2015, Califano et al. 2020), and are known to occur especially abundant in aquaculture (Ghaderiardakani et al. 2019, van der Loos et al. 2021). Similar results were observed in studies of cultivated kelp, including *Saccharina japonica* (Q. Han et al. 2021), *Saccharina latissima*, and *Alaria esculenta* (Davis et al. 2023), revealing a distinct microbiome during the nursery stage. In addition, we observed lower

diversity during the nursery stage and the first week compared to the rest of the experiment, similar to the lower diversity associated with young meristematic kelp tissue (Weigel and Pfister 2019, Lemay et al. 2021). Bacterial communities of different *Ulva* species reared in the same nursery (e.g., *Ulva fenestrata* and *U. linza* hatchlings reared for offshore cultivation during September–October 2022) were more similar than the bacterial communities of the same *Ulva* species reared in different nurseries (e.g., *Ulva fenestrata* grown in April 2020 for onshore cultivation and *U. fenestrata* grown in September 2022 for offshore cultivation). This suggests that the nursery itself is an important source pool for bacteria, in accordance with previous results indicating that *Ulva* acquires its bacterial symbionts through horizontal transmission rather than vertical transmission (Syukur et al. 2023).

The introduction of beneficial microorganisms onto a host does not always result in successful colonisation, particularly when the native microbiota has already established a relatively stable community. Prior disruption of the existing communities may be necessary to enable effective microbiota manipulation. Antibiotic treatments, such as those demonstrated in the case of brown algae *Ectocarpus* to illustrate the seaweed's reliance on bacteria for acclimation to salinity changes (Dittami et al. 2016), are often employed for this purpose. Other options include the use of chemicals such as essential oils and povidone-iodine (Burgunter-Delamare et al. 2021), or physical methods (Fernandes et al. 2011). Nappi et al. (2022) used a sonication treatment, resulting in the successful colonisation of *Ulva australis* tissue by the inoculated bacteria. Once the hatchling in our experiments were translocated to either onshore tanks or offshore lines, the bacterial composition rapidly changed in as little as seven days. This indicates that the bacterial community at this stage is still susceptible to new microbiota and that these controlled nursery conditions could provide the ideal opportunity for microbiota manipulation. The questions remain, however, whether the newly-acquired SBMs will persist the transition to larger cultivation settings.

3.5 Conclusions and perspective

In this study we characterised successional and seasonal dynamics in cultivated and non-cultivated *Ulva*-associated bacterial communities. Our findings highlight that the taxonomic composition of these communities constantly changes throughout the year or the cultivation period. The most pronounced differences were observed between the nursery stage and the outplanted thalli that were transferred to onshore tanks or offshore lines. The nursery stage was generally characterised by lower bacterial diversity and the dominance of 1–3 genera. However, as the hatchlings were exposed to natural conditions, their bacterial communities rapidly diversified, with fluctuating abundances of different bacteria over the course of the year. The controlled nursery conditions and the susceptibility of the bacterial biofilm to the acquisition of new bacteria could provide the ideal opportunity for microbiota manipulation to enhance seaweed production in aquaculture.

Acknowledgements

The authors thank the Formas-funded 'A manual for the use of sustainable marine resources' project [grant number 2022-00331] and the FWO PhD Fellowship fundamental research [grant number 3F020119] for financial support. Furthermore, we would like to thank Gunnar Cervin, Gunilla Toth, Kristoffer Stedt, and Alexandra Kinnby for their help during sample acquisition.

Author contributions

L.M.L.: Conceptualization, Data curation, Formal analysis, Investigation, Visualisation, Writing – original draft. **C.D.W.:** Data curation, Formal analysis, Writing – review & editing. **A.W.:** Supervision, Writing – review & editing. **O.D.C.:** Funding acquisition, Supervision, Writing – review & editing. **S.S.:** Conceptualization, Data curation, Funding acquisition, Investigation, Writing – review & editing.

Data availability statement

Raw sequence reads and metadata are deposited at SRA (BioProject PRJNA994710). All Electronic Supplementary Materials (Supplementary Figures and Tables) are available at Zenodo (DOI: 10.5281/zenodo.10732174).

Supplementary Materials & Methods

Supplementary Materials & Methods S3.01 Provasoli's Enriched Seawater Medium (PES)

To create 1L PES, add the following solutions together:

Solution I: Base solution	599 mL
Solution II: Fe	200 mL
Solution III: PII metals	200 mL
Solution IV: vitamins	1 mL

Solution I

Deonised water	599 mL
Tris buffer	4 g
$NaNO_3$	2.8 g
Na_2 glycerophosphate	0.4 g
Thiamine-HCl (vitamin B_1)	0.004 g

Solution II

Deonised water	1 L
$Fe(NH_4)_2(SO_4)_2 * 6H_20$	0.700 g
Na_2EDTA	0.600 g

Solution III

Deonised water	1 L
Na_2EDTA	1 g
H_3BO_3	1.140 g
$FeCl_3 * 6H_2O$	0.049 g
$MnSO_4 * H_2O$	0.130 g
$CoSO_3 * 7H_2O$	0.005 g
$ZnSO_4 * 7H_2O$	0.022 g

Solution IV

Deonised water	25 mL
Vitamin B_{12}	0.002 g
Biotin	0.001 g

Supplementary Figures

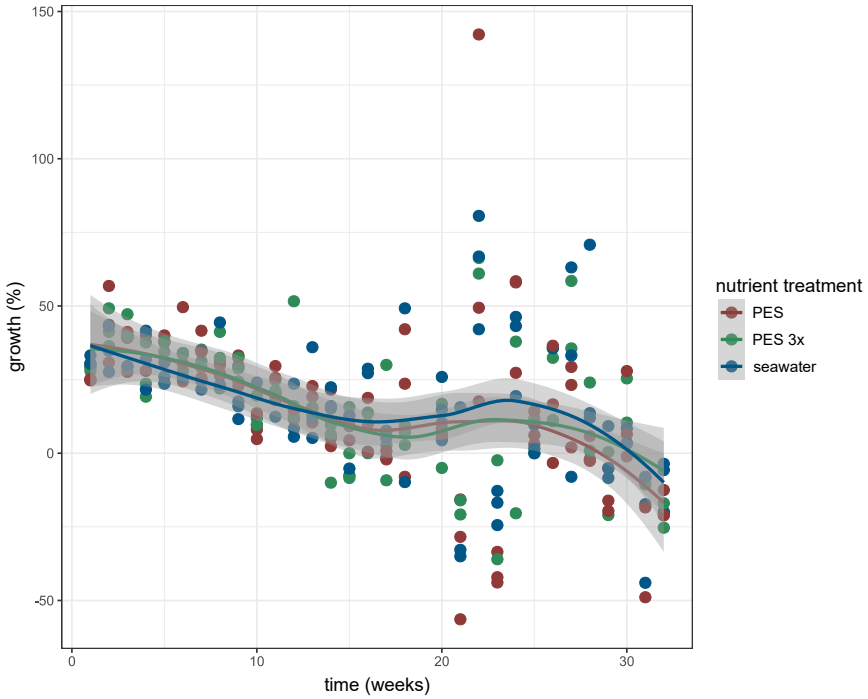

FIGURE S3.01 *Ulva fenestrata* growth (%) in a land-based aquaculture set-up (which consisted of nine experimental tanks) throughout a period of 32 weeks. Colour indicates nutrient treatment (blue = SW, red = 1x PES, green = 3x PES).

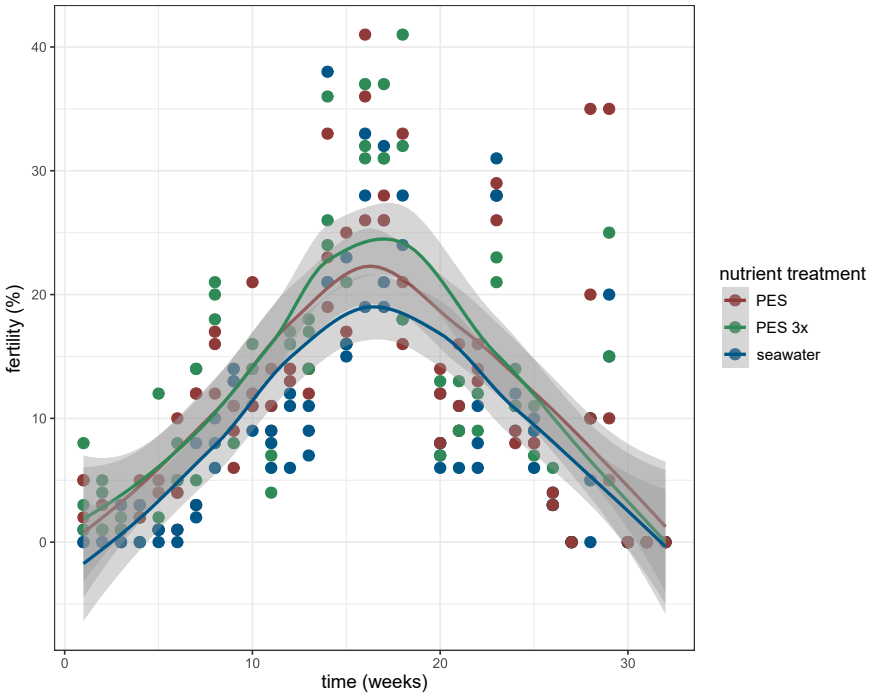

FIGURE S3.02 *Ulva fenestrata* fertility (%) in a land-based aquaculture set-up (which consisted of nine experimental tanks) throughout a period of 32 weeks. Colour indicates nutrient treatment (blue = SW, red = 1x PES, green = 3x PES).

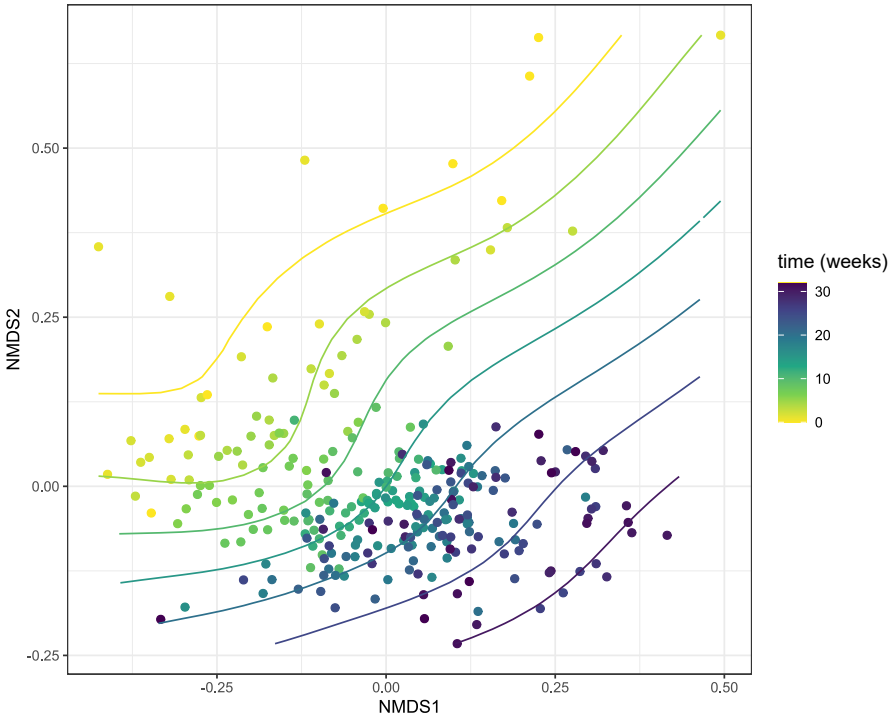

FIGURE S3.03 NMDS ordination of the microbial communities (genus level, Bray-Curtis dissimilarities) associated with Ulva fenestrata in a land-based aquaculture set-up (which consisted of nine experimental tanks) throughout a period of 32 weeks. Colour indicates time in weeks. Taxonomic assignment was based on the SILVA rRNA database.

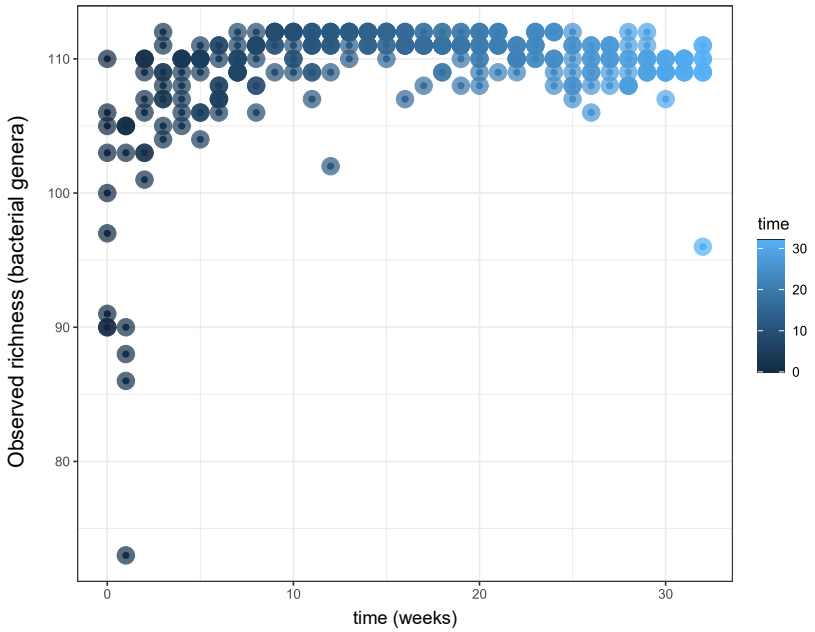

FIGURE S3.04. Observed alpha diversity (bacterial genera) over time (in weeks) of the bacterial communities associated with *Ulva fenestrata* in a land-based aquaculture set-up (which consisted of nine experimental tanks) throughout a period of 32 weeks.

“How inappropriate to call this planet Earth, when it is quite clearly Ocean.”

– Arthur C. Clarke

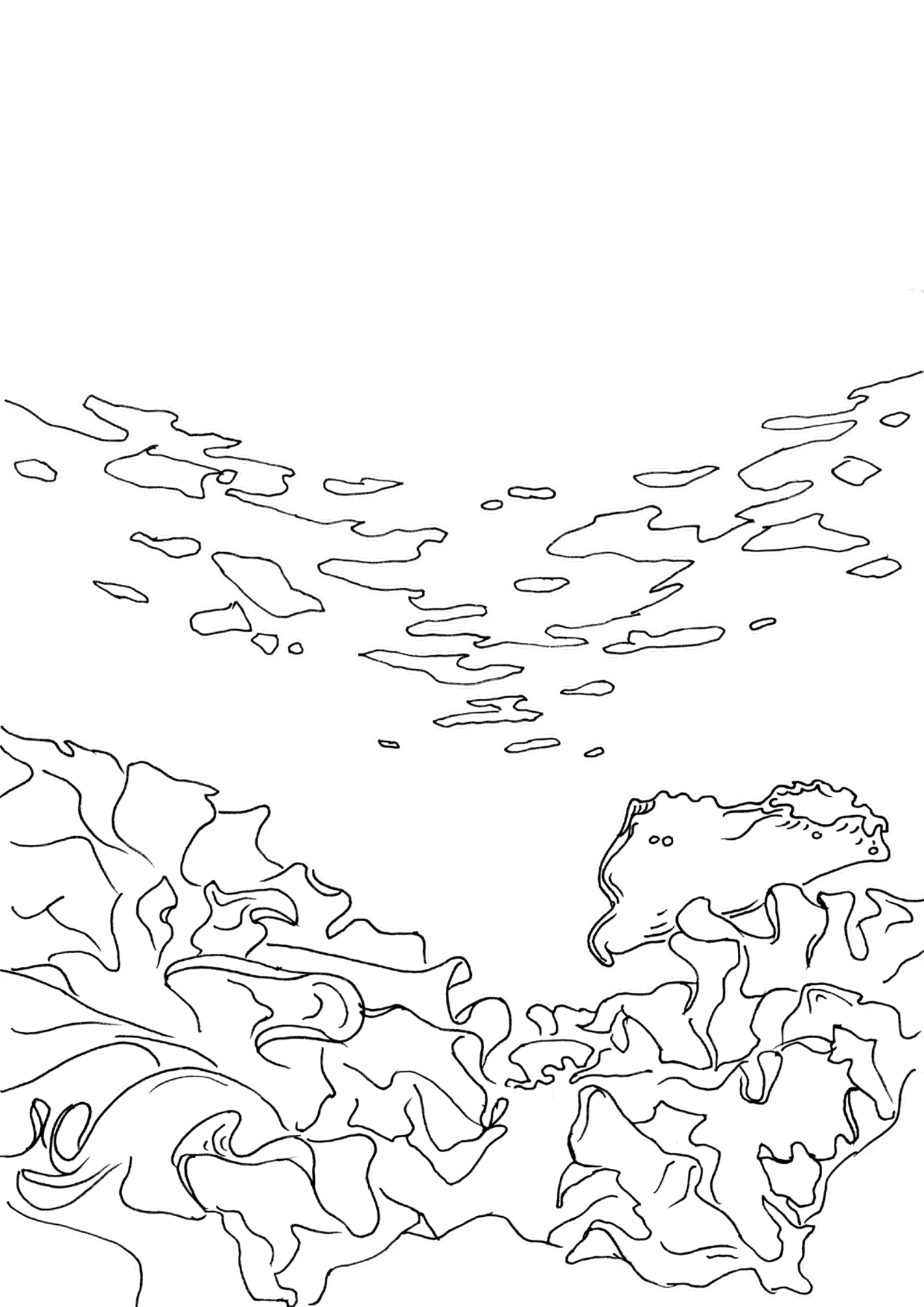

Chapter 4. Salinity and host drive *Ulva*-associated bacterial communities across the Atlantic–Baltic Sea gradient

This chapter has been published as:
L.M. van der Loos[1,2], S. D'hondt[1], A.H. Engelen[3], H. Pavia[4], G.B. Toth[4], A. Willems[2], F. Weinberger[5], O. De Clerck[1] & S, Steinhagen[4]. 2022. Salinity and host drive *Ulva* associated bacterial communities across the Atlantic–Baltic Sea gradient. *Molecular Ecology* 10.1111/mec.16462

[1] Phycology Research Group, Department of Biology, Ghent University, Ghent, Belgium
[2] Laboratory of Microbiology, Department Biochemistry and Microbiology, Ghent University, Ghent, Belgium
[3] Marine Microbial Ecology & Biotechnology, CCMAR, University of Algarve, Faro, Portugal
[4] Department of Marine Sciences-Tjärnö, University of Gothenburg, SE-452 96 Strömstad, Sweden
[5] GEOMAR Helmholtz Centre for Ocean Research Kiel, 24148, Kiel, Germany

Abstract

The green seaweed *Ulva* is a model system to study seaweed–bacteria interactions, but the impact of environmental drivers on the dynamics of these interactions is little understood. In this study, we investigated the stability and variability of the seaweed-associated bacteria across the Atlantic–Baltic Sea salinity gradient. We characterised the bacterial communities of 15 *Ulva sensu lato* species along 2,000 km coastline in a total of 481 samples. Our results demonstrate that *Ulva*-associated bacterial composition was strongly structured by both salinity and host species (together explaining between 34–91% of the variation in the abundance of the different bacterial genera). The largest shift in the bacterial consortia coincided with the horohalinicum (5–8 PSU, known as the transition zone from freshwater to marine conditions). Low salinity communities especially contained high relative abundances of *Luteolibacter*, *Cyanobium*, *Pirellula*, *Lacihabitans*, and an uncultured *Spirosomaceae*, whereas high salinity communities were predominantly enriched in *Litorimonas*, *Leucothrix*, *Sulfurovum*, *Algibacter*, and *Dokdonia*. We identified a small taxonomic core community (consisting of *Paracoccus*, *Sulfitobacter*, and an uncultured *Rhodobacteraceae*), which together contributed to 14% of the reads per sample, on average. Additional core taxa followed a gradient model, as more core taxa were shared between neighbouring salinity ranges than between ranges at opposite ends of the Atlantic–Baltic Sea gradient. Our results contradict earlier statements that *Ulva*-associated bacterial communities are taxonomically highly variable across individuals and largely stochastically defined. Characteristic bacterial communities associated with distinct salinity regions may therefore facilitate the host's adaptation across the environmental gradient.

4.1 Introduction

Bacteria are of vital importance to marine multicellular organisms and often play a crucial role throughout their host's life (McFall-Ngai et al. 2013, Bordenstein and Theis 2015). Seaweeds — important primary producers in coastal ecosystems worldwide — likewise depend on their associated microbiota for optimal functioning, including nutrient exchange, defence mechanisms, and reproduction (Weinberger et al. 2007, Egan et al. 2013). The algal host and its associated microbiome are often referred to as a holobiont: a single ecological unit (Egan et al. 2013). The members of these ecological units are connected through complex interactions on multiple levels (Pita et al. 2018). The dynamics of the seaweed holobiont, however, are little understood — especially with regards to environmental drivers (Egan et al. 2013, van der Loos et al. 2019).

The green seaweed *Ulva* is a model to study algae–bacteria interactions (Wichard et al. 2015, Kessler et al. 2018, Califano et al. 2020). *Ulva* relies on specific bacterial partners to obtain its typical morphology (e.g., a blade that is two-cells thick or a tube that is one-cell thick). In the absence of these specific bacteria, *Ulva* merely grows as a loose aggregation of cells without rhizoids or proper cell wall development. In addition to morphogenesis, bacteria are known to promote *Ulva* growth (Gemin et al. 2019), induce settlement of zoospores (Joint et al. 2000, Patel et al. 2003), and affect biochemical composition of the seaweed (Polikovsky et al. 2020).

As with other seaweeds, the entire spectrum of interactions between *Ulva*, its associated microbiome, and the environment remains largely unknown. Studies so far have only addressed variation in *Ulva*-associated bacterial diversity across small and larger geographical scales (see e.g., Tujula et al. 2010, Burke et al. 2011b, Roth-Schulze et al. 2018), but not across environmental gradients. In the absence of an explicit environmental gradient, neutral or stochastic processes are more likely to drive microbial community structure, thus causing high among-individual variation (Adair and Douglas 2017). In the presence of an environmental gradient, deterministic mechanisms (i.e., environmental selection) could govern variation in microbial composition (Martiny et al. 2006, Adair and Douglas 2017). Indeed, previous studies of *Ulva*-associated bacteria with samples

taken from one or a few locations have highlighted high levels of inter-individual variation (Burke et al. 2011b, Roth-Schulze et al. 2018). Other studies, however, found distinct differences among sampling habitats and *Ulva* host species (Comba González et al. 2021, van der Loos et al. 2021).

Closely related to questions on the variability of the *Ulva* microbiome across environmental gradients, is the question on its stability (the 'core' microbiome). Identifying stable key microbes is important in order to define 'healthy' microbial communities and — especially with regard to spatial and temporal distribution — gain insight in ecological functions (Risely 2020). Bonthond et al. (2020) for example identified various prokaryotic and eukaryotic core taxa associated with the red alga *Gracilaria vermiculophylla* on a global scale in both native and introduced populations. This implies that *Gracilaria*'s core taxa either have a worldwide distribution, or have been co-introduced with their host during the invasion process. The bacterial communities of the introduced Mediterranean *Caulerpa taxifolia* likewise showed high similarity to the communities of the native populations in eastern Australia (Meusnier et al. 2001, Arnaud-Haond et al. 2017). Core microbes may even facilitate successful introductions (Bonthond et al. 2021). Bacteria likely play an important role in acclimatisation and adaptation of *Ulva* to environmental changes, as has been demonstrated in the filamentous brown alga *Ectocarpus*, which depends on bacterial communities for acclimatisation to salinity changes (Dittami et al. 2016). Incorporating an environmental gradient can, therefore, inform us on the stochastic versus deterministic mechanisms controlling the variability and stability of microbial composition in general.

A study on the global, environmental distribution of bacterial diversity marked salinity as the most important driver of bacterial community composition, surpassing the effects of temperature and pH (Lozupone and Knight 2007). Salinity gradients are often studied in estuaries, but estuarine environments are dynamic and the constant mixing of water bodies causes unstable gradients. The Baltic Sea is the world's largest inland brackish sea and one of the most widely studied coastal areas. This area represents a relatively young (8,000 years), semi-enclosed postglacial sea that stands out by a successive transition from fully marine conditions of the North Sea (North-east Atlantic) towards a near freshwater state in its innermost parts (Reusch et al. 2018). The lack of tides, as well as the freshwater influx on one side of the gradient combined with limited exchange with North Sea water, allow for stable salinity regions over a large geographical distance. In addition, water retention time in the brackish central Baltic is high (between 3 to 30 years), especially compared to the more dynamic estuaries formed at river mouths (Herlemann et al. 2011). This makes the Baltic Sea an excellent area to study salinity gradients.

The steepest salinity change in the Baltic Sea can be observed at the Danish Straits (Johannesson et al. 2020), and species diversity and distribution are strongly defined by the prevailing salinity regime (Ojaveer et al. 2010). Marine species diversity generally decreases with decreasing salinity, while simultaneously freshwater species increase in number and abundance (Ojaveer et al. 2010). Consequently, only few marine species successfully establish along this entire environmental gradient (Johannesson et al. 2020). Although salinity does not affect bacterial species richness in seawater- and sediment-associated communities in the Baltic, it is a strong driving force behind bacterial community structure and composition (Herlemann et al. 2011, Klier et al. 2018). Work on bacterial communities in the Baltic region has been limited to bacterioplankton, bacteriobenthos, and bacteria as components of animal diets (Herlemann et al. 2011, Klier et al. 2018, Skrodenytė-Arbačiauskienė et al. 2021), while host-associated bacteria have rarely been investigated across the entire salinity gradient. The question therefore remains how host-associated bacterial communities are influenced by a gradual environmental transition, and whether the host itself or the prevailing salinity conditions have a larger effect on the associated microbiomes.

This study aims to 1) characterise the dynamics of seaweed-associated bacterial communities as a function of both host and a stable salinity gradient, and 2) assess whether we can define a taxonomical core community across the Atlantic–Baltic Sea gradient. We sampled 481 *Ulva sensu lato* individuals along 2,000 km of coastline, spanning the full 3.5–36 PSU salinity gradient in the Baltic Sea and adjacent areas. To examine to what extent the ecological dynamics of the *Ulva* associated bacterial communities are driven by ecological factors and host species, we generated full-length 16S rRNA gene amplicon sequences with Oxford Nanopore Technologies. Previous studies on *Ulva*-associated bacteria indicated that between-site effects were more important than between-species effects, likely due to the high morphological similarity and close phylogenetic relatedness between *Ulva* species (van der Loos et al. 2021). We therefore hypothesise that *Ulva*-associated bacterial community composition in the Baltic Sea is primarily established under the influence of the prevailing salinity gradient and secondarily affected by host species.

4.2 Materials and methods

4.2.1 Study area, field collection, and sample preparation

Samples of *Ulva sensu lato* individuals (n = 481, including *Ulva*, *Blidingia*, and *Kornmannia*) used in the present study were collected along the full salinity gradient present in the Baltic Sea and adjacent areas such as the Kattegat, Skagerrak, and the eastern North Sea (Fig. 4.01). *Ulva* species are commonly found in the Baltic Sea and on the North-east Atlantic coast, and are known for their high tolerance towards fluctuations in salinity (Rybak 2018). Under high nutrient conditions, some species are known to cause nuisance blooms (Smetacek and Zingone 2013). *Ulva* species are difficult to identify based on their simple morphological characteristics due to the high plasticity within species and high morphological similarities among species. Over ten species of *Ulva* have previously been identified based on genetic markers in the Baltic area (Steinhagen et al. 2019a). Many of these species occur in sympatry and can be found in a wide variety of habitats (Leskinen et al. 2004, Steinhagen et al. 2019a). *Ulva* has an isomorphic diplohaplontic life cycle. Morphologically, the gametophytic and sporophytic phases cannot be reliably distinguished (Wichard 2015). The life stage of the individuals sampled in this study was therefore not checked.

In total 146 sampling sites, of which 63 in Denmark, 53 in Sweden, 25 in Norway, and 5 in Germany, were visited during summer 2020 (June–September; see also Electronic Supplementary Table S4.01). The salinity ranged from 3.5 to 36 PSU and is presented in the figures in this study either on a continuous scale (0–36) or in salinity zones defined according to the Venice classification system (0.5–5 = oligohaline, 5–8 = horohalinicum, 8–18 = mesohaline, 18–30 = polyhaline, and 30–36 = euhaline) (Alves et al. 2009, Bleich et al. 2011, Hu et al. 2016). In addition, both water temperature (°C) and oxygen levels (mg L^{-1}) were measured at each site (Fig. S4.01, S4.02).

A variety of habitats, such as, rock pools, harbours, estuaries, fjords, drain channels, as well as exposed and sheltered coastal areas were visited. The different substrates (organic and inorganic) of the attached thalli were recorded. Sampling was performed in the supra- and mid-littoral zones using waders, which allowed for sampling to a depth of ~1.5 m below mean sea level. Additional samplings of the mid- and infralittoral zones of chosen sites were conducted via snorkelling. At each site, representative specimens of each morphotype and all observed populations were collected from the supralittoral to the sublittoral (in horizontal transects of ca. 50 m depending on site accessibility), including drifting and epiphytic green algae. All sampling work in the respective countries was conducted by a single person to ensure repeatability among sites. Sterilised disposable gloves

and sterilised equipment were used throughout the sampling procedure to minimize contamination. After rinsing each individual with ca. 30–50 mL sterile water to remove dirt, a cotton swab sample for microbiome analyses was generated by rubbing for 30 s on the tissue.

Furthermore, to enable DNA barcoding of the host, clean and epiphyte-free tissue samples (ca. 1 cm^2) of the respective individuals were collected. All samples were stored in a portable freezer (–20 °C) until transferred to –80 °C in the laboratory.

4.2.2 Molecular identification of the algae host

Genomic DNA was extracted from lyophilised host tissue using the Invisorb Spin Plant Mini Kit (Stratec, Birkenfeld, Germany) following the manufacturer's protocol and stored at –80 °C. The *tuf*A gene was used for species identification of the host. PCR amplicons were successfully generated for 461 samples following (Steinhagen et al. 2019a). The PCR products were first assessed by gel electrophoresis and subsequently purified using the QIAquick PCR Purification Kit, Qiagen (Hilden, Germany). Sanger sequencing of the purified amplicons was performed by Eurofins Genomics (Konstanz, Germany). Forward and reverse sequence reads were assembled in Sequencher (v. 4.1.4, Gene Codes Corporation, Ann Arbor, MI). Using the BLAST function in GenBank, first identifications via the specimens' *tuf*A sequences were made. To better resolve species identities, a set of peer-reviewed and annotated reference sequences downloaded from GenBank were used in subsequent phylogenetic analyses. Host species were identified according to the latest taxonomic revisions by Hughey et al. (2021). A multiple sequence alignment was constructed using MAFFT (Katoh et al. 2002). An optimal substitution model (GTR+G+I) was determined using MrModeltest software version v. 2.2. (Nylander 2004). Subsequently, a maximum likelihood analysis was performed using RAxML (v. 8; (Stamatakis 2014) with 1,000 bootstrap iterations. All sequences are publicly available in GenBank (see Electronic Supplementary Table S4.01 for accession numbers).

4.2.3 Molecular characterisation of the microbial communities

Bacterial communities were characterised with Oxford Nanopore sequencing following van der Loos et al. (2021). In short, total microbial DNA was extracted with the Qiagen DNeasy mini kit following the manufacturer's protocol, with the addition of a bead beating step before lysis using zirconium oxide beads (RETCH Mixer mill MM400; 5 minutes at 30 Hz). The full length 16S rRNA gene was amplified using the 27F_BCtail-FW (TTTCTGTTGGTGCTGATATTGC_AGAGTTTGATC MTGGCTCAG) and 1492R_BCtail-RV (ACTTGCCTGTCGCTC-TATCTTC_CGGTTACCT TGTTACGACTT) primers, each containing a 5′ extension allowing for subsequent barcoding by PCR. 16S rDNA PCRs were performed using the Phire Tissue direct PCR Master Mix (Thermo Fisher) and amplicons for each sample were barcoded using the Oxford Nanopore "PCR Barcoding Expansion Pack 1–96 (EXP-PBC096)". A total of 481 *Ulva*-associated samples were processed in nine PCRs and the final libraries were prepared with the ligation-based sequencing kit SQK-LSK109 according to manufacturer's protocol (Oxford Nanopore Technologies). The libraries were subsequently sequenced in six separate sequencing runs on a MinION (with R10.3 flow cells, Oxford Nanopore Technologies) for 72 h each. Six negative extraction samples were included in this study, as well as nine negative PCR controls, and four positive controls (ATCC microbial standard MSA-1002). In addition, two randomly chosen samples (DK043 from Denmark and NO118 from Norway) were included in all PCRs and divided over the six sequencing runs to verify comparability across PCRs and sequencing runs.

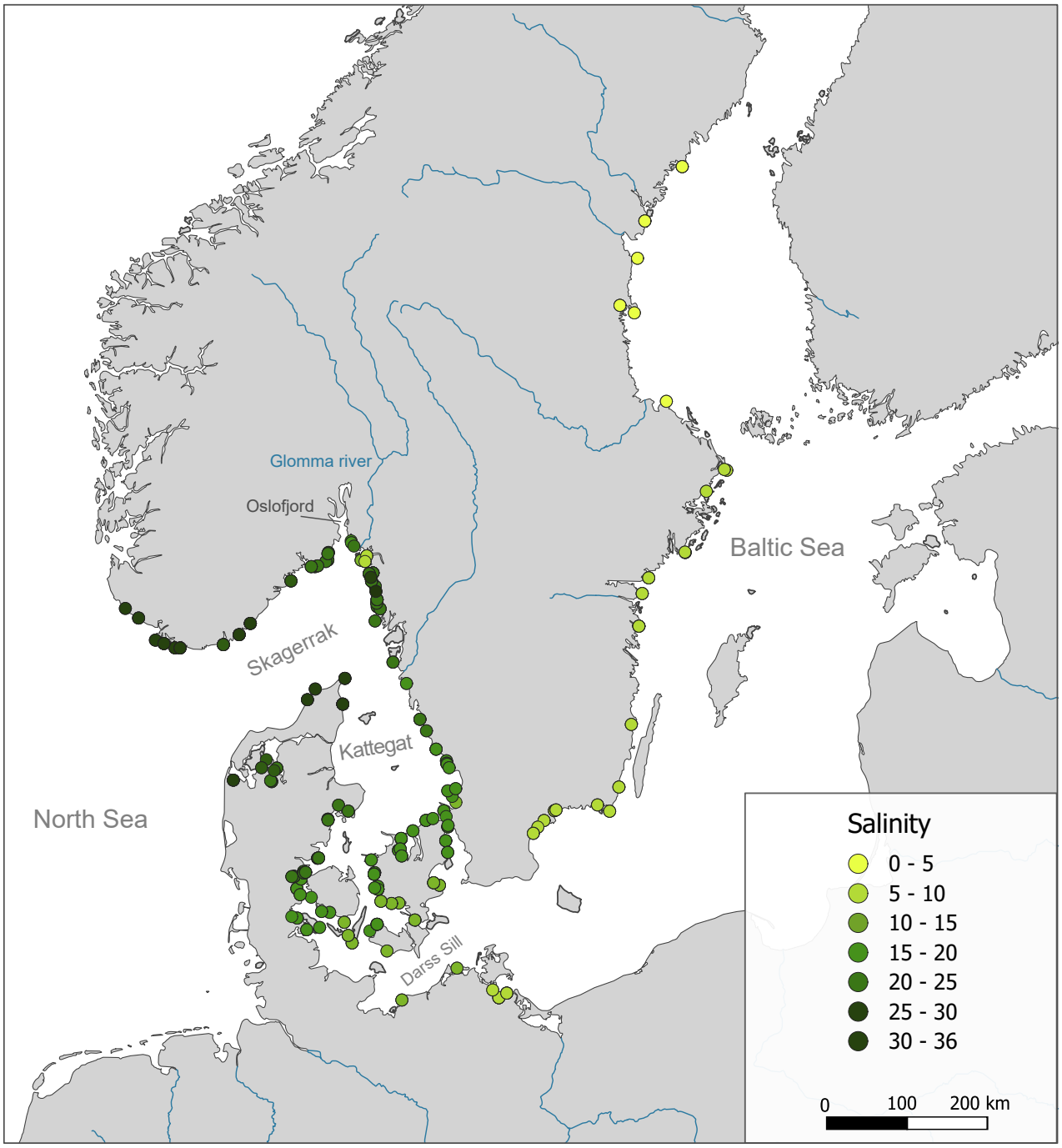

FIGURE 4.01 Geographic distribution of all 146 sampling sites in the Baltic Sea and adjacent areas (eastern North Sea, Skagerrak, and Kattegat) where 481 *Ulva sensu lato* samples were collected. The colour of the sites corresponds to the measured salinity. Major rivers are projected in blue.

The resulting raw FAST5 reads were basecalled and demultiplexed with Guppy (version 5.0.7, sup model, Oxford Nanopore Technologies). Data quality and length were first visually inspected with NanoPlot (De Coster et al. 2018). Subsequently, high-quality reads were obtained using chimaera removal with Yacrd (Marijon et al. 2020), and by filtering the dataset on quality (Q-score >8) and length (1,000–2,000 bp) with NanoFilt (De Coster et al. 2018). The resulting 23,955,915 high-quality reads were used to assign taxonomy at genus level with Kraken2 in combination with the SILVA 16S database (138.1 release) (Quast et al. 2013, Lu and Salzberg 2020). In the presented results and figures, we use the nomenclature as implemented in the SILVA database. The sequences are archived at SRA (BioProject PRJNA781821).

After taxonomic assignment, all chloroplast reads (3% of the high-quality reads) were removed from the dataset. In addition, rare taxa were discarded (optimal settings based on the positive controls retained OTUs found more than 70 times in at least 20% of the samples) to protect against OTUs with small mean and trivially large coefficient of variation. Finally, DESeq2 was used to account for sequencing depth with a variance stabilising transformation (Love et al. 2014).

4.2.4 Statistical analyses

To assess genus level differences in bacterial composition, Bray-Curtis dissimilarities were calculated and visualised with an NMDS ordination (Bray and Curtis 1957). Smooth surface lines were fitted to the ordination with the ordisurf function (vegan package) based on the correlation with salinity. The effect of salinity, host species, temperature, oxygen levels, and habitat (substrate from which the host was collected, being either rock, sand, concrete, epiphytic/epizoic, metal, plastic, wood/rubber/rope, or drift samples) on community composition was tested using the envfit function of the vegan package with 9,999 permutations (model included all factors, with $p < 0.05$ considered significant) (Oksanen et al. 2020). Multivariate comparisons with 9,999 permutations were made with pairwiseAdonis (Martinez Arbizu 2020) among all salinity zones and among all host species. A Mantel test was subsequently used to evaluate the correlation between the bacterial community dissimilarity matrix (at genus level) and the phylogenetic host species distance matrix. Alpha diversity was calculated as observed genus richness, as well as by using the Shannon Index, Simpson Index, and Chao1 Index (Jost 2007, Willis 2019). Differences in alpha diversity with salinity were assessed using a generalised linear mixed model based on a negative binomial family ($p < 0.05$ considered significant). The model included salinity, host species, and habitat, as well as the interaction between salinity and host. All categorical variables (host and habitat) were included as random effects.

Significantly differential abundant bacterial genera ($p < 0.01$, Benjamini-Hochberg corrected) were identified with DESeq2 (model included salinity, host species, and habitat, as well as the interaction between salinity and host) (Love et al. 2014). The amount of explained variation in abundance was quantified using the lme4 (Bates et al. 2015) and variancePartition (Hoffman and Schadt 2016) packages with a generalised linear mixed model fitted to a negative binomial family (model included salinity, host species, and habitat, as well as the interaction between salinity and host, and all categorical variables were included as random effects).

There are many different ways to define and calculate the core microbiome of a given dataset (Shade and Handelsman 2012, Risely 2020). Both core composition and size differ with relative abundance and prevalence (the number of samples in which the taxa were encountered) threshold settings, and as such defining a "core" microbiome remains relatively arbitrary. Here, the variation in core size (number of core taxa) was calculated for a range of different relative abundances (0.1–100%) and prevalences (50–90%) using the microbiome R package (Lahti and Shetty 2017).

All statistical tests were performed in R (R Core Team 2020) and data were visualised using the GGPLOT2 (Wickham 2016), METACODER (Foster et al. 2017), and PHYLOSEQ (McMurdie and Holmes 2013) packages.

4.3 Results

4.3.1 Taxonomic identification of host species

A total of 461 *Ulva sensu lato* samples were processed for species discrimination and identification based on *tuf*A sequence data. The full dataset was subject to phylogenetic analyses to allow for robust identification of host species (see Electronic Supplementary Table S4.01). The phylogenetic analyses separated the investigated specimens into 15 well-delimited taxonomic entities, including members of the genera *Blidingia*, *Kornmannia*, and *Ulva*. Eight entities of the genus *Ulva* could be resolved based on peer-reviewed reference sequences provided by GenBank. Five entities (represented by a total of 25 samples), could not be resolved to species level due to the absence of any similar GenBank entries.

More specifically, the taxa were identified as *Blidingia minima* (Nägli ex Kütz.) Kylin; see also (Steinhagen et al. 2021a) (n = 25 samples), *Kornmannia leptoderma* (Kjellmann) Bliding (n = 14), *Ulva australis* Areschoug (n = 2), *Ulva compressa* Linnaeus (n = 48), *Ulva fenestrata* Postels & Ruprecht (n = 36), *Ulva intestinalis* Linnaeus (n = 116), *Ulva lacinulata* (Kützing) Wittrock (n = 32), *Ulva linza* Linnaeus (n = 128), *Ulva prolifera* O.F. Müller (n = 7), *Ulva torta* (Mertens) Trevisan (n = 28), and unidentified *Ulva* sp. 1 (n = 1), *Ulva* sp. 2 (n = 15), *Ulva* sp. 3 (n = 2), *Ulva* sp. 4 (n = 4), and *Ulva* sp. 5 (n = 3).

Distinct distribution patterns across the salinity gradient were recorded for the host species. Corroborating previous studies focusing on different taxa, most of the green algal species investigated were absent east of the Danish Straits. *Ulva intestinalis* and *U. linza* showed the widest distribution and were present across the whole salinity gradient (present from 3.5 to >30 PSU). For details on the species distribution see Electronic Supplementary Table S4.02.

4.3.2 Bacterial alpha diversity associated with *Ulva sensu lato*

After filtering out rare taxa (using optimal settings based on the positive controls), we identified 96 bacterial genera, belonging to 28 families and 24 orders, associated with *Ulva*, *Blidingia*, and *Kornmannia*. Highly abundant orders across all *Ulva sensu lato* species included the Rhodobacterales, Sphingomonadales, Rhizobiales, and Flavobacteriales. Alpha diversity did not change with salinity when calculated as either observed richness ($p = 0.09$, $z = 1.71$; negative binomial model), or a Shannon Index ($p = 0.55$, $z = 0.59$; negative binomial model), Simpson Index ($p = 0.89$, $z = 0.14$; negative binomial model), or Chao1 Index ($p = 0.27$, $z = 1.11$; negative binomial model).

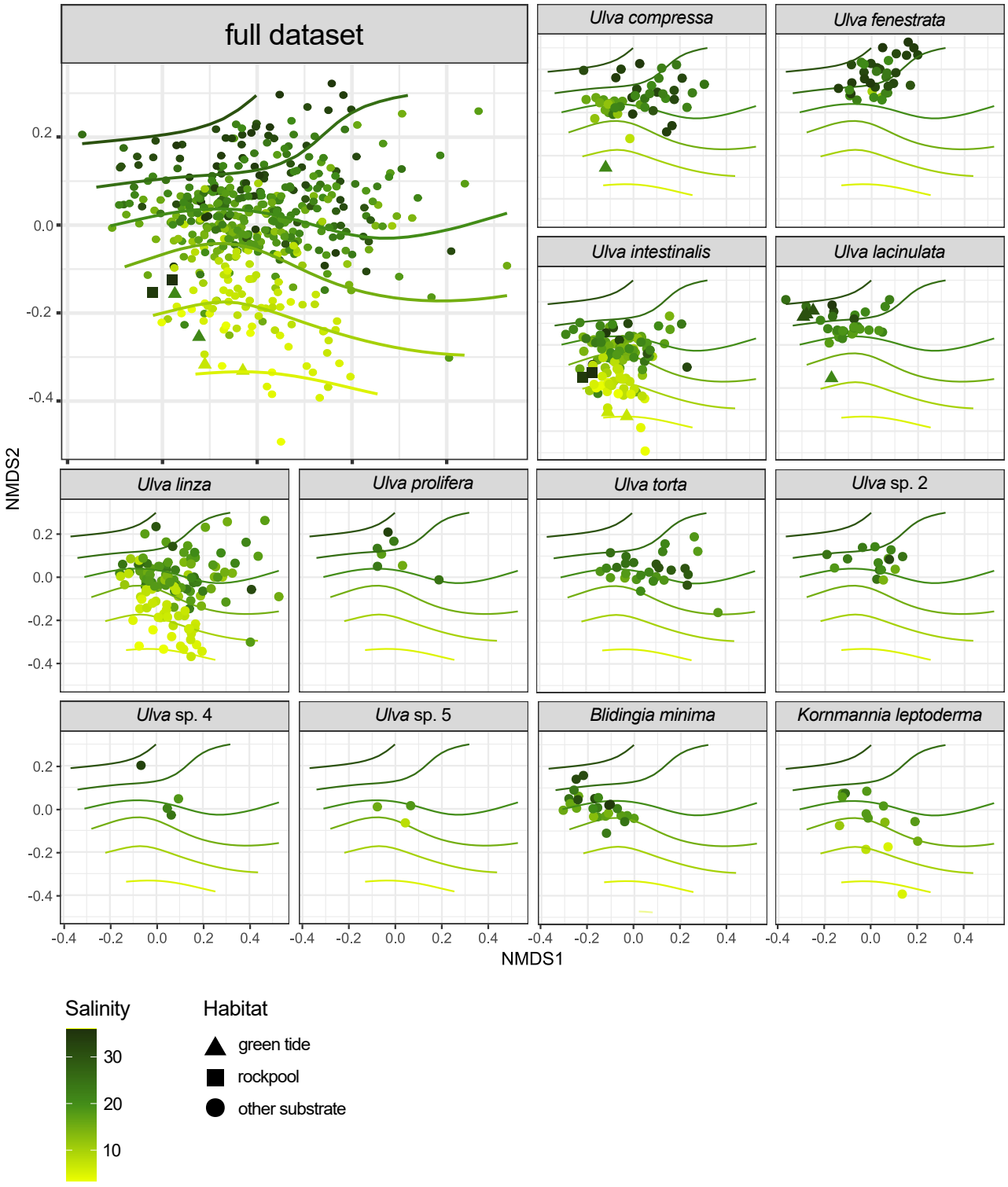

FIGURE 4.02 NMDS plots (stress = 0.01, k = 4) of *Ulva sensu lato* associated bacterial community composition (based on Bray-Curtis dissimilarities and genus level identifications). The first panel shows the full dataset (n = 481 samples). The remaining panels are split by host species (*Ulva compressa*, *Ulva fenestrata*, *Ulva intestinalis*, *Ulva lacinulata*, *Ulva linza*, *Ulva prolifera*, *Ulva torta*, *Ulva* sp. 2, *Ulva* sp. 4, *Ulva* sp. 5, *Blidingia minima*, and *Kornmannia leptoderma*). Note that separate plots for *Ulva australis*, *Ulva* sp. 1, and *Ulva* sp. 3 are not shown due to the few data points collected for these species. Colours represent salinity and symbols represent the habitat of the host species. The contour lines (smooth surface lines) are fitted to the ordination based on the correlation with salinity.

4.3.3 Effect of environment and host species on bacterial community

Bacterial community composition differed significantly with salinity ($p < 0.001$, R2 = 0.48) and host species ($p < 0.0001$, $R^2 = 0.34$). While pairwise comparisons showed that the oligohaline (0–0.5 PSU) and horohalinicum (5–8 PSU) shared similar bacterial communities ($p = 0.816$, $F = 1.77$; pairwise Adonis test), pairwise contrasts among all other salinity zones showed significant differences in bacterial communities (with $p < 0.001$ for all comparisons; pairwise Adonis test, Electronic Supplementary Table S4.03). Pairwise comparisons among all host species indicated that, amongst others, *U. linza* and *U. intestinalis* were associated with different bacterial communities ($p = 0.01$, $F = 25.97$; pairwise Adonis test), as well as *U. compressa* versus *U. fenestrata* ($p = 0.01$, $F = 6.09$; pairwise Adonis test), and *U. compressa* versus *U. lacinulata* ($p = 0.02$, $F = 5.03$; pairwise Adonis test). On the contrary, similar bacterial communities were shared between *U. compressa* versus *U. torta* ($p = 0.24$, $F = 3.66$; pairwise Adonis test), and *U. prolifera* versus *U. torta* ($p = 1.00$, $F = 2.23$; pairwise Adonis test). See Electronic Supplementary Table S4.04 for full statistics.

NMDS plots likewise showed a clear ordination influenced by the salinity gradient as well as host species (Fig. 4.02). This salinity effect was not only observed along the larger Atlantic–Baltic Sea gradient, but also on local scales (e.g., caused by freshwater river input). Sample sites located south in the Oslofjord (Norway, Skagerrak Strait) near the mouth of the Glomma river, for example, have a lower salinity compared to the predominantly higher surrounding salinity levels (Fig. 4.01). Bacterial community composition in these sites was generally more similar to samples collected in distant, low-saline sites in the Baltic Sea than to samples collected at neighbouring sites in the Skagerrak (Fig. S4.03).

Both habitat ($p < 0.0001$, $R^2 = 0.09$) and temperature ($p < 0.001$, $R^2 = 0.05$) were found to be significant as well, but with very low explanatory values. Several outliers in the NMDS plot however can be explained by habitat. For example, the bacterial communities of two *Ulva intestinalis* samples collected in high-saline rock pools located two and ten meters away from the main waterbody, were more similar to lower salinity communities (Fig. 4.02). The salinity of such rock pools is expected to vary a lot with rainfall and evaporation. Samples collected from green tides (mass accumulation events, n = 8), belonging to *Ulva compressa*, *Ulva lacinulata*, and *Ulva intestinalis*, were distinctly different from the general host species patterns (Fig. 4.02). Oxygen levels did not have a significant effect on bacterial community composition ($p = 0.69$, $R^2 \approx 0$).

4.3.4 Differentially abundant bacteria

The largest shift in bacterial community composition was observed passing the horohalinicum (salinity 5–8 PSU; Fig. 4.03A). This shift in community composition was attributed mostly to large differences in abundance, rather than presence/absence patterns. Lower salinity communities were enriched in *Cyanobiaceae* ($p < 0.0001$), *Rubritaleaceae* ($p = 0.0002$), *Sphingomonadaceae* ($p = 0.0002$), and *Spirosomaceae* ($p < 0.0001$) (contrasts between 0–5 PSU versus 30–36 PSU, all p-values Benjamini-Hochberg corrected; Fig. 4.03A). High-saline communities were characterised by high relative abundances of amongst others *Alteromonadaceae* ($p < 0.0001$), *Granulosicoccaceae* ($p = 0.001$), *Hyphomonadaceae* ($p < 0.0001$), *Sulfurovaceae* ($p < 0.0001$), and *Thiotrichaceae* ($p < 0.0001$) (contrasts between 0–5 PSU versus 30–36 PSU, all p-values Benjamini-Hochberg corrected; Fig. 4.03A). These differences become more pronounced when comparing oligohaline communities with increasingly higher salinity communities (i.e., the differences between the euhaline and oligohaline form a starker contrast than the differences between the mesohaline and oligohaline).

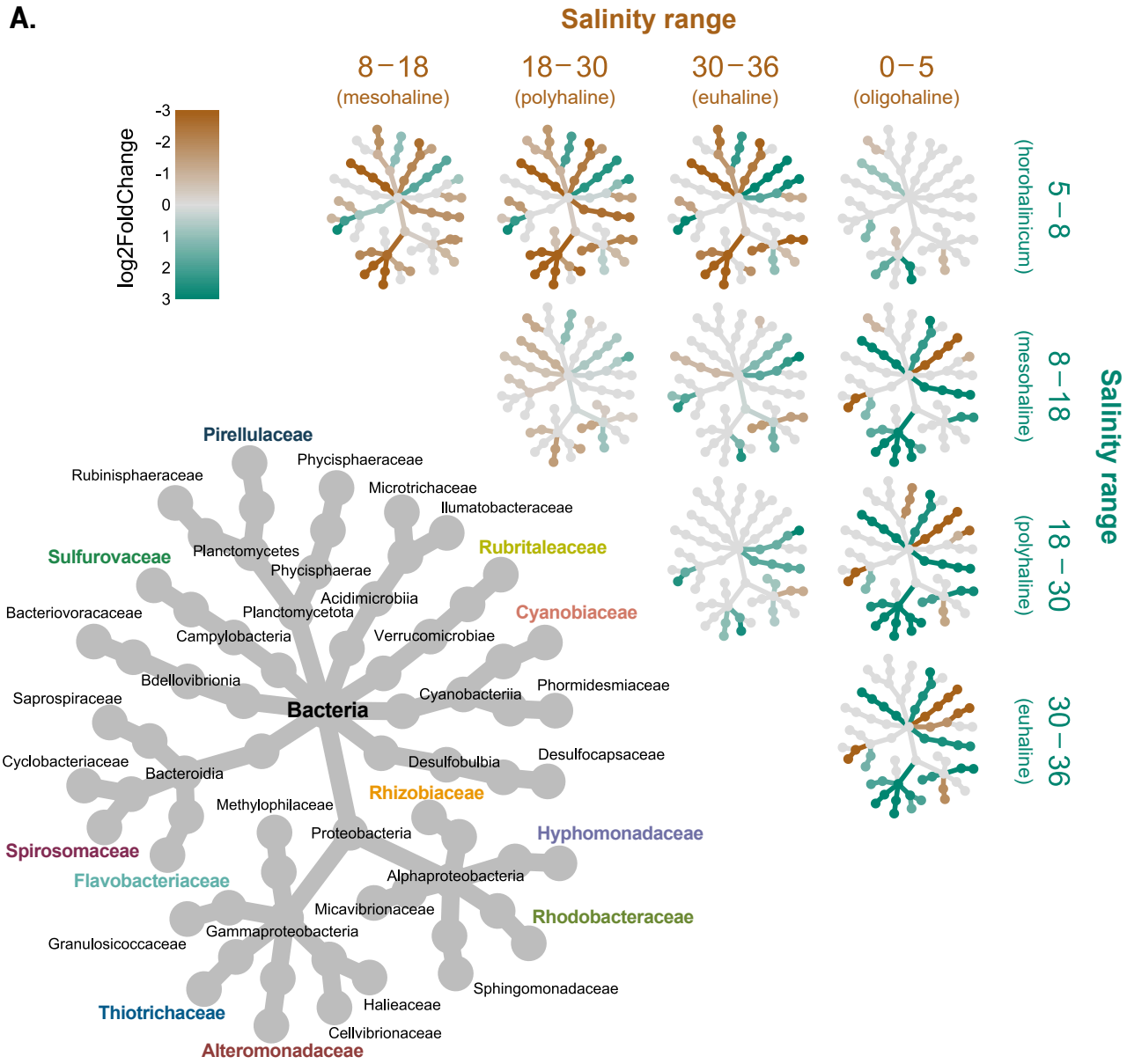
A.
Salinity range
8−18
(mesohaline)
18−30
(polyhaline)
30−36
(euhaline)
0−5
(oligohaline)
log2FoldChange
-3
-2
-1
0
1
2
3
5−8
(horohalinicum)
8−18
(mesohaline)
18−30
(polyhaline)
30−36
(euhaline)
Salinity range
Pirellulaceae
Phycisphaeraceae
Rubinisphaeraceae
Microtrichaceae
Ilumatobacteraceae
Rubritaleaceae
Sulfurovaceae
Planctomycetes
Phycisphaerae
Acidimicrobiia
Bacteriovoracaceae
Planctomycetota
Cyanobiaceae
Campylobacteria
Verrucomicrobiae
Bdellovibrionia
Saprospiraceae
Cyanobacteriia
Phormidesmiaceae
Bacteria
Cyclobacteriaceae
Bacteroidia
Desulfobulbia
Desulfocapsaceae
Rhizobiaceae
Methylophilaceae
Proteobacteria
Hyphomonadaceae
Spirosomaceae
Alphaproteobacteria
Flavobacteriaceae
Micavibrionaceae
Rhodobacteraceae
Gammaproteobacteria
Granulosicoccaceae
Sphingomonadaceae
Halieaceae
Thiotrichaceae
Cellvibrionaceae
Alteromonadaceae

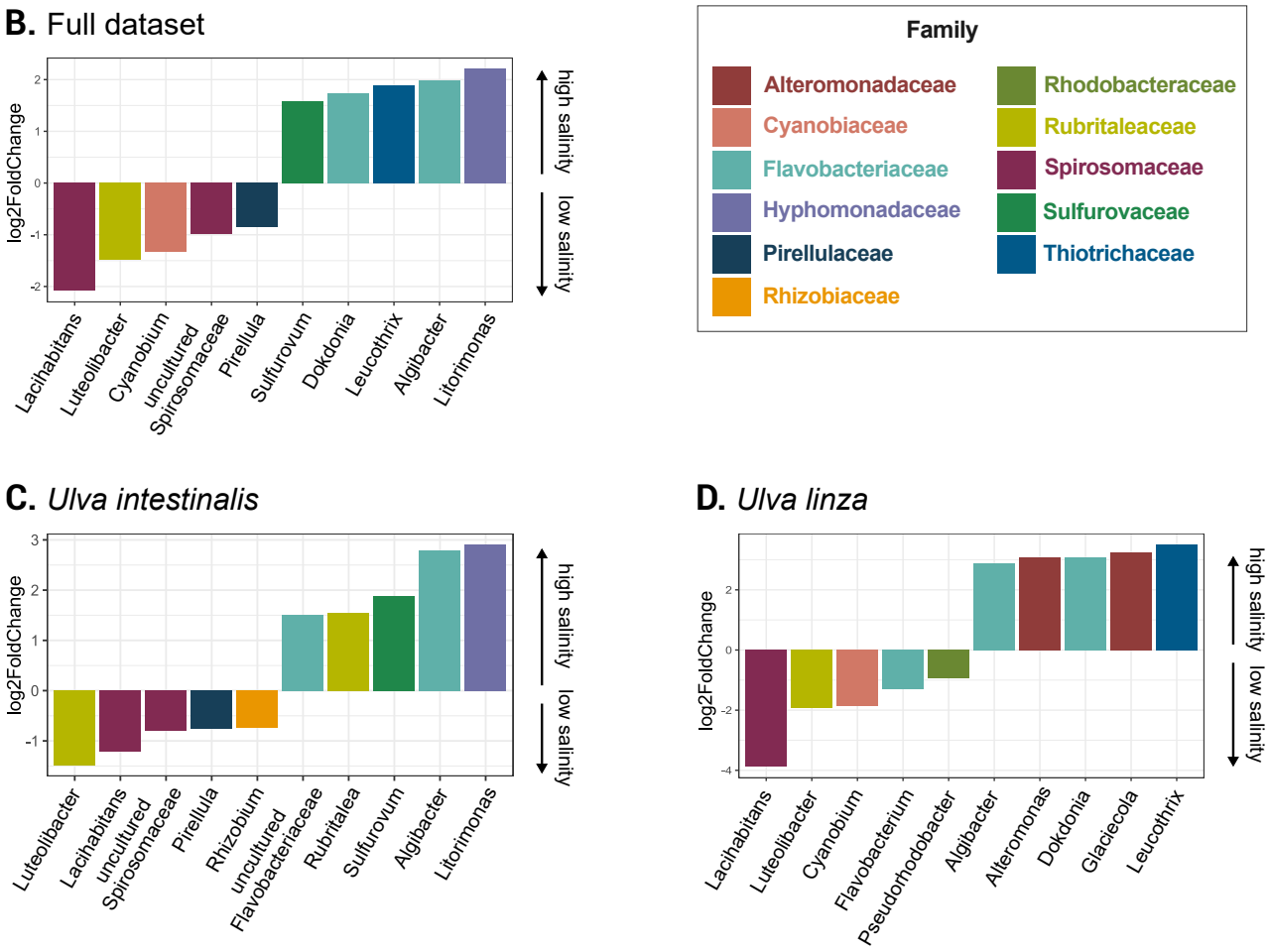

FIGURE 4.03 Overview of the significantly differential abundant bacterial families and genera associated with *Ulva sensu lato* across Atlantic–Baltic salinity ranges.

◀ Panel A) on the left page shows the pairwise comparisons of phylogenetic heat trees depicting the 28 bacterial families associated with *Ulva*, *Blidingia*, and *Kornmannia*. The larger, grey tree on the lower left functions as a taxonomic key for the smaller unlabelled trees. The smaller trees provide contrasts between five salinity zones: 0–5 PSU (oligohaline), 5–8 PSU (horohalinicum), 8–18 PSU (mesohaline), 18–30 PSU (polyhaline), and 30–36 PSU (euhaline). The colour (brown to green) of the nodes and edges corresponds to the log2FoldChange (only significant differences are coloured, $p < 0.05$, Benjamini-Hochberg corrected). Taxa coloured brown were enriched in the salinity zones in columns, whereas taxa coloured green were enriched in salinity zones in rows. For example, *Rubritaleaceae*, *Spirosomaceae*, and *Cyanobiaceae* were enriched in the oligohaline (brown) compared to most of the higher salinity zones (green).

▲ Panels B), C), and D) show bar graphs of the top 10 differentially abundant genera between high and low salinity, based on (B) the full dataset when controlled for host species, (C) *Ulva intestinalis* samples only, and (D) *Ulva linza* samples only. The log2FoldChange is expressed on the y-axis and genus on the x-axis. Colours of the bars correspond to family level (similar colours as used in the phylogenetic heat tree).

A total of 70 bacterial genera were differentially abundant with changing salinity levels (with $p < 0.01$, Benjamini-Hochberg corrected; see Electronic Supplementary Table S4.05 for an overview of all log2FoldChange and p-values). Low salinity communities especially contained high relative abundances of *Luteolibacter* (*Rubritaleaceae*), *Cyanobium* (*Cyanobiaceae*), *Pirellula* (*Pirellula*ceae), *Lacihabitans* (*Spirosomaceae*), and an uncultured *Spirosomaceae* (Fig. 4.03B). High salinity communities were predominantly enriched in *Litorimonas* (*Hyphomonadaceae*), *Leucothrix* (*Thiotrichaceae*), *Sulfurovum* (*Sulfurovaceae*), *Algibacter*, and *Dokdonia* (both *Flavobacteriaceae*) (Fig. 4.03B; Fig. S4.04).

As *Ulva intestinalis* and *Ulva linza* co-occurred over the entire salinity gradient from the North Sea to the Baltic Sea (Electronic Supplementary Table S4.02), they provided a good opportunity to assess differences in host species. Both *Ulva* species contained high relative abundances of *Luteolibacter* and *Lacihabitans* in low salinity sites, but *U. intestinalis*' low-saline communities were further characterised by *Pirellula*, *Rhizobium*, and an uncultured *Spirosomaceae*, whereas *U. linza* communities mainly contained *Cyanobium*, *Flavobacterium*, and *Pseudorhodobacter* (Fig. 4.03C, D). Likewise in high salinity environments, both host species had high abundances of *Algibacter*, but *U. intestinalis* had significantly more *Litorimonas*, *Sulfurovum*, *Rubritalea*, and an uncultured *Flavobacteriaceae* with increasing salinity. *U. linza* on the other hand typically contained more *Leucothrix*, *Glaciecola*, *Dokdonia*, and *Alteromonas* in high salinity (Fig. 4.03C, D).

When comparing the bacterial communities of *Ulva* species (*Ulvaceae*) with the more distantly related *Kornmannia leptoderma* (*Kornmannia*ceae), *Ulva* harboured significantly higher abundances of *Algitalea*, *Marinagarivorans*, and *Algibacter* compared to *Kornmannia leptoderma*, whereas the latter typically contained more *Cellulophaga*, *Sulfurovum*, and *Altererythrobacter* ($p < 0.01$, Benjamini-Hochberg corrected). Compared to *Blidingia minima* (*Kornmannia*ceae), *Ulva* was enriched in *Rubritalea*, *Algitalea*, and *Roseitalea*, while *Phormidesmis*, *Roseibacillus*, and *Jannaschia* were associated with *Blidingia* ($p < 0.01$, Benjamini-Hochberg corrected).

Despite host species having a clear effect on the associated bacteria, the correlation between host phylogeny and bacterial community composition was very weak (Mantel test, $p = 0.004$, $r = 0.03$).

4.3.5 Variance partitioning

Salinity, host species, and habitat together explained between 34–91% of the variation in the abundance of the bacterial genera (Fig. 4.04; Fig. S4.05). In concordance with the differential abundance analyses (based on log2FoldChange), the variation was best explained for *Lacihabitans* (91% variation explained), *Leucothrix* (86%), *Algitalea* (84%), *Dokdonia* (84%), *Luteolibacter* (83%), and *Algibacter* (81%). For most genera, the interaction between salinity and host species explained the highest proportion, followed by the single effects of salinity and host species (Fig. 4.04). Salinity explained a lot of variation for *Litorimonas* (39%) and *Cyanobium* (29%), whereas host species explained a high portion of the variation in *Mesorhizobium* (49%, especially abundant in *Ulva linza*), *Roseitalea* (47%, less abundant in *Blidingia* and *Kornmannia*), *Fuerstia* (44%, especially abundant in *U. compressa*, *U. fenestrata*, and *U. lacinulata*), *Ensifer* (43%, enriched in *Kornmannia*), *Marinagarivorans* (40%, enriched in *Kornmannia*), and *Jannaschia* (31%, enriched in *Blidingia*).

Habitat explained little of the variation in most genera, except for *Roseivivax* (61%) and *Olleya* (21%) (Fig. 4.04). Additional DESeq2 analysis indicated *Roseivivax* was especially abundant on algae collected from sandy habitats and *Olleya* on algae growing on metal. Although relatively few samples in green tide events were collected ($n = 8$), patterns could be distinguished. For example, the green tide in Gryt on the Baltic coast of Sweden (salinity = 7.0), consisted of *Ulva intestinalis* ($n = 2$ samples). These Gryt green tide algal microbiomes were mainly characterised by the abundant presence of *Rhodopirellula* and *Rubripirellula* (both Planctomycetota)

compared to the bacterial communities of non-green tide *Ulva intestinalis* specimens collected at the same site or neighbouring sites (n = 3 samples) (Fig. S4.06). The green tide in Frederikshavn in Denmark (salinity = 30.0) was caused by *Ulva lacinulata*. Compared to *U. lacinulata* specimens growing attached in the same harbour (n = 2), the green tide communities (n = 3) were enriched in *Thiothrix*, *Limibaculum*, *Pseudophaeobacter*, *Octadecabacter*, and *Sulfitobacter* (all Proteobacteria) (Fig. S4.06).

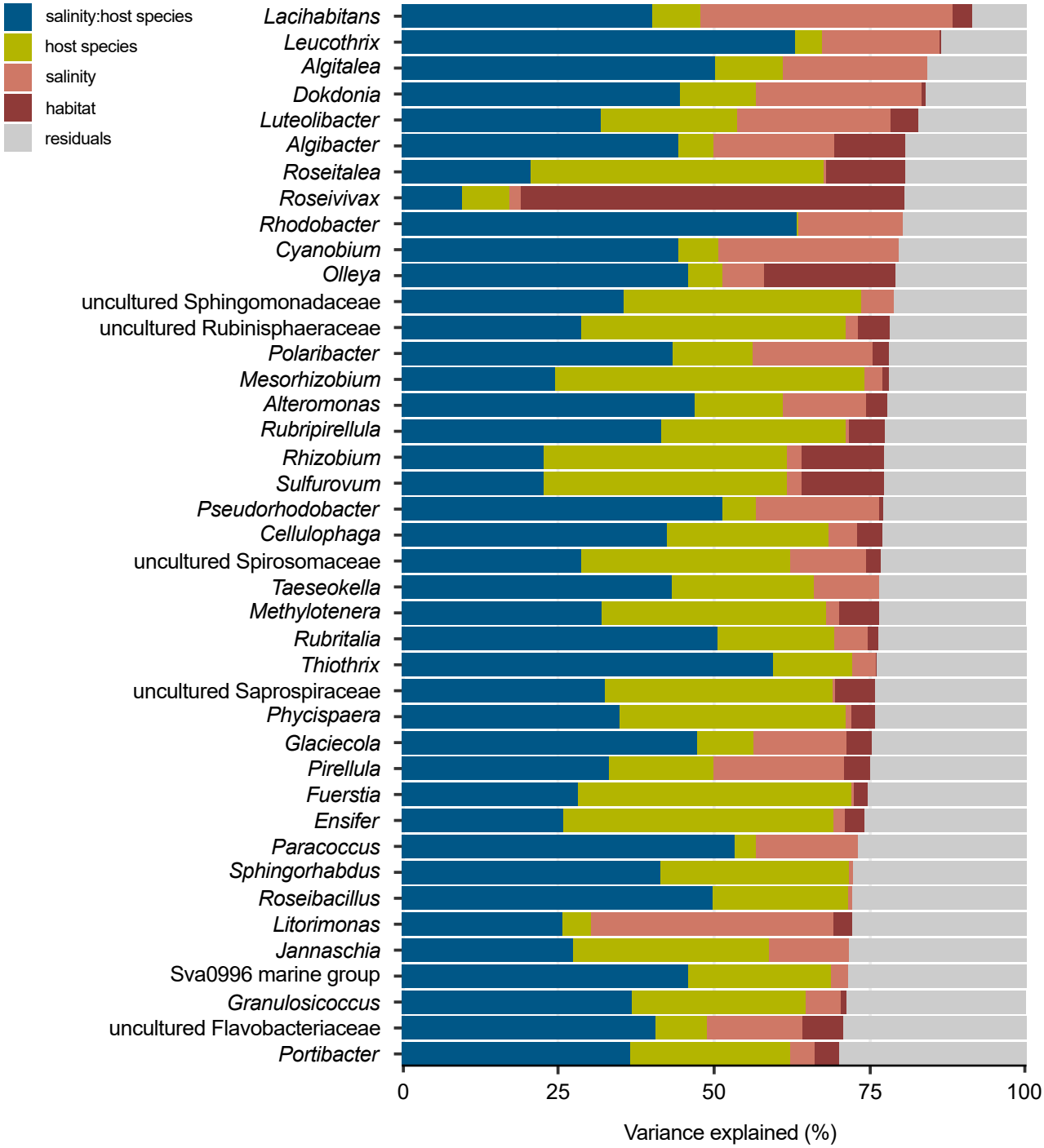

FIGURE 4.04 Variance partitioning plot showing the amount of variance in abundance of *Ulva sensu lato* associated bacterial genera explained (in %) by the interaction between salinity and host species (salinity:host species), host species, salinity, and habitat. Based on a generalised linear mixed model (negative binomial family). Only genera for which >70% of the variation was explained are shown. For a graph containing all genera, see Fig. S4.05.

4.3.6 Bacterial core

The number of core taxa and members of the core bacterial community varied tremendously depending on the threshold settings of relative abundance and prevalence (% of samples in which the taxa occurs) (Fig. 4.05). When setting the limits to ≥0.1% abundance and ≥50% prevalence, >60 genera were considered part of the core of *Ulva sensu lato* along the entire salinity gradient. However, with strict thresholds of ≥1% relative abundance and ≥90% prevalence, only two genera were defined as core taxa: an uncultured *Rhodobacteraceae* and *Sulfitobacter*. When the prevalence threshold was lowered to ≥80%, *Paracoccus* became part of the core bacterial community as well, and when the prevalence was set to ≥70%, an uncultured *Rhizobiaceae*, *Yoonia-Loktanella*, and an uncultured *Saprospiraceae* became additional members.

Across the salinity gradient, a shift in core community composition occurred. Five taxa were considered core across all species in the oligohaline region (0–5 PSU) and four taxa in the horohalinicum (5–8 PSU) with ≥75% prevalence and ≥1% relative abundance (Fig. 4.06A). In addition to the three taxa considered core across the entire salinity gradient (*Sulfitobacter*, *Paracoccus*, and an uncultured *Rhodobacteraceae*), these low salinity ranges also shared *Luteolibacter* as core genus. The mesohaline samples (8–18 PSU) contained five core taxa, the polyhaline samples (18–30 PSU) six core taxa, and the euhaline samples (30–36 PSU) five core taxa. These higher salinity regions all shared an uncultured *Rhizobiaceae* in their core. In addition, the mesohaline and polyhaline core both included *Yoonia-Loktonella*, and the polyhaline and euhaline shared an uncultured *Saprospiraceae* (Fig. 4.06A).

Core membership did not only shift with salinity. The different host species were also associated with distinct core consortia (Fig. 4.06B). *Ulva intestinalis* and *Ulva linza* shared the same geographical range, but the *U. intestinalis* core was larger (seven taxa) and included amongst others *Yoonia-Loktanella*, an uncultured *Sphingomonadaceae*, *Erythrobacter*, and *Roseovarius*, while the *U. linza* core was smaller (four taxa) and included only an uncultured *Saprospiraceae* in addition to the three main core members. *Ulva fenestrata*, a more typical marine species, was the only host with *Granulosicoccus* and *Blastopirellula* in its core. *Blidingia minima* shared a large proportion of its core with *Ulva intestinalis*, but additionally included *Jannaschia* and *Altererythrobacter*. *Kornmannia leptoderma* in particular had high relative abundances of core taxon *Altererythrobacter* as well.

4.4 Discussion

Seaweeds and associated bacteria show interdependent and complex dynamics. Here, we tested stability of *Ulva*-associated bacterial communities across a stable salinity gradient in the Atlantic–Baltic Sea. In addition, we made use of the rich diversity of *Ulva* species in the study area, with some species covering the entire salinity gradient, to characterise species-specific responses versus environmentally driven variation.

4.4.1 Salinity driven seaweed–bacterial interactions

The Baltic Sea is characterised by its strong and stable salinity gradient. Salinity has been identified as the most important structuring factor on seawater and sediment microbial consortia (Herlemann et al. 2011, Dupont et al. 2014). This agrees with our study, which showed that *Ulva*-associated bacterial composition is strongly structured primarily by salinity and secondarily by host species.

The largest shift in the bacterial consortia of *Ulva sensu lato* was observed passing the horohalinicum (5–8 PSU) from low salinity to higher salinity. The brackish to full marine transition has also been termed "critical salinity region", as this is the salinity range where many chemical, physical, and biological processes abruptly

change (Telesh and Khlebovich 2010). For example, the ion Ca/Cl ratio is stable down to 7 PSU, but below this salinity level the ratio drastically changes. Similar non-linear dynamics are observed for, e.g., silicon concentration, suspended matter concentration, and the stability of phosphorus compounds. In the Baltic Sea, the horohalinicum coincides with the Darss Sill (situated East of the Danish Straits; Fig. 4.01). This likely explains why most of the *Ulva* species' distribution is limited to the North Sea and Danish Straits. The distribution of bacteria associated with *Ulva sensu lato* is clearly affected as well and this study is the first report of a host-associated bacterial communities changing drastically in the horohalinicum.

The effect of salinity on seaweed bacteria has rarely been investigated in laboratory experiments. Two exceptions include the long-term mesocosm studies conducted on the red seaweed *Gracilaria vermiculophylla* collected at the North Sea coast of Germany (Saha et al. 2020b), and the brown seaweed *Fucus vesiculosus* collected in the Kiel fjord in the western Baltic (Stratil et al. 2014). *Gracilaria vermiculophylla* is non-native in Europe and has also been introduced in the Baltic Sea where it occurs across a wide salinity range. Both the bacterial communities of *Gracilaria* and *Fucus* were strongly impacted by salinity. Despite the occurrence of some shared bacterial taxa in *Ulva* and *Gracilaria* microbiomes, for example *Dokdonia* in higher salinity communities, the bacterial microbiomes of respective seaweeds are very different. Comparisons between *Ulva*- and *Fucus*-associated bacteria likewise result in very few shared taxa. Although salinity overall had a greater effect than host species in our study, it is possible that the evolutionary distances between the genera *Ulva*, *Gracilaria*, and *Fucus* are large enough to overrule salinity (Lachnit et al. 2009).

Our results may suggest that some of the typical low-salinity bacteria in *Ulva* microbiomes (e.g., *Lacihabitans*, *Luteolibacter*, and *Cyanobium*), could facilitate acclimation of the host to low salinity in the Baltic. The effect of specific bacterial taxa on host tolerance to lower salinities has so far only been tested in the brown algal genus *Ectocarpus* (Dittami et al. 2016). In *Ectocarpus*, two bacterial OTUs — *Haliea* and an uncultured Sphingomonadales — were linked to increased host performance when the algae were first cultivated in seawater medium and subsequently in freshwater medium (Dittami et al. 2016). Axenic (bacteria-free) cultures of an *Ectocarpus* strain originally isolated from a freshwater environment did not survive in freshwater medium, nor did they survive the change from seawater to freshwater medium. Acclimation to freshwater medium was only possible if the axenic strain was inoculated with medium containing bacteria of the non-axenic cultures (Dittami et al. 2016). To be able to experimentally test whether characteristic low-salinity consortia in *Ulva* bacterial communities likewise stimulate host acclimation to freshwater, isolation and cultivation of the associated bacteria and subsequent experimental work with axenic *Ulva* are required.

4.4.2 Disentangling the effects of spatial distance and salinity

In essence, all environmental gradients in the Baltic are spatial gradients in northeast–southwest direction. The samples in this study were collected on a 2,000 km transect. The shortest route across water from the most inland sampling site (Skepssmalen, Sweden) to the most outer sampling site (Egersund, Norway) was over 1,670 km. The spatial effect is statistically hard to separate from the environmental salinity gradient. However, 13 samples from five different sampling sites near the mouth of the Glomma river in the Oslofjord (Skagerrak; Fig. 4.01) provide a good test case. The Glomma is Norway's longest and most voluminous river. Sampling at the sites close to the Glomma river mouth took place in early July, right after its discharge flow peak in May–June (Frigstad et al. 2020). Measured salinity at these sites was between 5.1–13.6 PSU, which corresponds to prevailing central and northern Baltic salinity ranges, whilst the surrounding sites in the Skagerrak are characterised by salinity levels >20 PSU. As bacterial community composition at the sites influenced by the Glomma discharge

was in general more similar to central-northern Baltic microbiomes >1,000 km away, than to the Skagerrak sites only 20–50 km further south or west, salinity seems to overrule spatial distance (Fig. S4.03). The effect of host species is visible here as well. Regarding *Kornmannia leptoderma*, for example, the samples at the mouth of the Glomma river represent the lowest salinity levels in which the species was found in this study, but also the most northern records in our dataset. The samples were found at least 300 km more to the north than other *K. leptoderma* samples collected in the Danish Straits (salinity ~25 PSU), but are more similar to samples collected in the Baltic Proper (salinity ~7 PSU) that are geographically even further away. For seaweeds to recruit similar bacterial communities in specific environmental conditions despite large spatial distances, requires the bacteria to be widely dispersed in the environment. This agrees with the Baas-Becking hypothesis: "everything is everywhere but the environment selects." (Martiny et al. 2006).

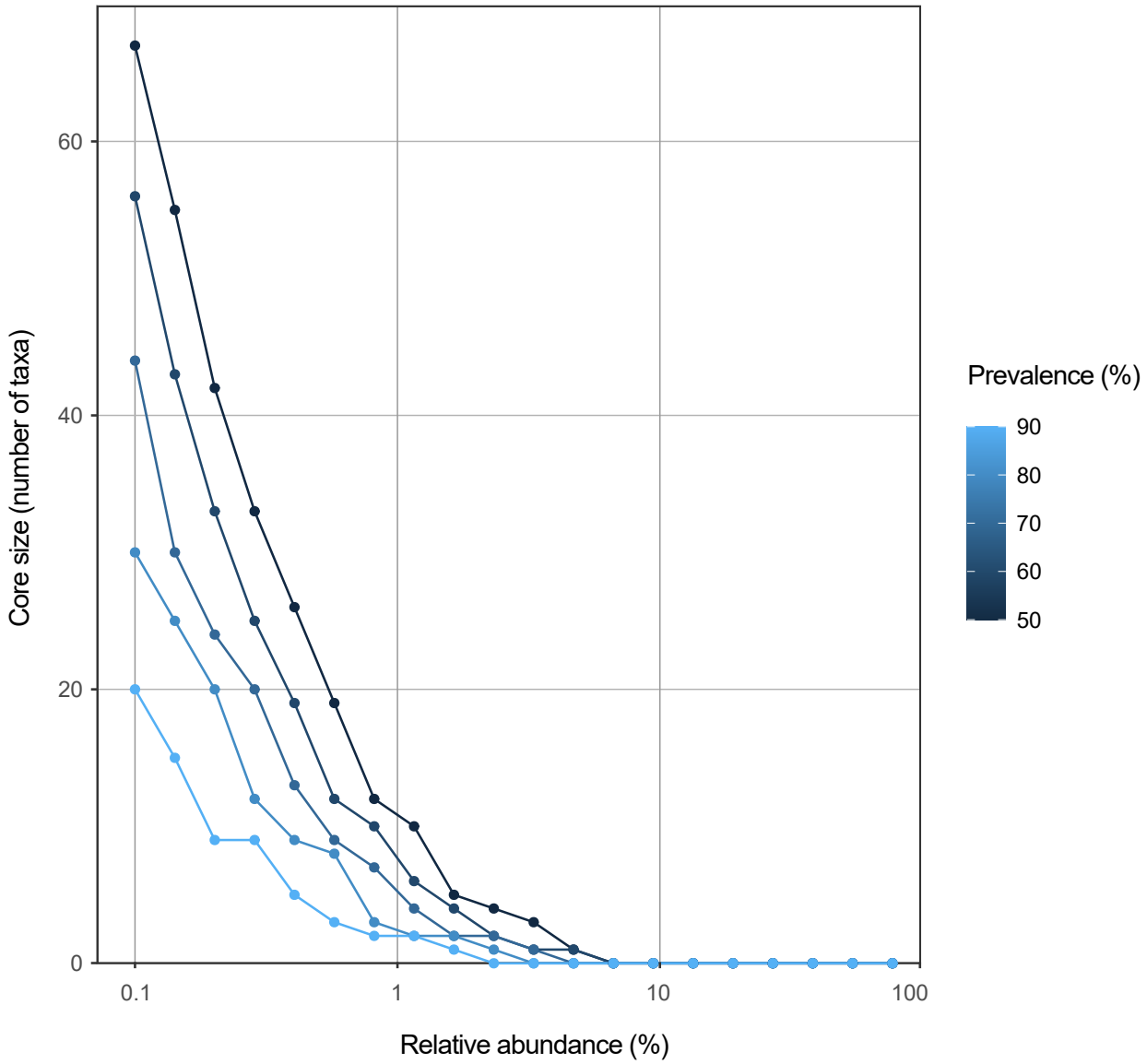

FIGURE 4.05 Bacterial core size (number of genera) of *Ulva sensu lato* across the entire Baltic salinity gradient with different relative abundance (based on read counts) and prevalence (based on the number of samples in which the taxa was encountered) thresholds.

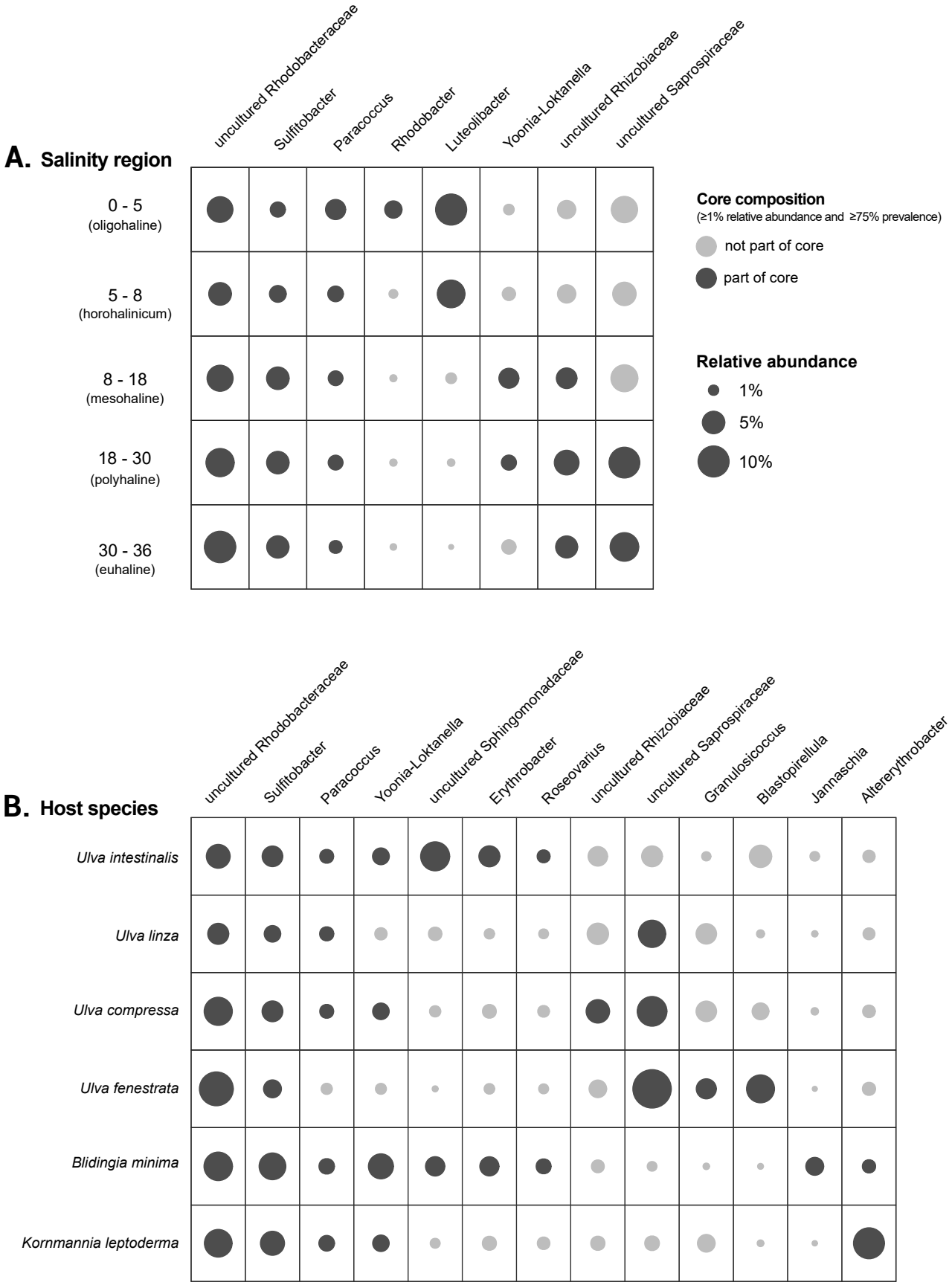

FIGURE 4.06 Mean relative abundance of bacterial core taxa of *Ulva sensu lato*, split by (A) salinity, and (B) host species. The circle size corresponds to relative abundance, and the dark grey shade indicates whether the taxon is part of the core community (based on >1% relative abundance and >75% prevalence).

4.4.3 The Baltic Sea and its multiple environmental gradients

Ulva sensu lato harbours distinct bacterial communities across the different salinity regions along the Atlantic–Baltic Sea transect. The Baltic, however, is not only characterised by a pronounced salinity gradient. Although less dramatic than the salinity gradient, the Baltic Sea also accommodates both a horizontal oxygen gradient (with the Kattegat and North Sea area being in general oxygen rich and the remainder of the Baltic Sea oxygen poor) and a vertical oxygen gradient (oxygen depletion at >50 m depth) (Villnäs and Norkko 2011). In addition, the Baltic experiences strong seasonal dynamics and is subjected to anthropogenic pressure (e.g., eutrophication, pollution, fisheries, shipping) (Ojaveer et al. 2010). Whilst both seawater surface temperature and oxygen levels were measured in this study and explained limited variance of bacterial community composition, the sample distribution was not designed to capture the full dynamics associated with these environmental factors.

The Baltic temperature gradient co-varies to some extent with salinity. In our study, lower temperatures were measured on the North Sea coast of Norway, and higher temperatures in the Baltic Proper (Fig. S4.01). As sampling was only carried out in Summer, yearly seasonal fluctuations were not represented. In addition, sampling was not restricted to a specific time of the day, hence small variations in the measured temperature between sites may have been caused by daily fluctuations. In Spring, sea surface temperatures usually increase earlier in the year in the south and west areas of the Baltic Sea compared to the northern and eastern areas (Mück and Heubel 2018). Bacterial community composition of seawater, therefore, does not only change with salinity as primary factor, but secondarily also with seasons (Andersson et al. 2010, Herlemann et al. 2016). In fact, these bacterioplankton community shifts display repeated patterns between years (Lindh et al. 2015). It is likely that, across the entire Baltic, *Ulva*-associated bacterial communities too experience seasonal dynamics, as has been shown before in local populations in the Kiel fjord (Lachnit et al. 2011), as well as in the Caribbean (Comba González et al. 2021).

Nutrients were not measured during this study but may drive some of the unexplained variation. The Atlantic–Baltic Sea salinity gradient is caused by freshwater input from sub-arctic rivers on one side of the gradient and limited water exchange with the marine water body of the North Sea on the opposite side of the gradient (Seidel et al. 2017). Freshwater river discharge does not only affect salinity, but simultaneously increases nutrient influx, including nitrate, phosphate, and dissolved organic carbon (Korth et al. 2012, Frigstad et al. 2020). Southern, high saline areas in the Baltic are characterised by high levels of autochthonous DOM (dissolved organic matter derived from e.g., phytoplankton primary production), whereas northern, low saline areas are richer in allochthonous DOM of terrestrial origin discharged by rivers (Rowe et al. 2018). This increased nutrient load is a major stimulator of bacterioplankton growth and pelagic productivity (Stepanauskas et al. 2002), and pelagic bacterial growth efficiency is highest in the low saline regions (Rowe et al. 2018). The community composition of bacteria living associated with *Ulva* may be impacted by prevailing nutrient conditions as well, but not necessarily following the same patterns as bacterioplankton, as the *Ulva* host likely provides its microbial partners (and other associates) with carbon and nutrients (Hudson et al. 2019).

4.4.4 Green tides: *Ulva* on the drift

Green tides are mass accumulations of unattached green seaweeds and are often caused by *Ulva* spp. They have profound negative effects on the environment, including reduced biodiversity, and smothering of the sea bed and its inhabitants (Ye et al. 2011, Wan et al. 2017). Decomposition of the *Ulva* biomass results in anoxic conditions and the release of gaseous sulphur compounds. In the Baltic Sea, where oxygen levels have already deteriorated over the past decades due to eutrophication, the anoxic conditions particularly pose a problem (Reusch

et al. 2018). In the formation of green tides too, eutrophication plays a major role (Smetacek and Zingone 2013). The microbial communities of green tide-forming ulvoid species have rarely been sequenced, but mass growth events of seaweeds are likely to induce a change in both the seaweed and environmental microbiome. Qu et al. (2020) for example demonstrated that sulphate-reducing bacteria and heterotrophic bacteria increased in abundance in sediment directly under an *Ulva prolifera* bloom in the Yellow Sea, especially towards the end of the bloom. In surface seawater samples, the abundance of heterotrophic diazotrophic bacteria increased likewise during *U. prolifera* blooms (Zhang et al. 2015). Diazotrophic bacteria are involved in N_2-fixation. Hence, altered microbial communities during green tide events may affect the sulphur and nitrogen cycles (Aires et al. 2019).

In the current study, green tides were encountered at Skive in Denmark (caused by *Ulva compressa* and *Ulva lacinulata*), Frederikshavn in the north of Denmark (caused by *Ulva lacinulata*), and Gryt in Sweden (caused by monostromatic *Ulva intestinalis*). Several of these samples were visible as distinct outliers in the NMDS plot (Fig. 4.02). In Frederikshavn, particularly high relative abundances of *Thiothrix* and *Sulfitobacter* were observed in green tide samples compared to attached thalli growing in the same harbour. These are sulphur-oxidising bacteria (SOB), and *Sulfitobacter* is additionally known to promote *Ulva* growth (Krishnani et al. 2010, Grueneberg et al. 2016). Growth-promoting bacteria produce metabolites and chemical compounds such as thallusin that induce cell division and thallus differentiation, including rhizoid formation and the proper development of cell walls, in *Ulva* (Alsufyani et al. 2020). In turn, *Ulva* can attract growth-promoting bacteria through the release of the chemoattractant dimethylsulfoniopropionate (DMSP). In some cases, SOB form visible mats on the sediment or on degrading organic material, such as seaweed tissue (Fenchel et al. 2012). Depending on the green tide phase, autotrophic as well as mixotrophic SOB could take advantage of degrading *Ulva* tissue for carbon and sulphur sources.

In Gryt, green tide samples were enriched in *Rhodopirellula* and *Rubripirellula* compared to non-green tide *U. intestinalis* thalli in neighbouring sites. Both bacterial genera belong to the Planctomycetota. These bacteria are adapted to life in marine biofilms, as they have a holdfast that accommodates surface colonisation, they can reproduce by budding, and can quickly adapt to environmental changes (Kallscheuer et al. 2020). In addition, they have large genomes that often encode for a large number of sulphatase genes. The genome of *Rhodopirellula baltica*, for example, contains 110 sulphatases (Wegner et al. 2013). Sulphatases enable the degradation of sulphated polysaccharides such as ulvan in the *Ulva* cell wall. Planctomycetota are known to be abundant on algal surfaces and their high abundance in green tide samples may simply be caused by the large accumulation of biomass (Bondoso et al. 2017, Wiegand et al. 2021).

Drifting seaweeds are not always necessarily green tides. All foliose *Ulva compressa* samples in this study were collected as unattached specimens, of which most without the occurrence of mass accumulations. Interestingly, all tubular shaped *U. compressa* were found growing attached to substrates, such as rock and concrete. The bacterial communities of foliose versus tubular *U. compressa* were distinctly different. However, all foliose samples were collected at low salinity (<20 PSU) and the tube-shaped at high salinity (>20 PSU). It is, therefore, not possible with the current dataset to resolve whether differences in the *U. compressa* bacterial communities fundamentally differ with morphology or salinity.

4.4.5 *Ulva* core bacterial communities along an environmental gradient

Although the *Ulva*-associated bacterial communities varied with salinity and host species, a small, stable consortium can be identified as well. The term "core microbiome" was initially used to describe a set of microbes or genes shared by the majority of host specimens in a given habitat (Turnbaugh et al. 2007). This is often referred to as a "common core", but the core concept has since been used in a broader context. Core microbiome members are, for example, hypothesised to play a key role in ecosystem functioning or may significantly affect host fitness and resilience to disturbance (Shade and Handelsman 2012). Such "functional cores" are based on commonly occurring functional genes rather than taxonomical units (Risely 2020). Whether based on taxonomy or function — the nature of a core can vary from being "substantial" (the majority of individuals/samples share a large proportion of the microbial consortia), to "minimal" (all individuals/samples only share a few core members), or even "non-existent" (no taxa or genes in common across the majority of individuals/samples) (Hamady and Knight 2009). In addition there are "gradient" core models (in which individuals close to each other on a gradient share more microbial components than individuals at opposite ends of the gradient) and "subpopulation" core models (distinct subpopulations of host species each have their own, unique core) (Hamady and Knight 2009).

Following the different core models described in Hamady and Knight (2009), we can define *Ulva*-associated bacterial communities across the Baltic as having a "minimal" taxonomic core (only three taxa are shared across the entire gradient), with in addition a "gradient" core (more taxa are shared between neighbouring salinity ranges than between ranges at opposite ends of the Atlantic–Baltic Sea gradient). Depending on the chosen prevalence and relative abundance settings, the minimal core consisted of *Sulfitobacter*, *Paracoccus*, and an uncultured *Rhodobacteraceae*. Together they made up on average 14% of the reads per sample. *Sulfitobacter* and *Paracoccus* are known growth-promoting and morphogenesis-inducing bacteria of *Ulva* (Ghaderiardakani et al. 2017, 2019), and are thus unsurprising core members. Possible beneficial interactions with the uncultured *Rhodobacteraceae* are unknown, but several of the reads assigned to this family did have a strong match to sequences in the NCBI database extracted from an *Ulva prolifera*-seawater interface (GenBank accession number JF769698.1).

Some gradient core taxa were clearly defined by differences in relative abundance. *Luteolibacter*, for example, was highly abundant in low salinity levels (7–9% % relative abundance) and scarcely present in higher salinity (<1% relative abundance), which was also demonstrated by the differential abundance analyses. Other gradient core taxa were defined predominantly by prevalence. An uncultured *Saprospiraceae*, for example, was quite abundant across the entire salinity gradient (5–9% relative abundance), but was only part of the bacterial core in higher salinities due to low prevalence at lower salinity levels. These varying prevalence levels might be due to differences among host species, as the uncultured *Saprospiraceae* was a highly abundant core member of *U. linza*, *U. compressa*, and *U. fenestrata*, but did not have a high prevalence and abundance in *U. intestinalis*, *Blidingia minima*, and *Kornmannia leptoderma*.

At host species level, the core consortia were slightly larger, varying from four to nine core members. Interestingly, the core community of *U. intestinalis* was more similar to the core of *Blidingia minima* than to *Ulva linza*, despite *U. intestinalis* and *U. linza* sharing a similar geographical range. The same pattern was observed in the NMDS plot, in which *U. intestinalis* and *B. minima* samples were clustered to the left of the plot, while the *U. linza* cluster was located to the right of the plot. The Mantel test showed that overall bacterial community composition did not differ with host phylogeny, indicating that differences in bacterial communities between host species were caused by intrinsic factors (e.g., biochemical composition and defence mechanism).

As the definition of a core community is flexible, the decision on which taxa should be considered core members and whether a core community exists at all remains arbitrary. Some studies define core taxa purely based on prevalence (Aires et al. 2015), others use both relative abundance and prevalence (Ainsworth et al. 2015), and again others use models (Shade and Stopnisek 2019, Bonthond et al. 2020). The threshold settings used vary tremendously as well, and rarely have biological justifications, hence the resulting core depends on the authors (Risely 2020). In *Ulva*, the taxonomic variability has often been deemed too large to contain a core consortium. A study on *Ulva australis*, for example, demonstrated only six bacterial species were consistently present in all samples (n = 6), and while these did make up on average 15.6% relative abundance per sample, a core was considered non-existent (Burke et al. 2011b). These results are relatively similar to our dataset, with three genera contributing up to 14% of the reads per sample. The larger the dataset and the wider the geographical scale investigated, the less likely it becomes to define a large core microbiome (Turnbaugh et al. 2007). Roth-Schulze et al. (2018) investigated the bacterial communities of three *Ulva* species in Spain and Australia, but found only one common OTU representing only 0.33% of the total number of sequences. On the contrary, >70% of the functional genes were shared across the microbiomes of all three *Ulva* species independent of biogeography, and the remaining 30% could possibly be linked to environmental adaptation. The large biogeographical scales in the aforementioned study, however, were not associated with obvious environmental gradients, and bacterial communities may therefore seem to be influenced mostly by stochastic processes. The results from our study, however, indicate a large deterministic effect of the environment. Future studies investigating the functional repertoire of bacterial communities across the Atlantic–Baltic gradient could show whether the *Ulva*-associated functional core likewise follows a gradient model, and if such functional patterns could be linked to the taxonomic core.

4.5. Conclusion

In conclusion, salinity and host play a major role in *Ulva*-associated bacterial community structure. Pronounced differences between low and high salinity communities manifest themselves through defined patterns in differential abundance rather than presence/absence patterns of certain bacteria. Deviations from the predominant pattern at a distinct salinity can often be ascribed to microhabitats (e.g., high saline rock pools, green tides, river mouths) that differ from the prevailing conditions on surrounding sites. We identified a small taxonomic core consortium with in addition a few gradient core members that change across the salinity gradient. Future studies with experimental work could focus on causal relationships between bacteria and host tolerance towards fluctuating salinity, as well as functional analyses across the entire Atlantic–Baltic salinity gradient.

Acknowledgements

The research leading to the results presented in this publication was carried out with infrastructure funded by the FWO PhD Fellowship fundamental research (3F020119), the EMBRC Belgium – FWO project I001621N, the Formas national research program for food (grant no 2020-03119), and Portuguese national funds from FCT - Foundation for Science and Technology through project UIDB/04326/2020 and contract CEEC-INST/00114/2018. We would like to thank Samanta Hoffmann for her assistance during field work.

Author contributions

L.M.L.: Methodology, Formal analysis, Investigation, Data curation, Writing – original draft, Visualisation. **S.D.:** Investigation, Resources, Writing - Review & Editing. **A.H.E.:** Conceptualizatio, Writing - Review & Editing. **H.P.:** Conceptualization, Writing - Review & Editing. **G.B.T.:** Conceptualization, Writing - Review & Editing. **A.W.:** Resources, Supervision, Writing - Review & Editing. **F.W.:** Investigation, Writing - Review & Editing. **O.D.C.:** Resources, Supervision, Funding acquisition, Writing - Review & Editing. **S.S.:** Conceptualization, Investigation, Writing - Review & Editing.

Data availability statement

Raw sequence reads and metadata are deposited at SRA (BioProject PRJNA781821). The *tuf*A sequences generated in this study to identify host species are deposited in GenBank and accession numbers can be found in Table S4.01. Supplementary data to this article can be found online at https://onlinelibrary.wiley.com/doi/full/10.1111/mec.16462.

Supplementary Figures

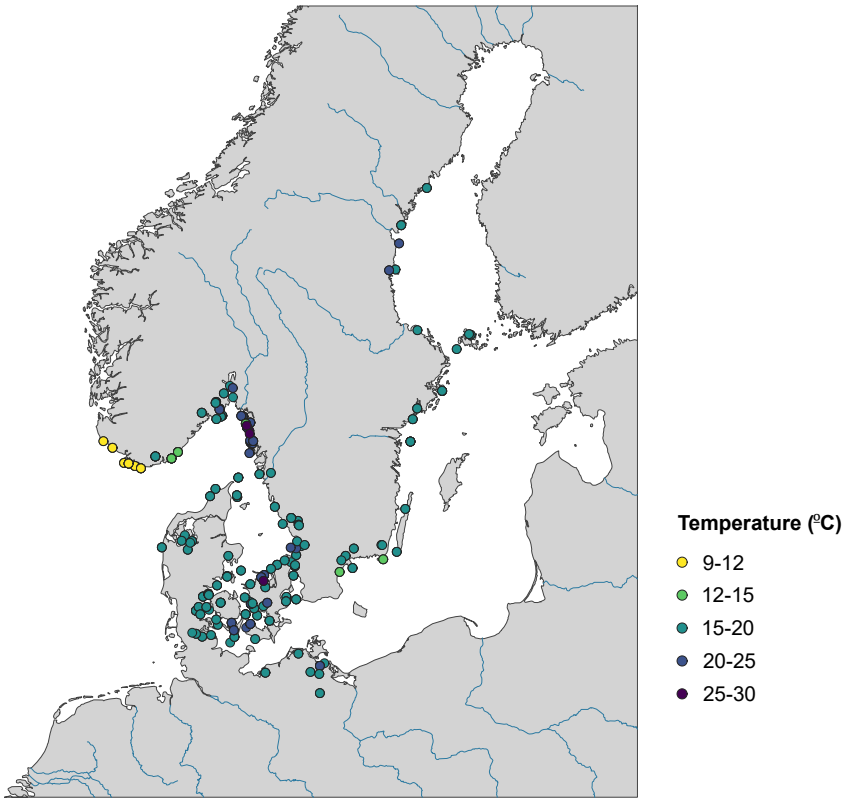

FIGURE S4.01 Map showing sample sites in the Baltic Sea and adjacent areas. The colour of the sites corresponds to the measured seawater temperature (°C). Major rivers are projected in blue.

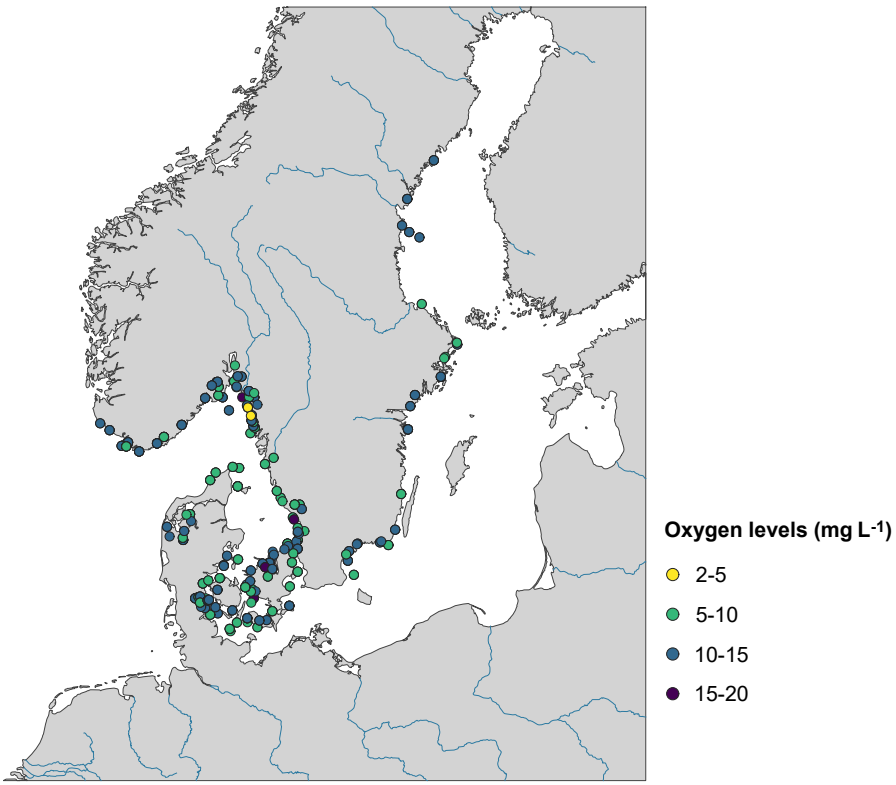

FIGURE S4.02 Map showing sample sites in the Baltic Sea and adjacent areas. The colour of the sites corresponds to the measured oxygen levels (mg L^{-1}). Major rivers are projected in blue.

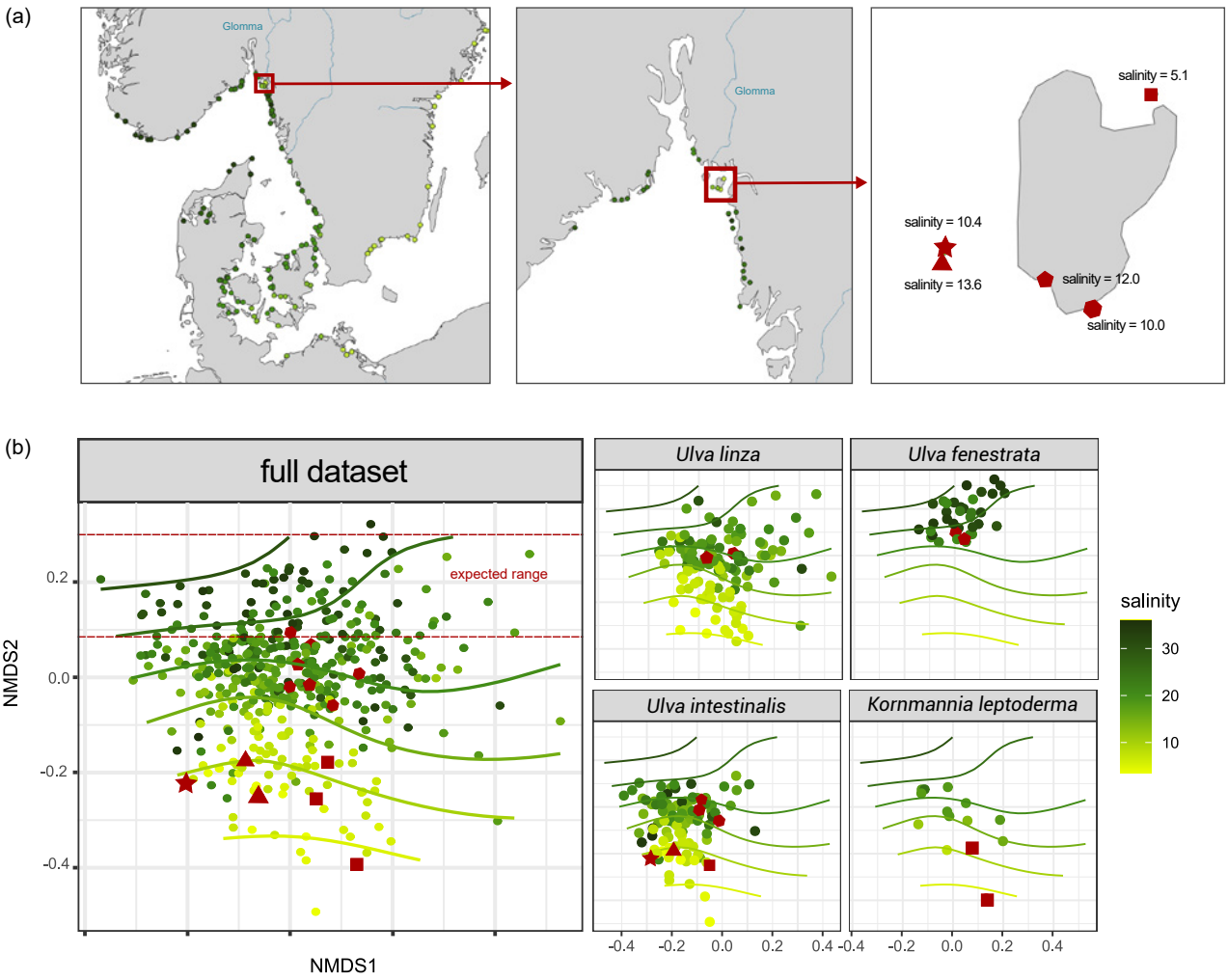

FIGURE S4.03 Overview of the sample sites near the Glomma river mouth. (A) map showing the location of the Glomma river sample sites. On the map on the right, the measured salinity at each of the 5 sites is given. The symbol shape of the sites matches the symbols in the NMDS plot. (B) NMDS plots (stress = 0.01, k = 4) of bacterial community composition (based on Bray-Curtis dissimilarities and genus level identifications). The first panel shows the full dataset (n = 481 samples). The remaining panels are split by host species (*Ulva linza*, *Ulva fenestrata*, *Ulva intestinalis*, and *Kornmannia leptoderma*). The NMDS plot is similar to Figure 2 (see main manuscript), with colours representing measured salinity, but the Glomma river samples are coloured red. The red dashes indicate the expected range of the samples with regards to their spatial distribution.

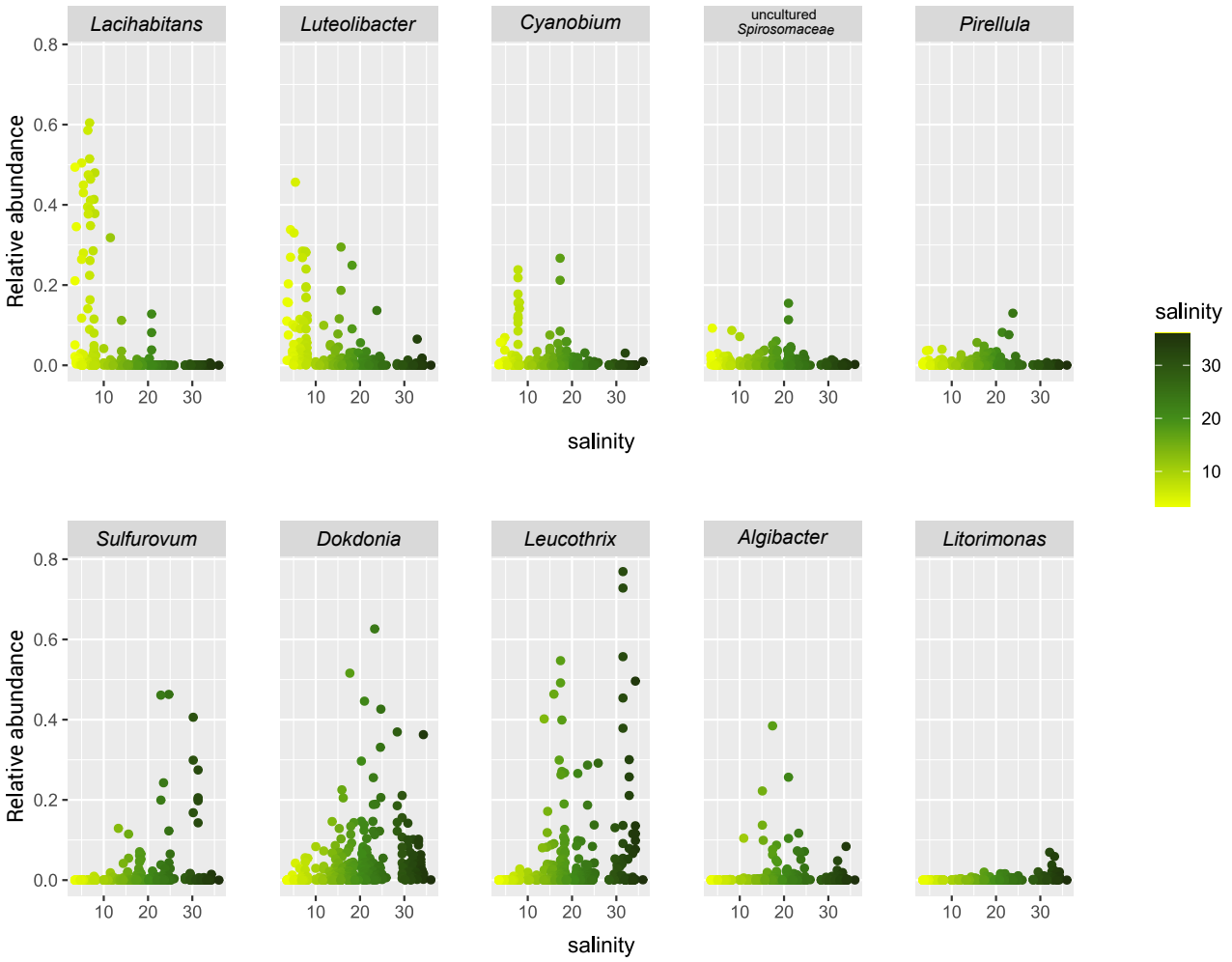

FIGURE S4.04 Scatterplots showing the relative abundance of the 10 most differentially abundant bacterial genera over salinity.

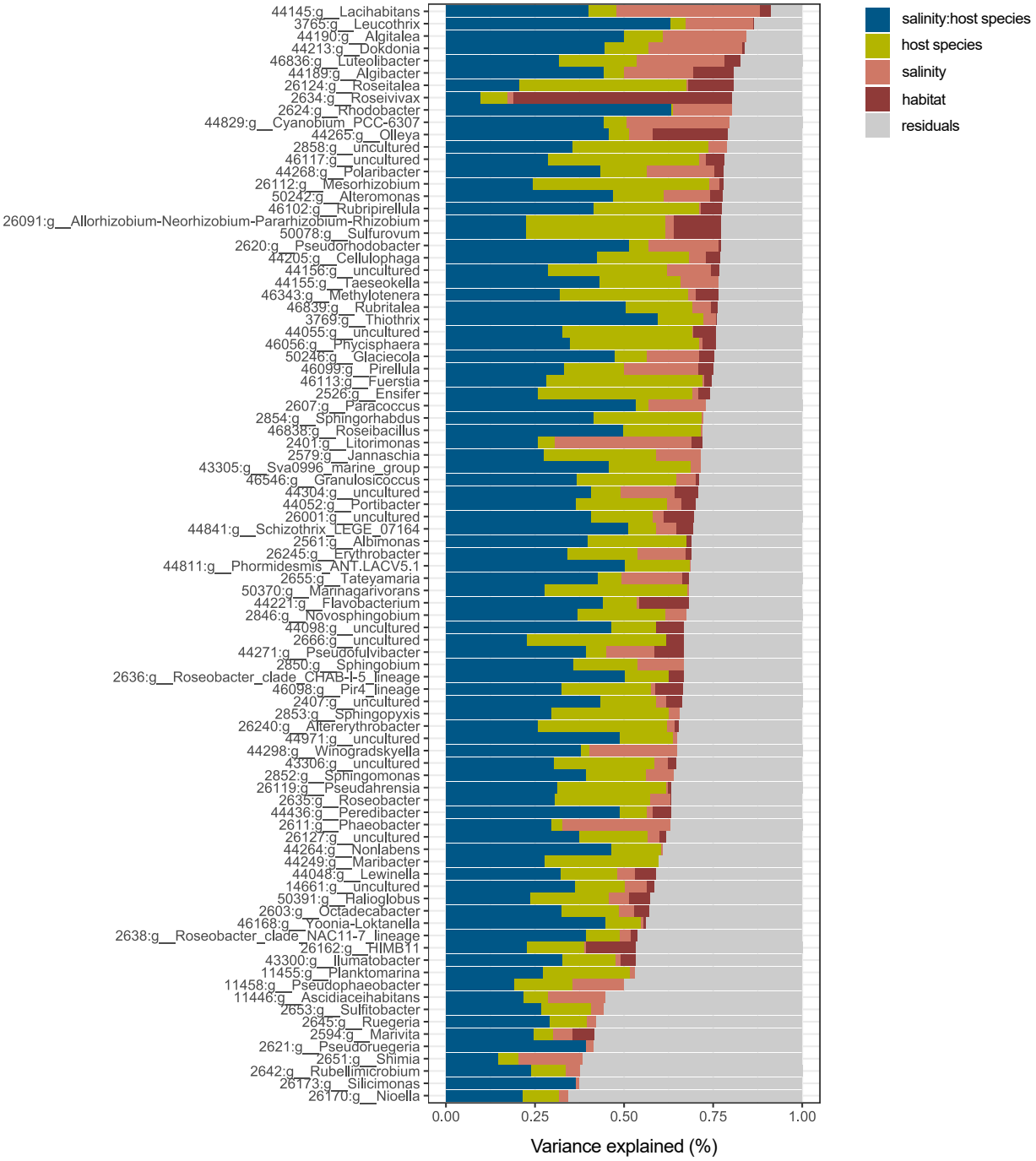

FIGURE S4.05 Variance partitioning, showing the amount of variance in abundance of bacterial genera explained (in %) by the interaction between salinity and host species (salinity:host species), host species, salinity, and habitat. Based on a generalised linear mixed model (negative binomial family).

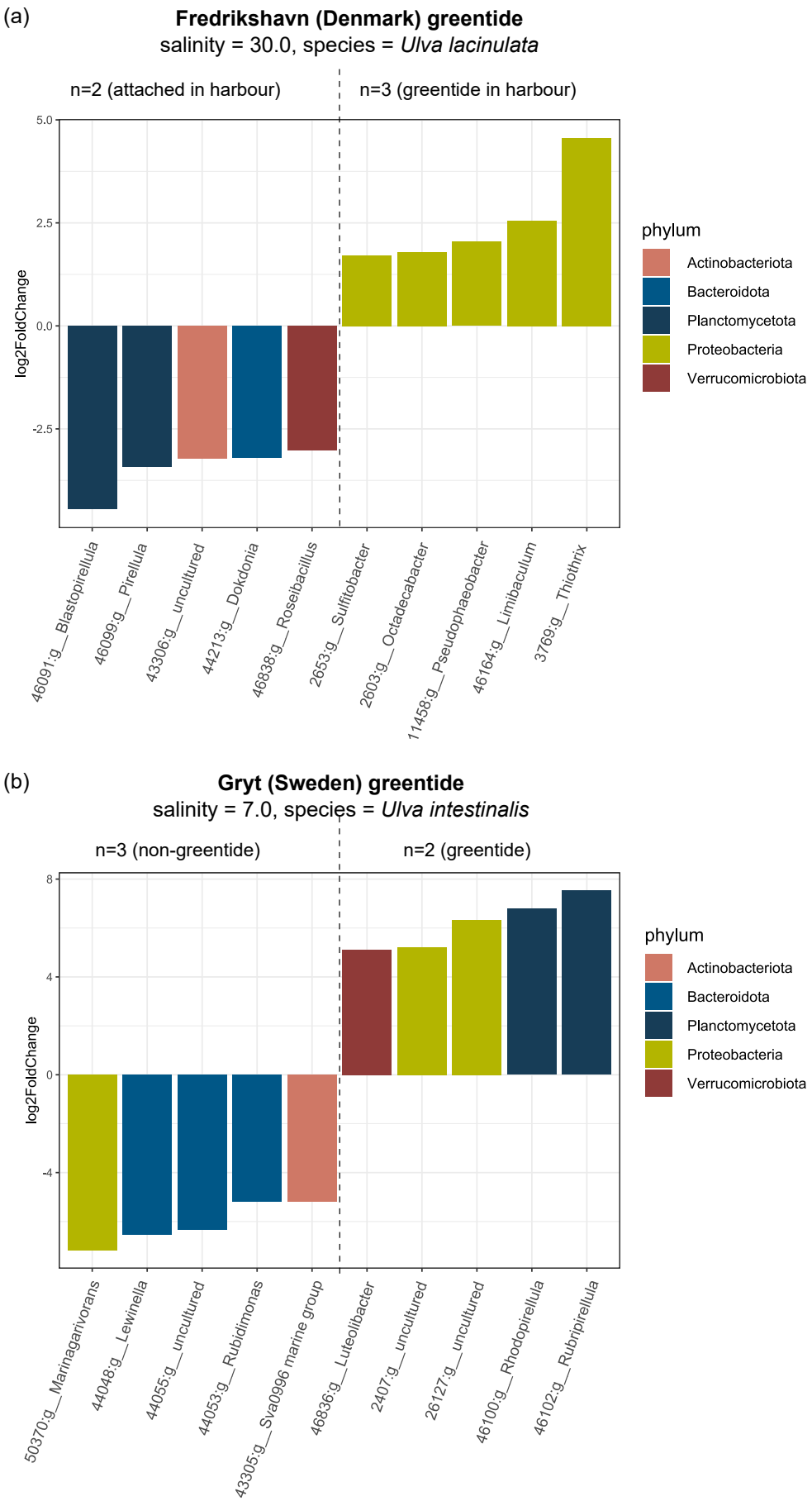

FIGURE S4.06 Bar graphs of the top 10 differentially abundant genera between greentide and non-greentide samples in (A) Fredrikshavn (Denmark), and (B) Gryt (Sweden).

“Zwiepend groen haar, als zeewier, wolkt in de golven.”

– Annet Schaap, in: Lampje

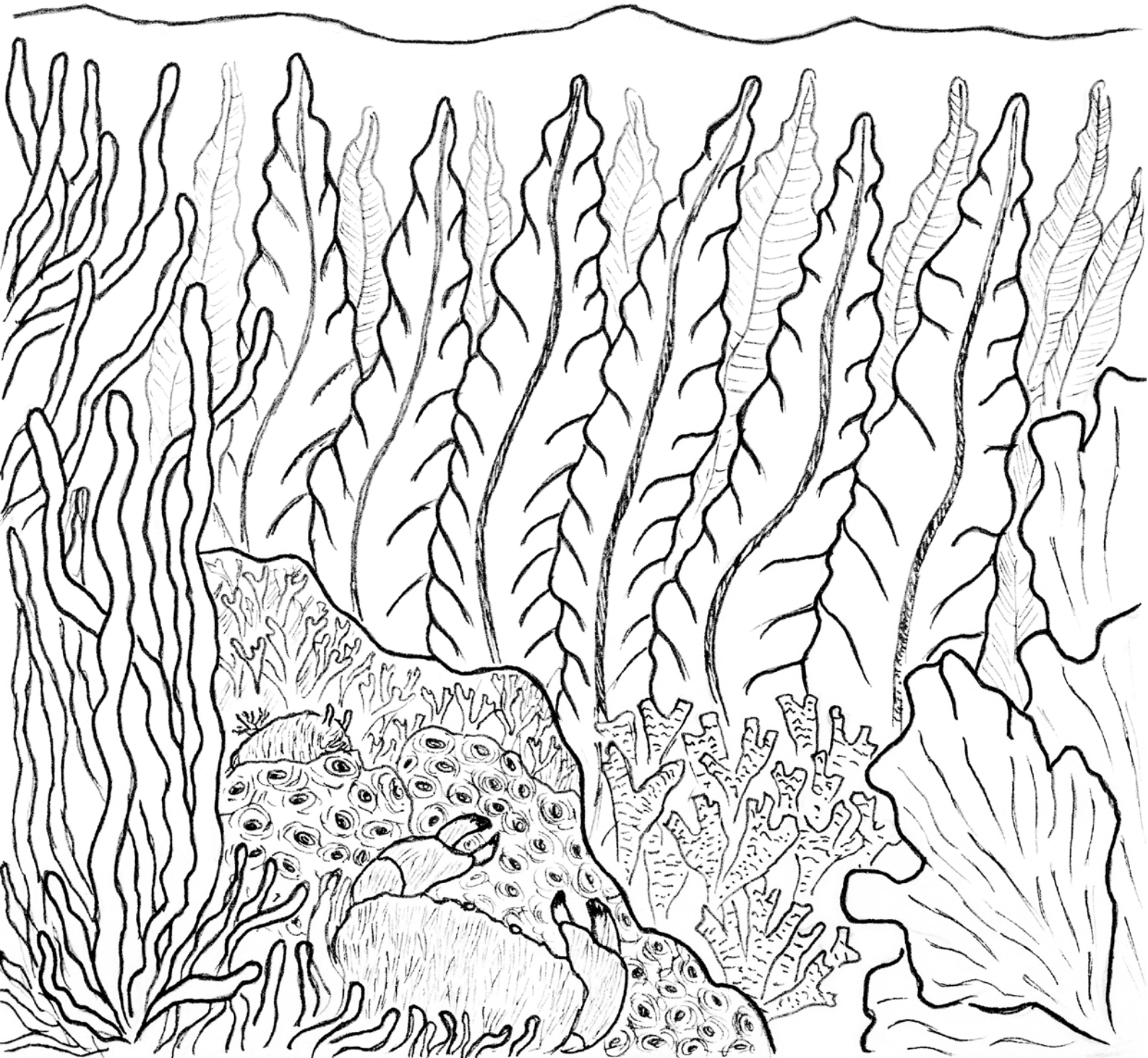

Chapter 5. Osmoregulation underpins functional stability of *Ulva*-associated bacterial communities in the Baltic Sea

Luna M. van der Loos[1,2], Sophie Steinhagen[3], Willem Stock[1], Florian Weinberger[4], Sofie D'hondt[1], Anne Willems[2], Olivier De Clerck[1]

[1] Phycology Research Group, Department of Biology, Ghent University, Ghent, Belgium

[2] Laboratory of Microbiology, Department Biochemistry and Microbiology, Ghent University, Ghent, Belgium

[3] Department of Marine Sciences-Tjärnö, University of Gothenburg, SE-452 96 Strömstad, Sweden

[4] GEOMAR Helmholtz Centre for Ocean Research Kiel, 24148, Kiel, Germany

Abstract

Marine macroalgae harbour a diverse and dynamic microbial community that is essential for host functioning. The green seaweed genus *Ulva* depends on its associated bacteria for morphogenesis and serves as a model system to study algal–bacterial interactions, yet we know very little about the functional potential of *Ulva*-associated bacterial communities, especially in relation to environmental change. In this study, we analysed the microbial community of 91 *Ulva* individuals sampled across a 2,000 km salinity gradient in the Atlantic–Baltic Sea using metagenomic sequencing. Metabolic reconstruction of 639 metagenome-assembled genomes (MAGs) revealed a widespread potential for carbon, sulphur, nitrogen, and vitamin metabolism, including amino acid and vitamin B biosynthesis. Compared to closely related seawater-isolated strains, typical *Ulva*-associated MAGs were defined by their ability to degrade the algal cell wall using polysaccharide lyases and glycoside hydrolases. Taxonomic turnover was substantial across the environmental gradient, with salinity explaining 70% of the observed taxonomic variation. In contrast, salinity accounted for only 17% of the observed functional variation in microbial communities. Despite prevalent functional redundancy across taxa, we identified salinity-associated changes in multiple functional pathways. High-salinity bacteria exhibited enrichment in genes related to thiamine (vitamin B_1), pyridoxal (vitamin B_6), and betaine biosynthesis, while low-salinity bacteria were more likely to contain genes necessary for arginine biosynthesis, D-glucuronate degradation, and phosphatidylcholine biosynthesis. These metabolic modules likely contribute to oxidative stress mitigation, cellular osmotic homeostasis, and membrane stabilisation in response to salinity variations. Our results emphasise the importance of conducting functional assessments to understand the seaweed holobiont and its collective response to environmental change.

5.1 Introduction

Microbial communities interact with eukaryotic hosts in every ecosystem, yet we know very little about how (variation in) microbial metabolisms impact host performance. Seaweeds, or macroalgae, are a group of important coastal inhabitants. As ecosystem engineers and primary producers, they are an essential source of food and they provide shelter and habitat for diverse marine organisms (Pessarrodona et al. 2022). Health, reproduction, and development of the macroalgal host — and indirectly their ecosystem functioning — are strongly dependent on the associated symbionts. Beyond the exchange of key nutrients, vitamins, and secondary metabolites, the microbial biofilm forms a physical and chemical barrier acting as a "second skin" that protects the host and modulates its interactions with the environment (Wahl et al. 2012, Egan et al. 2013, van der Loos et al. 2019). Beneficial bacteria can, for example, shield the host against pathogens (J. Li et al. 2022a), stimulate algal growth (Gemin et al. 2019), or mitigate the adverse effects of environmental pollution (Riquelme et al. 1997).

Species of the green seaweed *Ulva* are particularly well-studied and are considered a model system to study algal–bacterial interactions (Wichard et al. 2015, Wichard 2023). The relation between *Ulva* and its symbionts is so indispensable that the seaweed fails to develop its typical leaf- or tube-like morphology in the absence of particular bacteria (Provasoli 1958, Spoerner et al. 2012). Morphological development is induced by chemical compounds produced by bacteria that trigger cell wall development, rhizoid formation, and cell division (Weiss et al. 2017). Initial studies identified a combination of two complementary strains (a *Roseovarius* and a *Maribacter* strain) that were needed together for full morphogenesis in *Ulva mutabilis*. Since then, multiple strains have been identified that have the same capacity (Grueneberg et al. 2016). This functional redundancy across taxa is important for the host in relation to shifts in bacterial communities.

Seaweed-associated bacterial communities are far from static. Although a small core community can sometimes be identified, the bacteria form a highly dynamic community that fluctuates through time and space (Chapter 3, Bengtsson et al. 2010, Davis et al. 2023). Abiotic factors, such as temperature, light, and salinity influence the community composition, as does the host itself (Minich et al. 2018, Paix et al. 2021, Düsedau et al. 2023). Prior research has mainly focused on dynamics in the *taxonomic* composition of the communities rather than the *functional* potential that the community harbours. Taxonomic profiling is based on 16S rRNA amplicon sequencing that in recent years has become widely accessible due to increased speed and reduced costs. Genome-wide studies or metagenomic sequencing in comparison are more expensive and the sample size in those studies is often limited. Metagenomic functional profiling in, for example, *Sargassum* spp. (Glasl et al. 2021, Dai and Wang 2022), *Pyropia haitanensis* (J. Wang et al. 2022), and *Nereocystis luetkeana* (Weigel et al. 2022) highlighted the importance of the bacterial biofilm in terms of vitamin production, polysaccharide degradation, and nutrient cycling. However, to understand how the functional potential of a bacterial community responds to environmental change and to evaluate the potential consequences for the seaweed host, it is essential to expand functional profiling on a broader scale across diverse environmental gradients (Rath et al. 2019).

Ulva species are known for their broad salinity tolerance, thriving in environments ranging from freshwater habitats to highly saline conditions. The Baltic Sea is a particularly interesting area to study *Ulva*, as it hosts more than 15 species distributed across its distinctive salinity gradient (Steinhagen et al. 2023). This relatively stable gradient stretches across more than 2,000 km, transitioning from near freshwater conditions in the innermost parts towards fully marine conditions on the North Sea side (Reusch et al. 2018). While the distribution of certain *Ulva* species is confined to higher salinity levels, other species like *U. intestinalis* and *U. linza* can be found throughout the entire range. Salinity is a major driving force of global bacterial diversity and community structure too (Lozupone and Knight 2007). Previous studies showed that salinity strongly structures the taxonomic composition of *Ulva*-associated bacterial communities (van der Loos et al. 2022). The question remains, however, if these taxonomic changes across salinity are reflected in the changes in functional profile of the same bacterial communities as well, or whether functions are conserved (Green et al. 2008).

Here, we investigated the taxonomic and functional composition of *Ulva*-associated bacteria across the Baltic–Atlantic salinity gradient using metagenomic sequencing. The aim of this study was twofold: 1) to provide an overview of the functional profile of the *Ulva* bacteriome based on a large number of samples (n = 91), and 2) to assess if the functional potential of the microbial community changes across an environmental gradient.

5.2 Materials and Methods

5.2.1 Sample collection

Samples of *Ulva sensu lato* individuals (n = 91) were collected during June–August 2020 in the Baltic Sea area (Electronic Supplementary Table S5.01)[1]. Of each individual, a tissue sample was collected to identify the host species and a swab sample for microbiome analyses was generated by rubbing for 30 s on the tissue. Sterilised disposable gloves and sterilised equipment were used throughout the sampling procedure to minimize contamination. All samples were stored in a portable freezer (–20 °C) until transferred to –80 °C in the laboratory.

In total, 63 sampling sites were visited along a salinity gradient in the Baltic Sea and adjacent areas such as the Kattegat, Skagerrak, and the eastern North Sea (Fig. 5.01). The salinity ranged from 5.1 to 34.3 PSU and is presented in the figures in this study either on a continuous scale (0–35 PSU) or in salinity zones defined

according to the Venice classification system (5–8 = horohalinicum, 8–18 = mesohaline, 18–30 = polyhaline, and 30–35 = euhaline) (Alves et al. 2009, Bleich et al. 2011, Hu et al. 2016). In addition, water temperature (°C), oxygen levels (mg L^{-1}), and nutrients concentrations (NO_3^-, NO_2^-, silicate, PO_4^{3-} in µmol L^{-1}) were measured at each site (Table S5.01).

Molecular identification, based on the *tuf*A marker, confirmed the samples in our dataset represented seven different species: *Blidingia minima* (Nägeli ex Kützing) Kylin (n = 8), *Ulva compressa* Linnaeus (n = 10), *Ulva fenestrata* Postels & Ruprecht (n = 8), *Ulva intestinalis* Linnaeus (n = 29), *Ulva lacinulata* (Kützing) Wittrock (n = 10), *Ulva linza* Linnaeus (n = 20), and *Ulva torta* (Mertens) Trevisan (n = 6) [see van der Loos et al. (2022) and Steinhagen et al. (2023) for detailed molecular methods and additional results concerning *Ulva* diversity in the Baltic region]. Throughout this chapter, "*Ulva*" refers to *Ulva sensu lato* (including *Blidingia*).

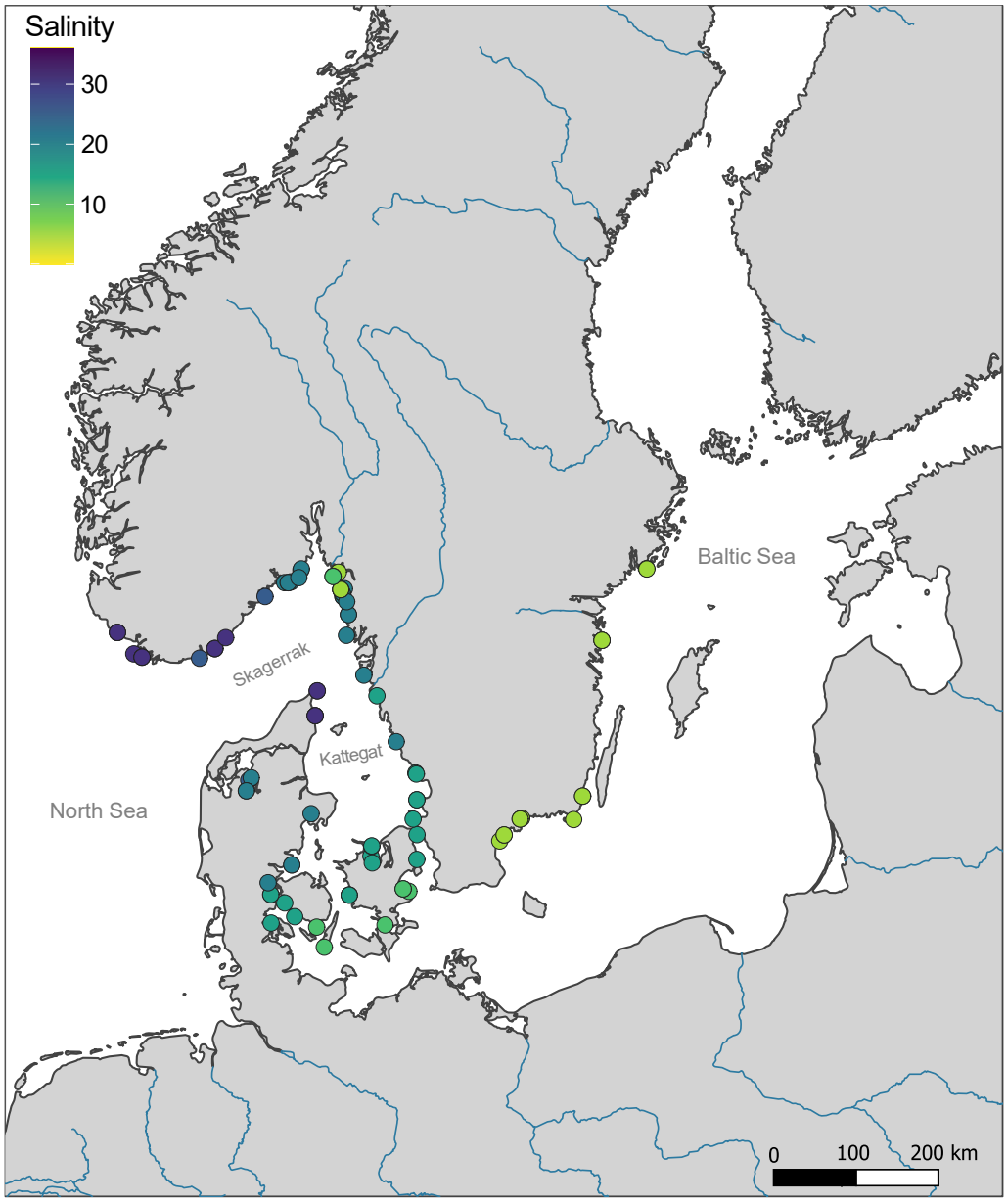

FIGURE 5.01 Geographic distribution of all 63 sampling sites in the Baltic Sea and adjacent areas (eastern North Sea, Skagerrak, and Kattegat) where 91 *Ulva sensu lato* samples were collected. The colour of the sites corresponds to the measured salinity. Major rivers are projected in blue.

5.2.2 DNA extraction and metagenomic sequencing

Total microbial DNA of the swab samples was extracted with the Qiagen DNeasy mini kit following the manufacturer's protocol, with the addition of a bead beating step before lysis using zirconium oxide beads (RETCH Mixer mill MM400; 5 minutes at 30 Hz). Quantity and quality of the DNA extracts were verified with Qubit (Life Technologies, Grand Island, USA) and NanoDrop (Thermo Scientific, Wilmington, USA). DNA extracts were sent to Novogene (Cambridge, United Kingdom) for library preparation and metagenomic sequencing on an Illumina NovaSeq 6000 (150 bp paired-end). A negative DNA extraction control and a positive control (ATCC microbial standard MSA-1002) were included. A total of 4,297,091,260 reads were generated (35,622,356 – 78,544,930 reads per sample). The sequences are archived at SRA (BioProject PRJNA1040445).

5.2.3 Bioinformatics and statistical analyses

The metagenomic sequencing data was processed with the ATLAS Snakemake workflow (Kieser et al. 2020), which integrates quality control, assembly, genomic binning, and annotation. In short, quality control was performed using the BBTools suite (Bushnell 2019). This includes removal of PCR duplicates and adapters, trimming and filtering of reads based on quality and length, and compressing the raw data files. Host sequences were removed based on an available *Ulva* reference genome (De Clerck et al. 2018). The de novo metagenome assembly was done using MEGAHIT v1.0 (Li et al. 2016). Next, metagenome-assembled genomes (MAGs) were predicted with binning tools MetaBAT 2 (Kang et al. 2019) and MaxBin 2.0 (Wu et al. 2016). Binning results were aggregated with DAS Tool (Sieber et al. 2018). Quality assessment of the resulting MAGs was performed with CheckM (Parks et al. 2015). MAGs were dereplicated across samples with dRep (Olm et al. 2017), and taxonomic classification was performed with GTDB-Tk (Parks et al. 2018). Finally, genes were predicted with Prodigal (Hyatt et al. 2010), redundant genes were clustered with linclust (Steinegger and Söding 2018), and annotated with eggNOG-mapper (Huerta-Cepas et al. 2017). This resulted in a classification of the genes following the Carbohydrate-Active EnZymes database (CAZy) (Cantarel et al. 2009) and Kyoto Encyclopedia of Genes and Genomes (KEGG) (Kanehisa and Goto 2000, Kanehisa et al. 2008) databases.

The effect of salinity, NO_x, and PO_4 on bacterial community composition at both MAG (taxonomic profile) and KO (KEGG Orthology; functional profile) levels was assessed using the envfit function from the vegan package with 9,999 permutations (Oksanen et al. 2020). Multivariate comparisons with 9,999 permutations were subsequently conducted with pairwiseAdonis among the different salinity zones (Martinez Arbizu 2020). Functional differences across salinity were visualised with a PCA ordination and smooth surface lines were fitted to the ordination with the ordisurf function (vegan package) based on the correlation with salinity (Oksanen et al. 2020). A LinDA linear regression was used to identify which MAGs and which KEGG modules (a set of genes with a specific reaction within a metabolic pathway) significantly changed across salinity and nutrient concentrations (Zhou et al. 2022). P-values were Benjamini & Hochberg corrected. Given the compositional nature of the data, read abundance values were transformed with the centric log-ratios (CLR) prior to the analyses (Gloor et al. 2017).

To gain a deeper understanding of what defines the metabolic potential of *Ulva* microbiomes, we compared the genomes of bacterial taxa isolated from *Ulva* to those isolated from seawater. In total, we selected 152 MAGs from our metagenomic dataset, representing 33 different genera. We then searched for publicly available genomes of bacteria from the same genera that were isolated from seawater (resulting in a set of 71 genomes) (Electronic Supplementary Table S5.02). These originated from a variety of geographical locations and habitats (e.g., surface water, deep sea, hydrothermal systems, and oceanic gyres). Subsequently, we conducted a com-

parative analysis based on odds ratios to identify potential enrichments of specific KO terms or CAZy families within bacteria of the same genus collected from *Ulva* versus seawater. For each KO term and CAZy family, the odds ratio was calculated as the number of discordant genome pairs in favour of the *Ulva* (term/family present in the *Ulva* bacterial genome, but not present in the seawater bacterial genome) divided by the number of discordant pairs in favour of seawater (term/family present in the seawater bacterial genome, but not present in the *Ulva* bacterial genome). An offset of 0.5 was added to the number of discordant pairs to prevent dividing by zero. As multiple genomes were available per genus, pairs were randomly assigned 1,000 times (permutations) and odds ratios were calculated for each permutation. The median odds ratio was retained. A term/family more frequent in *Ulva* bacterial genomes results in an odds ratio larger than one. The opposite results in an odds ratio smaller than one.

All statistical tests were performed in R (R Core Team 2020) and data were visualised using the GGPLOT2 (Wickham 2016) and PHYLOSEQ (McMurdie and Holmes 2013) packages.

5.3 Results

5.3.1 Taxonomic profile

A total of 639 metagenomic assembled genomes (MAGs) were found to be associated with *Ulva* in 91 samples collected across the Baltic–Atlantic salinity gradient, of which 413 had an estimated assembly completeness of >90% (Electronic Supplementary Table S5.03). The MAGs were classified in 52 different orders and 88 different families. The majority of these belonged to the orders Flavobacteriales (106 MAGs), Rhodobacterales (84 MAGs), and Chitinophagales (64 MAGs). The Flavobacteriales were the most abundant in the dataset (22% total relative abundance across all reads), followed by the Sphingomonadales (15.7%) and the Rhodobacterales (13.4%)[2].

At MAG level, there were relatively few core taxa [defined here as taxa that were present in at least 70% of the samples with a relative read abundance of 0.1% in each sample]. An unidentified *Rhizobiaceae* was present in at least 60% of the samples and a MAG of the genus *Sphingorhabdus* was present in at least 50% of the samples (both with a relative abundance of >0.1%). At genus level, a higher number of core taxa could be identified. *Pontixanthobacter* (*Sphingomonadaceae*), JAALLB01 (*Rhizobiaceae*), *Sphingorhabdus* (*Sphingomonadaceae*), *Lewinella* (*Saprospiraceae*), and *Dokdonia* (*Flavobacteriaceae*) were present in at least 70% of all samples with a relative abundance of at least 0.1%. Within specific salinity ranges, the number of core taxa increased. 14 core taxa were present in the 5–8 PSU range, 10 core taxa in 8–18 PSU, 5 core taxa in 18–30 PSU, and 4 core taxa in the 30–36 PSU range. In the higher salinity regions, for example, *Litorimonas* was a core taxon, and *Roseobacter* and *Alteraurantiacibacter* in the low salinity regions.

Salinity had a significant effect on bacterial community composition at MAG level ($p = 0.0001$, $R^2 = 0.70$), whereas nutrient concentrations only had a limited effect (NO_x, $p = 0.04$, $R^2=0.07$; PO_4, $p = 0.08$, $R^2=0.05$) (Fig. 5.02A). Pairwise comparisons showed that the taxonomic composition of *Ulva*-associated bacteria differed between all salinity regions (horohalinicum *vs* mesohaline *vs* polyhaline *vs* euhaline, $p < 0.01$ for all comparisons; pairwise Adonis test). In total, 294 MAGs changed in relative abundance across salinity ($p < 0.01$, LinDA linear regression) (Fig. 5.03) (Electronic Supplementary Table S5.03), of which 126 MAGs decreased with salinity and 168 MAGs increased with salinity. Several MAGs belonging to *Dokdonia*, *Leucothrix*, and *Litorimonas* for example increased with salinity, while *Alteraurantiacibacter*, *Rubripirellula*, and *Erythrobacter* decreased with salinity (Fig. 5.04).

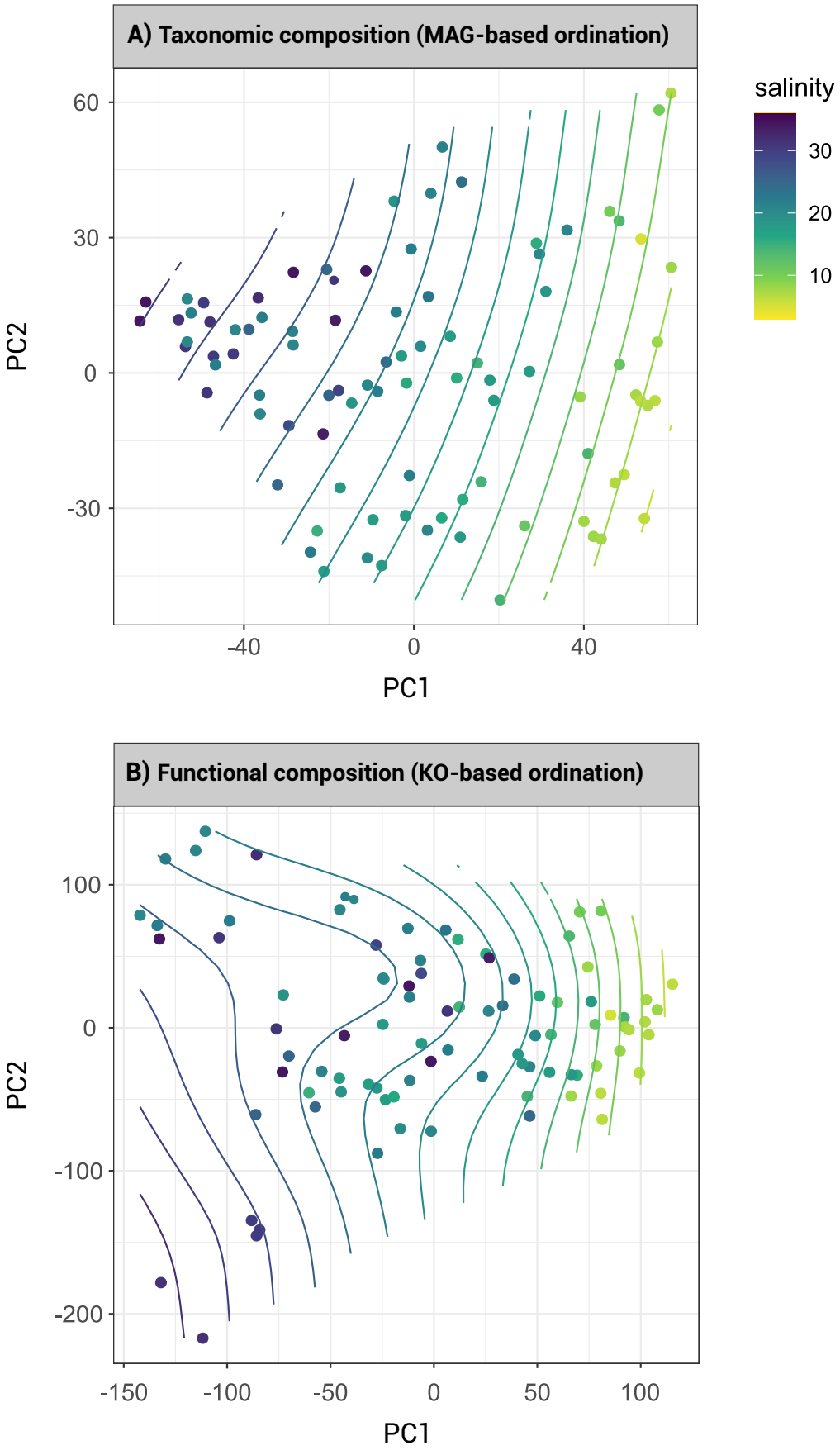

FIGURE 5.02 PCA plot of the A) taxonomic composition (MAG-based), and B) functional composition (KEGG Orthology-based) of *Ulva*-associated bacterial communities. Colours represent salinity. The contour lines (smooth surface lines) are fitted to the ordination based on the correlation with salinity.

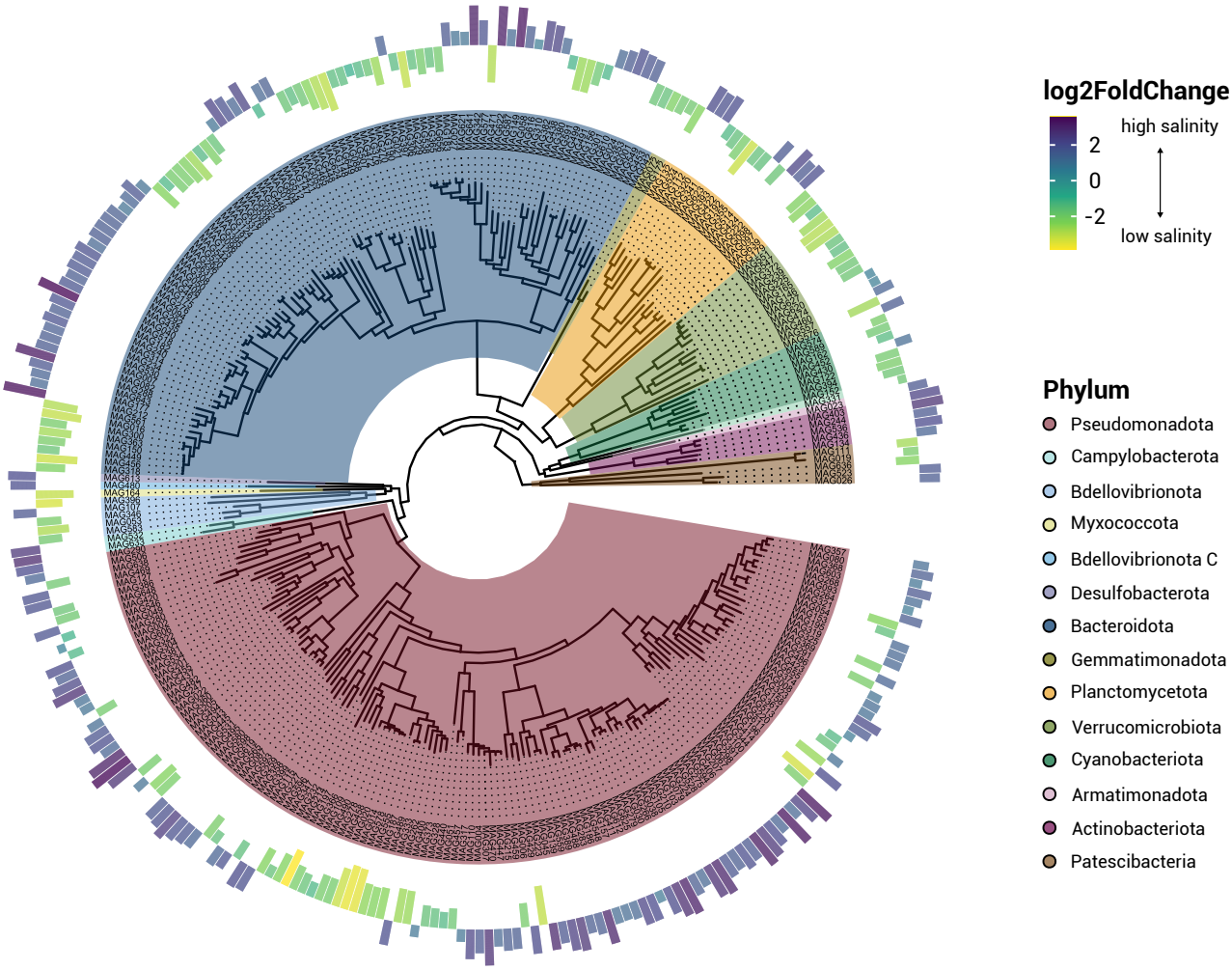

FIGURE 5.03 Phylogenetic tree of the 294 metagenome-assembled genomes (MAGs) that significantly differed ($p < 0.01$) in relative abundance across the salinity gradient. The outer ring represents the log2FoldChange (LinDA linear regression model), with the MAGs in yellow-green that are enriched in low salinity and the MAGs that are enriched in high salinity in purple-blue. The colours in the phylogenetic tree represent the bacterial phyla (the legend is ordered in clockwise order of appearance).

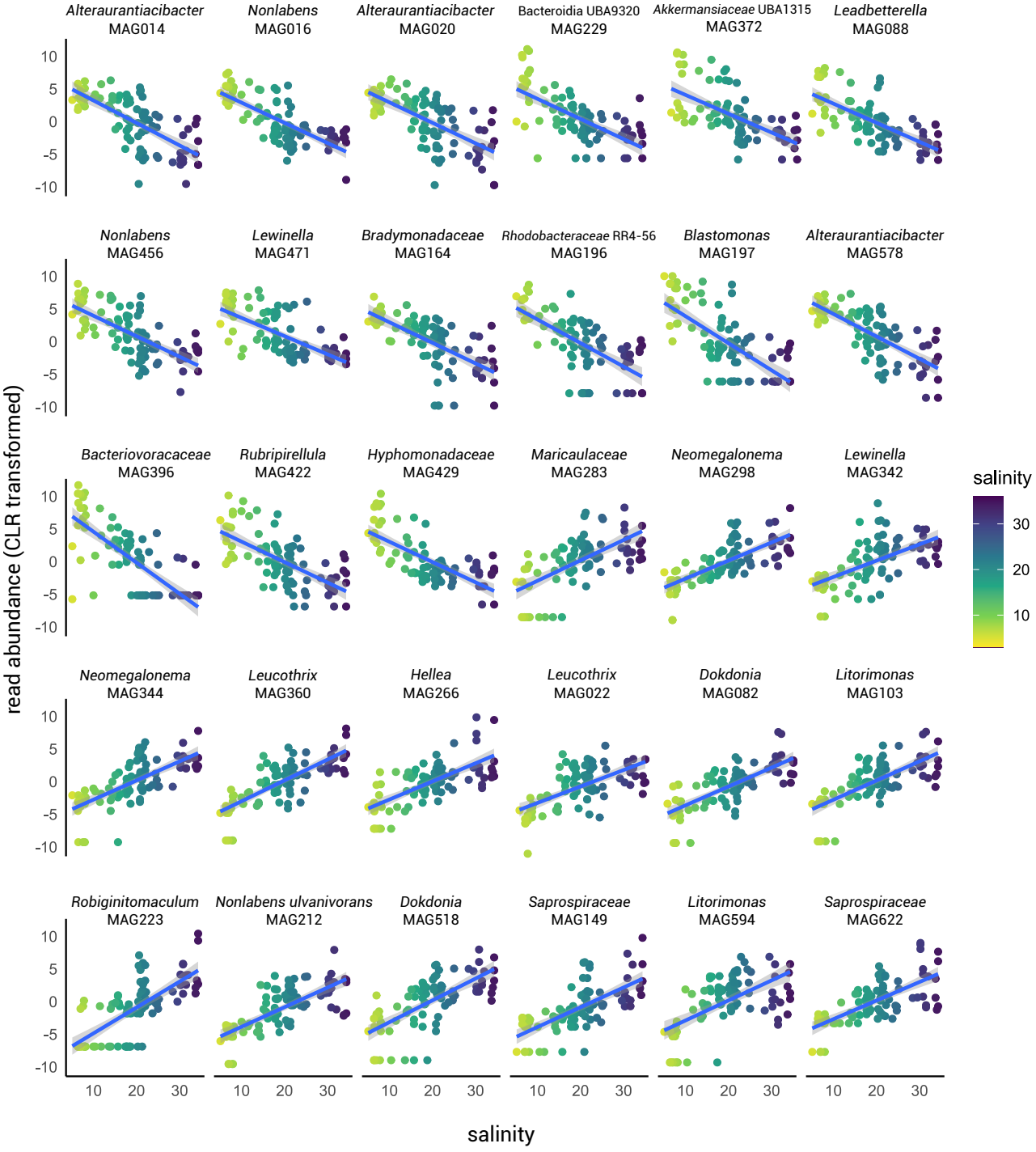

FIGURE 5.04 Read abundance of the 30 most differentially abundant metagenome-assembled genomes (MAGs) across salinity. The x-axis displays salinity (PSU) and the y-axis CLR-transformed read abundance. Colours represent salinity. Curves were fitted with a generalised linear model (GLM) using the R package GGPLOT2. Shaded areas represent the 0.95 confidence interval.

5.3.2 Functional profile

Across 91 *Ulva* microbiome samples and 639 MAGs, a total of 6,525 KO terms and 399 KEGG modules were identified (Electronic Supplementary Table S5.04). The MAGs with an estimated completeness of >90% contained on average 59 KEGG modules (ranging from 33–94 modules). The relative abundance of the modules (calculated as a matrix multiplication of the MAG counts per sample and the absence/presence matrix of the modules in each MAG) ranged from <0.001% to 1.73%. Apart from basic cellular metabolic pathways (e.g., fatty acid biosynthesis, RNA polymerases, DNA polymerases, ribosome, F-type ATPases, cytochrome C oxidase, etc.), the *Ulva*-associated bacterial communities contained a range of functions that are clearly linked to the association with its host. Below we detail the metabolic potential of the *Ulva* biofilm, focusing on carbon, sulphur, and nitrogen metabolism, algal cell wall degradation, amino acid biosynthesis, and vitamin pathways (summarized in Fig. 5.05).

Carbon, sulphur, and nitrogen metabolism

Carbon metabolism potential among *Ulva*-associated bacteria largely centred on the use of organic carbon. The vast majority of MAGs was able to utilise organic carbon as their primary energy source through, e.g., complex carbon degradation, glycolysis (KEGG modules M00001+M00002), and the tricarboxylic acid (TCA) cycle (M00009). In addition, we identified the potential for autotrophic carbon fixation through four different pathways. The most prevalent pathway was the reductive pentose phosphate cycle (Calvin cycle; M00165) [present in 166 MAGs and contributing to 0.6% of module relative abundance], followed by the 3-hydroxypropionate (3HP) bicycle (M00376) [present in 21 MAGs and contributing to 0.06% module relative abundance]. The reductive citrate cycle (Arnon-Buchanan cycle/reductive citrate cycle; M00173) was identified in only four MAGs [*Desulforhopalus*, *Sulfurovum*, *Lutibacter*, and an unknown DSM-100316] and the reductive acetyl-CoA pathway (Wood-Ljungdahl pathway) (M00377) was represented by a single MAG [*Desulforhopalus*].

Nitrogen metabolism potential largely centred on the conversion from nitrate and nitrite to ammonia. A large number of 174 MAGs contained the *nrfAH* or *nirBD* genes that are essential for nitrite reduction to ammonia, which is the final step in dissimilatory nitrate reduction to ammonia. A total of 30 MAGs exhibited the genes for the full dissimilatory nitrate process, utilising nitrate respiration for energy production (M00530). Only seven MAGs, all belonging to the Cyanobacteriia, demonstrated complete assimilatory nitrate reduction capability, involving the reduction of nitrate to ammonia for biosynthesis purposes (M00531). Nevertheless, the first step in this process (nitrate to nitrite reduction mediated by the *narB* gene) was identified in 53 MAGs, and the subsequent step (nitrite to ammonia reduction facilitated by the *nirA* gene) was detected in 45 MAGs. The *narB* gene was predominantly observed in *Flavobacteriaceae* and *Saprospiraceae*, while the *nirA* gene was prevalent in *Akkermansiaceae* and *Pirellulaceae*. Two MAGs harboured all the genes necessary for the denitrification process involving the reduction of nitrate and nitrite to nitrogen (M00529), while none of the MAGs carried genes associated with nitrification (the oxidation of ammonia to nitrate; M00528). Finally, ten MAGs from diverse families showed the capacity to fix nitrogen (M00175).

Sulphur metabolism potential was widespread. While only six MAGs, mainly belonging to the *Thiotrichaceae,* contained the necessary genes for dissimilatory sulphate reduction to sulphide (sulphate reduction for energy production; M00596), over 130 MAGs were capable of assimilatory sulphate reduction (M00176). 137 MAGs were able to oxidise thiosulphate (the result of the incomplete oxidation of sulphides) through sulphur-oxidising proteins *SoxAB* and *SoxXYZ* that together form the Sox complex (M00595). Metabolism of organic sulphur included, amongst others, cysteine synthase (which can be converted to homocysteine and methionine), as well as DMSO and DMSP metabolism. The capacity to convert DMSP to DMS was almost exclusively

restricted to members of the *Rhodobacteraceae* and *Rhizobiaceae*, like *Sulfitobacter*, *Roseovarius*, and *Jannaschia* (40 MAGs in total, with a combined relative abundance of 8.4% in the entire dataset). In addition, several MAGs displayed the ability to transport the sulphur-containing β-amino acid taurine via ABC transporters (*tauACB*) and convert the bioactive compound to sulphite via taurine dioxygenases (*tauD*). The *tauD* gene was identified in 33 MAGs (including several Acidimicrobiales, Burkholderiales, and Caulobacterales) and *tauACB* was present in >100 MAGs.

Algal cell wall degradation

Apart from examining carbon and sulphur metabolic functions organized in KEGG modules, we also screened the *Ulva*-associated bacterial MAGs for the presence of carbohydrate-active enzymes using the CAZy database. The CAZy database categorizes enzymes involved in degrading, modifying, or creating glycosidic bonds into families, including glycoside hydrolases (GHs) and polysaccharide lyases (PLs). A total of 121 different GH families and 26 different PL families were identified within *Ulva*-associated MAGs.

The most prevalent polysaccharide lyases in *Ulva*-associated bacteria were oligogalacturonate lyases [e.g., CAZY family P22; 327 MAGs], alginate lyases [amongst others CAZY family PL6, PL7, and PL17; 315 MAGs], and ulvan lyases [amongst others CAZY family P24, P25, and P37; 146 MAGs]. Endo-beta-1,4-glucuronan lyases were less abundant [CAZY family P20 and P31; 30 MAGs].

The most prevalent glycoside hydrolase families were GH3 [553 MAGs], GH23 [544 MAGs], GH13 [497 MAGs], GH16 [305 MAGs], and GH5 [299 MAGs]. Family GH3 includes, amongst others, xyloglucan-specific exo-β-1,4-glucosidase (EC 3.2.1.-), xylan β-1,4-xylosidase (EC 3.2.1.37), several glucanases, and several other glucosidases. Family GH23 includes activities of chitinase (EC 3.2.1.14), lysozyme (EC 3.2.1.17), and peptidoglycan lyase (EC 4.2.2.n1). Family GH13 is the major group of enzymes acting on substrates containing α-glucoside linkages. Enzymes of family GH16 are active on β-1,4 or β-1,3 glycosidic bonds in various glucans and galactans and includes xyloglucan:xyloglucosyl transferase (EC 2.4.1.207). Members of the GH5 family are mainly active on cellulose, but this family also includes high specificity xyloglucanases.

Most *Ulva*-associated MAGs contained at least five different GH families. In general, members of the *Spirosomaceae*, *Saprospiraceae*, and *Flavobacteriaceae* exhibited a relatively high number of distinct GH families, ranging from 19–27 on average. In contrast, the *Micavibrionaceae*, *Rhizobiaceae*, and *Rhodobacteraceae* contained relatively few glycoside hydralases (on average three to six distinct GH families). Among the identified MAGs, *Maribacter*, *Leadbetterella*, and *Lewinella* stood out with the highest numbers of GH families, particularly *Maribacter luteus*, containing as much as 48 distinct GH families. The prevalence of multiple polysaccharide lyases was sparser. Several MAGs identified as *Jejuia*, *Algibacter*, *Cellulophaga*, and *Glaciecola* each featured ten or more different PL families. Members of the *Micavibrionaceae* and *Rhizobiaceae* contained on average only one distinct PL family.

Vitamin pathways

The potential of vitamin B production was widely distributed within the *Ulva* microbiome. The capacity to produce tetrahydrofolate (a derivative of vitamin B_9; M00126) was most widespread and was identified in 110 MAGs from varying families, including the *Alteromonadaceae*, *Flavobacteriaceae*, *Granulosicoccaceae*, *Saprospiraceae*, and *Spirosomaceae*. This vitamin was the only vitamin that was part of the core functions of the *Ulva* microbiome, being consistently present in all samples with a minimum relative abundance of 0.1%. KEGG modules related to the production of vitamin B_1 (thiamine; M00127), vitamin B_2 (riboflavin; M00125), vitamin B_5 (pantothenate; M00119), vitamin B_6 (pyridoxal; M00124), vitamin B_7 (biotin; M00123), and vitamin B_{12}

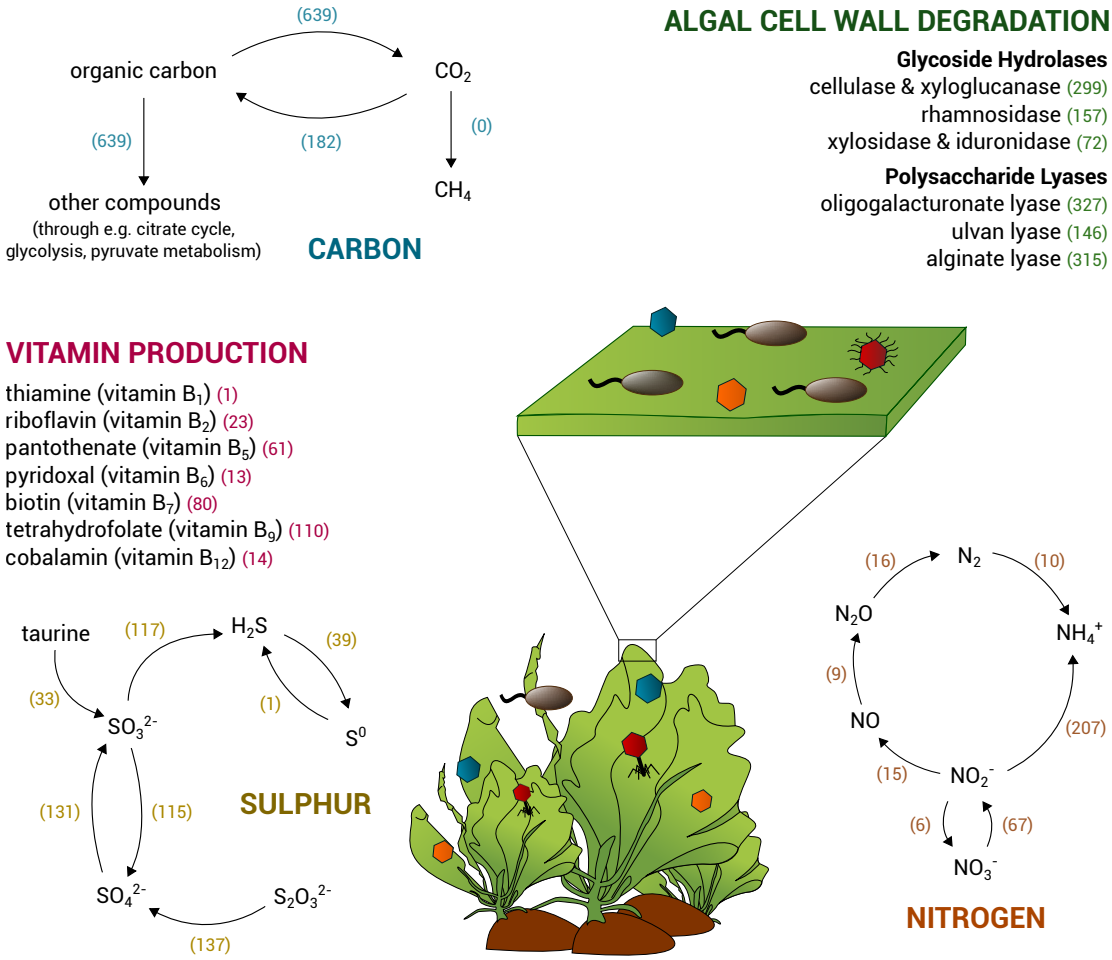

FIGURE 5.05 Overview of the metabolic potential of the *Ulva* microbiome, highlighting vitamin production (purple), algal cell wall degradation (green), and the metabolism of carbon (blue), nitrogen (orange), and sulphur (yellow). The number of identified metagenomic assembled genomes (MAGs) that are capable performing the reactions are displayed in brackets.

(cobalamin; M00122) were identified as well, although not as core functions. This could be attributed to either the absence of MAGs with the capacity to produce these vitamins in all samples or their presence in samples but not with high abundance.

Vitamin B_7 production potential was identified in 80 different MAGs. These mainly belonged to the *Akkermansiaceae* (e.g., *Roseibacillus*), *Micavibrionaceae* (with several unidentified genera), and *Pirellulaceae* (e.g., *Rubripirellula*). Vitamin B_5 was predominantly associated with *Roseibacillus*, *Dokdonia*, *Litorimonas*, *Robiginitomaculum*, and *Rhodopirellula* and was found in 61 MAGs in total. Biosynthesis of vitamin B_2 and vitamin B_6 were identified in 23 MAGs and 13 MAGs, respectively. Both sets of genes were mainly found in *Glaciecola* and *Alteromonas* (both *Alteromonadaceae*). The full set of genes essential for vitamin B_1 production was detected in only one MAG, a *Vibrio*. Five other MAGs (including *Alteromonas* and *Haloferula*) only missed a single gene necessary for the conversion of a adenylyl sulphur-carrier protein to a thiocarboxy sulphur-carrier protein. Although 158 MAGs possessed the final gene needed for the biosynthesis of vitamin B_{12}, only 14 MAGs contained the full module. These MAGs were identified as belonging to the genera *Burkholderia*, *Cupriavidus*, *Granulosicoc-*

cus, *Leucothrix*, *Neomegalonema*, *Paraglaciecola*, *Roseibaca*, *Vibrio*, and *Yoonia*. Additionally, 85 MAGs exhibited the ability to synthesise menaquinone (vitamin K_2; M00116), and six MAGs possessed the capacity for tocopherol production (vitamin E; M00112).

Amino acid biosynthesis

The biosynthesis of multiple amino acids was part of the core modules of the *Ulva*-associated bacteria (with 0.65–1.42 % relative abundance in at least 99% of samples). This included the biosynthesis of proline (M00015), threonine (M00018), lysine (M00016, M00526, M00527), valine/isoleucine (M00019), serine (M00020), cysteine (M00021), tryptophan (M00023), histidine (M00026), ornithine (M00028), leucine (M00432), and arginine (M00844). Of these core modules, cysteine biosynthesis was detected in the fewest number of MAGs (222 MAGs), while histidine biosynthesis was found in the highest number of MAGs (443 MAGs). Likewise, genes necessary for glycine biosynthesis (from threonine or serine), alanine biosynthesis (from pyruvate) and glutamine biosynthesis (from glutamate), as well as the conversion between aspartate and asparagine were prevalent in the majority of the MAGs.

Although the methionine biosynthesis module (M00017) was present in all samples, its relative abundance was low (0.04%). The potential to produce methionine was restricted to 15 MAGs, including *Ahrensia* and *Neomegalonema*. Similarly, the KEGG modules associated with phenylalanine biosynthesis (M00024) and tyrosine biosynthesis (M00025) exhibited low relative abundances and were only present in seven to eight MAGs, mainly *Burkholderiaceae*.

The definition of a typical *Ulva* microbiome

Our dataset provides a thorough overview of the functional profile of the *Ulva*-associated microbiome. To determine the functions contributing to a "typical" *Ulva* microbiome, we contrasted taxa isolated from *Ulva* with those isolated from seawater. In total, we selected 152 MAGs from our metagenomic dataset, representing 33 different genera. We then searched for publicly available genomes of bacteria from the same genera but isolated from seawater (71 genomes) (Electronic Supplementary Table S5.02). Subsequently, we conducted a comparative analysis based on odds ratios to identify potential enrichments of specific KEGG Orthology (KO) terms or Carbohydrate-Active enZymes (CAZys) in bacteria from the same genus collected from *Ulva* versus seawater.

Bacteria originally isolated from seawater more frequently harboured genes related to glyoxylate biosynthesis compared to their relatives isolated from the *Ulva* thallus. This included the reversible conversion from glycolate ⇔ glyoxylate (*katE*; K03781) and malate ⇔ glyoxylate (*aceB*; K01638), as well as malyl-CoA ⇔ glyoxylate (*mcl*; K08691) and malyl-CoA ⇔ malate (*mcl2*; K14451) conversions. Seawater-derived bacteria were also enriched in genes involved in alanine biosynthesis (pyruvate ⇔ alanine, K14260), cysteine biosynthesis (serine > cystathione > cysteine, K01697 & K01758), and several genes associated with tryptophan (K01817 & K01609), tyrosine (K00220), and phenylalaline (K01609) production.

Ulva-isolated bacteria on the other hand were more likely to contain genes related to the conversion between pyruvate and oxaloacetate (*ppdK*; K01006 & *ppc*; K01595), the conversion from betaine to glycine via sarcosine (K00315 & K00305), the conversion from glutamate to ornithine (K00620), and folate biosynthesis (K00287). In addition, they were enriched in ABC transporters facilitating the extracellular uptake of taurine (*tauACB*; K15552 & K10831), α-glucoside (*aglEFGK*; K10232, K10233 & K10234), fructose (*frcBCA*; K10552, K10553 & K10554), and rhamnose (*rhaSPQT*; K10559 & K10560).

Concerning CAZys, *Ulva*-associated bacteria were distinguished from their seawater-isolated counterparts by the presence of ulvan lyases (PL24, PL25, PL28, PL37, PL40), as well as α-L-rhamnosidases (GH106), and rhamnogalacturonan α-L-rhamnohydrolase (GH78). They also exhibited a higher likelihood of containing enzymes from the GH5 (cellulose and xyloglucan activity), PL42 (L-rhamnose-α-1,4-D-glucuronate lyase), and GH39 (β-xylosidase and α-L-iduronidase) families. Conversely, seawater-associated bacteria were enriched in enzymes from the GH28 (polygalacturonases), GH29 (α-fucosidases), GH117 (α-neoagarobiosidase), and GH168 (α-1,3-L-fucanase activity) families (Fig. S5.01).

5.3.3 Functional patterns across salinity

Salinity had a significant effect on the functional profile of the *Ulva*-associated bacterial community ($p = 0.0003$, $R^2 = 0.17$). However, the differences were less pronounced than in the taxonomic composition. The functional gene profile of the bacterial community in the horohalinicum (5–8 PSU) was significantly different from the higher salinity areas (18–30 PSU, $p = 0.04$; 30–35 PSU, $p = 0.04$, pairwise Adonis test), but not from the mesohaline (8–18 PSU, $p = 0.64$, pairwise Adonis test). The functional composition of bacterial communities in the mesohaline, polyhaline, and euhaline were not significantly different ($p > 0.05$ for all comparisons, pairwise Adonis test). Nutrients did not affect functional composition (NO_x, $p = 0.90$; PO_4, $p = 0.22$).

A PCA plot based on KEGG Orthology (KO) composition likewise demonstrated the importance of the salinity gradient toward structuring the functional composition (Fig. 5.02B). A total of 23 KEGG modules differed in abundance across the salinity region ($p < 0.05$, LinDA linear regression) (Fig. 5.06). MAGs of bacteria from high salinity areas, for example, were enriched in genes related to thiamine biosynthesis (M00127, $p < 0.0001$), F_{420} biosynthesis (M00378, $p = 0.0004$), pyridoxal biosynthesis (M00124, $p = 0.001$), ubiquinone biosynthesis (M00117, $p = 0.02$), and betaine biosynthesis (M00555, $p = 0.03$). On the other hand, MAGs of bacteria from low salinity areas were enriched in, e.g., arginine biosynthesis (M00845, $p = 0.0004$), D-glucuronate degradation (M00061, $p = 0.001$), and phosphatidylcholine biosynthesis (M00091, $p = 0.002$). In addition, MAGs from low salinity areas included more photosynthesis genes, related to beta-carotene biosynthesis (M00097, $p < 0.0001$) and photosystem I (M00163, $p = 0.001$).

Our results showed that the *taxonomic* composition of *Ulva*-associated bacterial communities ($p = 0.0001$, $R^2 = 0.70$) explained more of the observed variation across the Atlantic–Baltic salinity gradient than the *functional* composition of the same communities ($p = 0.0003$, $R^2 = 0.17$). This implies that taxonomic turnover was larger than the observed functional change and that several functions were performed across the salinity gradient by different taxa. Figure 5.07 gives a complete overview of the presence or absence of KEGG modules in the metagenomic assembled genomes of 26 taxa that are characteristic to a specific salinity region (5–8 PSU, 8–18 PSU, 18–30 PSU, or 30–36 PSU). Pantothenate (vitamin B_5), for example, can be produced at low to medium salinity (5–18 PSU) by an unknown *Saprospiraceae* (MAG591), but at medium to high salinity (18–36 PSU) this function in the community was taken over by *Robiginitomaculum* and another unknown *Saprospiraceae* (MAG149) (Fig. 5.07). Similarly, proline biosynthesis at low salinity can be conducted by *Alteraurantiacibacter* and *Rubripirellula* (5–8 PSU), at medium salinity by *Litorimonas* A (8–18 PSU), and was gradually taken over by *Neomegalonema* (18–30 PSU), and *Leucothrix* and *Litorimonas* at high salinity (30–36 PSU). In addition, most MAGs shared a set of core genes that are necessary for essential functions, including nucleotide metabolism, fatty acid biosynthesis, energy metabolism (F-type ATPases, succinate dehydrogenases, etc.), and genes encoding structural modules (e.g., ribosomes, RNA polymerase, and DNA polymerase) (Fig. 5.07).

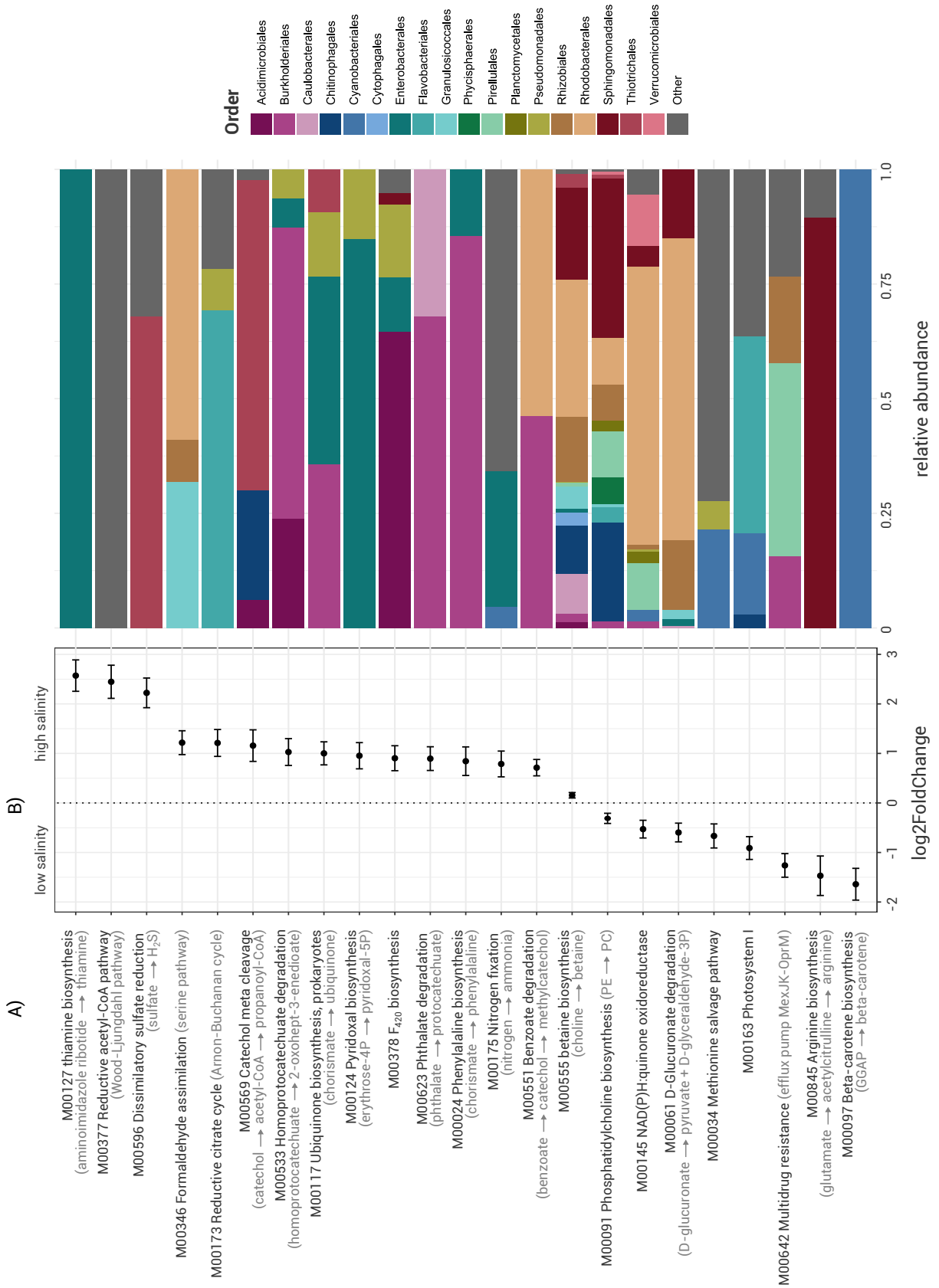

FIGURE 5.06 Functional changes in the *Ulva*-associated bacterial communities across salinity. Panel A) log-2FoldChange values (± standard error) of the KEGG modules that significantly ($p < 0.05$) differ in abundance with salinity. Panel B) Taxonomic composition (order level) of the metagenomic-assembled genomes (MAGs) that harbour the identified KEGG modules. The relative abundance is based on read counts of the orders across the entire dataset.

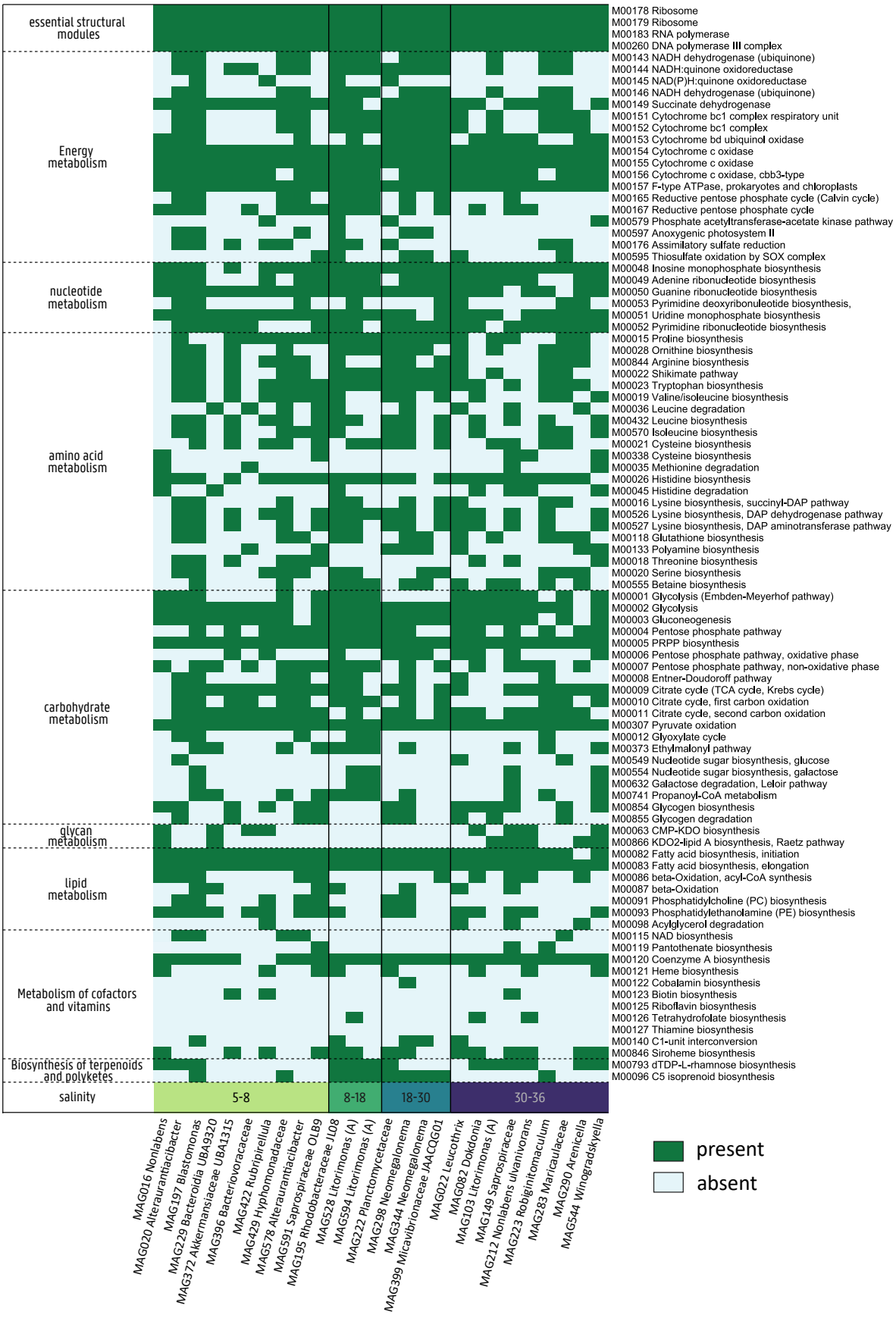

FIGURE 5.07 Heatmap depicting the presence (dark-green) or absence (light-blue) of KEGG modules in 26 metagenomic assembled genomes (MAGs) that are characteristic to a specific salinity region (5–8 PSU, 8–18 PSU, 18–30 PSU, or 30–35 PSU).

5.4 Discussion

5.4.1 Bacteria as important symbionts of macroalgae

Carbon and sulphur utilisation

Rich in organic carbon, oxygen, and nutrients, the algal surface provides an ideal habitat for the growth of microbes (Brock and Clyne 1984, Bengtsson et al. 2011, Lage and Graça 2016). The microbial community reciprocates by supplying the algal host with phosphate, nitrogen, and vitamins in return (Croft et al. 2006, Egan et al. 2013, Hollants et al. 2013a). Such an exchange of key nutrients is an essential feature of the *Ulva* holobiont.

Bacteria do not only live on the algal tissue, they live of it. Our results demonstrated that a substantial majority [97%] of the bacteria in *Ulva*-associated communities are capable of breaking down complex polysaccharides constituting the *Ulva* cell wall. The *Ulva* cell wall is mainly composed of cellulose, glucuronan, ulvan, and xyloglucan, which together make up 45% of the dry-weight biomass (Kidgell et al. 2019). Ulvan, a key component, is composed of sulphated rhamnose, xylose, and uronic acids (D-glucuronate and iduronic acid) (Kidgell et al. 2019). The initial steps in the breakdown of ulvan can be catalysed by ulvan lyases (sulphatases) (Tang et al. 2021), but additional glycoside hydrolases are needed to obtain monomeric sugars (Reisky et al. 2018). Through a comparative analysis of *Ulva*-associated bacteria and closely related taxa isolated from seawater, we showed that the *Ulva* community was significantly enriched in CAZys that specifically target and break down *Ulva*'s polysaccharides and cell wall components (e.g., ulvan, iduronic acid, cellulose, xyloglucan). In total, ulvan lyases were found in 146 MAGs, many of which were typical *Ulva*-associated bacteria, such as *Lewinella*, *Nonlabens*, *Algibacter*, *Glaciecola*, and *Polaribacter*. Furthermore, these *Ulva*-associated bacteria were enriched in ABC transporters, facilitating the uptake of small monosaccharides like fructose and rhamnose resulting from the degradation of the cell wall polysaccharides. This enrichment in enzymes capable of degrading *Ulva*'s cell wall components suggests that a defining aspect of an *Ulva* microbiome is its ability to utilise and break down the host organism, providing a partial answer to the question of what defines an *Ulva* microbiome.

In addition to the utilisation of polysaccharides, bacteria living in symbiosis with *Ulva* utilise sulphur compounds produced by the host. Due to the presence of sulphate esters in ulvan, *Ulva* species have a relatively high sulphur content (Wahlström et al. 2020a, Yang et al. 2021). Our findings align with the hypothesis that the widespread prevalence of sulphonates in marine algae contributes to the high abundance of sulphonate-degrading bacteria in marine habitats (Scholz et al. 2021). Sulphur metabolism related genes in *Ulva*-associated communities were predominantly involved with assimilatory sulphate reduction, leading to the formation of sulphite and, ultimately, sulphide.

Other prevalent sulphur cycling enzymes in *Ulva*-associated communities were related to dimethylsulfoniopropionate (DMSP) metabolism, an organosulphur compound produced by *Ulva* (Van Alstyne et al. 2007, L. Han et al. 2021). DMSP has a wide range of ecophysiological functions and in the model species *Ulva mutabilis* it is known to mediate the interaction with the symbiont *Roseovarius* sp. MS2. This symbiont releases morphogenetic compounds that stimulate algal morphogenesis and growth (Kessler et al. 2018). Interestingly, although the bacterial strain is attracted by the release of DMSP and rapidly takes up the compound, its growth is not affected by DMSP. Instead, DMSP is converted into dimethylsulphide (DMS) and methanethiol (MeSH). In our dataset, the capacity to convert DMSP to DMS was almost exclusively restricted to a few genera within the *Rhizobiaceae* (the undescribed genus JAALLB01) and *Rhodobacteraceae* (predominantly *Jannaschia*, *Roseovarius*, *Sulfitobacter*, and *Tateyamaria*). This observation aligns with previous findings that another well-known morphogenesis-inducing symbiont of *Ulva*, *Maribacter* sp. MS6 (belonging to the *Flavobacteriaceae*), is not attracted by DMSP (Kessler et al. 2018).

Finally, a wide range of MAGs displayed the capability to sequester the host-derived bioactive compound taurine and convert it to sulphite. Compared to related seawater taxa, *Ulva*-associated bacteria also showed an enrichment in *tauACB* transporter enzymes. In *Ulva bulbosa*, taurine content increases in response to low temperatures and as such has been identified as a cold stress marker (Ghaderiardakani et al. 2022). Taurine likely plays a role in oxidative stress regulation within the host, but can also serve as a significant carbon and energy source for the microbial community (Clifford et al. 2019).

Amino acid metabolism

Unlike animals, seaweeds can synthesise essential amino acids themselves and relatively little is known about the uptake of dissolved organic nitrogen compounds by seaweeds. It is likely, however, that seaweeds and bacteria do exchange amino acids, especially when dissolved inorganic nitrogen availability is low (Tyler et al. 2003). Previous studies, for example, demonstrated that observed amino acid uptake rates in *Ulva* were highest for glycine and alanine and that while *Ulva* prefers inorganic nitrogen, the organic compounds may also play a significant role (Tyler et al. 2005, Li et al. 2019). A transcriptomic study in *Laurencia dendroidea* showed that the associated bacteria had a higher relative contribution to amino acid metabolism than the host itself, indicating a symbiotic relation (Oliveira et al. 2012). Similarly, in *Pyropia haitanensis*, co-cultivation with a *Bacillus* sp. does not only result in an increased growth rate, but also in a downregulation of genes related to the biosynthesis of several amino acids and other metabolites (Xiong et al. 2018). As free amino acids are known to increase primary production of algae (Flynn and Wright 1986, Linares 2006), it is hypothesised that the release of amino acids by bacteria serves as one mechanism through which they may facilitate algal growth.

Vitamins

Vitamins are essential to a well-functioning central metabolism in both microbes and their hosts (LeBlanc et al. 2013, Ryback et al. 2022). Algae require a combination of different vitamins for growth, but are likely unable to synthesise some of these the organic compounds themselves (Droop 1957, Fries 1973, Croft et al. 2005). A study by Croft et al. (2006) for example showed that more than 50% of the algae studied by them required an exogenous supply of cobalamin, 22% required thiamine, and 5% required biotin. This vitamin auxotrophy suggests that the host is dependent on the production by its microbial symbionts. In *Ulva* species, the addition of vitamin B_{12} (cobalamin) and particularly vitamin B_6 (pyridoxal) to culture medium is necessary for growth and promotes nitrogen metabolism (Nasr and Bekheet 1969, Mohsen et al. 1974). The well-defined *Ulva* culture medium that is used for cultivating the lab strain *Ulva mutabilis* even contains a stock solution of most vitamin B types (Califano and Wichard 2018). Previous metagenomic studies in the red alga *Pyropia haitanensis* (J. Wang et al. 2022) and brown alga *Nereocystis luetkeana* (Weigel et al. 2022) have highlighted the potential of the bacterial symbionts to produce cobalamin. Here we showed that the capacity of seaweed-associated bacteria to biosynthesise multiple vitamins extends beyond vitamin B_{12} and is widespread within the *Ulva* microbiome.

5.4.2 Changing taxa, consistent functions?

Our results demonstrated that both the taxonomic composition and the functional composition of *Ulva*-associated bacteria significantly change across the salinity gradient. In some instances, shifts in taxa coincided with corresponding changes in functional potential. At low salinity, for example, we observed higher abundances of MAGs containing photosystem I. These mostly belonged to the Cyanobacteriota (*Prochlorotrichaceae*, *Phormidesmiaceae*, and *Cyanobacteriaceae*), along with a few instances in *Flavobacteriaceae* such as *Cellulophaga*

tyrosinoxydans. In addition, genes related to beta-carotene biosynthesis, which is essential for the assembly of photosynthetic complexes (Tóth et al. 2015), were enriched in low salinity conditions, primarily attributed to the increased prevalence of *Spirulina*, *Rippkaea*, and a *Geitlerinemaceae* (all Cyanobacteriales). The higher abundance of Cyanobacteriales at low salinity corresponds with previous 16S-based findings across the Atlantic–Baltic Sea gradient in both *Ulva*-associated communities (van der Loos et al. 2022) and seawater communities (Celepli et al. 2017, Olofsson et al. 2020).

However, our results also showed that the functional potential of the bacterial community across the salinity gradient was more conserved than the taxonomic profile. This conservation extends beyond a set of core genes encoding structural modules that are necessary for essential metabolism to include functions potentially relevant to the algal host. Both the low and high salinity communities exhibited the capacity to synthesise, for example, proline and tetrahydrofolate (vitamin B_9), despite the large difference in taxonomic composition. This functional redundancy across taxa has been observed previously in *Ulva*-communities (Burke et al. 2011a, Roth-Schulze et al. 2016) and may be indicative of a stable foundational relation between the host and symbionts. Although the niche width of *Ulva* appears to be broader than that of the bacterial taxa, both host and microbes must have been adapted to the local conditions along this large environmental gradient. In the next section, we discuss how the functional potential of the *Ulva*-associated bacterial community changes across salinity.

5.4.3 Functional and taxonomic patterns across salinity

Salinity as an environmental factor influences the *Ulva* host and its associated bacteria in several ways. First, as discussed in the previous paragraph, prevailing salinity conditions affect taxonomic and functional community composition. *Ulva* and bacterial species occurring in a specific salinity range are expected to have adapted to those salinity conditions through various mechanisms (Sleator and Hill 2002, Rybak 2018). Secondly, short-term fluctuations or prolonged deviations from the optimal salinity range, triggered by events such as increased river input or wind-driven exchange of water masses, can impose hypo- or hypersalinity stress that affect cell physiology. The turgor pressure of cells changes with fluctuating salinity due to changes in osmolarity, which in turn affects the efflux and influx of inorganic ions and water (Gregory and Boyd 2021). Salinity-induced osmotic changes trigger the overproduction of reactive oxygen species (ROS), causing oxidative stress (Jahnke and White 2003), damaging membrane lipids, proteins, nucleic acids, and chloroplasts (García-Caparrós et al. 2019). In *Ulva prolifera*, for example, both hyposaline and hypersaline treatments decrease growth rate and photosynthesis, with the hypersaline conditions resulting in increased hydrogen peroxide (H_2O_2) content and the upregulation of antioxidant activity and reactive oxygen scavenging enzymes such as catalase, superoxide dismutase, and glutathione reductase (Luo and Liu 2011). Similarly, *Ulva compressa* responds to hyposalinity by upregulating genes associated with protein repair, photosynthesis, and ROS scavenging (Xing et al. 2021). In bacteria too, the prevailing salinity conditions affect carbohydrate, energy, and amino acid metabolism, as well as fatty acid biosynthesis (Yaakop et al. 2016). Bacteria have developed a range of adaptive mechanisms to function optimally in either high or low salinity conditions and to cope with salinity fluctuations (Yaakop et al. 2016, Gregory and Boyd 2021). In our dataset, we identified several general patterns in how functional pathways of *Ulva*-associated bacteria differ across the salinity gradient, which we discuss in more detail below.

1) Vitamins and cofactors that reduce oxidative stress

MAGs that were abundant in high salinity areas more often contained the genes needed to produce factor F_{420}, in particular several MAGs belonging to the Acidimicrobiales, as well as *Alteromonas stellipolaris* and a *Vibrio* species. This cofactor is a low-potential hydride transfer agent and plays an important role in the primary and secondary metabolism of certain bacteria. Several antioxidant mechanisms are F_{420}-dependent (Gurumurthy et al. 2013) and cofactor F_{420} is known to help bacteria combat oxidative stress (Grinter and Greening 2021).

The ability to produce thiamine (vitamin B_1) and pyridoxal-5P (the active form of B_6) was enriched in high salinity areas as well. A total of 13 MAGs had the potential to produce pyridoxal-5P (including *Alteromonas stellipolaris*, and multiple *Glaciecola* and *Vibrio* species), and these were typical of the higher salinity bacterial communities. Only a single *Vibrio* MAG contained the genes necessary for the production of thiamine. This bacterium was nearly absent at the lower end of the salinity gradient, and much more abundant at high salinity levels. In terrestrial plants, both vitamin B_1 and B_6 are known to alleviate salinity stress, for example in *Arabidopsis thaliana* (Rapala-Kozik et al. 2012) and in milk thistle (Mosavikia et al. 2020), due to the stimulation of antioxidant enzyme activity and proline content. In addition to protecting from oxidative stress, pyridoxal-5P also increases photosynthetic pigment in wheat (Liu et al. 2019), and it facilitates growth through the reduction of ethylene accumulation that usually occurs under salinity stress in rice (Hussain et al. 2020). Similarly, gene expression of vitamin B_1 is upregulated in phytoplankton during salt stress and oxidative stress is thought to function as a stress signalling molecule (Faarghl 2012, Fern et al. 2017). It is possible that thiamine and pyrodixal-5P produced by bacteria also aid the *Ulva* cells against oxidative radicals that are more prevalent under high salinity levels.

2) Accumulation of compounds to maintain osmotic homeostasis

One of the best-known strategies in bacteria and eukaryotes alike is the accumulation of low molecular weight compounds, such as sugars and amino acids, that act as osmoprotectants to maintain osmotic homeostasis and turgor pressure. Glycine betaine, for example, is an osmolyte that acts as one of the preferred compatible solutes in the majority of prokaryotes (Sleator and Hill 2002, McParland et al. 2021). It is known to accumulate in bacterial cells with increasing salinity (Hu et al. 2020), and betaine transporters are enriched in bacterial communities originating from marine habitats compared to freshwater environments (Dupont et al. 2014). Although glycine betaine plays a more important role in higher plants than in algae as osmoprotectant (Kirst 1989), a transcriptomic dataset showed that three choline dehydrogenase genes (involved in the conversion from choline to betaine) were upregulated in *Ulva compressa* during a recovery period after hyposaline stress. In our dataset, MAGs containing the genes needed to produce betaine (e.g., *Litorimonas*, *Leucothrix, Neomegalonema*) were more abundant at high salinity levels. Similarly, the capacity to produce the essential amino acid phenylalanine was enriched at high salinity. Phenylalanine is known to accumulate in plants under high salinity conditions (Hattab et al. 2015) and increases salinity tolerance in maize (Zahra et al. 2020). In the brown alga *Ectocarpus siliculosus*, the intracellular phenylalanine concentration increases to 120–176% during both hypo- and hypersaline levels compared to controls (Dittami et al. 2011). Another amino acid, arginine, is also known as an osmoprotectant (Dittami et al. 2011, Kabiri et al. 2016), but the necessary genes in our dataset were mainly present in Sphingomonadales that were more abundant at lower salinities. Both arginine and proline are synthesised from glutamate, but we did not find evidence for enrichment of proline synthesis genes at high salinity. Instead, the potential to produce proline was abundantly present across the entire salinity range, with an average relative abundance of 1.1% and 388 out of the 639 MAGs demonstrating the ability to produce it.

The serine pathway of formaldehyde assimilation is another module that was enriched in high salinity MAGs. In this pathway, formaldehyde is assimilated to form intermediate compounds of central metabolic pathways such as serine, glycerate, malate, and acetyl-CoA that can subsequently be used for biosynthesis (Bar-Even 2016). Serine and malate can accumulate in plants in response to high salinity, particularly in plants that also accumulate proline, and act as osmoprotectants by maintaining turgor pressure (Stewart and Larher 1980, Whittington and Smith 1992). Genes associated with other well-known osmolytes and osmoprotectants, such as ectoine and trehalose, were comparatively less prevalent in our dataset (9 MAGs and 35 MAGs, respectively, were able to synthesise these compounds). However, it is important to keep in mind that these findings are solely derived from gene content analyses and do not reflect gene expression patterns. Future transcriptomic studies could shed more light on the up- or downregulation of specific genes by *Ulva* and its associated bacteria in response to changing salinity conditions.

3) Stabilising the cell membrane

Another well-known strategy of bacteria to cope with cell turgor pressure is to alter the membrane composition through changes in fatty acids or phospholipids (Oshone et al. 2017). The cell membrane separates the cell's interior from the external environment and is therefore the first structure to encounter the effects of fluctuating salinity and osmotic stress. The disruption of membranes affects many processes such as transport of compounds, enzyme activities, and signal transduction. It is therefore important to maintain the correct fluidity of the lipid bilayer (Los and Murata 2004). We found that many typical high-salinity MAGs were associated with the ability to synthesise ubiquinone. Ubiquinone (also called coenzyme Q) is a membrane-stabilising isoprenoid and the accumulation of this compound increases salt tolerance in bacteria, especially in the thin-walled gram-negative bacteria (Sévin and Sauer 2014, Sévin et al. 2016). In the Atlantic–Baltic Sea gradient, it was mainly found in gram-negative bacteria of the orders Burkholderiales, Enterobacterales, Pseudomonadales, and Thiotrichales. Ubiquinone alters the physicochemical properties of the membrane by increasing the lipid packing and density. This results in reduced membrane permeability (i.e., a slower release of small solutes) and increases the strength of the membrane (i.e., resistance to cell rupture) (Agmo Hernández et al. 2015).
By studying seawater and limnic bacterial communities across the Atlantic–Baltic Sea gradient, Dupont et al. (2014) found contrasting pathways in the biosynthesis of quinones. Biosynthetic pathways for ubiquinone were correlated with seawater communities, while the menaquinone pathway was correlated with freshwater communities. In our dataset, we did not find evidence for enriched pathways of menaquinone synthesis in low salinity communities, perhaps since we did not include true freshwater communities (the lowest salinity values were >5 PSU). However, we did find that the module for phosphatidylcholine biosynthesis was enriched in low salinity conditions. Phosphatidylcholine (PC) is a membrane-forming phospholipid that is synthesised from Phosphatidylethanolamine (PE) and studies found that PE levels increased in salt-adapted cells (Šajbidor 1997). It has been noted before that while PE is the more common phospholipid in bacteria, gram-negative bacteria with high proportions of unsaturated fatty acids often contain additional PC to maintain stable bilayers (Goldfine 1984). Indeed, in our dataset, the ability to convert PE to PC was mainly found in low salinity enriched Sphingomonadales (e.g., *Alteraurantiacibacter*, *Erythrobacter*) and Rhodobacterales (e.g., *Jannaschia*, *Pseudorhodobacter*). Membranes lacking PC are more fluid, have a higher permeability for small molecules and are more sensitive to osmotic changes (Geiger et al. 2013). Both quinone and phosphatidylcholine seem to stabilise the membrane to withstand changes in turgor pressure and maintain osmotic balance.

5.5 Conclusions and future perspectives

In this study we showed that both the taxonomic and functional composition of *Ulva*-associated bacterial communities change across a 2,000 km salinity gradient. The high turnover of microbial taxa is accompanied by functional redundancy, where guilds of taxa along the entire environmental gradient can perform crucial functions. These functions, including amino acid and vitamin B production, are potentially important to the seaweed host. Alongside functional redundancy, we identified distinct functional modules exhibiting enrichment in either low or high salinity areas. These modules are likely involved in mitigating oxidative stress, maintaining cellular osmotic homeostasis, and stabilising cell membranes. Furthermore, we provided an overview of the metabolic functions that characterise a typical *Ulva*-microbiome, highlighting the large metabolic potential inherent in bacterial–algal symbiosis. The holobiont concept, which regards the seaweed host and its associated microbes as an integrated functional unit, is essential when studying the physiological response of seaweeds to environmental change. Future laboratory experiments, involving the inoculation of seaweed cultures with targeted microbial communities, are needed to investigate whether bacteria can facilitate the acclimation of *Ulva* species to changes in salinity.

Acknowledgements

The research leading to the results presented in this publication was carried out with infrastructure funded by the FWO PhD Fellowship fundamental research (3F020119), the EMBRC Belgium – FWO project I001621N, and the Formas-funded 'A manual for the use of sustainable marine resources' project (Grant no. 2022-00331). We would like to thank Samanta Hoffmann for her assistance during field work and Nadja Stärck for assistance with nutrient analyses.

Author contributions

L.M.L.: Conceptualization, Methodology, Formal analysis, Data Curation, Writing - Original Draft, Visualisation. **S.S.:** Investigation, Writing - Review & Editing. **W.S.:** Resources, Writing - Review & Editing. **F.W.:** Writing - Review & Editing. **S.D.:** Methodology, Resources, Writing - Review & Editing. **A.W.:** Writing - Review & Editing, Supervision. **O.D.C.:** Writing - Review & Editing, Supervision, Funding acquisition.

Data availability statement

Raw whole-genome sequence reads and related metadata are deposited in the SRA (BioProject PRJNA1040445). All Electronic Supplementary Materials (Figures and Tables) are available at Zenodo (DOI: 10.5281/zenodo.10475438).

Notes

[1] The samples analysed in this study are a subset of the 481 samples described in Chapter 4 of this thesis. The samples for additional metagenomic analyses were selected to encompass a diverse representation of host species and to cover the distribution across the salinity gradient adequately. Furthermore, we conducted DNA quantity and quality measurements to ensure compliance with the requirements for metagenomic sequencing. Consequently, this screening process resulted in the exclusion of the majority of samples collected at salinity levels below 5 PSU due to insufficient DNA concentration.

[2] The taxonomic composition (including the most abundant bacterial orders, families, and genera) and the changes in taxonomic composition across salinity corresponded well to the patterns observed based on 16S amplicon data (Chapter 4). The metagenomic dataset revealed higher diversity, and changes across salinity sometimes deviated from the patterns observed at the genus level due to the increased taxonomic resolution. For instance, while the 16S amplicon dataset showed that a high percentage of variation in abundance of the genus *Leucothrix* was explained by salinity and host species, the metagenomic dataset revealed five *Leucothrix* metagenome-assembled genomes (MAGs), of which only three exhibited well-explained variations in abundance in response to salinity.

Supplementary Figures

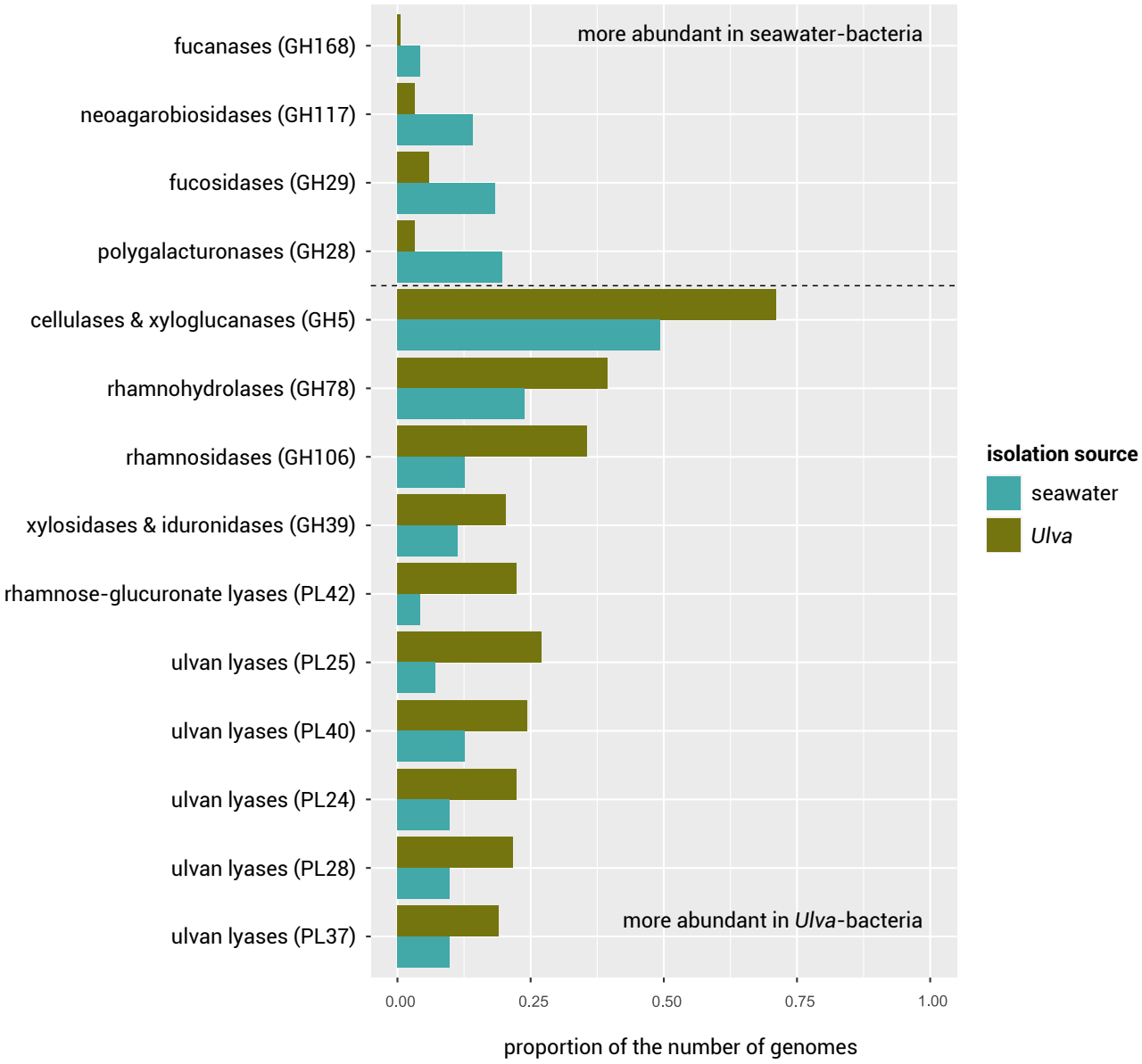

FIGURE S5.01 The proportion of the number of seawater-isolated (blue) or *Ulva*-isolated (green) bacterial genomes than contained a specific CAZY family (polysaccharide lyases = PL, glycoside hydrolases = GH).

“There is nothing more deceptive than an obvious fact.”

– Arthur Conan Doyle, in: The Adventures of Sherlock Holmes

Chapter 6.
How bacteria shape growth of the green seaweed *Ulva fenestrata* in low salinity environments

Luna M. van der Loos, Sophie Steinhagen, Peter Chaerle, Evelien De Canck, Sofie D'hondt, Liesbeth Lebbe, Francesca Petrucci, Frederik Leliaert, Anne Willems, Olivier De Clerck

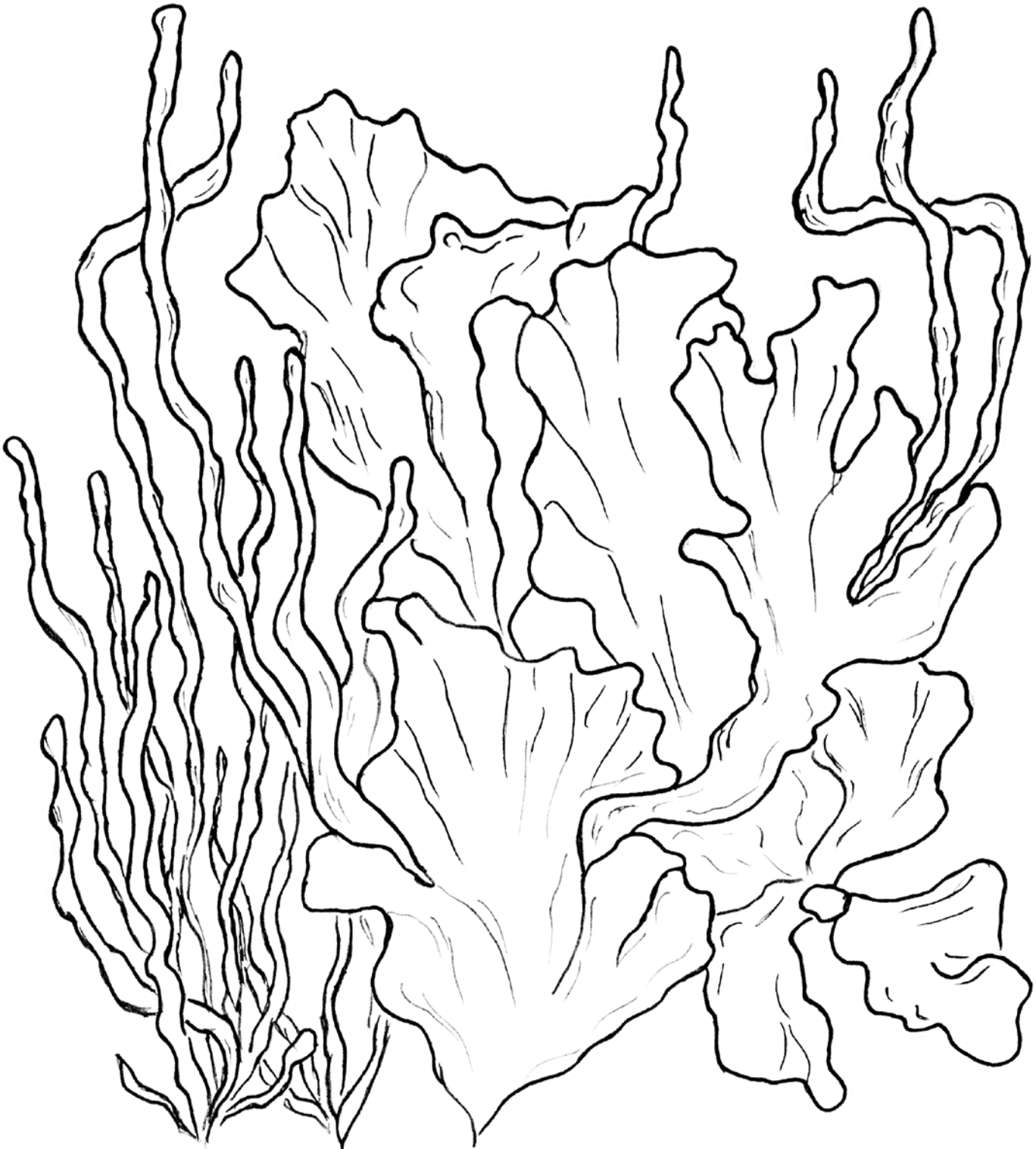

Chapter 6. How bacteria shape growth of the green seaweed *Ulva fenestrata* in low salinity environments

Luna M. van der Loos[1,2], Sophie Steinhagen[3], Peter Chaerle[4], Evelien De Canck[2], Sofie D'hondt[1], Liesbeth Lebbe[2], Francesca Petrucci[1], Frederik Leliaert[5], Anne Willems[2], Olivier De Clerck[1]

[1] Phycology Research Group, Department of Biology, Ghent University, Ghent, Belgium
[2] Laboratory of Microbiology, Department Biochemistry and Microbiology, Ghent University, Ghent, Belgium
[3] Department of Marine Sciences-Tjärnö, University of Gothenburg, SE-452 96 Strömstad, Sweden
[4] BCCM/DCG, Department of Biology, Ghent University, Ghent, Belgium
[5] Meise Botanic Garden, 1860 Meise, Belgium

Abstract

Salinity is one of the main drivers of species diversity in both macroalgae and microbial communities. Green seaweeds of the genus *Ulva* are known for their high tolerance to changing salinity conditions, ranging from freshwater to full marine conditions. Previous research indicated that the taxonomic and functional composition of *Ulva*-associated bacterial communities shift in response to salinity along a natural environmental gradient. Here, we exposed *Ulva fenestrata* cultures to two different salinity treatments (5 PSU and 32 PSU) using both germlings and adult tissue. We then investigated how *Ulva* growth was affected by the addition of 24 bacterial strains, of which 12 were typical to high salinity conditions and 12 were typical low salinity strains. We tested the effect of individual monocultures, as well as inoculants comprising randomly assembled communities of 3, 6 and 12 species following a broken stick model. We found that *Ulva* growth exhibited a 74–120% increase with the addition of an *Aquipuribacter* strain (originally isolated from low salinity), a *Maribacter*, or a *Zobellia* strain (both isolated from high salinity) compared to the effect of the other monocultures. Notably, the growth-enhancing effect was specific to germling cultures under low salinity conditions. Germling daily growth rate in low salinity exceeded that in the high salinity treatment by 138% when beneficial bacteria were introduced, despite the fact that distribution of *U. fenestrata* in natural environments is limited to high salinity conditions. In addition, *U. fenestrata* developed a tube-like morphology in the low salinity treatments, while this species is obligate foliose in natural systems. Our results underscore that life-history phases and environmental conditions are essential to understanding the dynamics of the seaweed holobiont.

6.1 Introduction

All organisms in an ecosystem are inextricably linked with one another and the environment through various interactions. This principle holds true for ecosystems at both macroscopic and microscopic scales. Each eukaryotic host, often colonised by millions of microbes, constitutes an ecosystem on its own. The host and its associated microbes collectively create a cohesive entity known as the "holobiont", representing a functional unity (Rosenberg and Zilber-Rosenberg 2016, Simon et al. 2019, Baedke et al. 2020). The holobiont concept is of particular importance within the context of environmental change, as not only the host but also the associated microbes react to changes in the environment (Egan et al. 2013, van der Loos et al. 2019).

The surface of seaweeds too, is covered with a plethora of microbes that rely on the host for food and habitat while reciprocally providing the seaweeds with a diverse array of services (Wahl et al. 2012, Egan et al. 2013). It becomes increasingly clear that these microbes are essential for the functioning of macroalgal life. Seaweed-associated bacterial communities are known to change when the host experiences environmentally-induced stresses, especially under the influence of elevated temperature (Webster et al. 2011, Saha et al. 2014, Mensch et al. 2020). A stable microbiome ensures host resilience to environmental stress, as has for example been demonstrated in rhodoliths under ocean acidification conditions (Cavalcanti et al. 2018). Certain bacteria can even help the seaweed host acclimate to environmental changes. For instance, the capacity to survive the transition from seawater to freshwater of *Ectocarpus*, a genus of small filamentous brown algae, is facilitated by a microbial community (Dittami et al. 2016). Removing the seaweed-associated bacteria deprived *Ectocarpus* cultures of their ability to survive in freshwater, while providing the seaweeds with an inoculant derived from an *Ectocarpus* strain that naturally inhabited freshwater environments, restored the ability to acclimate to salinity changes (Dittami et al. 2016).

Several biofertilisers (i.e., inoculants composed of plant growth-promoting bacteria) are commercially available in the agricultural industry (Mącik et al. 2020). These biofertilisers enhance crop yield by mitigating environmental stressors, such as salinity and drought (Olanrewaju et al. 2017, Mishra et al. 2021). The bacteria in the biofertilisers provide nutrients, release secondary metabolites, and protect the plants against pathogens. Growth-promoting inoculants have not been commercially developed for seaweeds yet. Nonetheless, several bacteria have been identified that promote seaweed growth, particularly within green seaweeds of the genus *Ulva* (Gemin et al. 2019, H. Wang et al. 2022). Moreover, *Ulva* exhibits a dependence on specific bacterial strains for morphological development, rendering it a model organism for investigating algal–bacterial interactions (Wichard et al. 2015).

Multiple *Ulva* species are known for their wide tolerance to salinity conditions, with some species occurring from freshwater to hyperhaline environments (Rybak 2018). Previous studies showed that salinity is a major driver of the taxonomic and functional composition of *Ulva*-associated bacterial communities and of *Ulva* species diversity (Chapter 4, Chapter 5, van der Loos et al. 2022, Steinhagen et al. 2023). This led us to hypothesise that associated bacteria help the host acclimate to salinity changes. In this study, we investigate the potential of bacteria to facilitate *Ulva fenestrata* growth under varying salinity conditions. We test this by subjecting *U. fenestrata* germlings and adult tissue to two different salinity treatments (high versus low salinity) accompanied by the introduction of bacteria that were originally isolated from *Ulva* growing in either high or low salinity environments. Given that the natural distribution of *U. fenestrata* is limited to euhaline and polyhaline salinity levels (20–34 PSU) (Steinhagen et al. 2023), we hypothesised that this species performs best in the high salinity treatment (HST) when supplemented with typical high salinity bacteria (HSB). In addition, we expected low salinity bacteria (LSB) to mitigate stress induced by the low salinity treatment (LST) by promoting *U. fenestrata* growth, but that these LSB cannot enhance growth in the HST.

6.2 Materials & Methods

6.2.1 Bacterial strain isolation and identification

The *Ulva*-associated bacteria used in this experiment were collected at different salinity conditions (2.8–35.0 PSU) across the Atlantic–Baltic Sea gradient, in Sweden, Denmark, and the Netherlands (Table 6.01, Electronic Supplementary Table S6.01). At each site, *Ulva* specimens were collected and gently rinsed in sterilised seawater to remove loosely attached bacteria. A piece of 2 cm^2 was cut from the thallus, blotted dry with sterilised filters, and stored in silica (Gherna and Reddy 2014). The samples were stored at 4 °C until isolation.

To isolate the *Ulva*-associated bacteria, the dried tissue was re-emersed in sterile seawater and rehydrated for 4 hours. The samples were then crushed with a mortar and pestle and 100 µL of the supernatant was plated on agar. Two different growth media were used: basic Marine Agar (with a total PSU of 30) and reduced salinity Marine Agar (with a total PSU of 6.5) (Table 6.01). The basic Marine Agar consisted of 5-g peptone, 1-g yeast extract, 15-g agar, salts (19.45-g sodium chloride, 8.8-g magnesium chloride, 3.24-g sodium sulphate, 1.8-g calcium chloride, 0.55-g potassium chloride), 0.1-g ferric citrate, 0.16-g sodium bicarbonate, 0.08-g potassium bromide, 34.0-mg strontium chloride, 22.0-mg boric acid, 4.0-mg sodium silicate, 2.4-mg sodium fluoride, 1.6-mg ammonium nitrate, and 8.0-mg disodium phosphate dissolved in 1 Liter milliQ water. The concentration of the salts was reduced by 5.6 times to create the reduced salinity Marine Agar. The agar plates were incubated

at 20 °C for 8–12 days. After growth was observed, individual colonies of different morphologies were picked and replated until pure. The pure bacterial strains were conserved in MicroBanks (Pro-Lab Diagnostics™) and stored at –80 °C.

The isolated strains were identified using 16S RNA gene sequencing. DNA of the bacterial cultures was extracted using an alkaline lysis. In summary, a small amount of biomass from a pure colony was harvested using a pipette tip and lysed in 20 µL alkaline lysis buffer at 95 °C for 15 minutes. The samples were cooled on ice immediately after. Subsequently, 180 µL sterile milli-Q was added to each sample, after which the samples were centrifuged for 5 minutes at maximum speed and stored at –20 °C. The full length 16S rRNA gene was amplified by PCR using the following primers: 27F (5'-AGAGTTTGATCCTGGCTCAG-3') and 1492R (5'-CGGTTACCTTGTTACGACTT-3') (Lane 1991). 16S rDNA amplification PCRs were performed using the Taq polymerase with a touchdown thermal profile: 5 min at 94 °C, 10 cycles of 30 s at 94 °C, 1 min at 65 °C and 1 min at 72 °C (during which the temperature of the annealing stage decreased with 0.5 °C every cycle from 65 °C to 60 °C), 20 cycles of 30 s at 94 °C, 1 min at 60 °C, and 1 min at 72 °C, and final extension of 10 min at 72 °C. The amplified products were sequenced with Sanger sequencing (Baseclear, the Netherlands). Sequences were identified using the EZBioCloud 16S rRNA database (Yoon et al. 2017).

In total, 218 pure strains were obtained (of which 98 strains with unique 16S sequences; Fig. S6.01). For use in the experiment, 12 typical low salinity bacteria and 12 typical high salinity bacteria were selected (Table 6.01). The low salinity strains were uniquely isolated from low salinity environments (<7 PSU), while the high salinity strains were exclusively isolated from high salinity sites (>25 PSU). In addition, strain selection was supported by previously collected 16S rDNA datasets (see Chapter 2, 3 & 4; van der Loos et al. 2021, 2022) and a metagenomic dataset (see Chapter 5) confirming the prevalence of these strains in either low or high salinity environments.

6.2.2 Whole-genome sequencing of isolated bacteria

The genomes of the 24 bacterial strains used in this experiment were sequenced using Oxford Nanopore Technologies. Cultured cells were suspended in 300 µL of 4 M UltraPure™ guanidine isothiocyanate solution (Invitrogen™ 15577018). High molecular weight genomic DNA was extracted using the Maxwell® RSC cultured cells DNA kit (AS1620, Promega, USA) and the Maxwell® RSC instrument (AS4500, Promega, USA) according to the manufacturer's instructions. DNA was eluted in a 10 mM Tris-HCl pH 8.5 elution buffer and subsequently treated with RNase (2mg/mL, 5 µL per 100 µL extract) and incubated at 37 °C for one hour.

The sequencing library was prepared with the Native Barcoding Kit 96 V14 (SQK-NBD114.96) according to the manufacturer's protocol (Oxford Nanopore Technologies), with an extension of the end-prep reaction duration (20 min at 20 °C and 20 min at 65 °C), the native barcode ligation duration (60 min at room temperature) and the adapter ligation duration (2 hours at room temperature). The library was subsequently sequenced on a MinION using an R10.4.1 flow cell for 72 h. The raw data was basecalled with MinKNOW core version 5.5.3 (using Guppy 6.5.7 and the SUP accuracy model), resulting in a total of 15,272,607 reads with an N50 of 8,395 bp.

The assembly of the genomes was performed with Flye v2.9.2 (Kolmogorov et al. 2019). The genomes were then checked for completeness with CheckM (Parks et al. 2015), annotated with Prokka (Seemann 2014) and visualised with GenoVi (Cumsille et al. 2023). The identification of the strains was confirmed again with GTDB-tk (Parks et al. 2018). The presence of KEGG modules was assigned with prokka2kegg (Lin 2021) and MicrobeAnnotator (Ruiz-Perez et al. 2021). To test if KEGG module composition varied with bacterial taxonomic classification, the ability to promote *Ulva* growth, and the typical salinity range, Bray-Curtis dissimilar-

ities were visualised with a Principal Coordinates Analysis (PCoA) and compared in a permutational analysis of variance (PERMANOVA) with 9,999 permutations. Differences in the presence/absence of KEGG modules between the different bacterial classes were tested with MaAsLin2 (Mallick et al. 2021). The reads are archived at SRA (BioProject PRJNA1036818). The genomes are archived at GenBank (for accession numbers, see Table 6.01).

6.2.3 Bacterial cultivation and quantification

The 24 bacterial strains that were selected to use in salinity experiments were recultivated on basic Marine Agar or reduced salinity Marine Agar and replated once to verify the absence of contamination. The colonies were then transferred to Marine Broth (Difco 2216) and cultivated for 7 days at 100 rpm shaking. To ensure the same number of bacterial cells were added to the experimental flasks, the concentration of the Marine Broth cultures was measured using an imaging flow cytometer. Subsamples of each of the bacterial culture were transferred to 1.5 mL Eppendorf tubes, stained with a SYBR® Green I nucleic acid gel stain (cat. no. S7563; Invitrogen; Thermo Fisher Scientific, USA) [working solution: 1:100 in DMSO (cat. no. D4540; Sigma-Aldrich; Merck KGaA, Germany), final stain concentration: 1:10000], incubated for 20 minutes at 37 °C in the dark, and analysed using the ImageStream®XMk II (Amnis part of Luminex, Austin, Texas, USA).

The template to acquire the data with the image flow cytometer was set as follows: per object, one bright field image (LED, 13.65 mW) was captured on Ch01 and the SYBR Green I signal on Ch02 (488 nm, 0.5 mW) of the first CCD camera, while the second bright field image (LED, 10.45 mW) was captured on Ch09 and the auto-fluorescent signal on Ch011 (642 nm, 0.5 mW) of the second CCD camera. The dark field (SSC, 785 nm, 1.0 mW) images were not retained for further analysis. Data acquisition ended when 30000 objects (within a predefined 2D region: x-axis [intensity Ch02: 200 – 1e06] and y-axis [intensity Ch011: -2000 – 1e04]) were measured or when a time of 5 minutes had passed. All images were captured with the instrument-specific Inspire software (v.201.1.0.765) and processed with the Ideas software (v.6.2.187.0). A single template created with the latter software was used to analyse all subsamples and to determine the concentration (objects/µL) of non-attached bacteria.

6.2.4 *Ulva* strain cultivation

The *Ulva fenestrata* strain used in this experiment was taken from a culture at Ghent University (Belgium) that originates from a long-term indoor tank culture at the Tjärnö Marine Laboratory (Sweden) where it was cultivated at a salinity of 33 PSU. The strain was originally collected in the Koster archipelago (Sweden), where the mean salinity of the surface seawater is 27.6 ± 3.3 PSU (±SD) (Steinhagen et al. 2021b). The species identification of the parental biomass has been confirmed with molecular methods (see Toth et al. 2020). The natural distribution of *U. fenestrata* in Europe includes the Netherlands, Great-Britain, France, Ireland, Denmark, Sweden, and Norway, where it is restricted to euhaline and polyhaline regions (34–20 PSU) (Steinhagen et al. 2023). The culture at Ghent University was maintained at 15 °C in 40 L cultivation tanks with natural seawater (sand-filtered and UV-filtered), constant aeration, and a 16:8 h (L:D) photo regime at an irradiance of 70 µmol m^{-2} s^{-1}.

Reproduction in *Ulva fenestrata* tissue to obtain germlings was induced following the protocol of Steinhagen et al. (2022). In short, discs with a diameter of 4 cm were perforated from the margins of mature thalli and transferred to a 10 L aquarium with constant aeration at 15 °C. After six days, fertile tissue was air-dried and re-emersed in sterile seawater to induce the release of swarmers. In the experiments described in this chapter, all germlings originated from a single parental individual[1].

TABLE 6.01 Overview of the bacterial strains used in the experimental set-up.

Bacterial isolates				Collection information			
Bacterial isolate	**Typical salinity range**	**Strain**	**Isolation medium**	**Site**	**Salinity (PSU)**	***Ulva* host**	**WGS accession number**
HSB01	HIGH	*Dokdonia* sp000355805	basic MA	Hirtshals, Denmark	33.4	*U. fenestrata* Postels & Ruprecht	CP138998
HSB02	HIGH	*Pseudoalteromonas* sp.	basic MA	Hirtshals, Denmark	33.4	*U. fenestrata* Postels & Ruprecht	JAXHCB000000000
HSB03	HIGH	*Sulfitobacter pontiacus*	basic MA	Hirtshals, Denmark	33.4	*U. fenestrata* Postels & Ruprecht	JAXHCA000000000
HSB04	HIGH	*Zobellia russellii*	basic MA	Hirtshals, Denmark	33.4	*U. fenestrata* Postels & Ruprecht	CP139000
HSB05	HIGH	*Alteromonas stellipolaris*	basic MA	Neeltje Jans, the Netherlands	35.0	*U. lacinulata* (Kützing) Wittrock	JAXHBV000000000
HSB06	HIGH	*Algibacter* sp.	basic MA	Yerseke, the Netherlands	25.0	*U. australis* Areschoug	CP138989
HSB07	HIGH	*Nonlabens ulvanivorans*	basic MA	Jacobahaven, the Netherlands	33.0	*U. australis* Areschoug	CP138994
HSB08	HIGH	*Maribacter* sp.	basic MA	Hirtshals, Denmark	33.4	*U. fenestrata* Postels & Ruprecht	CP138999
HSB09	HIGH	*Olleya* sp.	basic MA	Yerseke, the Netherlands	25.0	*U. lacinulata* (Kützing) Wittrock	CP138988
HSB10	HIGH	*Polaribacter* sp.	basic MA	Yerseke, the Netherlands	25.0	*U. australis* Areschoug	CP138992
HSB11	HIGH	*Vibrio* sp.	basic MA	Jacobahaven, the Netherlands	33.0	*U. australis* Areschoug	JAXHBS000000000
HSB12	HIGH	*Winogradskyella* sp.	basic MA	Yerseke, the Netherlands	25.0	*U. australis* Areschoug	CP138990
LSB01	LOW	*Albirhodobacter* sp.	reduced MA	Gryt, Sweden	6.6	*U. linza* Linnaeus	JAXHCH000000000
LSB02	LOW	*Aquipuribacter* sp.	reduced MA	Härnösand, Sweden	2.8	*U. intestinalis* Linnaeus	JAXHCD000000000
LSB03	LOW	*Bermanella* sp.	reduced MA	Härnösand, Sweden	2.8	*U. intestinalis* Linnaeus	CP139001
LSB04	LOW	*Bosea* sp.	reduced MA	Härnösand, Sweden	2.8	*U. intestinalis* Linnaeus	JAXHPY000000000
LSB05	LOW	*Brevundimonas* sp.	reduced MA	Gräddö, Sweden	5.3	*U. intestinalis* Linnaeus	CP139004
LSB06	LOW	*Frigoribacterium* sp001424645	reduced MA	Härnösand, Sweden	2.8	*U. intestinalis* Linnaeus	CP139002
LSB07	LOW	*Kineococcus* sp.	reduced MA	Härnösand, Sweden	2.8	*U. intestinalis* Linnaeus	JAXHCE000000000
LSB08	LOW	*Allorhizobium* sp001713475	reduced MA	Hudiksvall, Sweden	4.9	*U. intestinalis* Linnaeus	JAXHBX000000000
LSB09	LOW	*Rhodococcus fascians*	reduced MA	Härnösand, Sweden	2.8	*U. intestinalis* Linnaeus	JAXHCF000000000
LSB10	LOW	*Sphingomonas* sp.	reduced MA	Hudiksvall, Sweden	4.9	*U. intestinalis* Linnaeus	JAXHBZ000000000
LSB11	LOW	*Erythrobacter* sp.	reduced MA	Gryt, Sweden	6.6	*U. linza* Linnaeus	JAXHCJ000000000
LSB12	LOW	*Paracoccus* sp.	reduced MA	Gryt, Sweden	6.6	*U. linza* Linnaeus	JAXHPZ000000000

6.2.5 Experimental set-up

In the salinity experiment conducted in this study, *Ulva fenestrata* was cultivated in flasks in either high (32 PSU) or low (5 PSU) salinity conditions, and inoculated with either a high or low salinity bacterial community (Fig. 6.01). This resulted in the following experimental combinations: 1) high salinity treatment + high salinity bacteria (HST+HSB), 2) high salinity treatment + low salinity bacteria (HST+LSB), 3) low salinity treatment + high salinity bacteria (LST+HSB), and 4) low salinity treatment + low salinity bacteria (LST+LSB).

The experiment was conducted three times: 1) with discs (3 mm in diameter) perforated from two-month-old thalli cultivated in sterilised seawater, 2) with two-week-old germlings (on average 0.08 mm^2) in sterilised seawater, and 3) with two-week-old germlings (on average 0.05 mm^2) in synthetic *Ulva* culture medium (UCM; specifically developed to cultivate *Ulva mutabilis*) (Stratmann et al. 1996). At the start of the experiment, the germlings and discs were exposed to a sonication treatment to disrupt the bacterial biofilm present. This does not completely sterilise the tissue, but facilitates colonisation of the inoculant (5 minutes at 40 kHz, Branson 3200 Ultrasonic Cleaner)[2]. The efficiency of the disruption method was verified with DAPI staining and fluorescence microscopy (Supplementary Materials & Methods S6.01).

A total of 264 flasks (VWR Cell Culture Flasks, vented cap, 25 cm^2) were used in every experiment, each with three *Ulva* germlings or discs and 17 mL medium (either sterile seawater or UCM). The seawater (collected at Ostend, Belgium) was autoclaved and filter-sterilised, and supplemented with 500 µL GeO_2 (1 mg mL^{-1}) and 1 mL F/2 (Varicon Aqua, Cell-Hi F2P) nutrients per Liter seawater. The UCM was prepared following the methods in Stratmann et al. (1996). Low salinity seawater was prepared by diluting seawater with milliQ water. Low salinity UCM was prepared by reducing the salts in solution I by 5.7 times. The bacterial inoculant was added to each flask at a final concentration of 10^5 bacterial cells/mL seawater. This was done by measuring the concentration of the Marine Broth bacterial cultures using an imaging flow cytometer (see section 6.2.3 Bacterial cultivation and quantification). The Marine Broth cultures were then diluted with sterile, autoclaved seawater to a concentration of 1.42×10^5 bacterial cells/µL and 12 µL of the bacterial culture was added to each flask. In cases where the inoculum consisted of a community of multiple species, each individual strain was added at a reduced concentration, resulting in a combined concentration of 10^5 cells/mL (e.g., in an inoculum comprising three species, each strain was added at a concentration of 0.33×10^5 bacterial cells/mL, corresponding to 4 µL of the diluted Marine Broth culture).

To be able to test the effect of individual bacterial strains and mixed communities, as well as estimate the effect of bacterial richness, we used a broken stick design (Bell et al. 2005, Salles et al. 2009). In this design, a "stick" corresponds to a list of 12 bacterial species in a random order. This stick is then divided in the middle, generating two sticks of 6 species (forming two assemblages) (Fig. 6.02A). The sticks are divided again to generate four sticks of 3 species. By creating three 12–species sticks of the HSB (all containing the same strains but in a different order), we created six random communities of 6 species, and twelve random communities of 3 species. In order to increase the number of assemblages for the 6–species communities, we added three extra assemblages (each constituting to the first three and last three species of one of the full sticks). This process was repeated for the LSB, resulting in a total of eighteen 6–species assemblages and 24 3–species assemblages. In addition, we included three replicates of all monocultures, as well as negative controls and positive controls (Fig. 6.02B). The negative controls consisted of six flasks containing sonicated germlings without the addition of bacteria, and six flasks of non-sonicated germlings without bacteria. The positive controls consisted of six flasks resembling a natural high salinity bacterial community, and six flasks resembling a natural low salinity bacterial community. These natural communities were created by removing the epibiotic bacteria from *Ulva* collected at the same low and high salinity sites visited during the isolation campaign, following the method in Bonthond

et al. (2021). In short, 3 mL sterile seawater and 10 glass beads (3 mm) were added to a 15 mL tube containing the silica-dried *Ulva* tissue. After rehydrating for four hours, the tubes were vortexed for 6 minutes at maximum speed and centrifuged for 1 min at 5000×*g*. The resulting suspensions were mixed with glycerol (20% final glycerol concentration) and stored at –80 °C. In total, 34 samples were prepared from low salinity sites and 32 samples from high salinity sites. These were pooled to create a low salinity natural community and a high salinity natural community, respectively. For a full overview of the number of flasks and the composition of the bacterial inoculation, see Electronic Supplementary Table S6.02.

The experiments ran for 21 days each, in an incubator at 15 °C with a light intensity of 70 µmol photons m^{-2} s^{-1} (15:9 h L:D), and 70 rpm shaking. The position of the flasks within the incubator was randomized every 2–3 days. *Ulva* surface area was measured at the start and end of the experiment using ImageJ (Schneider et al. 2012). Growth was calculated as the increase in surface area in mm^2/day/individual (averaged over 3 individuals). A Kruskal-Wallis test was used to test for differences in *Ulva* growth between salinity treatments and Dunnett's test was used to assess differences in growth between the different bacterial inoculants.

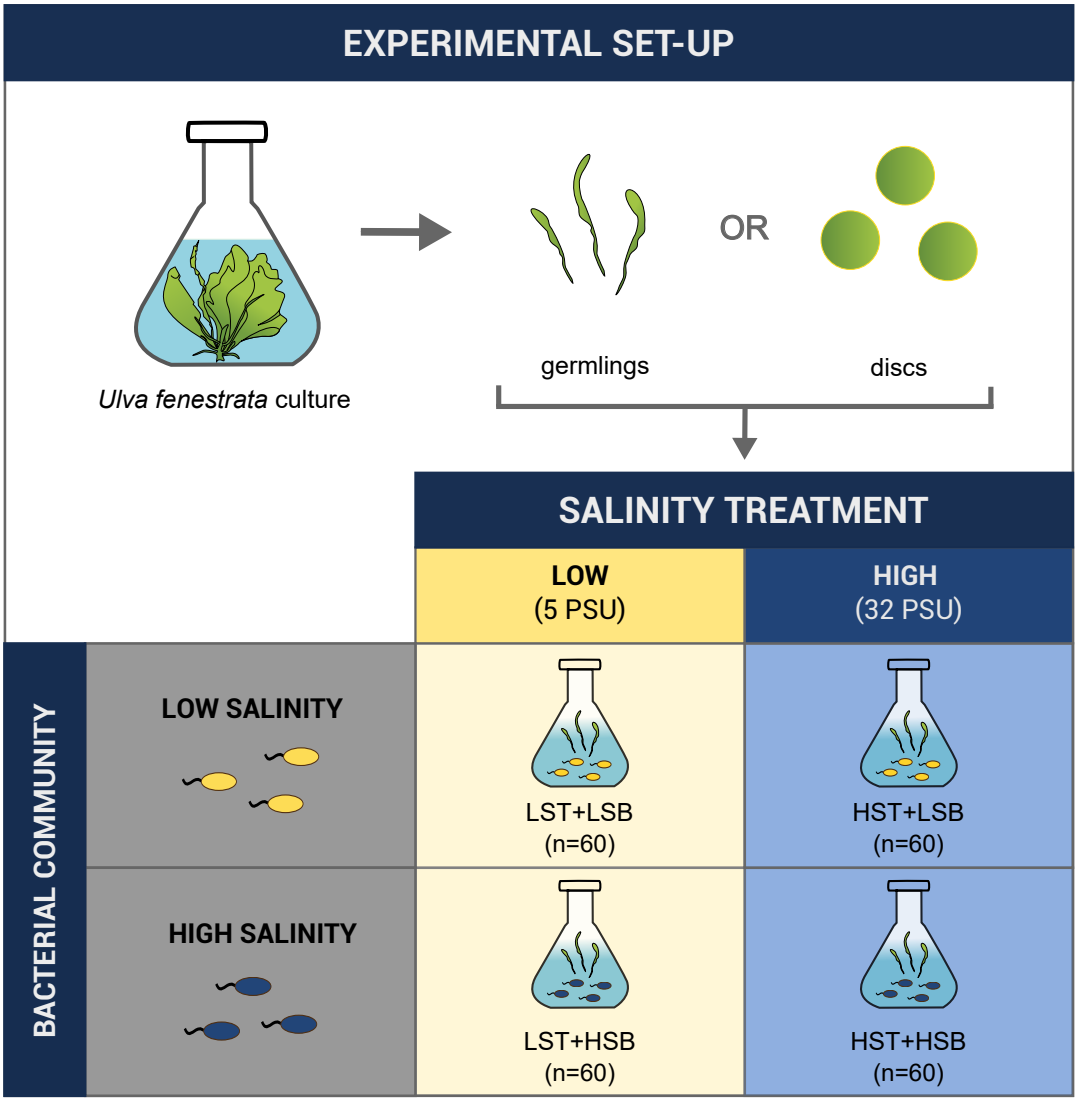

FIGURE 6.01 Schematic overview of the experimental set-up. Germlings or discs were obtained from a single *Ulva fenestrata* culture and three individuals (germlings or discs) were transferred to a flask. The flasks contained either low (LST) or high (HST) salinity medium (seawater or UCM) and were supplied with a bacterial inoculant containing typical low (LSB) or high (HSB) salinity bacteria.

A)

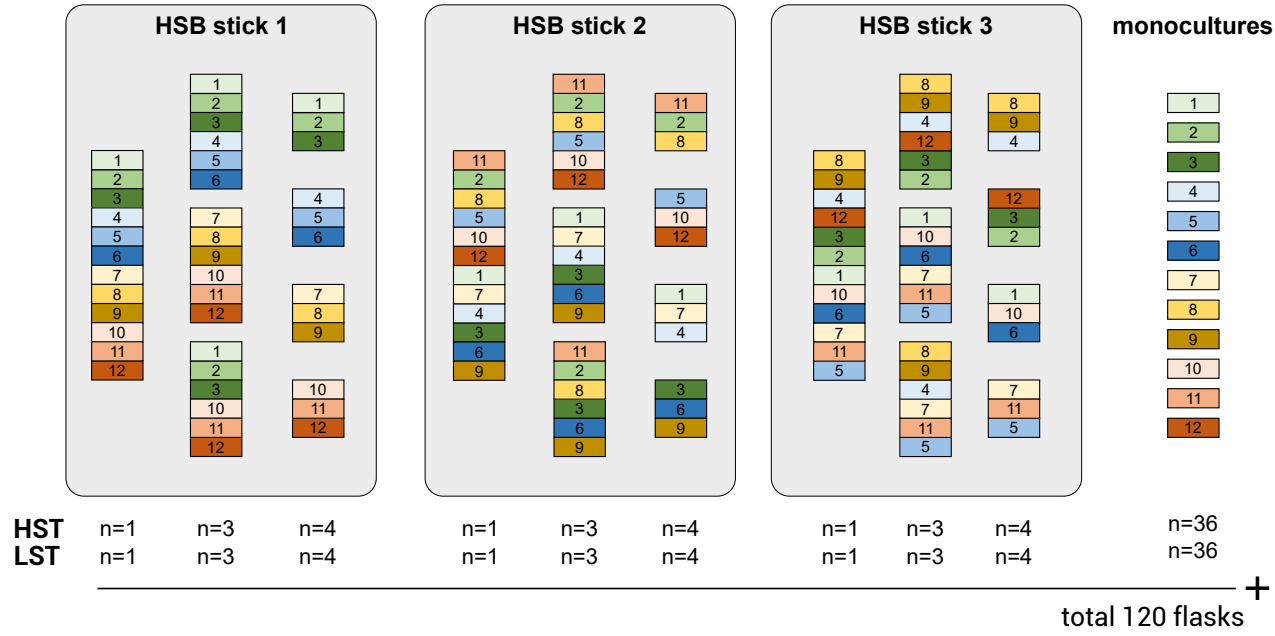

B)

	low salinity treatment (LST)	high salinity treatment (HST)	
synthetic community	60 flasks HSB	60 flasks HSB	120
	60 flasks LSB	60 flasks LSB	120
natural community	3 flasks HSB	3 flasks HSB	6
	3 flasks LSB	3 flasks LSB	6
negative control	6 flasks	6 flasks	12

total 264 flasks

FIGURE 6.02 A) Broken stick design used in this study to create random bacterial inoculants with twelve high salinity bacteria (HSB). Three different sticks were created for the low salinity bacteria (LSB). B) Overview of the number of flasks used in the experiment, divided over the low salinity treatment (LST) and high salinity treatment (HST).

6.3 Results

6.3.1 *Ulva* growth with varying salinity conditions

Ulva fenestrata growth varied between the low and high salinity treatment and with the culture medium. Adult tissue (experiment conducted on discs) displayed higher growth rates in high salinity conditions (on average 7.02 mm^2/day) than in low salinity conditions (on average 1.37 mm^2/day) ($p = 2.2\times10^{-16}$, $\chi^2 = 189.3$, Kruskal-Wallis test) (Fig. 6.03A). Two-week-old germlings (grown in sterilised seawater), on the contrary, showed slightly higher growth rates in the low salinity treatment (7.70 mm^2/day compared to 5.55 mm^2/day in the high salinity treatment) ($p = 2.7\times10^{-6}$, $\chi^2 = 22.0$, Kruskal-Wallis test) (Fig. 6.03B). In synthetic UCM, all germlings died in the high salinity treatment[3]. In low salinity UCM, the germlings in general showed very low growth rates (Fig. 6.03C). The growth rates displayed considerable variation within both low and high salinity treatments, depending on the bacterial inoculant.

Morphological development also differed between salinity treatments. In the HST, germlings initially displayed a tubular morphology, transitioning into a blade-like form during the second week of the experiment (developing a narrow stipe and a broadened, flattened blade) (Fig. 6.04). On the contrary, in the LST, germlings remained tubular and frequently showed signs of inflation with air (Fig. 6.04).

6.3.2 Effect of bacteria on *Ulva* growth

In the germlings cultivated in low-salinity UCM, growth was significantly higher compared to the negative controls if the bacterial communities contained either strain HSB04 (*Zobellia*) ($p = 2.7\times10^{-13}$, Dunnett's test), HSB08 (*Maribacter*) ($p = 2.8\times10^{-11}$, Dunnett's test), or LSB02 (*Aquipuribacter*) ($p = 1.2\times10^{-14}$, Dunnett's test) (Fig. 6.05A, Fig. 6.06A). In the monocultures, growth was on average 5.5 ± 0.8 (SE) mm^2/day/individual with HSB04, 5.0 ± 0.9 mm^2/day/individual with HSB08 and 4.7 ± 0.8 mm^2/day/individual with LSB02, compared to an average of 0.09 ± 0.01 mm^2/day/individual in the other monocultures. Likewise, if a 3–species or 6–species community contained one or several of these three strains, *Ulva* growth was significantly higher. The addition of the full 12–species communities also increased growth, but to a lesser extent than in the monocultures. Mean growth was 1.9 ± 0.08 mm^2/day/individual for the HSB community ($p = 2.1\times10^{-5}$, Dunnett's test) and 0.7 ± 0.08 mm^2/day/individual for the LSB community ($p = 0.002$, Dunnett's test).

In the germlings cultivated in sterile seawater, the addition of strain HSB04, HSB08, and LSB02 also increased *Ulva* growth compared to the negative controls, but this effect was only visible in the low salinity treatment (Fig. 6.05B, D; Fig. 6.06B, D) (HSB04, $p = 0.03$; HSB08, $p = 0.001$; LSB02, $p = 0.003$, Dunnett's tests). The effect was less pronounced than in the UCM experiment. In the monocultures, growth was on average 10.5 ± 0.7 (SE) mm^2/day/individual with HSB04, 13.3 ± 0.5 mm^2/day/individual with HSB08 and 12.1 ± 0.6 mm^2/day/individual with LSB02, compared to an average of 6.0 ± 0.4 mm^2/day/individual in the other monocultures (mean values for LST only). In the high salinity treatment, none of the bacterial communities affected *Ulva* growth (all comparisons $p > 0.05$, Dunnett's tests).

In the experiment conducted on adult tissue, we observed no effect of the bacterial inoculants on *Ulva* growth, either in the high salinity treatment or low salinity treatment (all pairwise comparisons in Dunnett's test $p > 0.05$) (Fig. 6.05C, E; Fig. 6.06C, E).

Even though the positive controls (glycerol stocks resembling natural communities) contained *Maribacter*, *Zobellia*, and *Aquipuribacter* (verified with 16S sequencing), there was no significant effect of these positive controls on *Ulva* growth compared to the negative controls in any of the three experiments or the two salinity treatments (all pairwise comparisons in Dunnett's test $p > 0.05$).

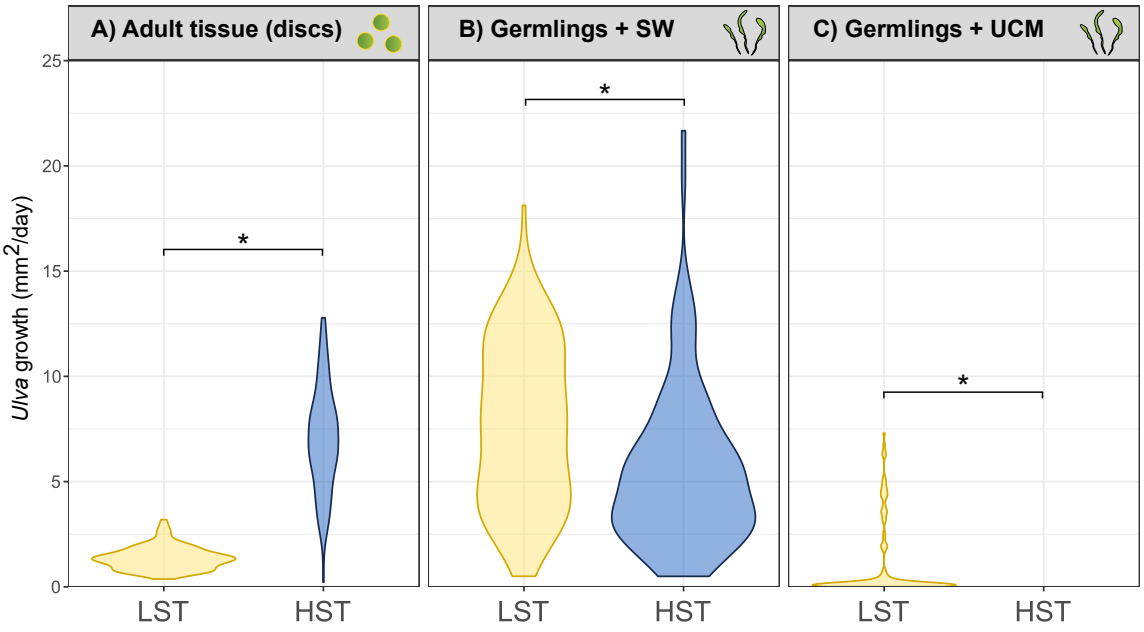

FIGURE 6.03 *Ulva* growth rates (mm²/day) in the low salinity treatment (LST; yellow) and the high salinity treatment (HST; blue), using A) *Ulva* adult tissue (discs), B) *Ulva* germlings cultivated in seawater, and C) *Ulva* germlings cultivated in UCM.

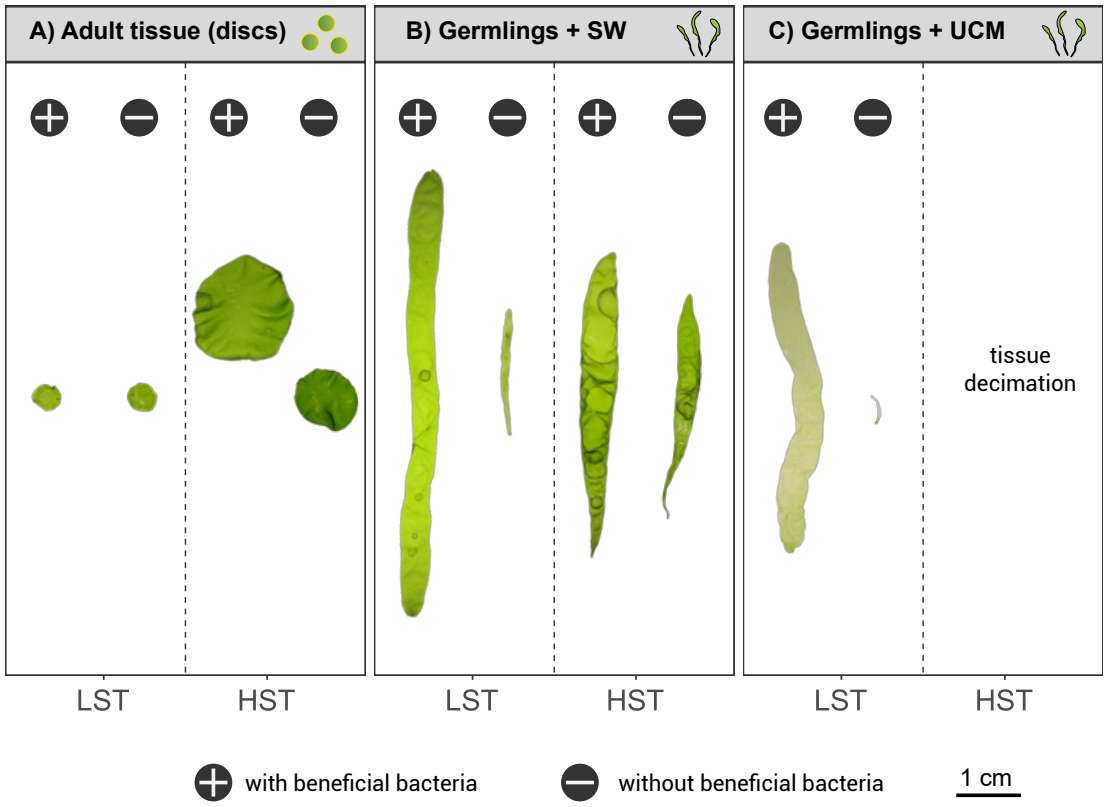

FIGURE 6.04 Example of *Ulva* morphological development in the low (LST) and high (HST) salinity treatment, supplemented with beneficial bacteria (bacterial strain HSB04, HSB08, or LSB02) and without the addition of beneficial bacteria. A) *Ulva* adult tissue (discs), B) *Ulva* germlings cultivated in seawater, and C) *Ulva* germlings cultivated in UCM.

6.3.3 Bacterial genome assemblies and functional groups

The assembled genomes of the 24 bacterial strains varied from 98.1–100% estimated completeness and contained 1–18 contigs (with the assemblies of 17 out of 24 strains containing merely 1–2 contigs). Genome size varied between 3.2 Mbp to 6.1 Mbp and the number of predicted genes varied between 2,887–5,597. See Fig. 6.07 as example (genome configuration of HSB04), and Electronic Supplementary Table S6.01 and Electronic Supplementary Figures S6.02A–X for a full overview of the assembly statistics and annotations.

The presence of specific functional groups of genes (COG categories and KEGG modules) mainly reflected the taxonomic classification (class, order and family level) of the isolated strains ($p = 0.0001$, $R^2 = 0.74$, PERMANOVA) (Fig. 6.08). Strains belonging to the class Actinomycetia, which were only isolated from low salinity areas, for example contained all the genes needed to produce trehalose (KEGG module M00565; $p < 0.001$, MaAsLin2 test), while these genes were absent from the other classes (Bacteroidia, Gammaproteobacteria, and Alphaproteobacteria). They also contained the genes necessary for ornithine production (M00028; $p < 0.001$, MaAsLin2 test), but lacked the full gene set necessary for module M00082 (fatty acid biosynthesis; $p < 0.001$, MaAsLin2 test) that the other classes did contain. The isolated Bacteroidia strains, which all belonged to the *Flavobacteriaceae*, were only found in marine locations (this is in accordance with previous findings that this family is more abundant in higher salinity areas; see Chapter 4). They lacked some genes that were present in the other strains, e.g., all the genes needed for betaine biosynthesis (M00555; $p = 0.002$, MaAsLin2 test), most of the genes related to C5 isoprenoid biosynthesis (M00096; $p = 0.01$, MaAsLin2 test), and an incomplete set of genes for leucine biosynthesis (M00432; $p < 0.001$, MaAsLin2 test). The genomes of the isolated Gammaproteobacteria uniquely contained the modules necessary for ubiquinone biosynthesis (M00117, $p < 0.001$, MaAsLin2 test), NAD biosynthesis (M00115; $p = 0.01$, MaAsLin2 test), pyridoxal-P biosynthesis (active form of vitamin B6, module M00124; $p < 0.001$, MaAsLin2 test), and glutathione biosynthesis (M00118; $p < 0.001$, MaAsLin2 test).

6.4 Discussion

Under natural conditions *Ulva fenestrata* is an obligate foliose species that is restricted to euhaline and polyhaline regions in coastal habitats (Steinhagen et al. 2023). This led us to hypothesise that a salinity of ~30 PSU provides optimal growth conditions for *U. fenestrata*, while lower salinity levels impose a certain degree of stress. This was true for the adult tissue, which exhibited higher growth rates in high salinity conditions, despite an increased sporulation prevalence. Surprisingly, however, germlings displayed overall higher growth rates in the low salinity treatment. Given that the negative controls (without bacteria added) showed similar growth rates in low versus high salinity seawater, the increased growth can likely be attributed to the influence of the bacteria. Our results demonstrate that three of the 24 tested bacterial strains (*Aquipuribacter* LSB02 isolated from a low salinity environment, and *Maribacter* HSB08 as well as *Zobellia* HSB04 from a high salinity environment) significantly increased the growth rate of *Ulva fenestrata*. Interestingly, this effect was observed exclusively in low salinity conditions. This contradicts our expectations that high salinity bacteria would facilitate *Ulva fenestrata* growth in high salinity conditions, while low salinity bacteria, conversely, would promote growth in low salinity conditions. Moreover, the growth-promoting effect of specific bacteria was only evident in the experiments involving germlings and was not observed in the experiment using adult tissue. These results emphasise the importance of life-history-phases and environmental conditions in assessing the effects of algal–bacterial interactions and potential adaptability.

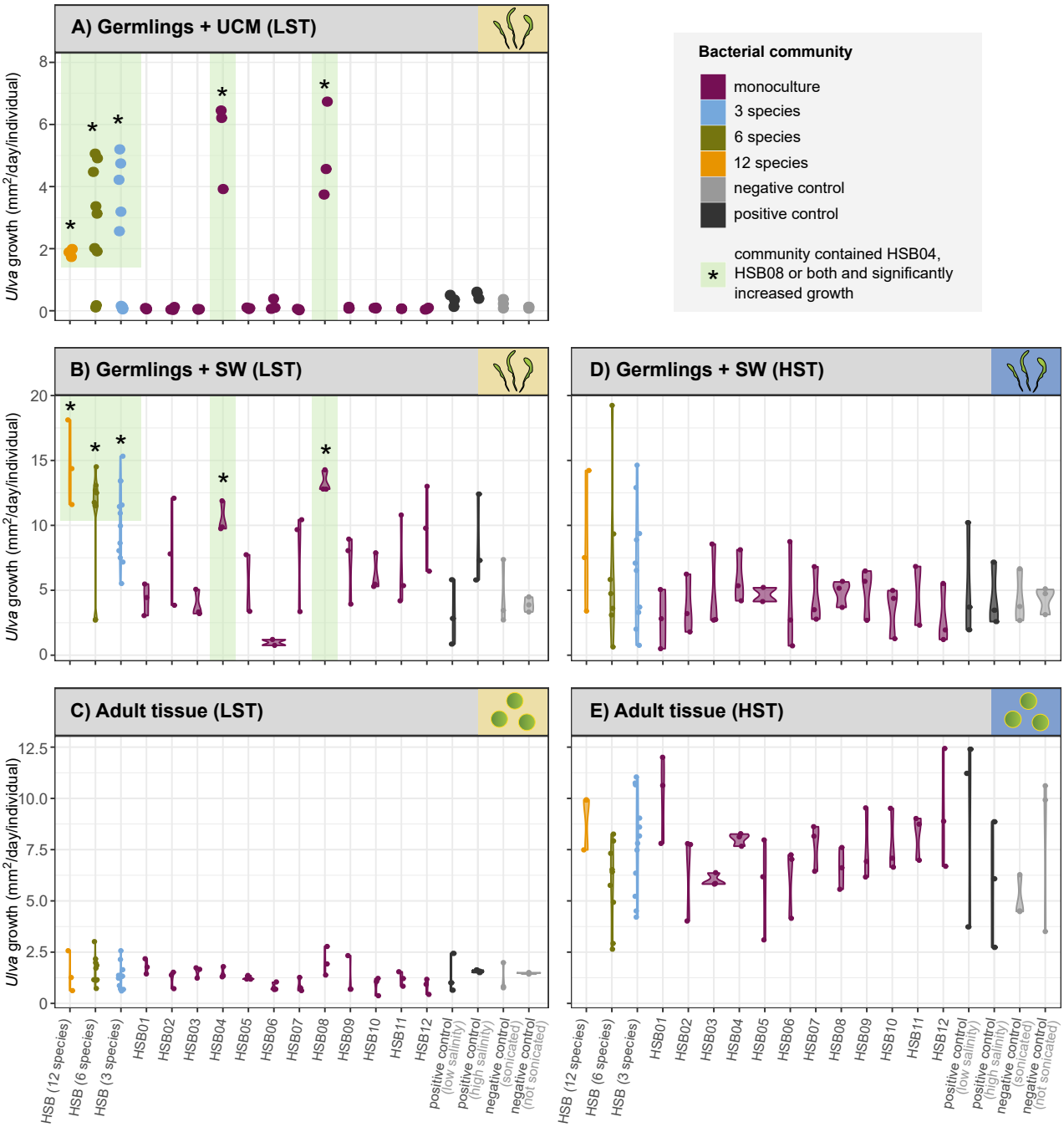

FIGURE 6.05 Scatter plots of *Ulva* growth (mm²/day/individual) with different HSB (high salinity) bacterial communities in A) germlings cultivated with low-salinity UCM, B) germlings cultivated in low-salinity seawater, C) adult tissue (discs) cultivated in low salinity seawater, D) germlings cultivated in high salinity seawater, and E) adult tissue (discs) cultivated in high salinity seawater. Colours indicate the number of bacterial strains in the inoculant. Bacterial treatments with significantly increased growth compared to the negative controls are denoted with an asterisk.

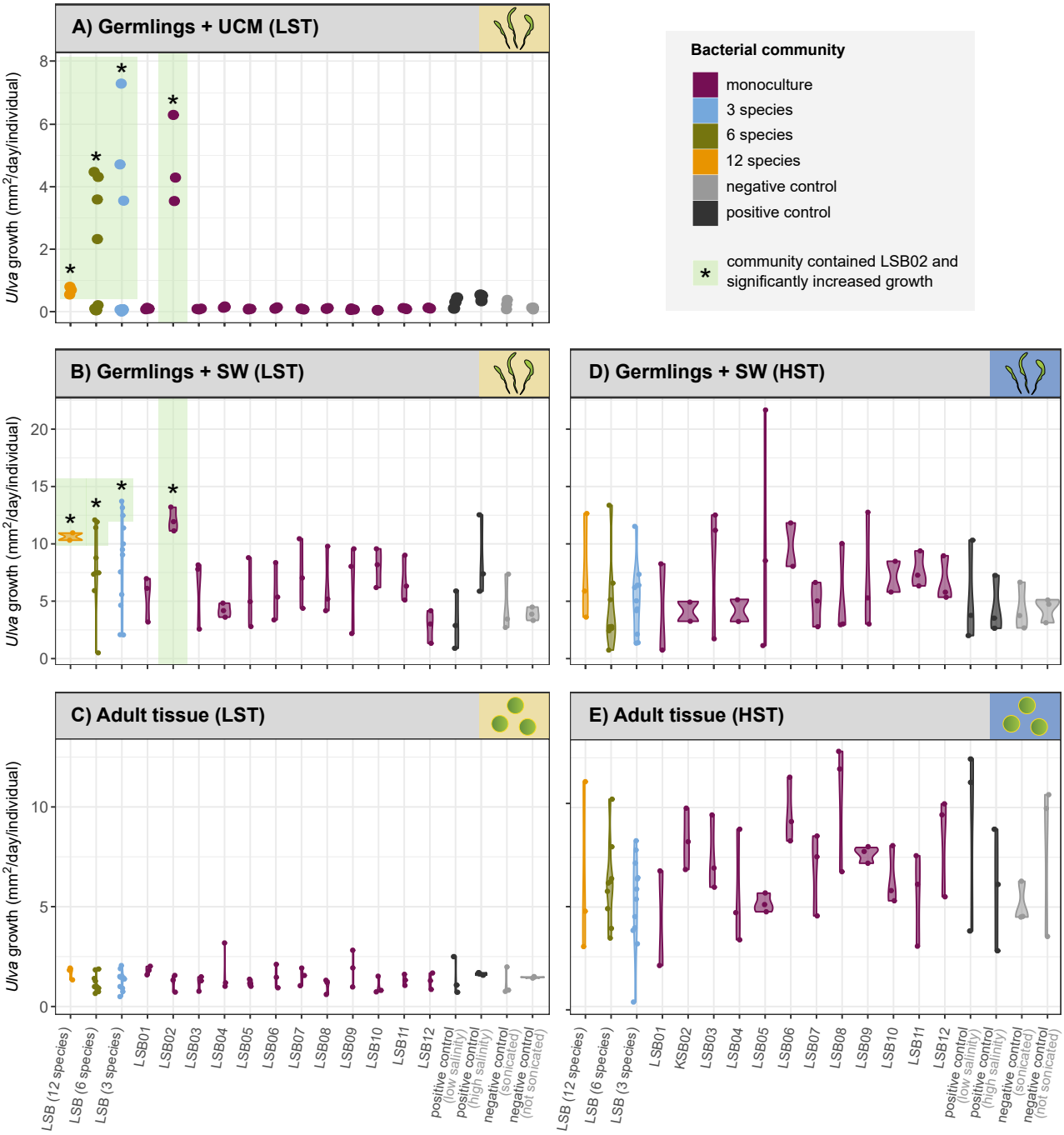

FIGURE 6.06 Scatter plots of *Ulva* growth (mm²/day/individual) with different LSB (low salinity) bacterial communities in A) germlings cultivated with low-salinity UCM, B) germlings cultivated in low-salinity seawater, C) adult tissue (discs) cultivated in low salinity seawater, D) germlings cultivated in high salinity seawater, and E) adult tissue (discs) cultivated in high salinity seawater. Colours indicate the number of bacterial strains in the inoculant. Bacterial treatments with significantly increased growth compared to the negative controls are denoted with an asterisk.

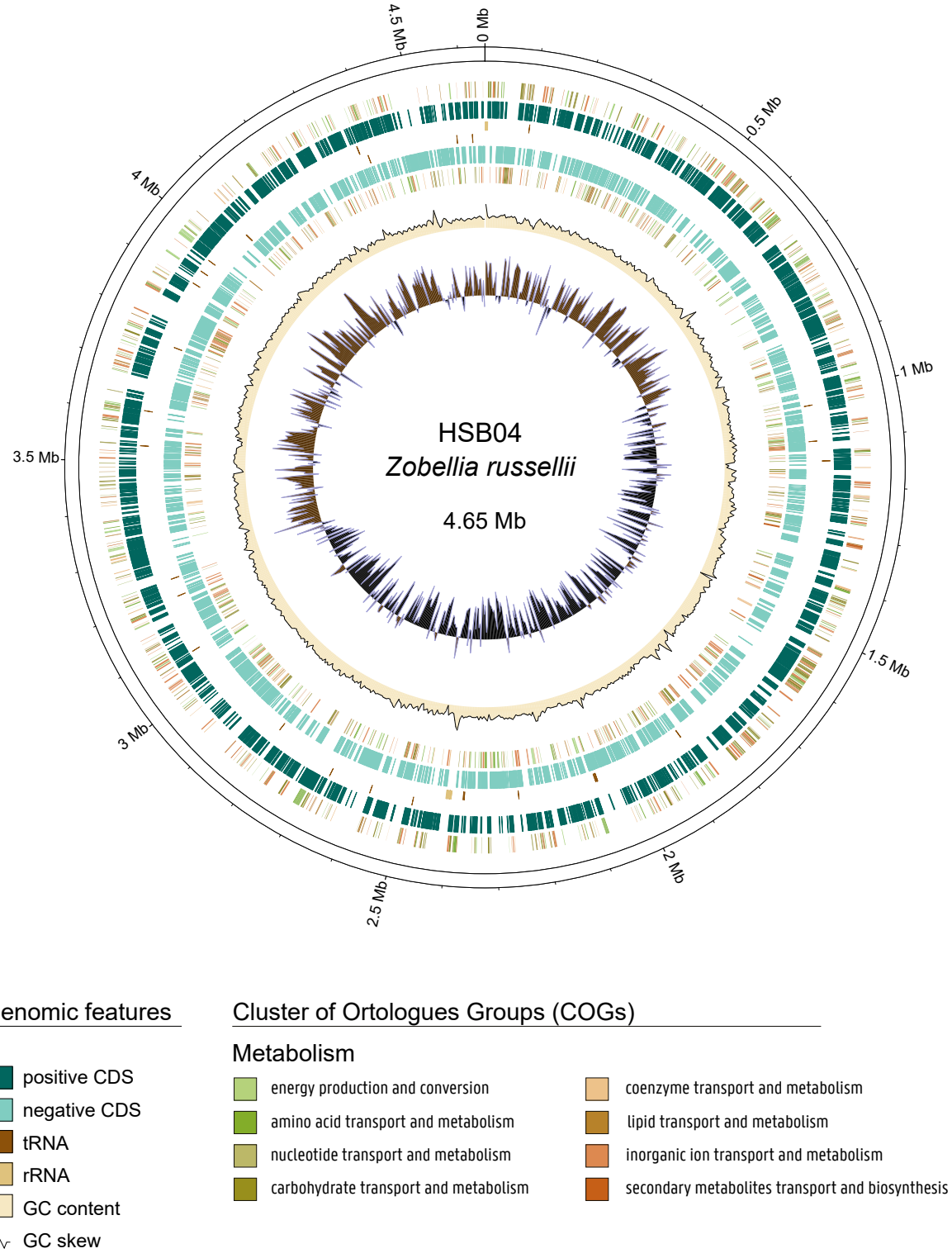

FIGURE 6.07 Genome overview of HSB04 (*Zobellia russellii*). Labelling from outside to the inside: contigs; COGs on the forward strand; positive CDS; tRNAs and rRNAs on the forward strand; tRNAs and rRNAs on the reverse strand; negative CDS; COGs on the reverse strand; GC content; GC skew. Positive GC skew (indicating guanine richness) is visualised in brown and negative GC skew (indicating cytosine richness) is visualised in black.

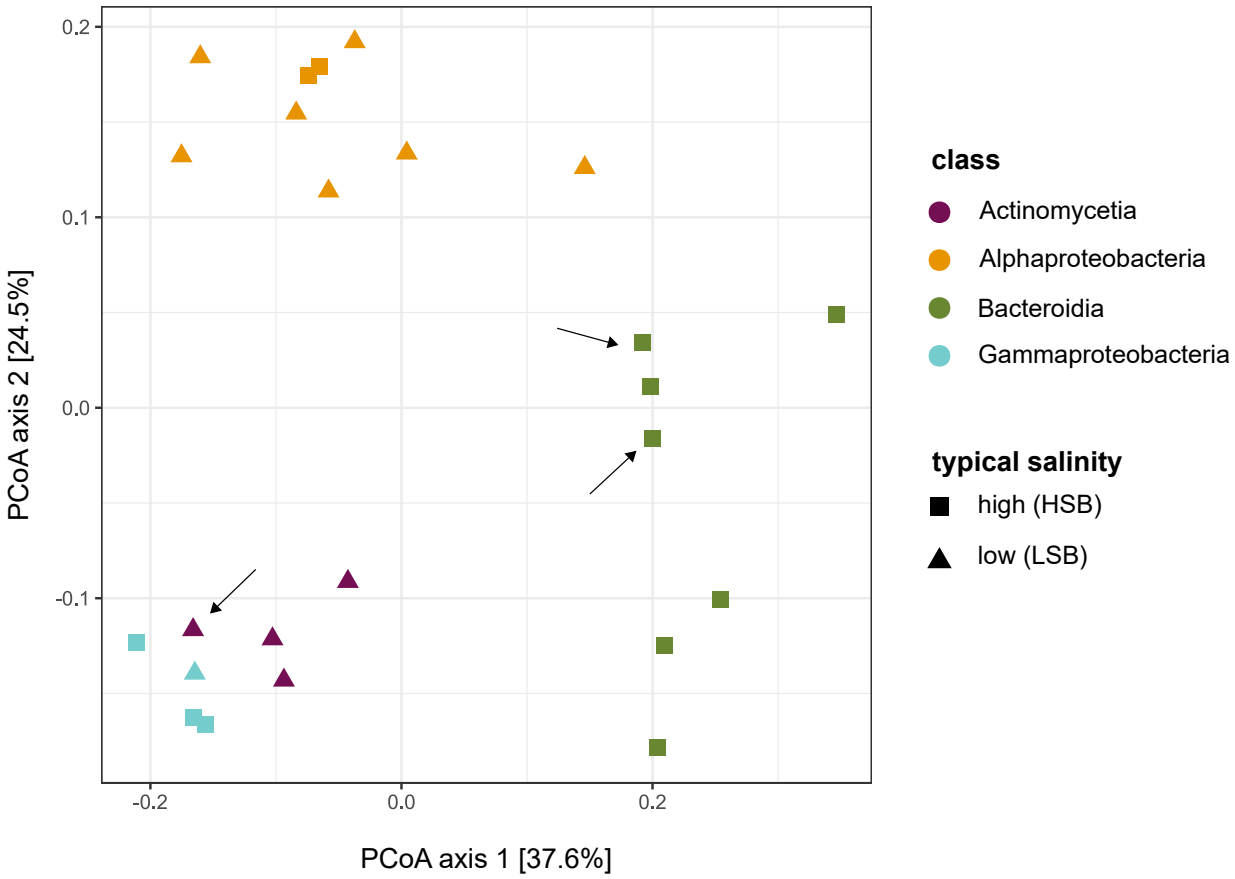

FIGURE 6.08 PCoA ordination plot based on the presence/absence of KEGG modules in the bacterial genomes of strain HSB01–HSB12 and LSB01–LSB12. Colours represent taxonomic class of the bacterial strains and symbols represent the typical salinity range (HSB = high salinity bacteria, LSB = low salinity bacteria). *Ulva*-growth promoting bacteria (HSB04, HSB08 and LSB02) are indicated with an arrow.

6.4.1 Growth-promoting bacteria have a larger effect on germlings than on adult tissue

The growth-promoting bacterial strains identified in this study only had an effect on *Ulva fenestrata* germlings, not on discs cut from adult tissue. *Ulva* species are known for their obligate relationship with bacteria. Under axenic (bacteria-free) conditions, these green seaweeds fail to develop a normal morphology, instead growing as a loose aggregation of cells (Provasoli 1958, Marshall et al. 2006). *Ulva* morphogenesis, encompassing processes like rhizoid formation, cell wall development, and blade cell division, requires the presence of two functional bacterial strains (Spoerner et al. 2012). Multiple strains that can trigger one or all of these morphogenesis processes in the model species *Ulva mutabilis* have been identified, many of which belong to the *Rhodobacteraceae* (e.g., *Roseovarius*, *Paracoccus*, *Sulfitobacter*) and the *Flavobacteriaceae* (e.g., *Maribacter*, *Zobellia*, *Polaribacter*) (Grueneberg et al. 2016). *Maribacter* and *Zobellia* strains specifically are known to produce the waterborne compound thallusin, a morphogen that induces rhizoid and cell wall formation (Matsuo et al. 2005, Alsufyani et al. 2020). It is possible that the *Maribacter* HSB08 and *Zobellia* HSB04 strain in this study are also capable of producing thallusin. Thallusin mainly acts on processes that are especially important during the early life stages (i.e., rhizoid and cell wall formation) (Alsufyani et al. 2020), which possibly explains the effect of the bacteria observed in germlings and not in adult tissue. An alternative explanation is that the germlings used in this experiment represented a complete individual, whereas the discs consisted solely of cells from the central

region of the blade. A complete *Ulva* thallus is composed of three different types of cells: the blade consists of blade cells and the basal region is composed of rhizoidal cells and stem cells (Løvlie 1969, Fjeld 1972). Unlike rhizoidal and stem cells, isolated blade cells (e.g., by cutting discs) are not totipotent and cannot develop into complete germlings anymore. Additional experiments on a larger scale with fully developed adult individuals are imperative to assess whether the identified beneficial bacteria can also affect adult tissue.

The ability to induce morphogenesis in *Ulva* is not confined to the *Rhodobacteraceae* and *Flavobacteriaceae* bacterial families. Similar properties have been documented for strains such as *Algoriphagus* Ul-9 (*Cyclobacteriaceae*), *Alteromonas* Ul-12 (*Alteromonadaceae*), and *Bacillus cereus* U5-30 (*Bacillaceae*) (Grueneberg et al. 2016, Gemin et al. 2019, H. Wang et al. 2022). Our results are the first indication that an *Aquipuribacter* strain (belonging to the *Aquipuribacteraceae*) is also capable of promoting *Ulva* growth. However, growth-promoting characteristics seem to be strain-dependent rather than genus-dependent. Gemin et al. (2019), for example, reported positive effects of *Alteromonas* strain Ul-12 on *Ulva clathrata*, and Grueneberg et al. (2016) showed that *Polaribacter* isolate RFB F06 completely recovered the morphology of *Ulva mutabilis*, while the *Alteromonas* HSB05 and *Polaribacter* HSB10 strains used in our experiments did not appear to enhance *Ulva* growth.

Our understanding of the mechanisms through which bacteria promote algal growth is limited. Beyond the documented production of thallusin, bacteria could also stimulate algal growth through alternative mechanisms, such as providing the host with vitamins, amino acids, or as-yet-unidentified compounds. To date, thallusin is the only morphogen that has been isolated and characterised (Dhiman et al. 2022), and even for this compound the signalling pathway leading to *Ulva* morphogenesis as well as the genes within the bacterial genomes necessary for thallusin production remain to be identified. Our genomic comparisons between the three growth-promoting strains and the 21 non-growth-promoting strains did not allow us to identify a clear set of genes as potential candidates for thallusin production. Comparative genomic analyses with a larger number of strains known to be able to produce thallusin, coupled with transcriptomic experiments, will be necessary to identify the genetic pathways.

6.4.2 Growth-promoting bacteria have a larger effect in low salinity conditions

The growth-promoting effect of bacteria was only prevalent in the low salinity treatment — regardless of whether these bacteria were originally isolated from low or high salinity environments. Both *Maribacter* HSB08 and *Zobellia* HSB04 were originally isolated from *Ulva fenestrata* thalli growing at 33.4 PSU, while the *Aquipuribacter* LSB02 strain was isolated from *Ulva intestinalis* collected at 2.8 PSU. With the addition of either of these three strains, *Ulva* experienced a 138% higher daily growth rate in low salinity compared to high salinity (12 mm^2/day/individual versus 5.0 mm^2/day/individual). Comparing growth rates in the other monocultures yielded very similar growth rates in low and high salinity (5.5–6.0 mm^2/day/individual). Curiously, the positive controls, which contained natural *Ulva*-associated communities, did not significantly increase growth compared to the negative controls. It is possible that the natural community lacked the beneficial strains in sufficient concentrations, or that the method used to isolate these natural communities by removing epibiotic bacteria from *Ulva* resulted in cell death of the beneficial strains.

The difference in Ulva growth with and without the addition of beneficial strains was even more striking when using *Ulva* culture medium instead of seawater. The use of UCM (which has been designed specifically to cultivate *Ulva mutabilis*) apparently imposed a certain level of stress on *Ulva fenestrata*. In low saline UCM, the germlings barely managed to survive without the addition of strain HSB04, HSB08, or LSB02, and in high saline conditions even the addition of these beneficial bacteria was not enough to keep the germlings alive. Growth,

however, is not the only indicator of fitness — other parameters like biochemical composition, protein content, photosynthesis, nutrient uptake, morphological development, and reproduction are also potentially affected by salinity (Olsson et al. 2020a, Cardoso et al. 2023).

Morphological development of germlings in low salinity was different from their counterparts in the high salinity treatment. Under conditions mirroring salinity levels of *U. fenestrata's* natural distribution (30 PSU), germlings initially assumed a tubular form, but continued to develop a small, narrow stipe and a flattened, broadened blade during the second week of the experiment (four-week-old individuals). In contrast, at 5 PSU, the thalli remained tubular, growing elongated rather than wider, often becoming inflated with air. In addition, both germlings and adult tissue at low salinity levels were paler in colour compared to individuals in the high salinity treatment. Morphological plasticity under different salinity conditions has been documented in other *Ulva* species before. *Ulva compressa*, for example, can be found as tubular, attached morphology at salinities >15 PSU, while it is predominantly foliose and free-floating at lower salinity levels (although it has not been recorded below 7.5 PSU) (Steinhagen et al. 2019b, 2023). *Ulva prolifera* is known to grow more numerous, but shorter branches in low salinity compared to high salinity (Gao et al. 2016). As a general rule, we only find tubular morphologies (not foliose strains) in freshwater and brackish water <5 PSU in natural environments (Rybak 2018, Steinhagen et al. 2023). In controlled experiments, tubular strains also grow better in low salinity than foliose strains (Cardoso et al. 2023). The question remains whether a tubular morphology gives *Ulva* species an advantage in low salinity and whether *U. fenestrata* acclimates to lower salinity conditions with morphological plasticity in natural environments.

6.5 Conclusions and future perspectives

In this study we showed that *Ulva* growth is increased by a *Maribacter*, *Zobellia*, and *Aquipuribacter* strain. The magnitude of the effect depends on the life-history phase and environmental conditions, with the most pronounced effects observed in germlings cultivated in low salinity. The growth-enhancing effect of certain bacterial strains on *Ulva* germlings, even when the germlings are not fully axenic, is very interesting from an aquaculture perspective. Supplying *Ulva* germlings with an inoculant of growth-promoting bacteria during the nursery stage is a good example of how 'microbiome engineering' (i.e., the manipulation of microbial communities through biological, chemical or physical means) can support sustainable seaweed aquaculture (Ke et al. 2021, Li et al. 2023). To extrapolate these findings to larger cultivation scales, future studies need to clarify whether the effect of the bacteria also persists in fully developed adult thalli, and which concentrations of bacteria are necessary to obtain optimal growth. Furthermore, elucidating the genetic pathway that controls thallusin production in bacteria, along with identifying additional morphogens stimulating algal growth, will be necessary for the effective screening and discovery of additional beneficial bacteria.

Acknowledgements

The research leading to the results presented in this publication was carried out with infrastructure funded by the FWO PhD Fellowship fundamental research (3F020119) and by EMBRC Belgium - FWO international research infrastructure I001621N. The authors thank the Formas-funded 'A manual for the use of sustainable marine resources' project (Grant no. 2022-00331) for financial support.

Author contributions

L.M.L.: Conceptualization, Methodology, Formal analysis, Investigation, Data Curation, Writing - Original Draft, Visualisation. **S.S.:** Resources, Writing - Review & Editing. **F.L.:** Writing - Review & Editing, Supervision. **S.D.:** Methodology, Formal analysis. **P.C.:** Methodology, Formal analysis. **A.W.:** Resources, Writing - Review & Editing, Supervision, Funding acquisition. **O.D.C.:** Conceptualization, Writing - Review & Editing, Supervision, Funding acquisition.

Data availability statement

Raw whole-genome sequence reads are deposited in the SRA (BioProject PRJNA1036818). Related metadata are also stored in SRA (BioProject PRJNA1036818) and can be found in Table 6.01 and Supplementary Table S6.01. The genomes are archived at GenBank (for accession numbers, see Table 6.01). All Electronic Supplementary Materials are available at Zenodo (DOI: 10.5281/zenodo.10475355)

Notes

[1] In the experiments described in this chapter, all germlings originated from a single parental individual and all discs were cut from a single parental blade. This ensured that the same phenotype was used across all treatments and avoids differences due to genetic variation. Nevertheless, genetic variability naturally exists in real-world ecosystems. Future studies could focus on how the introduction of beneficial bacterial inoculants influences various phenotypes, thereby enhancing our understanding of their potential impact.

[2] The *Ulva* individuals used in this study were not fully axenic. To obtain true axenic *Ulva* cultures, it is necessary to separate the reproductive cells from their bacterial symbionts following the procedure outlined in Califano and Wichard (2018). This protocol makes use of the phototactic behaviour of gametes and spores by passing them through glass pipettes equipped with a light source at the tips. Due to the rapid swimming speed of the swarmers, they effectively outcompete the accompanying bacteria, enabling the collection of sterile swarmers at the pipette tip after repeating this process three or four times. These axenic *Ulva* cultures serve as valuable tools for evaluating the effect of individual bacterial strains on *Ulva*'s morphological development (see for example (Grueneberg et al. 2016). However, given that a combination of two specific bacterial strains is typically necessary for complete morphological development, *Ulva* cultures in such investigations often exhibit atypical growth patterns. Consequently, comparing growth across treatments becomes challenging. Moreover, it is also important to determine whether the addition of bacteria affects non-axenic *Ulva*. We therefore decided to use non-axenic *Ulva* and disrupt the existing bacterial community through sonication to facilitate colonisation by the inoculated bacteria. This ensured normal morphological development across all treatments, facilitating meaningful growth comparisons.

[3] The reasons behind the suboptimal growth (i.e., general low growth rates in the low salinity treatment and tissue decimation in the high salinity treatment) observed in *Ulva fenestrata* cultivated in *Ulva* culture medium (UCM) remain unclear. One possibility is that the synthetic medium lacks an important component (e.g., organic matter) that is present in natural seawater, although this would not immediately explain the difference in tissue decimation between low and high salinity UCM. Another possibility is that antagonists (e.g., fungi or oomycetes) that grow well in high salinity could have been introduced during the inoculation process (although this is not likely, as the bacterial cultures were pure when verified on agar plates).

Supplementary Materials & Methods

Supplementary Materials & Methods S6.01 Testing the efficiency of sonication using DAPI staining and fluorescence microscopy

To verify that sonication (5 minutes at 40 kHz, Branson 3200 Ultrasonic Cleaner) did indeed disrupt the microbial biofilm of the *Ulva* surface, we stained non-sonicated and sonicated *Ulva* discs (1 cm diameter) with DAPI following the protocol in (Shishlyannikov et al. 2011). After staining, the bacteria can be visualised under a fluorescence microscope. The fluorescence microscopy photos of DAPI-stained *Ulva* tissue below clearly show that a large biofilm is present before sonication, while this biofilm is not visible anymore after sonication.

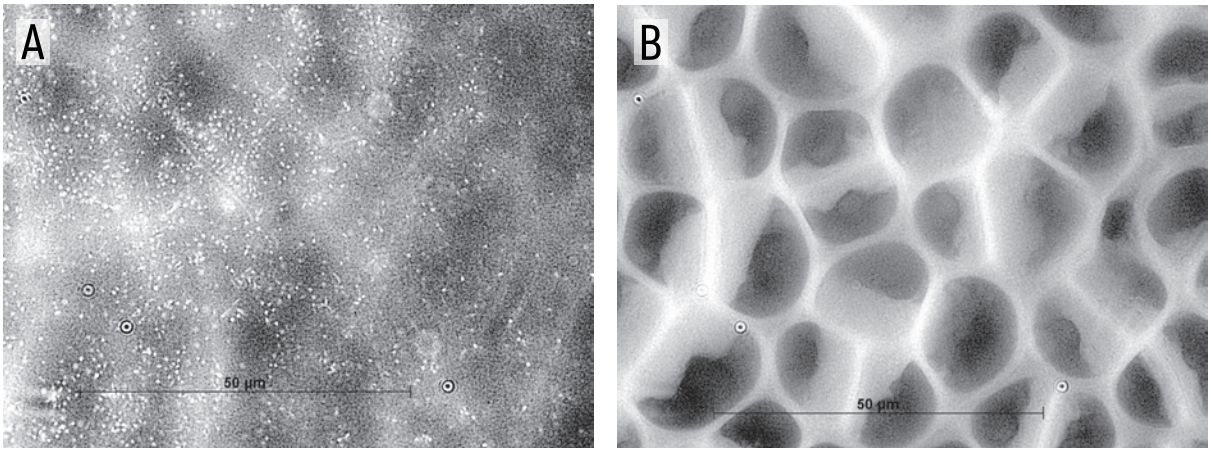

Fluorescence microscopy photos with DAPI-stained *Ulva* tissue. A) *Ulva* surface without sonication. B) *Ulva* surface after sonication.

“I wish the world was twice as big — and half of it was still unexplored.”

– Sir David Attenborough

Chapter 7.
Highly divergent CRESS and picorna-like viruses associated with bleached thalli of the green seaweed *Ulva*

Luna M. van der Loos, Lander De Coninck, Roland Zell, Sebastian Lequime, Anne Willems, Olivier De Clerck, Jelle Matthijnssens

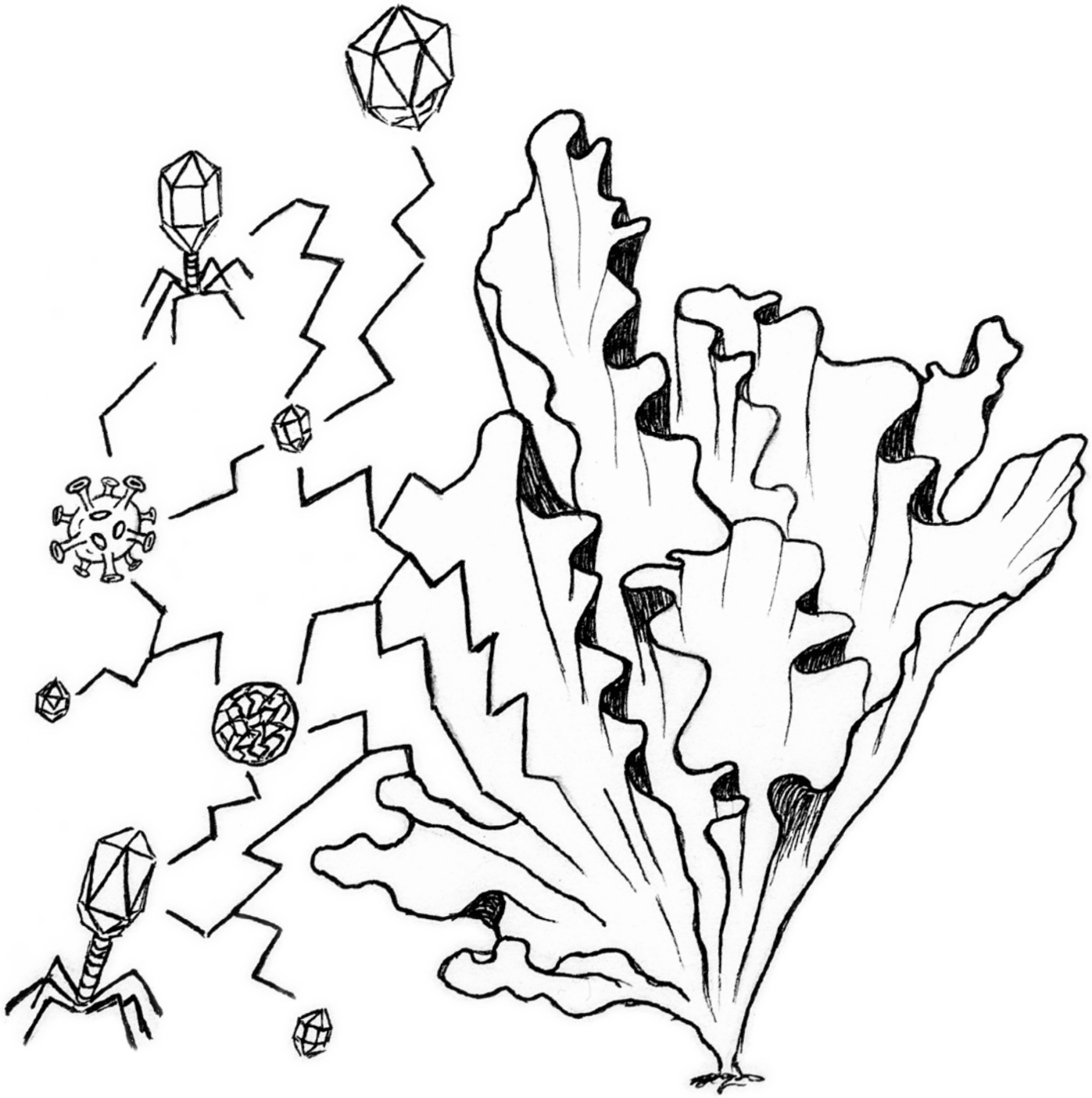

Chapter 7. Highly divergent CRESS and picorna-like viruses associated with bleached thalli of the green seaweed *Ulva*

This chapter has been published as:
L.M. van der Loos, L. De Coninck, R. Zell, S. Lequime, A. Willems, O. De Clerck & J. Matthijnssens. 2023. Highly divergent CRESS DNA and picorna-like viruses associated with bleached thalli of the green seaweed *Ulva*. *Microbiology Spectrum* 11:5 e00255-23.

[1] Phycology Research Group, Department of Biology, Ghent University, Ghent, Belgium
[2] Laboratory of Microbiology, Department Biochemistry and Microbiology, Ghent University, Ghent, Belgium
[3] Laboratory of Clinical and Epidemiological Virology, Laboratory of Viral Metagenomics, Department of Microbiology, Immunology and Transplantation, Rega Institute, KU Leuven, Leuven, Belgium
[4] Section of Experimental Virology, Institute for Medical Microbiology, Jena University Hospital, Friedrich Schiller University, Jena, Germany
5 Cluster of Microbial Ecology, Groningen Institute for Evolutionary Life Sciences, University of Groningen, Groningen, The Netherlands

Abstract

Marine macroalgae (seaweeds) are important primary producers and foundation species in coastal ecosystems around the world. Seaweeds currently contribute to an estimated 51% of the global mariculture production, with a long-term growth rate of 6% per year, and an estimated market value of more than US$11.3 billion. Viral infections could have a substantial impact on the ecology and aquaculture of seaweeds, but surprisingly little is known about virus diversity in macroalgal hosts. Using metagenomic sequencing, we characterised viral communities associated with healthy and bleached specimens of the commercially important green seaweed *Ulva*. We identified 20 putative new and divergent viruses, of which the majority belonged to the CRESS viruses (single-stranded (ss)DNA genomes), *Durnavirales* (double-stranded (ds)RNA), *Picornavirales* (ssRNA). Other newly identified RNA viruses were related to the *Ghabrivirales*, the *Mitoviridae*, and the *Tombusviridae*. Bleached *Ulva* samples contained particularly high viral read numbers. While reads matching assembled CRESS DNA viruses and picorna-like viruses were nearly absent from the healthy *Ulva* samples (confirmed by qPCR), they were very abundant in the bleached specimens. Therefore, bleaching in *Ulva* could be caused by one or a combination of the identified viruses, but may also be the result of another causative agent or abiotic stress, with the viruses simply proliferating in already unhealthy seaweed tissue. This study highlights how little we know about the diversity and ecology of seaweed viruses, especially in relation to health and diseases of the algal host, and emphasises the need to better characterise the algal virosphere.

7.1 Introduction

Viruses are widespread and abundantly present in the marine environment (Middelboe and Brussaard 2017). In fact, with millions of virus-like particles per millilitre of seawater and an estimated 10^{23} viral infections occurring every second, viruses are the most abundant lifeform in the ocean (Suttle 2007). They play a fundamental role in ecological processes as drivers of biogeochemical cycles and microbial community compositions (Fuhrman 1999, Suttle 2007). Viral infections kill an estimated 20% of the marine microbial biomass per day and are causative agents of high mortality rates in heterotrophic and autotrophic phytoplankton blooms (Brussaard 2004, Brum et al. 2013). For example, viral lysis can quickly stop bloom formations of the cosmopolitan coccolithophore *Emiliania huxleyi* (Prymnesiophyceae), whose calcite shells constitute around 1/3 of the total marine $CaCO_3$ production (Vardi et al. 2012). Viral infections also potentially introduce new genetic information into the infected organism, and viruses, as a whole, comprise an untapped reservoir of genetic diversity (Suttle 2007). Although our knowledge of the impact of viruses in marine environments is increasing, remarkably little is known about viral diversity associated with specific groups of eukaryotes, such as marine macroalgae.

Marine macroalgae (seaweeds) occur worldwide from tropical to arctic coastal ecosystems. As ecosystem engineers and foundation species, they provide food, shelter, and habitat for a wide variety of marine life and are important contributors to total primary productivity (Pessarrodona et al. 2022). In addition, approximately 30% of the global aquaculture production is derived from seaweeds (Cai et al. 2021). While it becomes increasingly clear that microbes significantly impact their seaweed host, we are largely ignorant about viruses in macroalgae (Fig. 7.01). Likely the most studied seaweeds with regard to viral infections are the brown, filamentous species belonging to the Ectocarpales. Viral-like particles were first observed in *Ectocarpus siliculosus* laboratory cultures that showed a defect in gametangium (reproductive structures) formation (Müller et al. 1990). These hexagonal particles were released in the culture medium after the host cells burst and were able to infect healthy cultures. Similar viral particles, identified as phycodnaviruses, were later observed in *Kuckuckia, Hincksia*, and *Feldmannia* (Müller 1996). More recently, double-stranded and single-stranded DNA viruses were found

to be associated with several brown macroalgal kelp species (McKeown et al. 2017, Beattie et al. 2018), and the first RNA virome characterisation was completed by Lachnit et al. (2016) on a red alga, *Delisea pulchra*. To our best knowledge, viral communities of green macroalgae have not been characterised before.

Although prior studies showed that macroalgae harbour a wide diversity of viruses, the biology and ecology of seaweed viruses are poorly understood. Especially the role of viruses in the health and diseases of seaweeds remains a black box (Gachon et al. 2010). The *Ectocarpus siliculosus* virus 1 (EsV-1 virus) is the best studied organism, as the virus has been isolated and its genome has been sequenced. The virus is considered pathogenic, as infected *Ectocarpus* thalli become partially or fully sterile (del Campo et al. 1997). In *Feldmannia*, photosynthetic performance is significantly reduced in infected individuals (Robledo et al. 1994). In red seaweeds, only a single disease has been causatively linked to a virus — green spot disease in *Pyropia* — but the viral genome has not been sequenced (G. H. Kim et al. 2016). In brown seaweeds, bleached kelp has been associated with elevated levels of Circular Rep-Encoding Single-Stranded (CRESS) DNA viruses (Beattie et al. 2018), and similarly bleaching in the green seaweed *Ulva* was also hypothesised to result from virus-like particles (Loret et al. 2020).

Green seaweeds of the genus *Ulva* — commonly known as sea lettuce — are ecologically and economically important seaweed species. Their biomass can be used as a sustainable feedstock due to their high protein content or in the context of bioremediation (i.e., removing excess nutrients) and integrated multi-trophic aquaculture systems (Steinhagen et al. 2021b). However, *Ulva* species are notorious for developing extensive blooms known as green tides. These mass accumulation events have been increasingly observed worldwide and profoundly affect the environment due to the resulting anoxic conditions and the release of gaseous sulphur compounds (Ye et al. 2011, Wan et al. 2017). In addition, *Ulva* species are often used to study algal–bacterial interactions and morphogenesis (Wichard 2015, 2023). *Ulva* species depend on appropriate bacterial communities for morphological development and in the absence of specific bacterial strains merely grow as a loose callus-like aggregate of cells (Spoerner et al. 2012). In addition to morphogenesis, bacteria play an important role in seaweed growth (Gemin et al. 2019), biochemical composition (Polikovsky et al. 2020), and the settlement of gametes and spores (Joint et al. 2000, Patel et al. 2003). While the *Ulva* holobiont is considered a model system to study microbial interactions with the algal host, nothing is known about associated viral communities.

Characterising viral communities associated with *Ulva* is the first step towards understanding the role of viruses in the ecology (e.g., the occurrence of green tides) and aquaculture of this green seaweed. In this study, we characterised *Ulva*-associated DNA and RNA viruses from cultivated and natural populations, as well as bleached and healthy thalli, using metagenomic analyses.

7.2 Materials and Methods

7.2.1 Sample collection and algal cultures

Six *Ulva* tissue samples were collected from three different cultures (Fig. 7.02). The first culture, *Ulva fenestrata*, was originally collected in Sweden and had been maintained for one year at Ghent University (Belgium) at the moment of sampling (n = 2). Cultures were maintained in 50 L tanks at 15 °C with constant aeration, a 15:9 light:dark photoperiod, and a photon flux density of 55 µmol photons m^{-2} s^{-2}. The second culture, *Ulva australis*, was originally collected in Zeeland (the Netherlands) and was maintained at the aquaculture facilities of the Royal Netherlands Institute for Sea Research (NIOZ) (n = 2). The third culture, *Ulva lacinulata*, was originally collected in Texel (the Netherlands) and likewise cultivated at the aquaculture facilities at NIOZ, the Netherlands

(n = 2). Both NIOZ strains had been in culture for one year at the moment of sampling. In addition, two individuals from a natural population in Zeeland, the Netherlands (51°38'35.3"N, 3°42'26.5"E) were collected. 1–2 cm^2 tissue from two different individuals was sampled from each culture or site. All samples were rinsed in autoclaved seawater and immediately stored at –80 °C.

All cultures and sampled individuals looked healthy except for the *Ulva australis* aquaculture samples (Fig. 7.02). Most individuals in this culture looked healthy at first but suddenly sprouted white spots that continuously became larger until the entire tissue degraded. Sporulation was not observed in any of the tissues.

7.2.2 RNA and DNA extraction and sequencing

Total DNA and RNA were extracted following the NetoVIR protocol optimised for viral metagenomics (Conceição-Neto et al. 2015)[1]. Briefly, all samples were homogenised with 2.8 mm zirconium oxide beads, centrifuged, and filtered (using a 0.8 µm filter) to remove prokaryotic and eukaryotic organisms, as well as cellular debris. Subsequently, the samples were treated with benzonase (VWR) and micrococcal nuclease (NEB) to remove free-floating nucleic acids. DNA and RNA were extracted with the QiaAmp Viral RNA Mini kit (QIAGEN). Nucleic acids were randomly amplified with a modified whole-transcriptome amplification 2 (WTA2) kit procedure (Sigma-Aldrich). The amplified products were purified using the MSB®Spin PCRapace purification kit (INVITEK), and the final sequencing library was prepared using the Nextera XT kit (Illumina). Sequencing of the samples was performed on the NextSeq500 platform (Illumina) for 300 cycles (2x150 bp paired ends), with an estimated 10 million reads per sample.

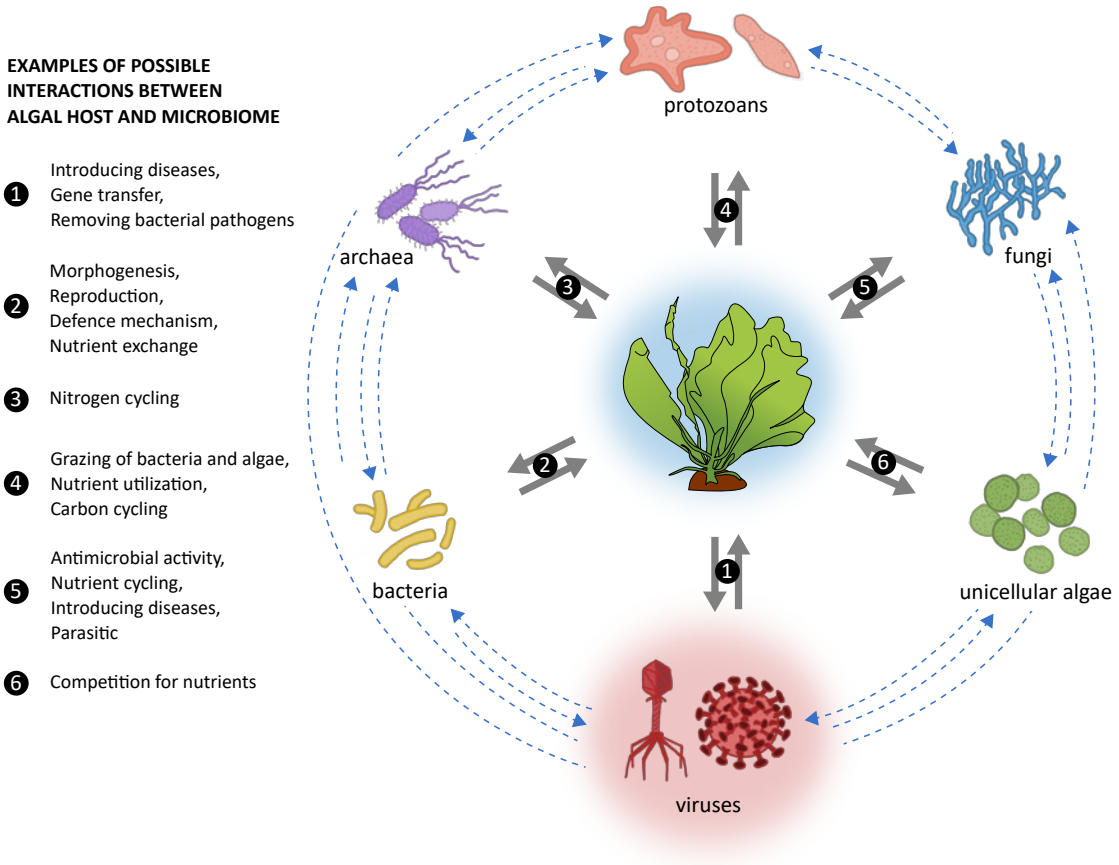

FIGURE 7.01 Possible roles and relationships between the algal host, viruses, and the other components of the microbiome. Image concept based on Peixoto et al. (Peixoto et al. 2017).

7.2.3 Bioinformatics

Obtained raw reads were processed with ViPER (https://github.com/Matthijnssenslab/ViPER). Briefly, the raw Illumina reads were filtered for quality and adapters were trimmed using Trimmomatic v0.39. This resulted in a total of 60,952,693 high-quality reads (*Ulva fenestrata* culture replicate 1 = 1,274,891 reads; *Ulva fenestrata* culture replicate 2 = 11,243,808; *Ulva australis* culture replicate 1 = 7,628,339; *Ulva australis* culture replicate 2 = 12,926,447; *Ulva lacinulata* culture replicate 1 = 4,071,840; *Ulva lacinulata* culture replicate 2 = 4,027,069; *Ulva australis* natural population replicate 1 = 9,995,302; *Ulva australis* natural population replicate 2 = 9,784,997). The reads were subsequently mapped with Bowtie2 v2.4.2 on the very sensitive setting to a reference *Ulva* genome (BioProject PRJEB25750) (De Clerck et al. 2018) to remove host-derived reads and to an assembled contaminome from a sequenced negative control to remove possible contamination. The remaining high-quality reads were *de novo* assembled into contigs using metaSPAdes v3.15. Contigs were then filtered on a length of at least 500 bp and clustered at 95% nucleotide identity over 85% of the length of the shortest contig to remove redundancy in the data using BLAST v2.11 (Altschul et al. 1990) and the clustering algorithm shipped with the CheckV package (Nayfach et al. 2021). All reads were then mapped to the non-redundant contigs with bwa-mem2 v2.2.1 (Md et al. 2019). The abundance of contigs that were less than 50% covered was set to 0 to exclude false positive detections. All contigs were classified by DIAMOND v2.0.11 on the sensitive setting against the NCBI nr database (Buchfink et al. 2014). Finally, KronaTools v2.8 (Ondov et al. 2011) and the Phyloseq R package were used to visualise data (McMurdie and Holmes 2013, R Core Team 2020).

7.2.4 Phylogenetic analyses

Contigs annotated as eukaryotic viruses were retained and putative new viruses were identified (only contigs with >500 reads that likely represented near-complete genomes were considered). For each of the putatively new viruses, Open Reading Frames (ORF) were predicted using ORFfinder (https://www.ncbi.nlm.nih.gov/orffinder/). Phylogenetic trees were generated based on amino acid sequences of the RNA-dependent RNA-polymerase for the RNA viruses (proteinase + RdRp polymerase in the case of the *Picornavirales*), and replicase for the CRESS DNA viruses. Reference amino acid sequences were retrieved from NCBI GenBank. The sequences were aligned with MAFFT v7.154b (Katoh et al. 2002) and trimmed with trimAl v1.2rev59 (using gappyout settings) (Capella-Gutiérrez et al. 2009). Maximum likelihood phylogenetic trees were generated with IQ-Tree v1.6.12 on an automated model finder with at least 10,000 ultrafast bootstraps (Nguyen et al. 2015).

The genome of one putative new virus (see Results; Ulva picorna-like virus 1) was represented by two fragmented contigs. The largest contig was first extended using ContigExtender (Deng and Delwart 2021), which revealed the correct orientation of the second contig in relation to the viral genome. To obtain an accurate full genome for this virus, the missing overlapping fragment between the two contigs was sequenced with Sanger sequencing. The PCR was performed with the OneStep RT-PCR kit (Qiagen) using the following primers: TGGTTTGGTTGCTTTTCGGT (forward) and CAGCGTTAACAACCATGCGT (reverse). The thermal profile was set to: RT (50 °C, 30 min), initial denaturation (95 °C, 15 min), 40 cycles (denaturation at 94 °C for 30 s, annealing at 51 °C for 30 s, and extension at 72 °C for 90 s), final extension (72 °C, 10 min). Finally, the complete genome was assembled using Geneious Prime (v2022.1.1).

7.2.5 qRT-PCR analyses

To verify the presence or absence of the putative new viruses in each of the samples, SYBR Green qRT-PCRs were performed with the *Power* SYBR™ Green RNA-to-CT™ *1-Step* Kit (Applied Biosystems) on an Applied Biosystems 7500 Real-Time PCR System. Primers for each virus were designed with Geneious Prime v2023.1.2 (see Electronic Supplementary Table S7.01). Each reaction consisted of 2 µL sample, 10 µL *Power* SYBR mix, 1 µL of 10 µM forward primer, 1 µL of 10 µM reverse primer and 0.16 µL RT enzyme mix, complemented with H_2O to a total reaction volume of 20 µL. Thermal cycling conditions comprised a 48 °C reverse transcription step for 30 min and a 95 °C denaturation step for 10 min initially, followed by 40 cycles of 95 ˚C for 15 s and 60 ˚C for 1 min as per manufacturer's instructions. All samples were quantified in duplicate for each virus and average Ct (cycle threshold) values of the duplicates were calculated.

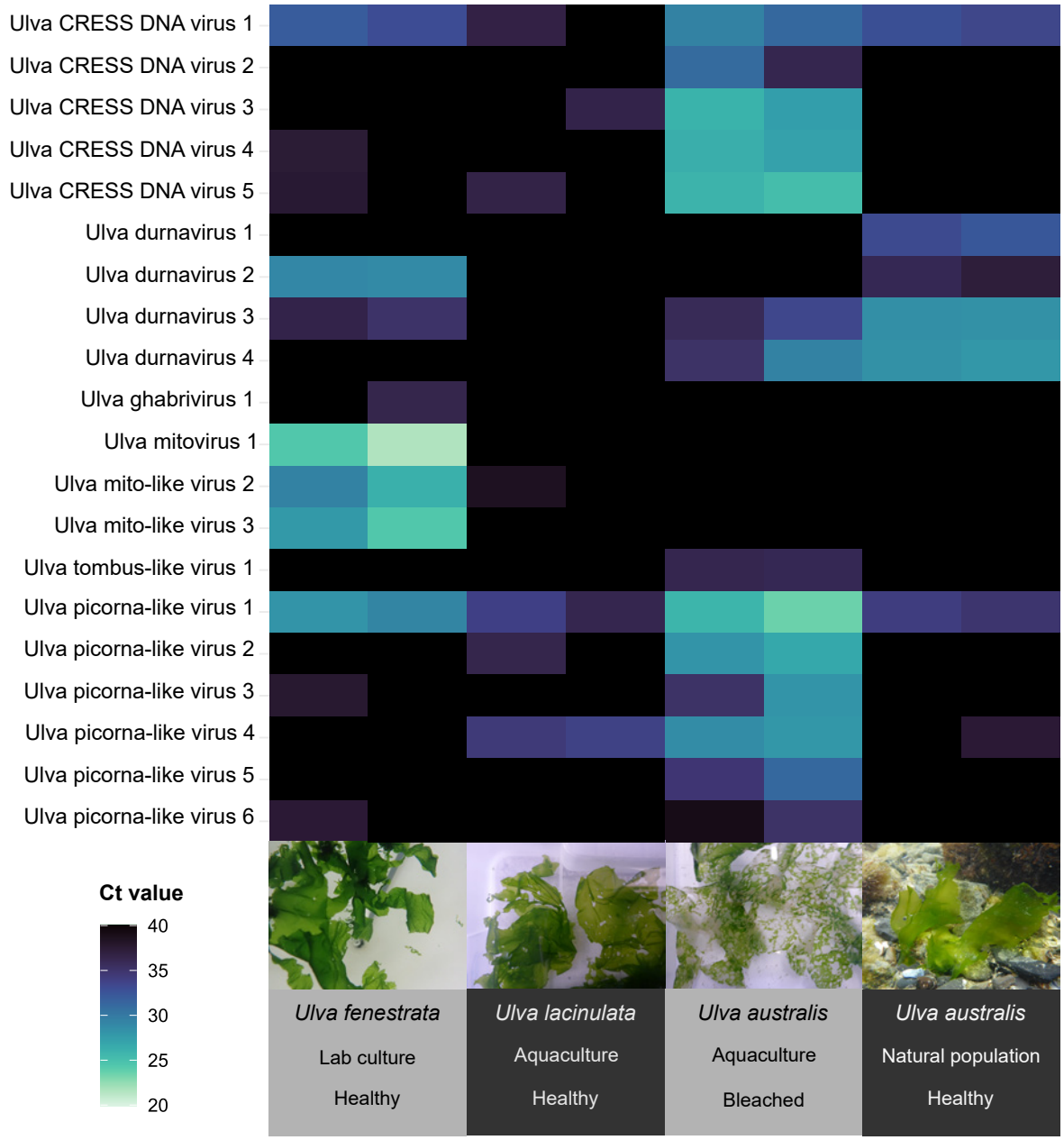

FIGURE 7.02 Heatmap showing mean Ct (cycle threshold) qPCR values for the 20 putative new viruses associated with the green seaweed *Ulva*. Low Ct values correspond to high viral load. From each culture or site, 1–2 cm^2 tissue from two different individuals was sampled.

7.3 Results

7.3.1 The *Ulva* virome composition of healthy and bleached specimens

A total of 60,952,693 high-quality reads were obtained across all eight samples, varying between 1,274,891 and 12,926,447 reads per sample. The majority of the reads were assigned to bacteria, the *Ulva* host, and prokaryotic viruses (i.e., phages that infect prokaryotes). A total of 591,075 reads — 1% of the total read number — across all eight samples were assigned to eukaryotic viruses (i.e., viruses that infect eukaryotes). The bleached *Ulva australis* samples had the highest number of eukaryotic viral reads (replicate 1 = 272,229 reads; replicate 2 = 202,349 reads), followed by the natural and presumably healthy *Ulva australis* populations (replicate 1 = 88,101 reads; replicate 2 = 22,359 reads) (Fig. 7.03A). The healthy aquaculture samples (*Ulva fenestrata* and *Ulva lacinulata*) contained the least reads assigned to eukaryotic viruses (varying between 216 and 4,857 viral reads) (Fig. 7.03A).

Across all samples, 144 unique eukaryotic virus contigs were identified. Most reads were assigned to viral contigs classified as belonging to the phyla *Pisuviricota* (70% of the eukaryotic viral reads) and *Cressdnaviricota* (4.4% of the eukaryotic viral reads). However, a large proportion of the viral contigs could not be classified at phylum level (i.e., contigs that matched uncultured marine viruses in the NCBI nr database), accounting for 23% of the eukaryotic viral reads. Within the *Pisuviricota*, healthy and bleached samples contained high read numbers of *Durnavirales* (109,420 reads in healthy samples versus 124,339 reads in the bleached samples) (Fig. 7.03B, C). The bleached samples also contained many reads mapping to contigs belonging to the *Picornavirales* (179,476 reads) (Fig. 7.03B). These results are based on the closest match in the NCBI database. However, the similarity (percentage identity) to the closest match is, in many cases, very low and the identifications should therefore be treated with caution (Table 7.01). For example, based on the initial BLAST results, 3.7% of the eukaryotic viral reads were assigned to the order *Cirlivirales* (*Cressdnaviricota*). Our phylogenetic analyses (see section 3.2.1), however, indicate that *Ulva*-associated CRESS DNA viruses likely belong to undescribed orders and families within the *Cressdnaviricota*.

7.3.2 Phylogenetic analyses of putative new viruses

In total, we identified 20 putative new (near complete) viral sequences using a standard sequence similarity search against the NCBI nr reference database (Table 7.01). The presence or absence of the 20 putative new viruses was verified by qRT-PCR in each of the samples. The putative new viruses exhibited low sequence similarity to existing replicase amino acid sequences (Rep in the case of DNA viruses and RdRp in the case of RNA viruses), with amino acid percentage similarities to the closest matching sequence ranging from 25.6 to 55.6%. They primarily belonged to single-stranded DNA viruses (ssDNA), double-stranded RNA viruses (dsRNA), or single-stranded positive-sense RNA viruses (ssRNA(+)). Together they represented 82% of the eukaryotic viral reads. The qPCR assay showed that Ulva CRESS DNA viruses and Ulva picorna-like viruses were especially abundant in bleached *Ulva* specimens, while absent or present in very low numbers (high cycle thresholds) in the healthy samples (Fig. 7.02; Fig. S7.01), which would not be expected for transcribed endogenous viral elements. Mitoviruses and mito-like viruses were especially abundant in the *Ulva fenestrata* lab culture, and Ulva durnaviruses were mainly present in both healthy and bleached *Ulva australis* (Fig. 7.02; Fig. S7.01).

The putative new viruses are most likely exogenous, as the same viral contigs were found in each of the duplicated samples, and the viral contigs assembled without attachment of *Ulva* genome fragments on either side. In addition, many of the putative new viruses were absent in the healthy *Ulva* samples, which would be

unexpected if the contigs belonged to endogenous viral elements. Finally, we extracted total DNA and RNA following the NetoVir protocol, which is optimised for virus-like particles (endogenous viral elements are not protected by a capsid and are therefore not extracted using NetoVir) (Conceição-Neto et al. 2015).

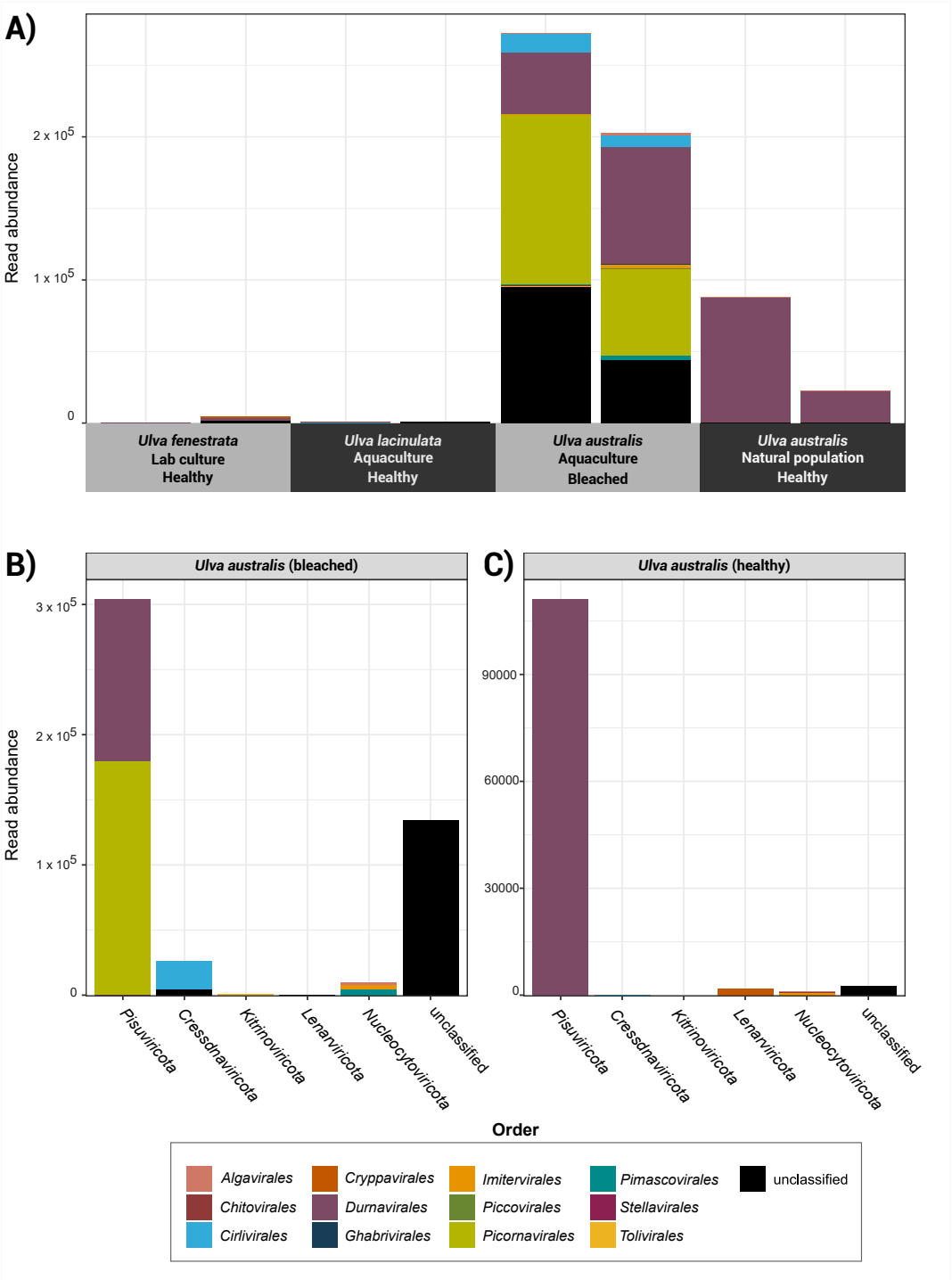

FIGURE 7.03 Eukaryotic viral read numbers. A) Total eukaryotic viral reads per sample (n = 8; 2 replicates per sample type); B) Total eukaryotic viral reads from bleached *Ulva australis* viromes that were assigned to the phyla *Pisuviricota*, *Cressdnaviricota*, *Kitrinoviricota*, *Lenarviricota*, *Nucleocytoviricota*, and unclassified viruses (sum of two replicates, total eukaryotic viral reads = 474,578); C) Total eukaryotic viral reads from healthy *Ulva australis* samples from natural populations (sum of two replicates, total eukaryotic viral reads = 110,460). Identifications are based on BLAST with the NCBI database. Colours represent different orders.

TABLE 7.01 BLASTx results of the 20 putative new virus-like sequences against the NCBI nr database

Putative new virus	GenBank accession number	Contig nudeotide length (bp)	BLASTx Hit GenBank accession	%ID with BLAST hit	e-Value	BLASTx hit organism	BLASTx hit taxonomy	BLASTx hit host
Ulva CRESS DNA virus 1	OP924572	3208	AXH74985.1	47.83	3.00E-84	CRESS virus sp.	*Cressdnaviricota*	Minnow (freshwater fish)
Ulva CRESS DNA virus 2	OP924573	2160	YP009163922.1	55.62	7.00E-68	Gammarus sp. Amphipod associated circular virus	*Circoviridae*	*Gammarus* sp. (amphipod)
Ulva CRESS DNA virus 3	OP924574	2668	YP009551434.1	44.19	1.00E-24	Mosquito VEM virus SDRBAJ	Unclassified DNA virus	Mosquito
Ulva CRESS DNA virus 4	OP924575	2402	YP009126884.1	46.44	2.00E-78	Avon-Heathcote Estuary associated circular virus 5	*Circoviridae*	*Austrovenus stutchburyi* (marine bivalve)
Ulva CRESS DNA virus 5	OP924576	3939	YP009553245	29.8	2.00E-05	Lolium perenne-associated virus	Unclassified DNA virus	*Lolium perenne* (plant)
Ulva durnavirus 1	OP924591	2971	QOW97231.1	44.49	4.00E-60	Amalga-like boulavirus	*Partitiviridae*	*Kraftionema allantoideum* (microalga)
Ulva durnavirus 2	OP924592	2730	QOW97231.1	41.78	3.00E-50	Amalga-like boulavirus	*Partitiviridae*	*Kraftionema allantoideum* (microalga)
Ulva durnavirus 3	OP924593	3198	QOW97231.1	40.09	1.00E-39	Amalga-like boulavirus	*Partitiviridae*	*Kraftionema allantoideum* (microalga)
Ulva durnavirus 4	OP924594	1909	QOW97235.1	25.63	6.00E-20	Partiti-like lacotivirus	*Partitiviridae*	*Ostreobium* sp. (microalgae)
Ulva ghabrivirus 1	OP924595	2825	BBZ90078.1	30.81	2.00E-76	Diatom RNA virus 1	Unclassified *Riboviria*	*Melosira* sp. (diatom)
Ulva mitovirus 1	OP924596	2200	AZG04294.1	35.6	1.00E-59	Hymenoscyphus fraxineus mitovirus 1	*Mitoviridae*	*Hymenoscyphus albidus* (fungus)
Ulva mito-like virus 2	OP924597	2513	APG77166.1	43.61	6.00E-50	Shahe narna-like virus 6	Unclassified *Riboviria*	Freshwater isoptera
Ulva mito-like virus 3	OP924598	2539	QOW97242.1	28.6	2.00E-45	Mito-like babylonusvirus	Unclassified *Riboviria*	*Ostreobium* sp. (microalgae)
Ulva tombus-like virus 1	OP924599	3717	YP009337737.1	42.79	3.00E-103	Hubei tombus-like virus 6	Unclassified *Riboviria*	Myriapoda
Ulva picorna-like virus 1	OP924600	8432	AVP71827.1	27.01	8.00E-56	Macrobrachium rosenbergii dicistrovirus 2	*Dicistroviridae*	*Macrobrachium rosenbergii* (shrimp)
Ulva picorna-like virus 2	OP924601	7847	QKK13171.1	41	2.00E-79	Kummerowia striata dicistrovirus	*Dicistroviridae*	*Kummerowia striata* (plant)
Ulva picorna-like virus 3	OP924602	7479	QKK82970.1	36.23	0	Trichosanthes kirilowii picorna-like virus	*Picornavirales*	*Trichosanthes kirilowii* (plant)
Ulva picorna-like virus 4	OP924603	8334	QKK82968.1	31.14	1.00E-53	Trichosanthes kirilowii picorna-like virus	*Picornavirales*	*Trichosanthes kirilowii* (plant)
Ulva picorna-like virus 5	OP924604	10369	YP009330008.1	28.68	2.00E-41	Changjiang crawfish virus 4	Unclassified *Riboviria*	Crayfish
Ulva picorna-like virus 6	OP924605	7970	YP009336663.1	28.98	3.00E-75	Wenling picorna-like virus 6	Unclassified *Riboviria*	Crustacean

CRESS (Circular Rep-Encoding Single-Stranded) DNA Viruses

Five viral assembled contigs associated with *Ulva* exhibited similarity to CRESS DNA viruses (*Cressdnaviricota*) belonging to the classes *Arfiviricetes* and *Repensiviricetes* (Fig. 7.04). CRESS DNA viruses have small, circular genomes, with a genome size often ranging from 1.0 to 6.5 kb (Krupovic et al. 2020). Many of these genomes contain only two major ORFs that encode the replication initiator protein (Rep) and the capsid protein (Cap). CRESS DNA viruses are believed to infect a wide variety of hosts, including mammals, birds, insects, fungi, diatoms, and plants (Rosario et al. 2017).

The five *Ulva*-associated CRESS DNA viruses grouped with very diverse orders and families (Fig. 7.05). Four contigs belonged to the *Arfiviricetes*, and one was positioned within the *Repensiviricetes* clade. Ulva CRESS DNA virus 1 was placed in an unidentified clade most closely related to the family *Smacoviridae* in the order *Cremevirales* (Fig. 7.06A). Ulva CRESS DNA virus 2 was located within the CRESS5 clade (Krupovic et al. 2019). This group also contained Rep-A viruses associated with *Ecklonia radiata* (a brown algal kelp species), as well as many other marine viruses associated with, amongst others, tunicates, amphipods, ctenophores, and marine snails (Fig. 7.06B). Ulva CRESS DNA virus 3 and 4 were positioned in a clade most closely related to the family *Circoviridae* and most likely belong to the order *Cirlivirales*. This clade also contained several viruses isolated from marine organisms and environments (Fig. 7.06C). Ulva CRESS DNA virus 5 grouped between the families *Geminiviridae* and *Genomoviridae* (*Geplafuvirales*, *Repensiviricetes*) (Fig. 7.06D). *Geminiviridae* and *Genomoviridae* viruses are mostly known to infect plants and fungi, respectively.

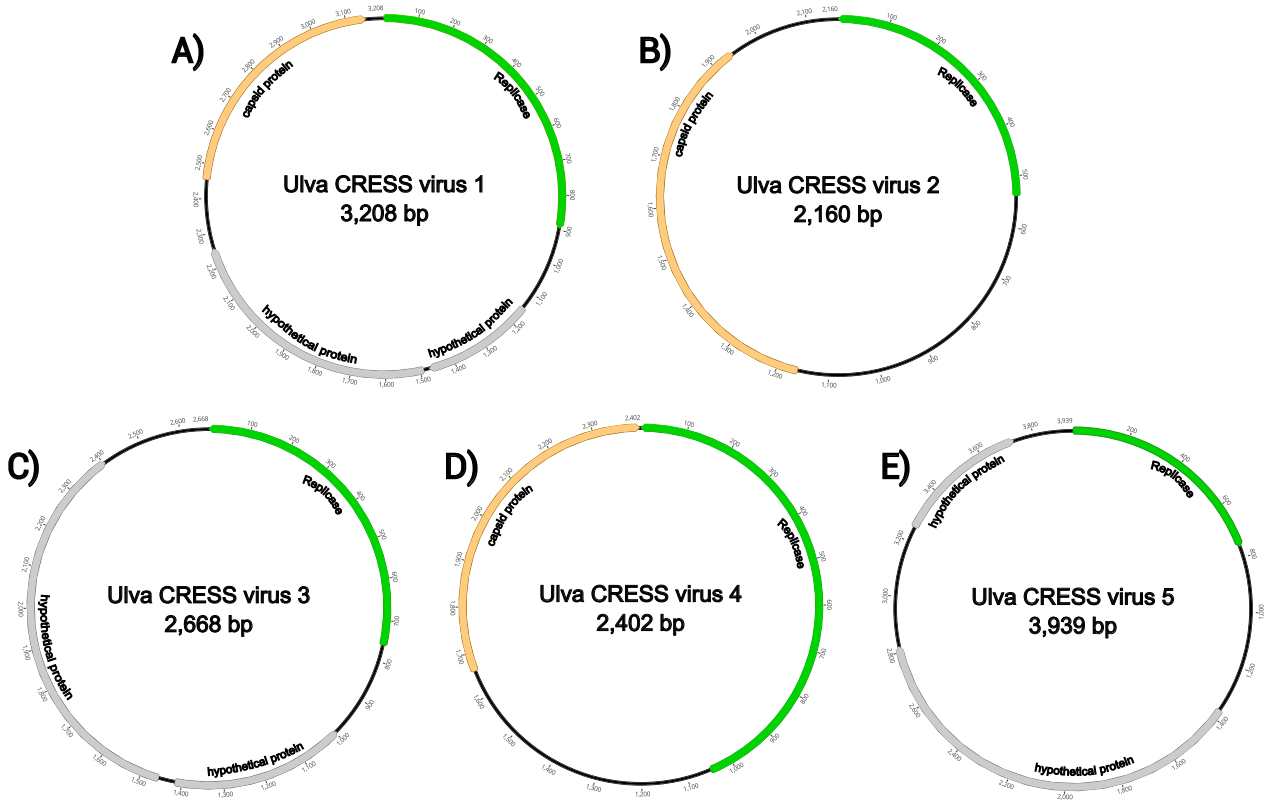

FIGURE 7.04 The genome organization of the five Ulva CRESS viruses, including replicase and capsid protein genes. Open Reading Frames (ORF) were predicted using ORFfinder (https://www.ncbi.nlm.nih.gov/orffinder/).

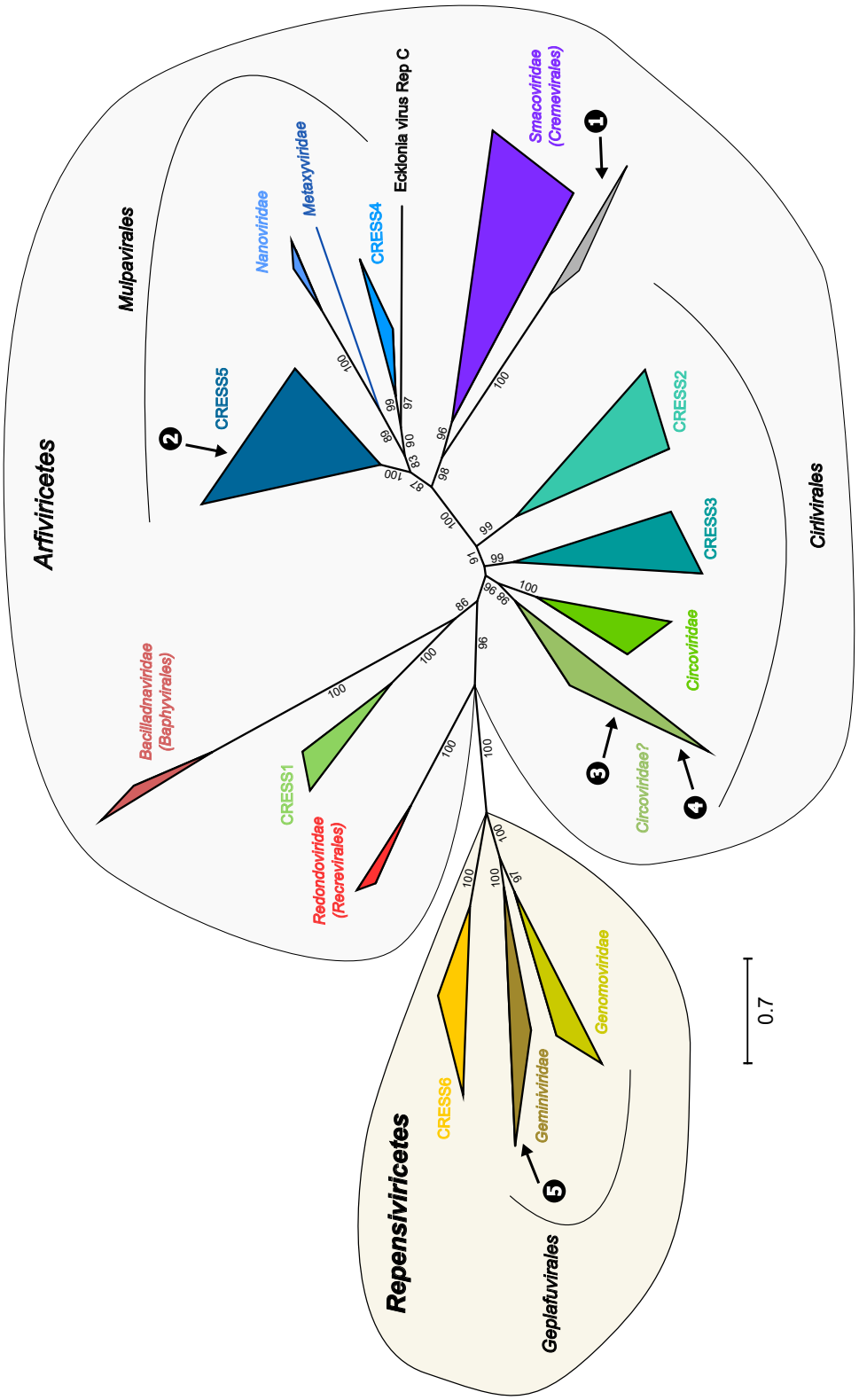

FIGURE 7.05 Unrooted maximum likelihood phylogenetic tree of Rep proteins from CRESS DNA viruses estimated using IQ-TREE with ultrafast bootstrap replicates (values below 70 are not displayed). Closely related sequence groups are collapsed into triangles, whose side lengths are proportional to the distances between the closest and farthest leaf nodes. The locations of the *Ulva*-associated CRESS DNA viruses are marked with numbered arrows. The numbers correspond to Ulva CRESS DNA virus 1–5. Branch lengths are scaled according to the number of amino acid substitutions per site.

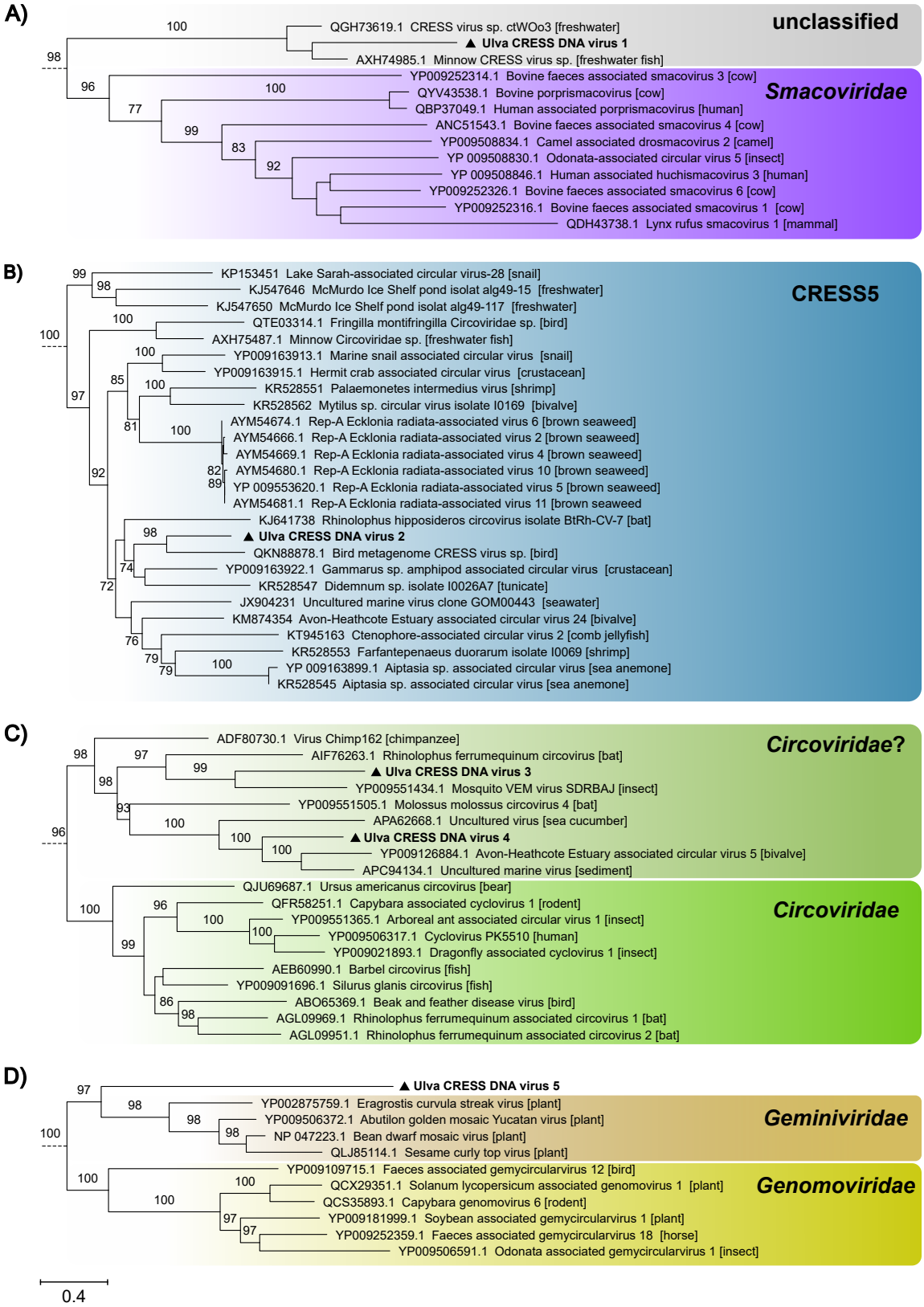

FIGURE 7.06 Details of the phylogeny of CRESS DNA viruses based on the Rep protein. A) the *Smacoviridae* and unclassified group, B) CRESS5 group, C) *Circoviridae*, D) *Repensiviricetes* (*Genomoviridae* and *Geminiviridae*). Newly discovered viruses from *Ulva* spp. are highlighted in bold. Each viral sequence's putative eukaryotic host (or sample habitat) is displayed in brackets. Maximum likelihood tree estimated using IQ-TREE with ultrafast bootstrap replicates (values below 70 are not displayed). The tree is mid-point rooted. Branch lengths are scaled according to the number of amino acid substitutions per site.

Durna-like dsRNA Viruses

Four putative new viruses were found to belong to the *Durnavirales*. This order currently includes six families (*Partitiviridae*, *Amalgaviridae*, *Picobirnaviridae*, *Hypoviridae*, *Fusariviridae*, and *Curvulaviridae*). Viruses belonging to the *Durnavirales* are mostly known to infect plants, fungi, and protists (Krupovic et al. 2015). The RdRp amino acid pairwise identity between the four *Ulva*-associated durnaviruses was relatively low but variable (14.7–61.8%). The ICTV currently uses 85% RdRp amino acid sequence identity as a demarcation criterion for the genus *Amalgavirus* (Sabanadzovic et al. 2018). We therefore assume that the four *Ulva*-associated sequences each represent a new virus genus or higher taxonomical rank.

Three of the newly described viral sequences exhibited RdRp amino acid sequence similarity to Amalga-like sequences (relatives of the *Amalgaviridae*) (Fig. 7.07A). *Amalgaviridae* have linear dsRNA genomes of ~3.5 kb containing two overlapping ORFs (Krupovic et al. 2015). The contig lengths of the putative new viruses varied from 2,730–3,198 nt, and they likely represent (near) complete genomes (Fig. 7.07B). Each genome contained 2 ORFs, of which the largest one coded for the RdRp and the smaller one did not exhibit similarity to known proteins (Fig. 7.07B). Ulva durnavirus 1, 2, and 3 were most closely related to Amalga-like boulavirus isolated from *Kraftionema allantoideum* (a microalga belonging to the Ulvophyceae) (Fig. 7.07A). The other viruses in this clade were related to the *Ostreobium* sp. and *Bryopsis* mitochondria-associated dsRNA viruses (both hosts belong to the Ulvophyceae). The latter was initially described as dsRNA associated with mitochondria in the green macroalga *Bryopsis cinicola* (Koga et al. 1998), but likely also represents a virus (Koga et al. 2003). Charon et al. (2020) hypothesised that these viruses formed a Ulvophyceae-infecting viral clade.

Ulva durnavirus 4 was positioned within a clade most closely related to the *Hypoviridae*, together with Partiti-like viruses associated with *Ostreobium* sp. (Ulvophyceae) (Fig. 7.07A). The contig of Ulva durnavirus 4 only contained one ORF (coding for RdRp) (Fig. 7.07B). As this was a relatively small contig (1,909 nt), it is likely that the genome of this virus is segmented (or incomplete), similar to viruses belonging to the *Partitiviridae* and *Picobirnaviridae* (Ghabrial et al. 2008). Linking additional genomic segments for this virus, however, is not possible based solely on metagenomics analysis.

***Ghabrivirales* (linear dsRNA viruses)**

One *Ulva*-associated contig displayed RdRp amino acid sequence similarity to two diatom-associated viruses (31–32%). These viruses form a clade closely related to the *Megabirnaviridae*, a predominantly fungi-infecting family within the order *Ghabrivirales* (Fig. 7.08A) (Abdoulaye et al. 2019). Other families within the *Ghabrivirales* include the *Chrysoviridae* (infecting plants and fungi), the *Quadriviridae* (infecting fungi), and the *Totiviridae* (infecting fungi and red macroalgae) (Lachnit et al. 2016, Sato et al. 2019). It is unclear whether the *Ulva*- and diatom-associated viruses form a new family within the *Ghabrivirales* or represent members of the *Megabirnaviridae*.

The genomes of the *Megabirnaviridae*, *Chrysoviridae*, and *Quadriviridae* are segmented, containing two to seven segments ranging from 2.7–9 kb in size (Chiba et al. 2018, Sato et al. 2019, Kotta-Loizou et al. 2020). It is therefore likely that the contig of Ulva ghabrivirus 1 (2,825 nt, containing 1 ORF coding for RdRp) only represents a partial genome (Fig. 7.08B).

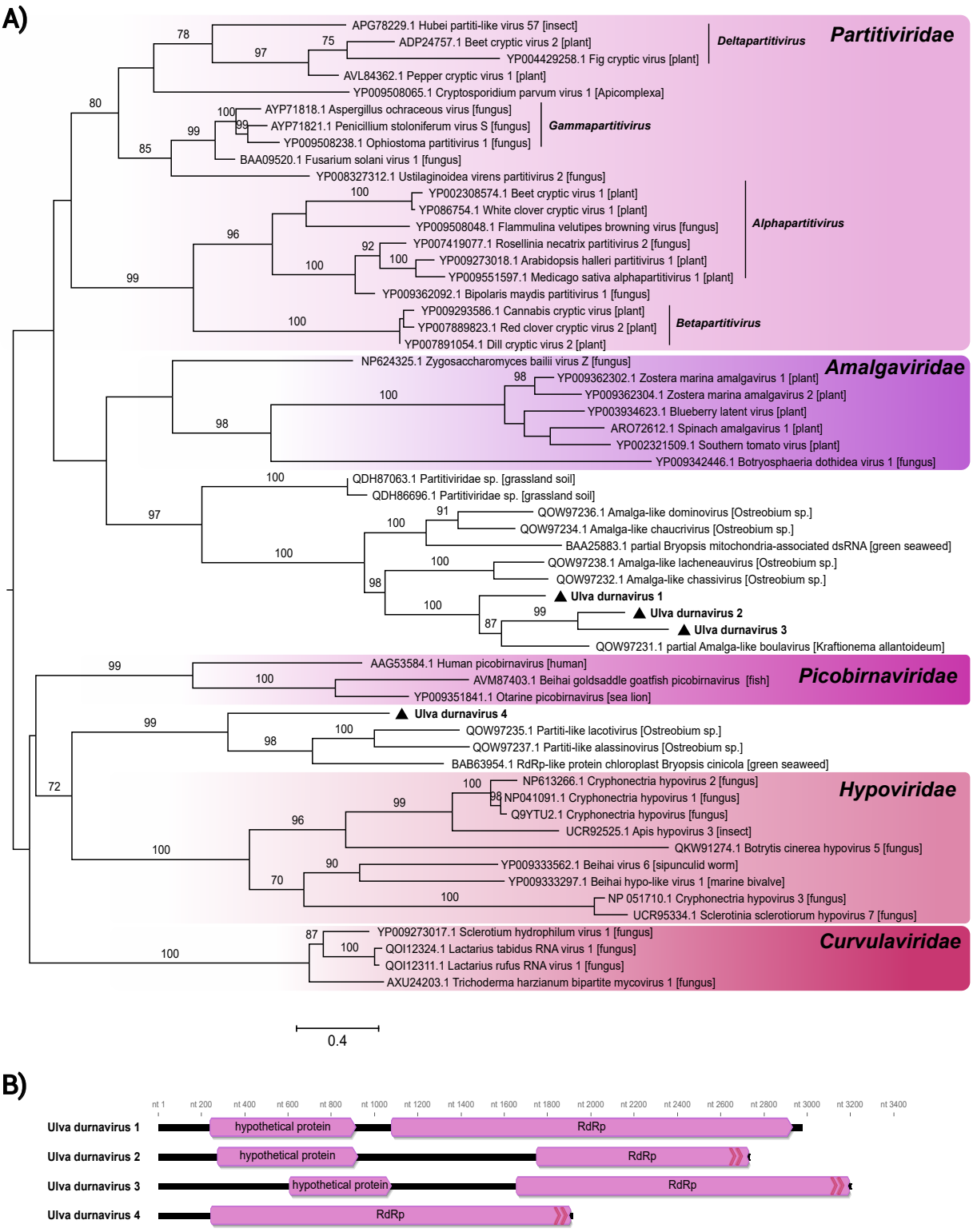

FIGURE 7.07 Phylogeny and genome organization of the Ulva durnaviruses. A) Phylogentic tree of the order *Durnavirales* based on the RdRp protein. Newly discovered viruses from *Ulva* spp. are highlighted in bold and indicated with a triangle. Each viral sequence's putative eukaryotic host (or sample habitat) is displayed in brackets. Maximum likelihood tree estimated using IQ-TREE with ultrafast bootstrap replicates (values <70 are not displayed). The tree is mid-point rooted. Branch lengths are scaled according to the number of amino acid substitutions per site. B) Genome organization, including RNA-dependent RNA polymerase (RdRp) genes. Open Reading Frames (ORF) were predicted using ORFFINDER (https://www.ncbi.nlm.nih.gov/orffinder/).

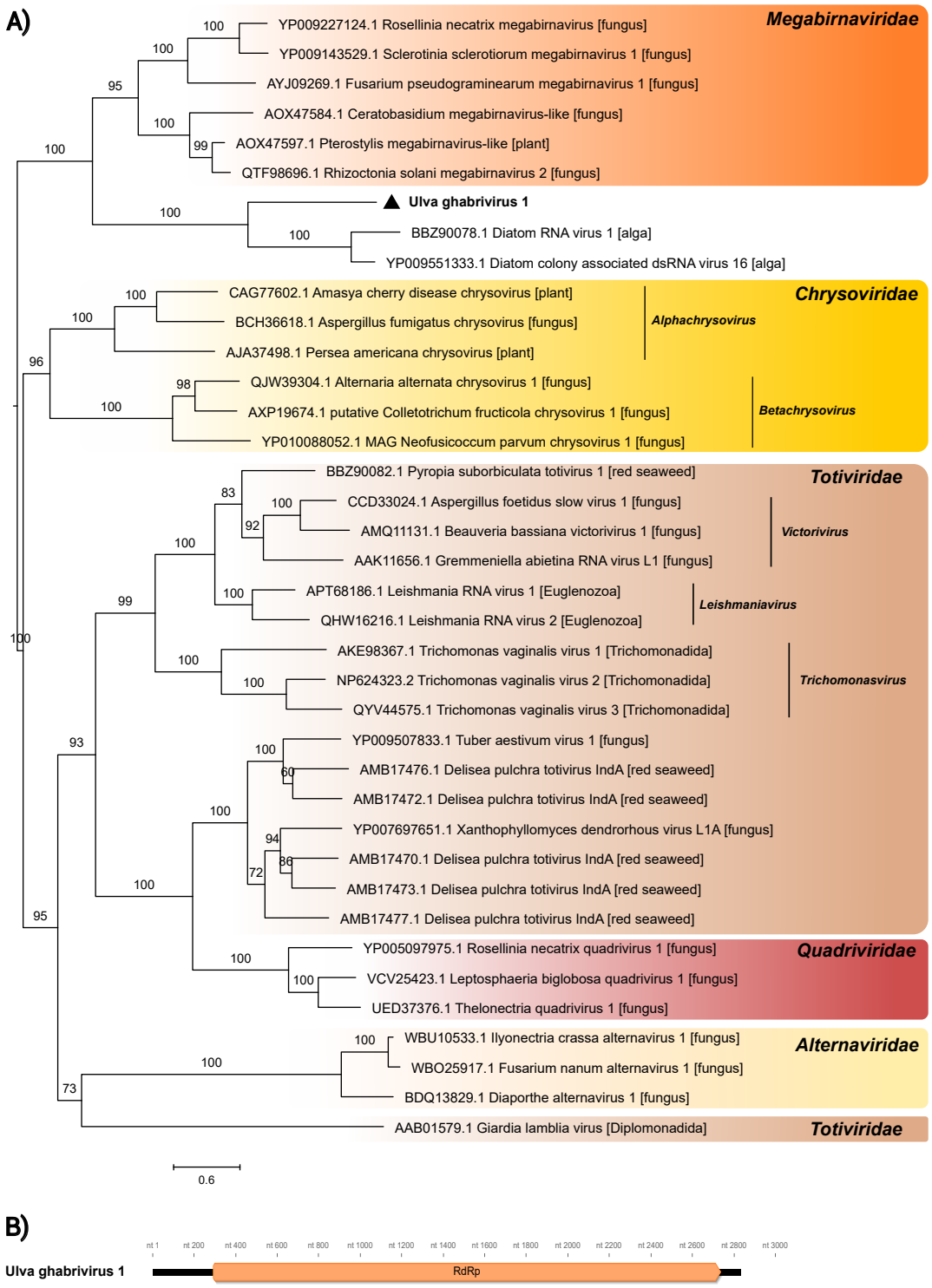

FIGURE 7.08 Phylogeny and genome organization of Ulva ghabrivirus 1. A) Phylogenetic tree of the *Ghabrivirales* based on the RdRp protein. The newly discovered Ulva ghabrivirus is highlighted in bold and indicated with a triangle. Each viral sequence's putative eukaryotic host (or sample habitat) is displayed in brackets. Maximum likelihood tree estimated using IQ-TREE with ultrafast bootstrap replicates (values <70 are not displayed). The tree is mid-point rooted. Branch lengths are scaled according to the number of amino acid substitutions per site. B) Genome organization, including the RNA-dependent RNA polymerase (RdRp) gene. The genomes of the *Ghabrivirales* are segmented, it is therefore likely that the contig of Ulva ghabrivirus 1 only represents a partial genome. Open Reading Frames (ORF) were predicted using ORFFINDER (https://www.ncbi.nlm.nih.gov/orffinder/).

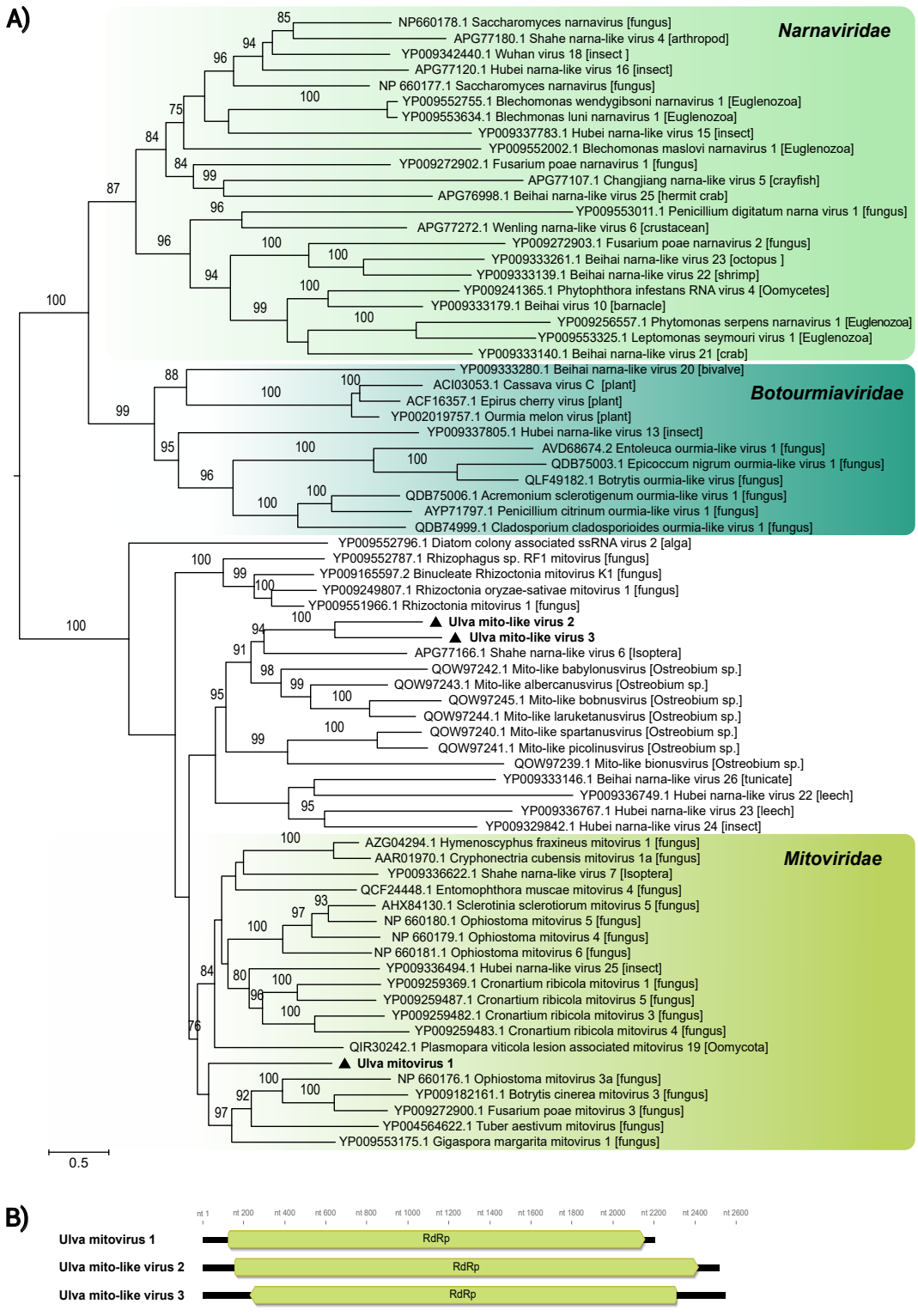

FIGURE 7.09 Phylogeny and genome organization of Ulva mitoviruses and mito-like viruses. A) Phylogenetic tree of the *Narnaviridae*, *Botourmiaviridae*, and *Mitoviridae* based on the RdRp protein. Newly discovered viruses from *Ulva* spp. are highlighted in bold and indicated with a triangle. Each viral sequence's putative eukaryotic host (or sample habitat) is displayed in brackets. Maximum likelihood tree estimated using IQ-Tree with ultrafast bootstrap replicates (values <70 are not displayed). The tree is mid-point rooted. Branch lengths are scaled according to the number of amino acid substitutions per site. B) Genome organization, including RNA-dependent RNA polymerase (RdRp) genes. Open Reading Frames (ORF) were predicted using ORFfinder (https://www.ncbi.nlm.nih.gov/orffinder/).

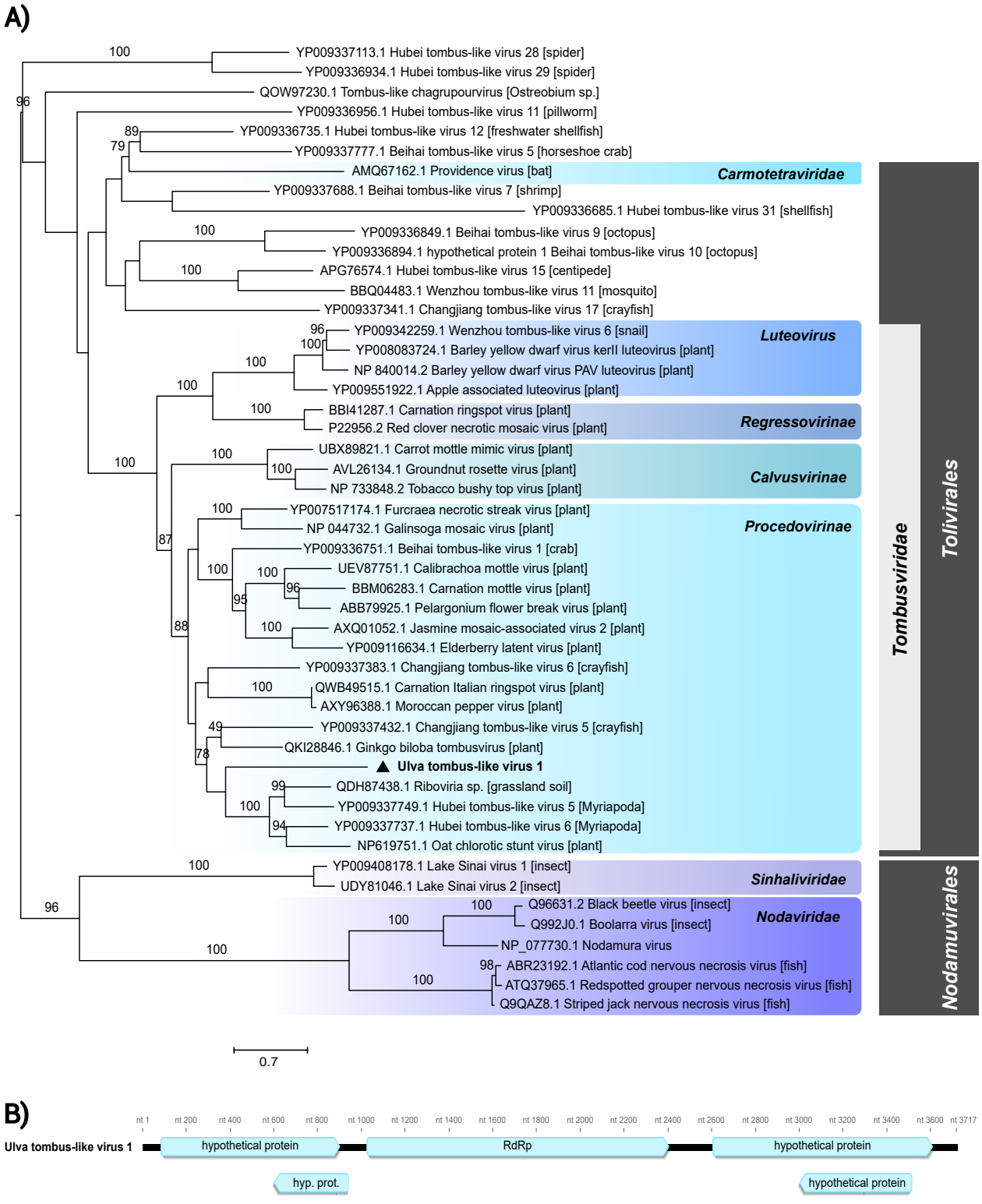

FIGURE 7.10 Phylogeny and genome organization of Ulva tombus-like virus 1. A) Phylogenetic tree of the *Tolivirales* (*Tombusviridae* and *Carmotetraviridae*), and the *Nodamuvirales* based on the RdRp protein. The newly discovered Ulva tombus-like virus is highlighted in bold and indicated with a triangle. Each viral sequence's putative eukaryotic host (or sample habitat) is displayed in brackets. Maximum likelihood tree estimated using IQ-Tree with ultrafast bootstrap replicates (values <70 are not displayed). The tree is mid-point rooted. Branch lengths are scaled according to the number of amino acid substitutions per site. B) Genome organization, including RNA-dependent RNA polymerase (RdRp) genes. Open Reading Frames (ORF) were predicted using ORFfinder (https://www.ncbi.nlm.nih.gov/orffinder/).

Mito-like ssRNA(+) Viruses

Three viral contigs associated with *Ulva* were related to the *Mitoviridae* (Fig. 7.09A). *Mitoviridae* is currently the only family recognised within the order *Cryppavirales*. Viruses of this family have small genomes of up to 3 kb containing a single ORF encoding an RdRp gene (Thekke-Veetil et al. 2020). *Mitoviridae* have mostly been reported from fungi, but to a lesser degree, have been found associated with insects (Le Lay et al. 2020, Ortiz-Baez et al. 2021), algae (Charon et al. 2020), and plants (Chen et al. 2021). The contig size of the viruses sequenced in this study varied between 2,200–2,539 bp, which is within the standard size ranges of viruses belonging to the family *Mitoviridae*. All three viral sequences contained a single ORF encoding for the RdRp domain (pfam05919) (Fig. 7.09B).

Ulva mitovirus 1 was positioned within a clade formed by the family *Mitoviridae*. This clade is dominated by viruses infecting fungi. Ulva mito-like virus 2 and 3 were closely related to each other (42% RdRp similarity) and seven mito-like viruses associated with the green microalga *Ostreobium* sp. (Ulvophyceae) (ranging from 25 to 45% similarity). This clade possibly represents a new genus within the family *Mitoviridae* or a new family within the order *Cryppavirales*.

Tombus-like ss(+)RNA Viruses

One contig, Ulva tombus-like virus 1, exhibited similarity to members of the *Tombusviridae* (a plant-infecting family of ssRNA(+) viruses) and clustered within the subfamily *Procedovirinae* (Fig. 7.10A). Viral genomes of members of the *Tombusviridae* range in size from 3.7–4.8 kb and contain 4–6 ORFs (Lommel et al. 2008). These ORFs encode replication-associated proteins, movement proteins, and capsid proteins. Ulva tombus-like virus 1 was represented by a 3.7 kb contig that included 5 ORFs (Fig. 7.10B). The largest ORF encoded the RdRp gene. The remaining 4 ORFs did not match with any reference protein sequences.

Ulva tombus-like virus 1 was most closely related to tombus-like viruses associated with grassland soil, Myriapoda, and Oat chlorotic stunt virus (a plant pathogen). RdRP amino acid similarity between Ulva tombus-like virus 1 and the latter three viruses ranged from 22–43%, which is well below the species demarcation criteria currently recognised within the different genera of the *Tombusviridae* by the ICTV (57–93%) (King et al. 2012a).

Picorna-like ss(+)RNA Viruses

Six *Ulva*-associated viruses were classified as belonging to the order *Picornavirales*. The *Picornavirales* is a diverse order, currently containing nine families. Members of the *Picornavirales* are known to infect invertebrates (families *Dicistroviridae*, *Iflaviridae*, *Polycipiviridae*, *Noraviridae*, and *Solinviviridae*), vertebrates (family *Picornaviridae*, *Caliciviridae*), plants (family *Secoviridae*), and algae (family *Marnaviridae*) (Lommel et al. 2008). They also occur widely and abundant in environments such as oceans (Vlok et al. 2019), rivers (Zell et al. 2022), and lakes (Yau and Seth-Pasricha 2019). Members of the *Picornavirales* have mono- or bipartite genomes (7,000–12,500 nt) encoding at least one polyprotein. These polyproteins include a replication block with three domains: a superfamily III helicase (Hel), a proteinase (Pro), and a superfamily I RdRp (Pol) (King et al. 2012b).

Ulva picorna-like virus 1 and 2 were related to each other and members of the *Dicistroviridae* (Fig. 7.11). The closest relatives were Havel picorna-like virus 56 and Havel picorna-like virus 63 (both isolated from a river), which belong to a Dicistro-like cluster 3 (Zell et al. 2022). For Ulva picorna-like virus 1 a near complete, dicistronic genome was obtained, and for Ulva picorna-like virus 2 a partial genome, lacking the 3'end (Fig. 7.12A–B). Ulva picorna-like virus 2 likely has a dicistronic genome as well, containing two polyproteins.

Ulva picorna-like virus 3 and 4 clustered within Dicistro-like cluster 4 (Zell et al. 2022), together with *Trichosanthes kirilowii* picorna-like virus (closest relative), and several other unclassified *Picornavirales* members associated with arthropods, snails, plants and bivalves (Fig. 7.11). The contig of Ulva picorna-like virus 3 represented an almost complete dicistronic genome, with polyprotein 1 encoding the nonstructural protein and a polyprotein 2 encoding the capsid protein (Fig. 7.12C). Two capsid protein domains with similarity to the cd00205 protein family (rhv-like) including conserved amino acids of the drug-binding pocket, were identified by Pfam. This drug-binding pocket is conserved in the three major capsid proteins of all rhinoviruses and enteroviruses, in the capsid proteins of almost all picornaviruses, and in many capsid proteins of picorna-like viruses, making this a good indication of a jellyroll fold of a capsid protein. The putative helicase exhibited a modified Walker A motif (GxxGxMKS). A proteinase domain was not detected using the PFAM conserved domain search tool. However, there was a modified active site sequence (AxCG rather than GxCG). Ulva picorna-like virus 4 likewise had a dicistronic genome containing 2 polyproteins (Fig. 7.12D). Both ORFs were separated by only 90 nt, suggesting either an unknown type of internal ribosome entry site (IRES) or another mechanism of translation initiation, e.g., transcription of subgenomic RNA.

Ulva picorna-like virus 5 was highly divergent (Fig. 7.11). The first ORF in the dicistronic genome encoded an exceptionally long polyprotein 1 (2,630 aa) with picorna-like helicase, proteinase, and polymerase domains (Fig. 7.12E). The N-terminal (1,000 aa) shared no similarity to any known protein. Polyprotein 2 (781 aa) did not share similarity to known sequences either but is expected to encode capsid proteins.

Ulva picorna-like virus 6 clustered with several picorna-like viruses isolated from the Havel river (Zell et al. 2022), and with other unclassified picorna-like viruses associated with crustaceans and insects (Fig. 7.11). Ulva picorna-like virus 6 had a monocistronic genome encoding a single polyprotein (~2,600 aa) with N-terminal nonstructural proteins (Hel-Prot-RdRp) and C-terminal capsid proteins (two rhv domains with drug binding pockets identified by a conserved domain search) (Fig. 7.12F).

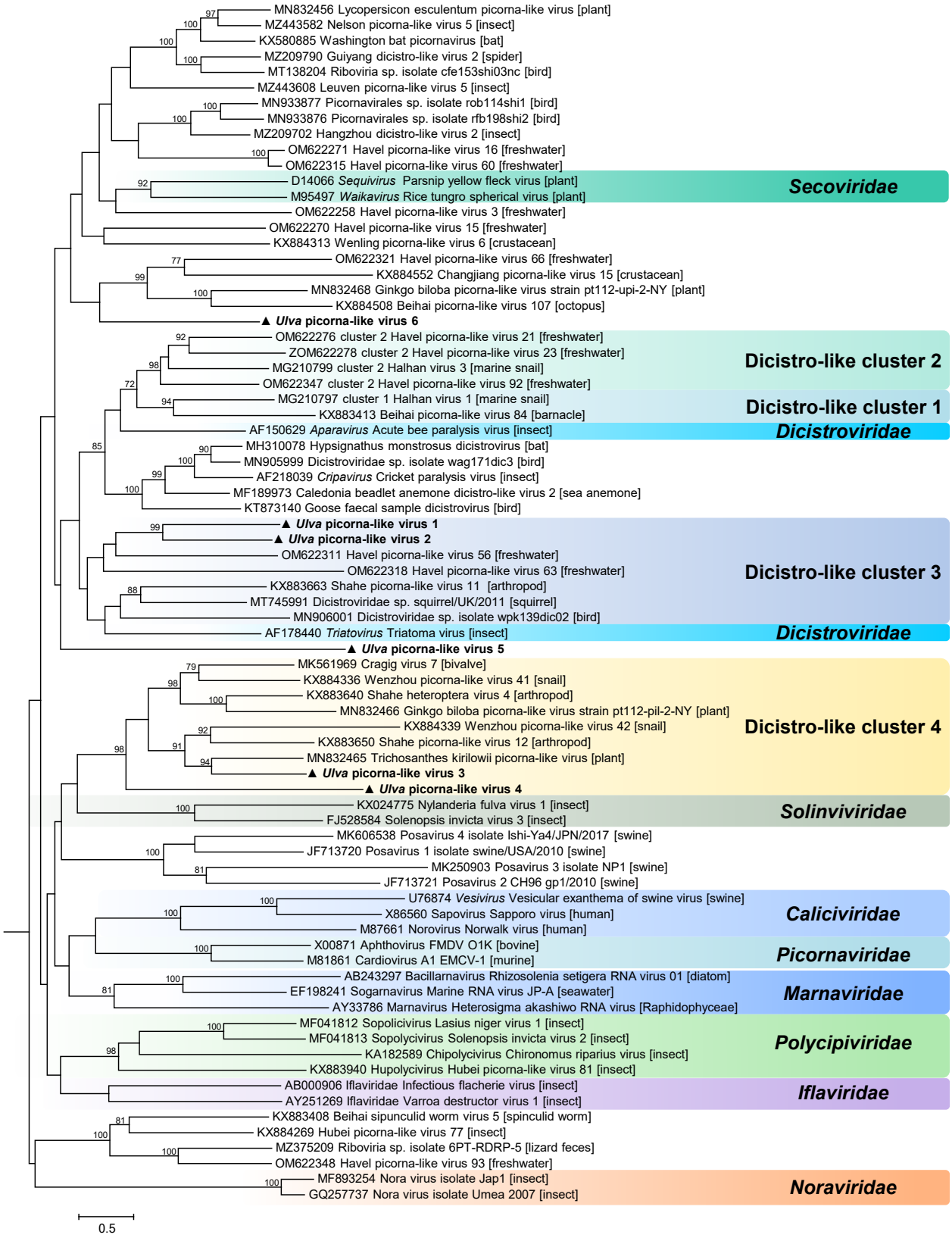

FIGURE 7.11 Phylogeny of the *Picornavirales* based on the proteinase/polymerase gene region. Newly discovered viruses from *Ulva* spp. are highlighted in bold. Each viral sequence's putative eukaryotic host (or sample habitat) is displayed in brackets. Maximum likelihood tree estimated using IQ-TREE with ultrafast bootstrap replicates (values <70 are not displayed). The tree is mid-point rooted. Branch lengths are scaled according to the number of amino acid substitutions per site.

A) Ulva picorna-like virus 1

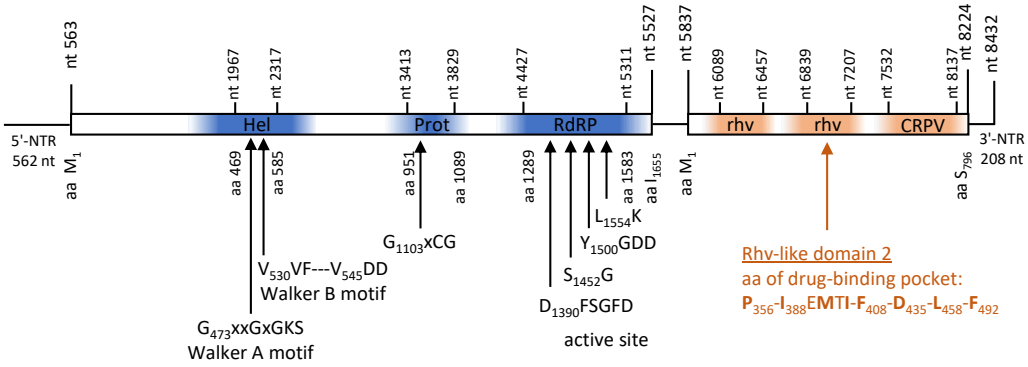

B) Ulva picorna-like virus 2

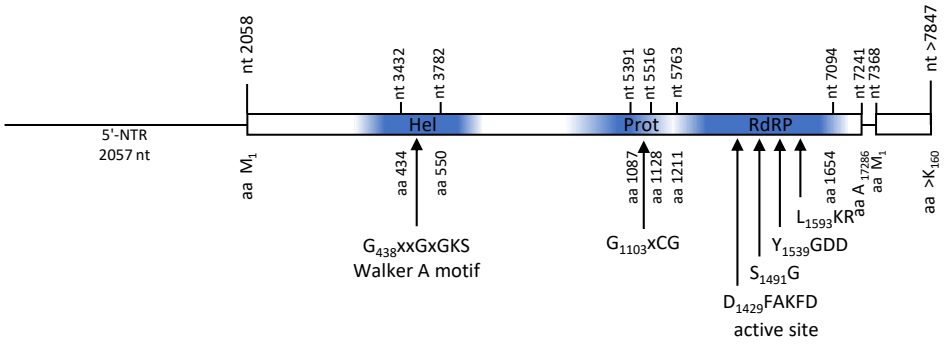

C) Ulva picorna-like virus 3

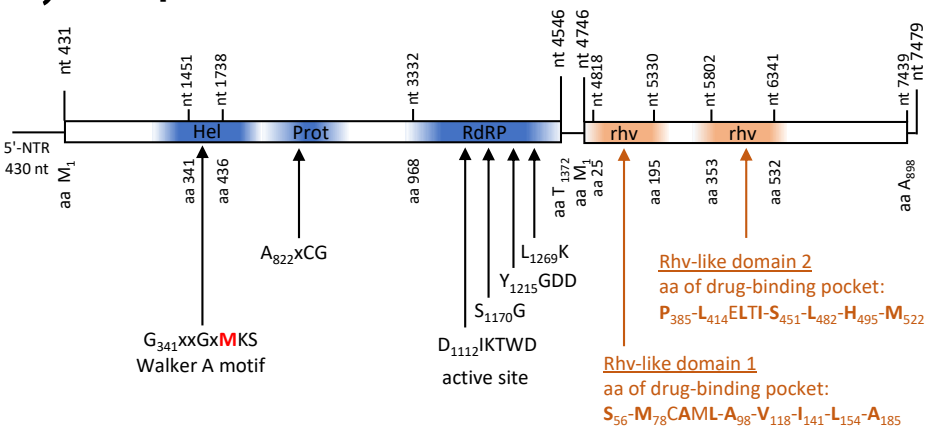

D) Ulva picorna-like virus 4

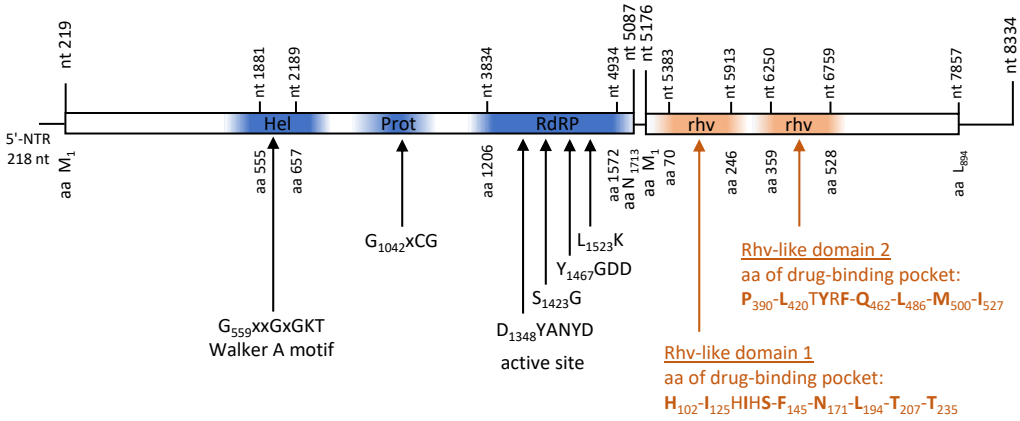

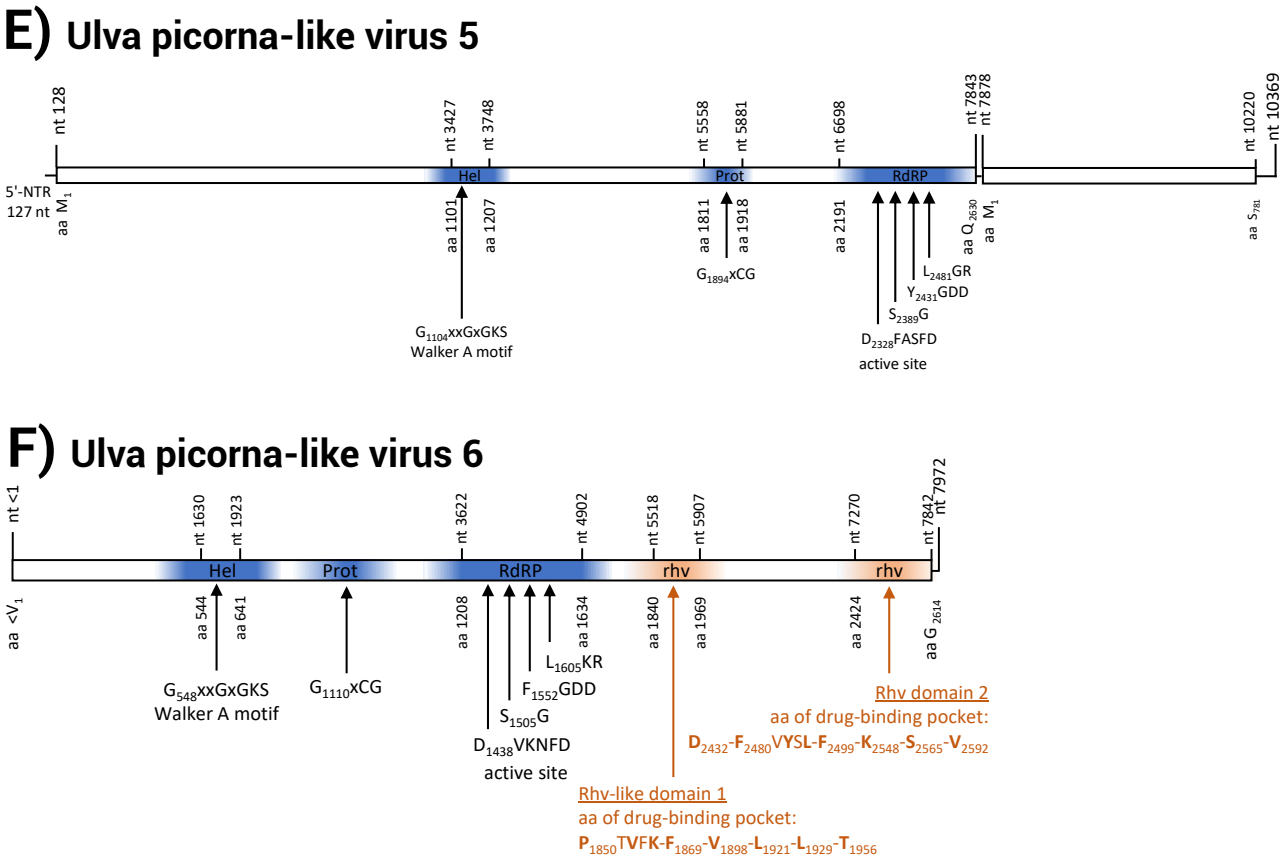

FIGURE 7.12 The genome organization and conserved picornaviral motifs of the six Ulva picorna-like viruses. Arrows indicate conserved motifs (Walker A and B motifs, proteinase active site motif, polymerase motifs, and drug-binding pockets of capsid proteins). Rhinovirus-like (rhv-like) domains, including conserved amino acids of the drug-binding pocket, were also identified. Conserved motifs were identified with Pfam and Phyre2.

7.4 Discussion

It is becoming increasingly clear that viruses are important components of microbial communities. Their role in seaweed health and disease, however, remains poorly studied. We aimed to characterise the DNA and RNA virosphere of the green seaweed *Ulva*. After analysing eight samples (originating from three different *Ulva* cultures and a natural population), we identified 20 putative new and divergent viruses, of which the majority was especially abundant in bleached *Ulva* specimens. However, it is important to remember that based on metagenomic data alone, it is not possible to establish whether these newly discovered viruses truly infect green algae (i.e., the source of the sequences does not necessarily represent the actual host) (Cobbin et al. 2021). The question, therefore, remains whether some of the newly identified viruses may have been associated with other hosts, e.g., fungi or diatoms. While the cultures used in this study were not axenic, the overwhelming majority of eukaryotic reads in our samples were assigned to the genus *Ulva*, making it likely that most of these 20 putative new viruses indeed infect green seaweeds rather than associated eukaryotic microbes.

7.4.1 Comparing the *Ulva* virome to other seaweeds and microalgae

This study is the first attempt at characterising the virosphere of a green macroalga. Viromes of green microalgae have received considerably more attention than their larger counterparts, especially in relation to phytoplankton blooms. The impact of viral lysis on phytoplankton mortality can be tremendous (Fuhrman 1999), and as most algal viruses have a specific host range, they effectively control bloom dynamics (Brussaard 2004). Nucleocytoplasmic large DNA viruses, for example, are known to infect the green unicellular prasinophytes *Micromonas pusilla* and *Ostreococcus tauri* (Derelle et al. 2008, Middelboe and Brussaard 2017), with interactions being strongly affected by environmental factors. For instance, continuous light (24:0 light:dark) increased the maximum virus production rate of prasinovirus MpoV-45T, and higher seawater temperature led to earlier algal cell lysis (Piedade et al. 2018). Phycodnaviruses are also found in association with brown seaweeds, including multiple species of kelp (Laminariales) (McKeown et al. 2017, 2018) and filamentous species (Ectocarpales) (Lanka et al. 1993, Müller 1996, Van Etten et al. 2002). Overall, 40–100% of *Ectocarpus* individuals and 35% of kelp individuals collected in Europe were found to be infected with phaeoviruses (McKeown et al. 2018), but their biological and ecological relevance is still unknown. Members of the *Phycodnaviridae* were also present in a small proportion of reads in our dataset (in the bleached *Ulva* specimens) based on NCBI blast results, but as these viruses contain relatively large genomes, we did not obtain (near) complete genome assemblies of the *Phycodnaviridae* members in this study.

Although research on microalgal virospheres has primarily focused on DNA viruses, recent studies have also demonstrated a large diversity of algae-associated RNA viruses (Charon et al. 2020, 2021, Chiba et al. 2020). One of these studies included two Ulvophyceaen hosts, *Kraftionema allantoideum* and an *Ostreobium* sp. (Charon et al. 2020). Similar to the *Ulva* virosphere, the viral communities of *K. allantoideum* and *Ostreobium* sp. were rich in members of the *Durnavirales*. The Ulvophyceaen viruses formed two separate clades most closely related to the *Amalgaviridae* and *Hypoviridae*. The virome of *Ostreobium* sp. also contained multiple mito-like viruses closely related to the mito-like viruses found here in *Ulva*. *Picornavirales* were not found in *Ostreobium* and *Kraftionema* cultures (Charon et al. 2020), but have been sequenced from non-green algae such as *Delisea pulchra* (Rhodophyta) (Lachnit et al. 2016), *Vaucheria litorea* (Xanthophyceae), *Symbiodinium* sp. (Dinophyceae), and *Thalassiothrix antarctica* (Bacillariophyta) (Charon et al. 2021). These picorna-like viruses, however, all belonged to the family of the *Marnaviridae* (data not shown) and are, therefore, not closely related to the

Picornavirales members found in the current study. Most viral genomes sequenced from algal hosts represent putative new viruses, often belonging to unidentified families or even orders. We have likely only touched the surface with regard to the diversity of algal viruses.

7.4.2 High viral load in bleached *Ulva*

The high number of viral reads in bleached *Ulva* specimens especially stands out. Only a handful of studies have shown a link between viruses and diseases in seaweeds (Ward et al. 2020). Green-spot disease, the most common disease in Korean *Pyropia* seaweed farms, is the only known red seaweed disease confirmed to be caused by a virus (G. H. Kim et al. 2016). This chloroplast-infecting virus PyroV1 causes cellular lysis, resulting in green spots on the purple-red seaweed tissue, eventually leading to lysis of the whole blade. Infection experiments showed that PyroV1 could infect at least three *Pyropia* species (*P. dentata*, *P. tenera* and *P. yezoensis*), but not more distantly related red seaweeds like *Bostrychia tenuissima* and *Dasysiphonia chejuensis*, displaying host-specificity to a certain extent (G. H. Kim et al. 2016). Interestingly, the *Pyropia* species were only susceptible to infection throughout their gametophyte stage (during which they are blade-shaped), not in their conchocelis phase (tetrasporophytic filamentous growths that are often shell-boring) (G. H. Kim et al. 2016). The latent period (i.e., the time required for the disease to become visible in a newly infected host) was 36–54 hours, meaning the disease could spread quickly within aquaculture facilities. Seaweed aquaculture currently represents 51.3% of the total marine and coastal aquaculture production (Chopin and Tacon 2021), and is still growing worldwide (Duarte et al. 2021). As most crops are cultivated as monocultures, with a higher vulnerability to disseminating diseases, virus detection may become increasingly important.

In brown seaweeds, CRESS DNA viruses were found to be associated in high abundance with bleached phenotypes of the habitat-forming kelp *Ecklonia radiata* (Beattie et al. 2018). These ssDNA viruses belong to the CRESS5 clade, together with other marine-habitat viruses, such as crustaceans, sea anemones, and Ulva CRESS DNA virus 2 from this study (Fig. 7.5). Our bleached *Ulva* specimens were associated with several CRESS DNA viruses and picorna-like viruses that were not found, or only found in low abundance, in healthy specimens. The highly abundant durnaviruses were also found in the natural, healthy population and are therefore not likely to induce bleaching. It is possible that bleaching in *Ulva* is caused by one or a combination of the CRESS DNA viruses or picorna-like viruses, possibly inducing cell lysis similarly to the chloroplast-infecting virus in *Pyropia*. However, as the viruses were not isolated, an unequivocal link between a virus and the bleaching disease could not be verified. Confirming such a link requires additional studies including the isolation of viruses and infection assays. Bleaching of the *Ulva* thalli may also have other causative agents (e.g., bacteria, fungi, abiotic stress), simply allowing the proliferation of viruses in the already unhealthy seaweeds.

To our knowledge, diseases in green seaweeds — whether caused by bacteria, fungi, or viruses — have not been reported. Bleaching in *Ulva* has however been observed in the bay of Marseille (Mediterranean Sea) (Loret et al. 2020). Contrary to many other coastal areas, the bay of Marseille does not experience green tides (i.e., mass accumulation events of unattached green seaweeds), despite high nutrient availability. When *Ulva* was collected from Brittany (Atlantic coast of France where green tides frequently occur but no bleaching is observed) and cultivated in Marseille seawater, bleaching was rapidly induced, with the thalli sometimes turning white within one day. Bleaching coincided with the observation of virus-like particles in seawater, which led Loret et al. (2020) to hypothesise that a marine virus prevents *Ulva prolifera*tion and green tides in the bay of Marseille. Green tides also happen frequently in the Yellow Sea in China and are becoming a growing concern (Ye et al. 2011). A recent study that characterised viral communities in seawater surrounding algal blooms in

the coastal waters of the Yellow Sea showed that viral richness and community composition changed throughout the different phases of the green tide. For example, *Phycodnaviridae* — known to infect algal hosts — were found to drastically increase during green tides and in the post-bloom phase, as did the proportion of lytic viruses in general (Du et al. 2023). In addition, the viral communities were influenced by other environmental parameters, such as total organic carbon, dissolved oxygen, nutrients, and chlorophyll a concentrations. The above examples emphasise how little we know of seaweed viruses, while the effect of these viruses on ecosystems and aquaculture could be tremendous.

Acknowledgements

The research leading to the results presented in this publication was carried out with infrastructure funded by the VLIZ Brilliant Marine Research Idea and FWO PhD Fellowships fundamental research for LvdL (3F020119) and LDC (11L1323N). We thank Lander Blommaert for providing the *Ulva australis* and *Ulva lacinulata* NIOZ aquaculture strains and Sophie Steinhagen for the *Ulva fenestrata* cultures. This research was facilitated by infrastructure funded by EMBRC Belgium - FWO project GOH3817N and I001621N.

Author contributions

L.M.L.: Conceptualization, Data curation, Formal analysis, Investigation, Visualisation, Writing – original draft. **L.D.C.:** Data curation, Formal analysis, Methodology, Writing – review and editing. **R.L.:** Formal analysis, Visualisation, Writing – review and editing. **S.L.:** Conceptualization, Methodology, Writing – review and editing. **A.W.:** Conceptualization, Supervision, Writing – review and editing. **O.D.C.:** Conceptualization, Funding acquisition, Supervision, Writing – review and editing. **J.M.:** Funding acquisition, Methodology, Resources, Supervision, Writing – review and editing.

Data availability statement

Raw sequence reads and metadata are deposited at SRA (BioProject PRJNA902394). The genome sequences of the putative new viruses are archived at GenBank (accession numbers OP924572-OP924576 and OP924591-OP924605). Supplementary data to this article can be found online at https://journals.asm.org/doi/10.1128/spectrum.00255-23.

Notes

[1] Sequencing host-related viruses often proves challenging due to the prevalence of DNA from other organisms, such as bacteria and the host itself. To address this, optimised DNA and RNA extraction methods are important to get rid of the majority of bacteria while retaining viral particles. In this study, we used the NetoVIR protocol (Conceição-Neto et al. 2015). Conceição-Neto et al. (2015) tested the effect of various homogenisation, filtration, and centrifugation methods, as well as the impact of chloroform treatment and random amplification on the viral and bacterial communities obtained by sequencing. They found that homogenisation at 3,000 rpm led to reduced viral particle loss compared to homogenisation at 5,000 rpm. Centrifugation for 3 minutes at 17,000×*g* effectively reduced bacterial particles without significant loss of viral particles. Filtering with a 0.8 µm PES filter proved more efficient in removing bacteria than a 0.8 µm PC filter. Using smaller filter sizes (e.g., 0.45 µm or

0.22 µm) altered the abundance of larger viruses. A chloroform treatment likewise efficiently removed bacteria, but also altered viral abundances and was therefore not advised to use. Finally, viral genetic material is often present in low amounts, random amplification, despite introducing bias, is frequently necessary for adequate detection.

Supplementary Figures

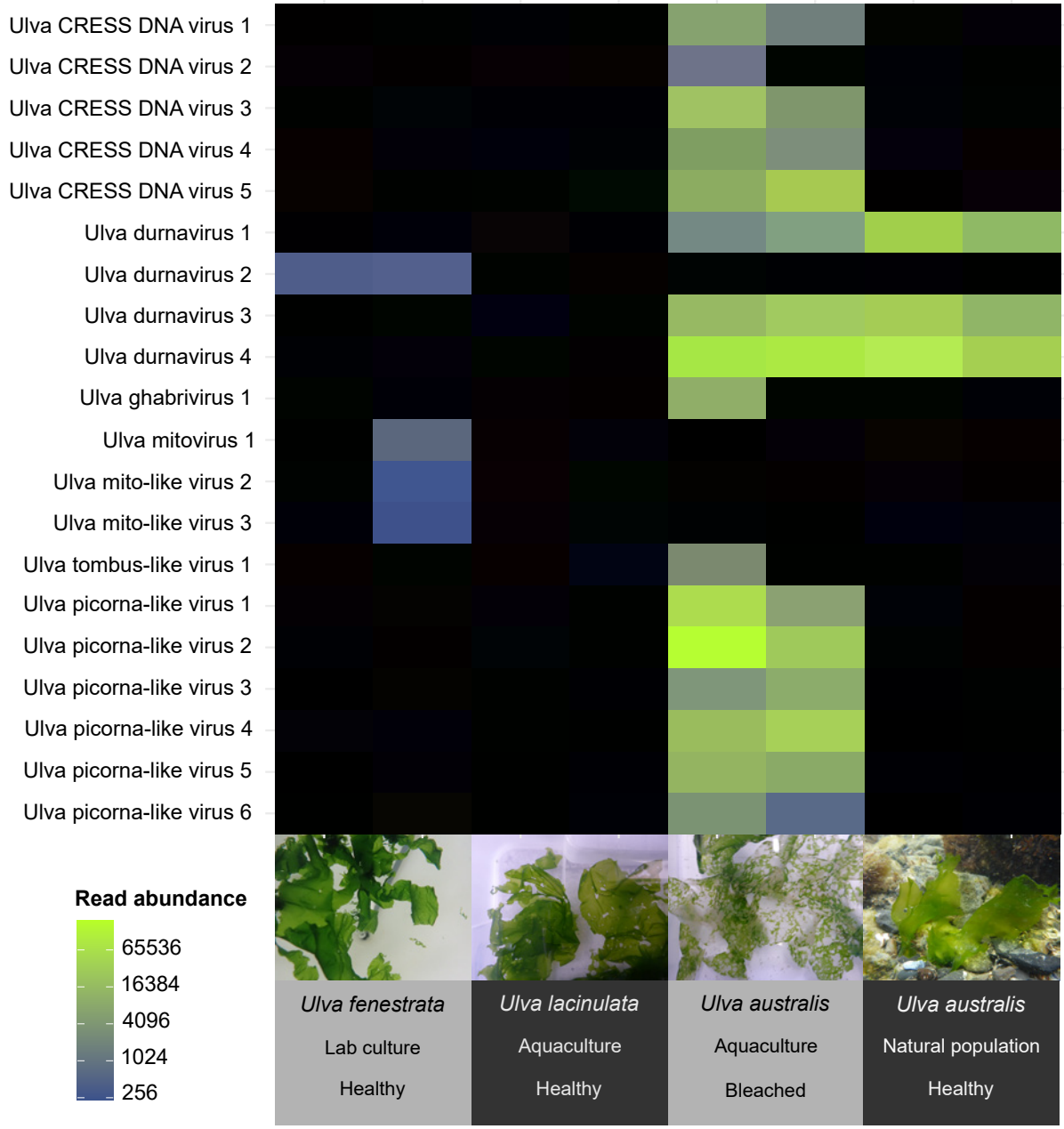

FIGURE S7.01 Heatmap showing normalized read number for the 20 putative new viruses associated with the green seaweed *Ulva*. From each culture or site, 1–2 cm^2 tissue from two different individuals was sampled.

"Beneath our superficial differences we are all of us walking communities of bacteria. The world shimmers, a pointillist landscape made of tiny living beings."

– Lynn Margulis & Dorion Saga, in: 'Microcosmos: Four Billion Years of Microbial Evolution'

Chapter 8.
Synthesis

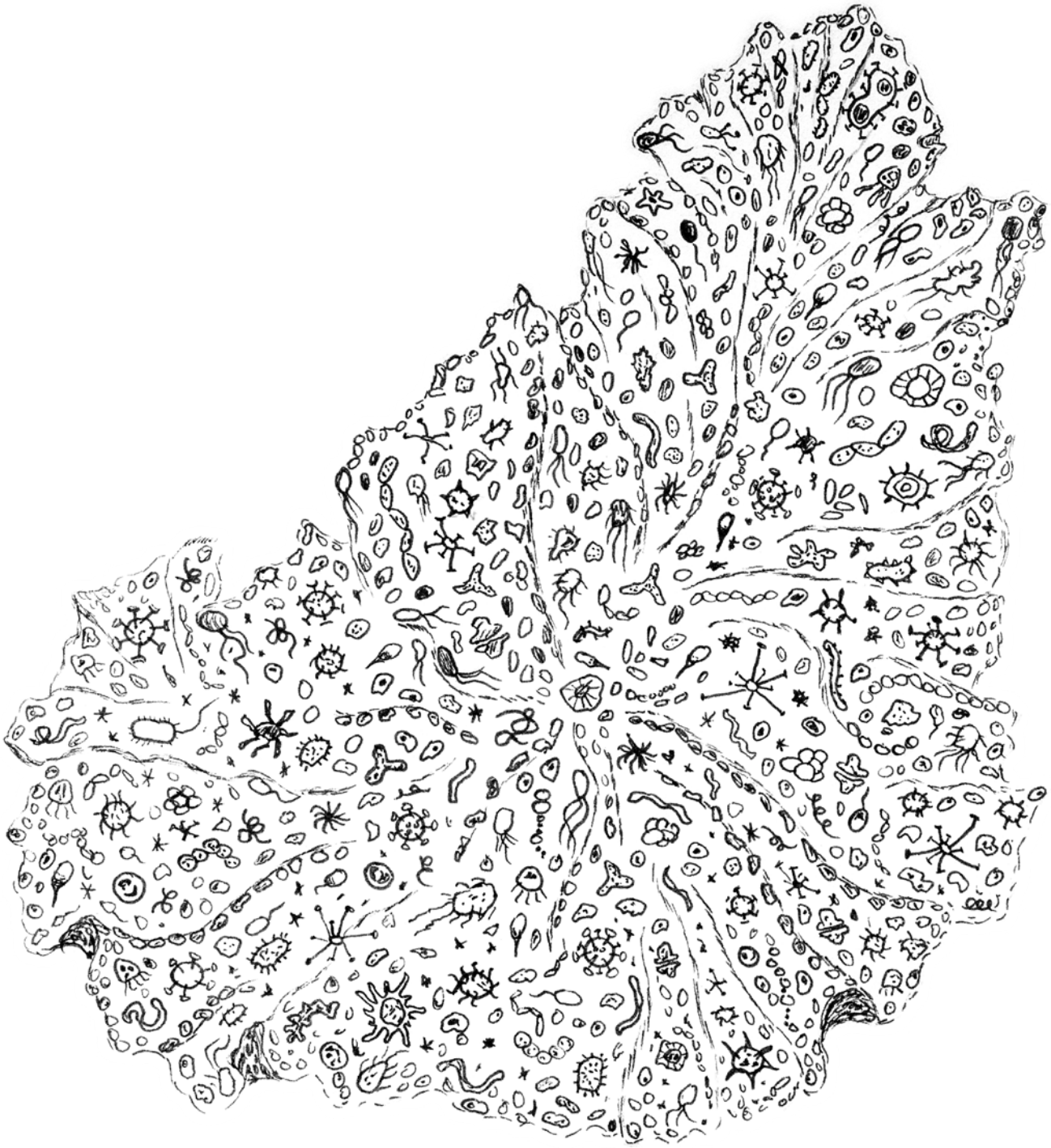

Chapter 8. Synthesis

Studying a seaweed unavoidably also involves studying its microbiome. Seaweeds and their associated microorganisms are inextricably connected, forming a dynamic entity that interacts with an equally dynamic environment. This thesis presents a collection of studies on the microbial communities of the green seaweed *Ulva* in relation to the environment, focusing on salinity as key environmental driver. To study the *Ulva*-microbial dynamics, we combined taxonomic characterisations, functional profiling, whole-genome sequencing, and controlled laboratory experiments. One of our main conclusions is that the environment strongly determines the taxonomic and functional composition of bacterial communities, affecting the ability of bacteria to optimise host performance. Below, we integrate and discuss the results from the individual research chapters in a broader context, highlighting future perspectives.

8.1 Bacteria-mediated acclimation: what we can learn from *Ulva*'s salinity tolerance

The main objective of this thesis was to evaluate the response of the *Ulva* holobiont to environmental change and investigate the potential role of bacteria in assisting the host's acclimatisation to changing conditions. The Atlantic–Baltic Sea salinity gradient provided an excellent environment to study this topic. The environmental gradient extends over 2,000 km of distance and is established by a continuous influx of freshwater into the innermost parts of the Baltic Sea, combined with limited exchange with North Sea water on the Atlantic end. This results in a relatively stable gradient across a large geographical distance that is characterised by high water retention time in the brackish central Baltic (Reusch et al. 2018). *Ulva* species are common in this area and biodiversity is high, with more than 15 species occurring in sympatry (Steinhagen et al. 2023). In addition, *Ulva* species are known for their tolerance to varying salinity conditions (Rybak 2018). Certain species, such as *U. intestinalis* and *U. linza*, demonstrate higher salinity tolerance compared to other species, like *U. fenestrata*, leading to distinct species distribution patterns across the Atlantic–Baltic Sea gradient. Consequently, salinity can be considered a suitable environmental factor to study the acclimation of *Ulva* and its microbiome to the environment.

Our results showed that the taxonomic composition of *Ulva*-associated bacterial communities strongly correlated with salinity (Chapter 4; van der Loos et al., 2022). This is exemplified by the bacterial communities in the vicinity of the Glomma river output (Norway), which were more similar to distant (>1,000 km away) low saline sites in the Baltic Sea than to samples collected at neighbouring sites (20–50 km away) in the North Sea. We also observed changes in the functional composition of the bacterial communities across the salinity gradient (Chapter 5). These included a range of functions that may impact host metabolism and functioning and are likely involved in mitigating oxidative stress and maintaining cellular homeostasis. Finally, we created synthetic bacterial communities representing typical low and high salinity consortia. We used these communities to perform controlled salinity experiments with a low salinity treatment (5 PSU, corresponding to oligohaline and horohaline conditions in the Baltic Sea) and a high salinity treatment (32 PSU, corresponding to euhaline conditions in the North Sea). We found that certain bacteria increased *Ulva fenestrata* growth, but this effect was only visible in low salinity conditions. Overall, if supplied with growth-enhancing bacteria, *Ulva* germling growth was higher in low salinity conditions than in the high salinity treatment. This was surprising, considering that *Ulva fenestrata* in its natural habitat is typically only found in euhaline and polyhaline conditions.

So, what can we learn from *Ulva*'s tolerance to salinity? Even a species considered less tolerant to low salinity levels, demonstrated high tolerance when transitioning from high to low salinity. This leads us to the question whether low salinity indeed represented a stressor for the seaweed. While growth results alone suggest that *U. fenestrata* is not stressed by low salinity, observed changes in morphology and tissue colour indicate potential stress on other aspects of its biology. Unintentionally, we also introduced the effect of another stressor: the use of *Ulva* culture medium in one repetition of the salinity experiment. Although UCM has been optimised for growth of *Ulva mutabilis*, it adversely affected *Ulva fenestrata*, causing very low growth rates in low salinity conditions, even leading to thalli decimation in high salinity conditions. The three growth-promoting strains enabled *U. fenestrata* to overcome UCM-induced stress in low salinity conditions. However, the provided resilience did not extend to the high salinity treatment. Contrary to the hypothesis that the origin of bacteria influences their effectiveness (i.e., bacteria collected from low salinity improving growth in the low salinity treatment, and vice versa), strains collected from both low and high salinity localities showed the capacity to enhance *Ulva* growth in low salinity conditions. Although bacteria can facilitate *Ulva*'s acclimation to the environment, it appears that the environment determines their ability to affect host performance.

Our combined studies and experiments answered several important question in microbial ecology identified by Antwis et al. (2017), linked to the relative contribution of host-associated and environmental factors determining community composition, the amount of functional redundancy across spatial scales, and how microbial communities affect the phenotype of the host. To delve deeper into host–microbe–environment interactions, additional laboratory experiments will be necessary. Future transcriptomic analyses, for example, can indicate which genes are upregulated or downregulated under high and low salinity conditions in both *Ulva* and the synthetic bacterial communities. Such analyses will provide insights into the mechanisms through which growth-promoting bacteria work and how these mechanism are influenced by salinity. Furthermore, testing repeated fluctuations between low and high salinity, in addition to the previous comparison between low and high salinity conditions in Chapter 6, can provide valuable insight into short-term acclimation processes.

Finally, the concept of eco-evolutionary dynamics, which posits that ecology and evolution mutually influence each other and operate within similar time frames, offers a valuable framework for understanding how the environment interacts with the host and the microbial communities (Hairston et al. 2005, Rodríguez-Verdugo et al. 2017). Our results, for example, have highlighted distinct differences in the bacterial communities of closely related hosts. Conducting controlled laboratory experiments with multiple *Ulva* species, including *U. intestinalis* and *U. linza* which naturally occur across the entire salinity range, will provide a better understanding of how the *Ulva* holobiont acclimates to salinity. Likewise, testing whether the beneficial bacterial strains identified in this study evoke consistent growth-promoting effects across various *Ulva* genotypes and considering different life stages (sporophytes and gametophytes) can provide additional insights into the interplay between host genetic diversity and the microbiome. This approach may also explain some of the inter-individual variation that we have observed in the current study. By taking into account eco-evo dynamics we may gain a deeper understanding of why *Ulva* would benefit from outsourcing key abilities to develop, survive, and adapt to environments to bacteria from an evolutionary perspective.

8.2 Monitoring and utilising microbes in aquaculture

Ulva species are gaining increased attention for their potential in seaweed aquaculture (Bolton et al. 2016, Steinhagen et al. 2021b), and microbes may significantly contribute to optimising the cultivation system. This hypothesis is supported by the findings in this thesis, which demonstrated that cultivated *Ulva* harbours a bacterial community that is distinct from its counterparts in natural ecosystems. Observations presented in this thesis include, amongst others, a higher abundance of growth-promoting bacteria in aquaculture-derived samples (Chapter 2; van der Loos et al., 2021), differences in bacterial communities associated with hatchlings in the nursery stage compared to later cultivation stages (Chapter 3), the identification of the nursery environment as an important microbial source pool (Chapter 3), and the capability of specific bacteria to enhance *Ulva* growth (Chapter 6). We therefore conclude that microbiome research can be applied in seaweed aquaculture in two ways: 1) through continuous monitoring of microbial dynamics in aquaculture systems to identify (un-)desirable changes, and 2) through microbiome engineering (i.e., the manipulation and modification of the seaweed-associated microbial communities).

8.2.1 Developing rapid and cost-effective microbiome screening

Monitoring seaweed-associated microbial communities in a cultivation setting can aim to detect microorganisms that are favoured (e.g., microbes that promote seaweed growth or increase protein content) or undesired (e.g., strains that are potentially pathogenic to the seaweed). Such a screening method has to be both rapid and cost-effective. Several aspects have to be taken into consideration when developing a screening method, including the sampling frequency, the number of replicates during each sampling occasion, the detection threshold, and the required level of microbial identification. For instance, 16S rRNA-based sequencing techniques are rapid and relatively cheap, but the resulting taxonomic identifications are typically restricted to genus or, at most, species levels. Given that pathogenic and non-pathogenic strains can belong to the same species (Georgiades and Raoult 2011, Jung et al. 2017), certain applications may require strain-level identifications using metagenomic sequencing.

A wide range of screening methods are available, and the choice of a specific method depends on the detection objectives. In this thesis, we mainly focused on molecular techniques. In Chapter 2, we tested Oxford Nanopore Technologies for 16S-based sequencing and subsequently applied it on a larger scale in Chapter 3 and 4. This long-read sequencing technique is continually evolving in terms of read accuracy and length, sequencing speed, performance in complex genome regions, as well as the advancement of automated library preparation methods and adaptive sequencing (De Meulenaere et al. 2023, MacKenzie and Argyropoulos 2023, Weilguny et al. 2023). Consequently, whole-genome sequencing and metagenomic sequencing are becoming increasingly accessible, as demonstrated in Chapter 6. Buytaers et al. (2021), for example, showed that a toxin-producing *Escherichia coli* strain can be reliably detected in food samples within one hour of MinION metagenomic sequencing or within five hours using the cheaper Flongle flow cell. Other viable screening methods include flow cytometry (De Roy et al. 2012, Props et al. 2016) and MALDI-TOF MS (Ashfaq et al. 2022, Haider et al. 2023). Finally, in the context of introducing beneficial microbes to a closed cultivation setup, screening methods can also verify the inoculation success.

8.2.2 Microbiome engineering

The utilisation of microbes as alternative fertilisers has been extensively investigated in terrestrial agriculture and is now starting to gain interest in seaweed cultivation as well. Within this thesis, we identified three bacterial strains that had a positive effect on *Ulva* growth. To develop effective inoculants, it will be essential to conduct screenings for additional beneficial microbes, particularly for different seaweed species commonly employed in aquaculture.

In addition to screening for growth-promoting microbes, screening efforts should focus on beneficial strains that protect the host against pathogens. For example, several strains have been identified that reduce the risk of bleaching and disease in *Saccharina japonica* (Ma et al. 2023), *Gracilaria vermiculophylla* (J. Li et al. 2022b), and *Pyropia yezoensis* (Weng et al. 2024). Endophytic bacteria and fungi represent a relatively unexplored source of potentially bioactive strains, as demonstrated by Deutsch et al. (2021). They isolated 173 endophytes from 16 seaweed species, of which 88 strains exhibited inhibition of common aquaculture pathogens. Endophytic strains were also identified in *Ulva*, even though these species are only one to two cells thick, and the feasibility of re-inoculating the endophytes was verified using a Green Fluorescent Protein reporter gene (Deutsch et al. 2023).

Finally, seaweed-associated microbes could also protect other organisms from pathogens. An *Ulva*-associated *Phaeobacter* strain, for example, reduced *Vibrio*-induced fish mortality within Integrated Multi-Trophic Aquaculture Recirculation Systems (IMTA-RAS) (Pintado et al. 2023). This shows how microbiome engineering can benefit multiple aquaculture purposes. Before we can effectively use microbiome engineering, however, additional research is needed on a number of topics:

- *What concentration of bacteria yields optimal performance?*
  Supplying an insufficient number of bacterial cells may fail to elicit the desired host response, while an excessively high concentration could prove detrimental. The optimal concentration is likely strain dependent (Mangmang et al. 2015), but is generally estimated to fall within the range of 10^5–10^6 cells/mL (Bashan 1986, Loffredo et al. 2021). This topic closely links to the viability of upscaling to larger aquaculture facilities. In Chapter 6, we investigated the effect of bacterial inoculants on *Ulva* growth on a small cultivation scale (i.e., culture flasks with 17 mL medium). The bacterial concentration of the individual strains varied from 10^5 cells/mL in the monocultures to ~8,300 cells/mL in the 12–species communities. Interestingly, monocultures containing beneficial strains exhibited a larger effect on *Ulva* growth than the 12–species communities (containing the same beneficial strains but in lower concentrations) when utilising UCM, but this was not the case for sterilised seawater. Evaluating the optimal concentration in 10–100 L cultivation tanks will be essential for the upscaling process.
- *Is it necessary to disturb the seaweed biofilm prior to inoculation?*
  This topic is closely connected to the question of how the addition of an inoculum influences the composition and dynamics of pre-existing communities. Competition in bacterial biofilms is high (Song et al. 2023), and the pre-existing microbes may either collaborate with the inoculated bacteria or act antagonistically (J. Li et al. 2022b). Multiple disruption methods have been used in prior research, including antibiotic treatment and mechanic disruptions. In Chapter 6, for example, we used sonication to facilitate strain colonisation of the inoculated microbiota. Various methods, including fluorescence imaging and quantitative PCRs, are available to assess colonisation success. Fluorescence in situ hybridization (FISH), for example, can be used to visualise the distribution of existing communities across the seaweed tissue (Remus-Emsermann et al. 2014, Shi et al. 2020). Moreover, bacterial strains within an inoculum can be genetically engineered to express different fluorescent protein markers, enabling

mapping of spatial interaction patterns between inoculated strains and the host (Germaine et al. 2004, Vergani et al. 2024). These methods can also serve to evaluate priority effects in complex communities, which refer to the importance of order and timing of species arrival during community assembly in shaping community structure (Svoboda et al. 2018, Debray et al. 2022).

- *What factors promote stability of the introduced bacteria within the assembled community?*
  Our findings in Chapter 3 demonstrated the dynamic nature of the seaweed microbiome. In such dynamic community assemblages, merely establishing colonisation of the host does not automatically guarantee the persistence of introduced microbiota in the biofilm over time. To successfully manipulate a seaweed microbiome with lasting effects, it is crucial to evaluate the factors that can facilitate the stability of the biofilm post-inoculation. Generally, stability in microbial communities is enhanced by minimizing positive feedback and weakening ecological interactions (Coyte et al. 2015). High nutrient concentrations, for example, have been shown to create stronger interactions between bacteria, leading to decreased stability and loss of biodiversity, whereas low nutrient concentrations increased stability and co-existence (Ratzke et al. 2020).
- *When is the optimal time to introduce an inoculum?*
  Our results suggested that the introduction of bacteria had the most pronounced impact on germlings, particularly under nursery conditions. Previous research on plants likewise indicated that inoculation during early life stages yielded larger response (Bashan 1986, Sohn et al. 2003). Given that *Ulva* individuals do not inherit the microbiome from their parents through vertical transmission (Syukur et al. 2023), the benefits of inoculation may be realized as early as the gamete/zoospore phase. Re-inoculation may also be necessary throughout the cultivation period.
- *Which cellular and genetic mechanisms drive the beneficial effect of bacteria?*
  Although it is established that certain bacteria enhance seaweed growth, the underlying mechanisms remain unknown. Microbes hold the potential to supply the host with essential vitamins and amino acids, produce morphogens, or alter the dynamics of host–microbial interactions. However, our understanding of the genetic responses triggered in host cells by these microbial products is limited, and confirming causative relationships proves challenging. To address this issue, genome-wide comparisons can be used to identify complementarity between the host and selected microbial strains (Burgunter-Delamare et al. 2020). Additionally, techniques such as isotope labelling and fluorescent probing, combined with gene expression analyses, can confirm the uptake of bacterial-derived compounds by the host and vice versa (Lawrence et al. 2018, Ferrier-Pagès et al. 2021).
- *What potential drawbacks and ethical considerations should be considered?*
  The potential benefits of microbial engineering are substantial, but microbiome engineering may also have its drawbacks. Unintended consequences, including unpredictable changes in the microbial community and host functioning, may arise. Long-term effects are not fully understood, and microbes may develop resistance or adapt to engineered interventions, potentially diminishing the effectiveness over time. Extreme caution is necessary when non-native microbes could be introduced into the natural environment. It is recommended to prioritize working with native microbial strains and to apply microbiome engineering solely in closed-systems, such as land-based cultivation or nursery conditions. Finally, it is important to keep in mind that seaweed cultivation alone cannot and should not be the solution to all our problems. While increasing the productivity and quality of seaweed crops offers many advantages, these improvements should not come at the expense of ecosystem functioning. The holobiont concept encourages us to adopt a holistic point of view — both at microscopic and macroscopic level.

8.3 Perspectives beyond bacteria

It is without doubt that bacteria are essential to a thriving *Ulva*. With the strong focus on algal–bacterial interactions, it is easy to forget that the seaweed microbiome encompasses a multitude of additional microorganisms. Seaweed-associated viruses, fungi, protozoa, oomycetes, and archaea are very diverse but remain notably understudied. Many fundamental questions still need answering: what species of microbes are associated with *Ulva* and seaweeds in general? To what extent do these microbes exhibit host specificity and biogeography? Are there fluctuations in their abundance corresponding to seasons or environmental conditions? Can we cultivate these as-yet-unidentified microorganisms? Acquiring such fundamental knowledge is imperative before we can explore their role in seaweed symbioses and assess how they affect seaweed physiology and ecology.

8.3.1 Viruses

In Chapter 7 (van der Loos et al. 2023), we presented a first characterisation of the *Ulva* virome. Although based on a limited number of samples derived from *Ulva* culture collections and natural ecosystem, we identified 20 putative new and divergent viruses. The majority of these novel viruses belonged to undescribed families, showing that we have only uncovered the tip of the iceberg regarding seaweed-associated viral biodiversity in marine systems. If anything, our results highlighted the significant gaps in our understanding of the diversity and ecology of seaweed viruses, particularly in the context of their symbiotic relationship with the algal host.

Our analyses focused on viruses possibly infecting the algal host — especially in relation to the bleached phenotype of an *Ulva australis* culture — but our dataset also included over 3.6 million reads assigned to bacteriophages. These viruses specifically target and kill bacteria and are likely the most abundant entities on earth (Duckworth 1976, Clokie et al. 2011). We assembled 37 near-complete (>90%) bacteriophage genomes associated with the *Ulva* biofilm, adding another layer of complexity to *Ulva*-bacterial interactions. Phage species often infect a small range of bacterial strains and the identified bacteriophages in our dataset included multiple phages specifically infecting, amongst others, *Alteromonas*, *Cellulophaga*, *Loktanella*, *Nonlabens*, *Polaribacter*, *Roseobacter*, *Roseovarius*, *Ruegeria*, and *Sulfitobacter*. The bacteria that are infected by these phages are well-known symbiotic partners of the *Ulva* biofilm and some play a pivotal role in *Ulva* growth and morphogenesis.

The interactions between phages and bacteria within biofilms are complex and diverse. Phages are not merely killing machines of bacteria, but can also promote biofilm formation and establish symbiotic relationships (Pires et al. 2021). The induction of prophages into the lytic cycle has, for example, been found to stimulate the release of biofilm-promoting molecules by bacteria (Carrolo et al. 2010, Gödeke et al. 2011). Furthermore, phages serve as sources of genetic innovation by encoding accessory genes and act as vectors of horizontal gene transfer (Wendling 2023). They can exert selective pressure and drive rapid mutation in bacteria (Fernández et al. 2018). In addition, virulent phages play a role in suppressing the most common bacteria, thereby maintaining bacterial diversity. Through these mechanisms, phages can shape the taxonomic and functional composition of bacterial communities (Chevallereau et al. 2022). Higher order interactions, wherein phages affect the nature of the interaction between bacteria and the seaweed host, may play a more important role in the seaweed holobiont than we currently know. The intricate relationships between phages, bacteria, and seaweed in biofilms offer a wide-open road and unexplored terrain for further exploration and discovery.

8.3.2 Fungi and oomycetes

Fungi and oomycetes are predominantly known for their parasitic roles in seaweed microbiomes. The fungal endophytes *Haloguignardia* and *Massarina*, for example, induce gall formation in brown algae (Apt 1988, Harvey and Goff 2010) and oomycetes of the genus *Pythium* are notorious for causing red rot disease in the commercially important red algae *Porphyra* and *Pyropia* (Park et al. 2000). A single *Pythium* strain has been isolated from a filamentous *Ulva* in the Oslo fjord in Norway and was shown to infect *U. intestinalis* at a salinity of 0, 15 and 30 PSU. While the infection did not progress beyond two weeks at salinity levels of 15 and 30 PSU, the mycelium completely killed its host at 0 PSU (Herrero et al. 2020). It is unknown whether the *Pythium* strain can also infect foliose *Ulva* species and whether this could affect their distribution at lower salinity.

To date, only a handful of fungi have been isolated from *Ulva* tissue, including *Neptunomuces aureus* (Gonçalves et al. 2019, 2020) and *Ascochyta salicorniae* (Osterhage et al. 2000), but these have not been linked to diseases or changes in morphology. An exception is the fungal symbiont *Turgidosculum ulvae*, which causes the formation of dark spots in *Blidingia minima* (a species closely related to the genus *Ulva* and morphologically very similar) (Kohlmeyer and Volkmann-Kohlmeyer 2003). Interestingly, the symbiosis with this fungus appears to benefit the host by significantly reducing grazing pressure from predatory gastropods, illustrating that algal-fungal interactions can be mutualistic as well (Cubit 1975).

Novel interactions between fungi and seaweeds continue to be discovered. Seaweed-isolated fungi have, for example, demonstrated the capacity to degrade algal polymers (Patyshakuliyeva et al. 2019). Our functional profile results (Chapter 5) revealed that an *Ulva*-associated bacterial community is characterised by its ability to degrade the host's cell walls. This principle might extend to the mycobiota of seaweeds. Furthermore, sequencing results have indicated that the fungal diversity associated with *Ulva* is very high (Agusman and Danqing 2017), with many of these fungi exhibiting inhibitory effects on bacterial growth (Rahaweman et al. 2016, Parthasarathy et al. 2020). Similar to viruses, fungi and oomycetes are likely to influence *Ulva*–bacterial dynamics as well directly impact the seaweed host.

8.3.3 Moving forwards with friends and foes

The recent rapid advances in (meta)genomic and (meta)transcriptomic research have significantly improved our understanding of the abundance and taxonomic diversity of microorganisms associated with a range of eukaryotic hosts (Gibb et al. 2021, Nelson et al. 2021). While exploratory and descriptive studies are of great importance for uncovering unexplored microorganisms on a large scale, the nature of such datasets does not allow the establishment of causal relationships. In seaweed–microbial research, bacteria stand out as an exception having progressed to controlled laboratory experiments, while research on other groups of microorganisms remains predominantly in the descriptive stage. To transition from addressing the question of 'who is there?' to 'what role do they play in seaweed ecology?', we need to move beyond descriptive studies. This will require the isolation of many microorganisms, the establishment of culture collections, and the assignment of biological reference material to newly described species (Nissimov et al. 2022). Such efforts are particularly important in the context of algal diseases, which are expected to become more prevalent in the future with growing aquaculture and environmental change (Gachon et al. 2010, Murúa et al. 2023). Future research should therefore also study how the seaweed host reacts to a (pathogenic) infection from a molecular point of view (e.g., focusing on the signalling pathways that are activated upon infection and throughout the disease). It is clear that a wealth of seaweed-associated microorganisms and symbiotic relationships remain to be discovered, if we look beyond bacteria.

8.4 Future perspectives: the seaweed holobiont in a changing ocean

This PhD thesis focused on the interactions between the seaweed holobiont and its environment, emphasising the role of salinity. Salinity, however, represents only one of many environmental parameters influencing the seaweed holobiont. Rising seawater temperatures, ocean acidification, oxygen depletion, increased frequency of green tides, eutrophication: anthropogenically induced stressors are anticipated to expose the seaweed holobiont to an array of climate changes in the near future. The manner in which a changing ocean will lead to alterations in the seaweed holobiont — along with subsequent cascading effects on the ecosystem — largely remains an unanswered question. This uncertainty leads to many additional questions with respect to resilience of microbial communities in the face of ecosystem disturbances and whether microbial communities can be used for restoration purposes.

To answer these questions, we need to progress beyond mere correlations and work towards establishing causative relationships and developing predictive models that advance our understanding of holobiont dynamics (Antwis et al. 2017). Achieving this goal will require the integration of -omics data output, including metagenomics, transcriptomics, metabolomics, and proteomics (Khan et al. 2023, Lin 2023). Moreover, new techniques in microbiome research are continually developed. Examples of the last years include spatial metatranscriptomics (Minton 2023), single cell analysis (Sharma and Thaiss 2020), genome engineering and genetic manipulation (Blomme et al. 2021, Chen et al. 2023), and protein sequencing (Wang et al. 2023). These emerging platforms will provide a robust toolkit to unravel the complex facets of host–microbiome research in the context of climate change.

References

Abdoulaye, A.H., Foda, M.F. & Kotta-loizou, I. 2019. Viruses infecting the plant pathogenic fungus *Rhizoctonia solani*. *Viruses*. 11:113.

Adair, K.L. & Douglas, A.E. 2017. Making a microbiome: the many determinants of host-associated microbial community composition. *Curr. Opin. Microbiol.* 35:23–29.

Agarwala, R., Barrett, T., Beck, J., Benson, D.A., Bollin, C., Bolton, E., Bourexis, D. et al. 2018. Database resources of the National Center for Biotechnology Information. *Nucleic Acids Res.* 46:D8–13.

Agler, M.T., Ruhe, J., Kroll, S., Morhenn, C., Kim, S.T., Weigel, D. & Kemen, E.M. 2016. Microbial hub taxa link host and abiotic factors to plant microbiome variation. *PLoS Biol.* 14:1–31.

Agmo Hernández, V., Eriksson, E.K. & Edwards, K. 2015. Ubiquinone-10 alters mechanical properties and increases stability of phospholipid membranes. *Biochim. Biophys. Acta BBA - Biomembr.* 1848:2233–2243.

Agusman, A. & Danqing, F. 2017. Fungal community structure of macroalga *Ulva intestinalis* revealed by MiSeq sequencing. *Squalen Bull. Mar. Fish. Postharvest Biotechnol.* 12:99.

Ainsworth, T.D., Krause, L., Bridge, T., Torda, G., Raina, J.B., Zakrzewski, M., Gates, R.D. et al. 2015. The coral core microbiome identifies rare bacterial taxa as ubiquitous endosymbionts. *ISME J.* 9:2261–2274.

Aires, T., Moalic, Y., Serrao, E.A. & Arnaud-Haond, S. 2015. Hologenome theory supported by cooccurrence networks of Species-specific bacterial communities in siphonous algae (*Caulerpa*). *FEMS Microbiol. Ecol.* 91:1–14.

Aires, T., Muyzer, G., Serrão, E.A. & Engelen, A.H. 2019. Seaweed loads cause stronger bacterial community shifts in coastal lagoon sediments than nutrient loads. *Front. Microbiol.* 10:1–18.

Al-Hafedh, Y.S., Alam, A. & Buschmann, A.H. 2015. Bioremediation potential, growth and biomass yield of the green seaweed, *Ulva lactuca* in an integrated marine aquaculture system at the Red Sea coast of Saudi Arabia at different stocking densities and effluent flow rates. *Rev. Aquac.* 7:161–171.

Alsufyani, T., Califano, G., Deicke, M., Grueneberg, J., Weiss, A., Engelen, A.H., Kwantes, M. et al. 2020. Macroalgal-bacterial interactions: Identification and role of thallusin in morphogenesis of the seaweed *Ulva* (Chlorophyta). *J. Exp. Bot.* 71:3340–3330.

Alsufyani, T., Engelen, A.H., Diekmann, O.E., Kuegler, S. & Wichard, T. 2014. Prevalence and mechanism of polyunsaturated aldehydes production in the green tide forming macroalgal genus *Ulva* (Ulvales, Chlorophyta). *Chem. Phys. Lipids*. 183:100–109.

Altschul, S.F., Gish, W., Miller, W., Myers, E.W. & Lipman, D.J. 1990. Basic local alignment search tool. *J. Mol. Biol.* 215:403–410.

Alves, A.S., Adão, H., Patrício, J., Neto, J.M., Costa, M.J. & Marques, J.C. 2009. Spatial distribution of subtidal meiobenthos along estuarine gradients in two southern European estuaries (Portugal). *J. Mar. Biol. Assoc. U. K.* 89:1529–1540.

Amin, S.A., Hmelo, L.R., van Tol, H.M., Durham, B.P., Carlson, L.T., Heal, K.R., Morales, R.L. et al. 2015. Interaction and signalling between a cosmopolitan phytoplankton and associated bacteria. *Nature*. 522:98–101.

Anderson, M.J. 2017. Permutational Multivariate Analysis of Variance (PERMANOVA). *Wiley StatsRef Stat. Ref. Online*. 1–15.

Anderson, R.J., Monteiro, P.M.S. & Levitt, G.J. 1996. The effect of localised eutrophication on competition between *Ulva lactuca* (Ulvaceae, Chlorophyta) and a commercial resource of *Gracilaria verrucosa* (Gracilariaceae, Rhodophyta). *In Hydrobiologia*. pp. 291–296.

Andersson, A.F., Riemann, L. & Bertilsson, S. 2010. Pyrosequencing reveals contrasting seasonal dynamics of taxa within Baltic Sea bacterioplankton communities. *ISME J.* 4:171–181.

Antwis, R.E., Griffiths, S.M., Harrison, X.A., Aranega-Bou, P., Arce, A., Bettridge, A.S., Brailsford, F.L. et al. 2017. Fifty important research questions in microbial ecology. *FEMS Microbiol. Ecol.* 93:10.1093/femsec/fix044.

Appeltans, W., Ahyong, S.T., Anderson, G., Angel, M.V., Artois, T., Bailly, N., Bamber, R. et al. 2012. The magnitude of global marine species diversity. *Curr. Biol.* 22:2189–2202.

Apt, K. 1988. Galls and tumor-like growths on marine macroalgae. *Dis. Aquat. Organ.* 4:211–217.

Arnaud-Haond, S., Aires, T., Candeias, R., Teixeira, S.J.L., Duarte, C.M., Valero, M. & Serrão, E.A. 2017. Entangled fates of holobiont genomes during invasion: nested bacterial and host diversities in *Caulerpa taxifolia*. *Mol. Ecol.* 26:2379–2391.

Ashfaq, M.Y., Da'na, D.A. & Al-Ghouti, M.A. 2022. Application of MALDI-TOF MS for identification of environmental bacteria: A review. *J. Environ. Manage.* 305:114359.

Ashrafuzzaman, M., Hossen, F.A., Ismail, M.R., Hoque, A., Zahurul, M., Shahidullah, S.M. & Meon, S. 2009. Efficiency of plant growth-promoting rhizobacteria (PGPR) for the enhancement of rice growth. 8:1247–1252.

Baedke, J., Tejeda, A.F. & Delgado, A.N. 2020. The holobiont concept before Margulis. *JEZ-B* 334:149–155.

Balar, N.B. & Mantri, V.A. 2020. Insights into life cycle patterns, spore formation, induction of reproduction, biochemical and molecular aspects of sporulation in green algal genus *Ulva*: Implications for commercial cultivation. *J. Appl. Phycol.* 32:473–484.

Barakat, K.M., El-Sayed, H.S., Khairy, H.M., El-Sheikh, M.A., Al-Rashed, S.A., Arif, I.A. & Elshobary, M.E. 2021. Effects of ocean acidification on the growth and biochemical composition of a green alga (*Ulva fasciata*) and its associated microbiota. *Saudi J. Biol. Sci.* 28:5106–5114.

Bar-Even, A. 2016. Formate assimilation: the metabolic architecture of natural and synthetic pathways. *Biochemistry*. 55:3851–3863.

Barott, K.L., Rodriguez-Brito, B., Janouškovec, J., Marhaver, K.L., Smith, J.E., Keeling, P. & Rohwer, F.L. 2011. Microbial diversity associated with four functional groups of benthic reef algae and the reef-building coral *Montastraea annularis*. *Environ. Microbiol.* 13:1192–204.

Bashan, Y. 1986. Significance of timing and level of inoculation with rhizosphere bacteria on wheat plants. *Soil Biol. Biochem.* 18:297–301.

Bates, D., Mächler, M., Bolker, B.M. & Walker, S.C. 2015. Fitting linear mixed-effects models using lme4. *J. Stat. Softw.* 67.

Beattie, D.T., Lachnit, T., Dinsdale, E.A., Thomas, T. & Steinberg, P.D. 2018. Novel ssDNA viruses detected in the virome of

bleached, habitat-forming kelp *Ecklonia radiata*. *Front. Mar. Sci.* 4:1–10.
Beer, S. 2022. Photosynthetic traits of the ubiquitous and prolific macroalga *Ulva* (Chlorophyta): A review. *Eur. J. Phycol.* 4:390–398.
Bell, T., Newman, J.A., Silverman, B.W., Turner, S.L. & Lilley, A.K. 2005. The contribution of species richness and composition to bacterial services. *Nature*. 436:1157–1160.
Bengtsson, M.M., Sjøtun, K. & Øvreås, L. 2010. Seasonal dynamics of bacterial biofilms on the kelp *Laminaria hyperborea*. *Aquat. Microb. Ecol.* 60:71–83.
Bengtsson, M.M., Sjøtun, K., Storesund, J.E. & Øvreas, L. 2011. Utilization of kelp-derived carbon sources by kelp surface-associated bacteria. *Aquat. Microb. Ecol.* 62:191–199.
Bentzon-Tilia, M., Sonnenschein, E.C. & Gram, L. 2016. Monitoring and managing microbes in aquaculture – towards a sustainable industry. *Microb. Biotechnol.* 9:576–584.
Berg, G., Kusstatscher, P., Abdelfattah, A., Cernava, T. & Smalla, K. 2021. Microbiome modulation—toward a better understanding of plant microbiome response to microbial inoculants. *Front. Microbiol.* 12:1–12.
Bikker, P., van Krimpen, M.M., van Wikselaar, P., Houweling-Tan, B., Scaccia, N., van Hal, J.W., Huijgen, W.J.J. et al. 2016. Biorefinery of the green seaweed *Ulva lactuca* to produce animal feed, chemicals and biofuels. *J. Appl. Phycol.* 28:3511–3525.
Bleich, S., Powilleit, M., Seifert, T. & Graf, G. 2011. B-diversity as a measure of species turnover along the salinity gradient in the Baltic Sea, and its consistency with the Venice System. *Mar. Ecol. Prog. Ser.* 436:101–118.
Blomme, J., Liu, X., Jacobs, T.B. & De Clerck, O. 2021. A molecular toolkit for the green seaweed *Ulva mutabilis*. *Plant Physiol.* 186:1442–1454.
Blomme, J., Wichard, T., Jacobs, T.B. & De Clerck, O. 2023. *Ulva*: An emerging green seaweed model for systems biology. *J. Phycol.* 59:433–440.
Bolinches, J., Lemos, M.L. & Barja, J.L. 1988. Population dynamics of heterotrophic bacterial communities associated with *Fucus vesiculosus* and *Ulva rigida* in an estuary. *Microb. Ecol.* 15:345–357.
Bolton, J.J., Cyrus, M.D., Brand, M.J., Joubert, M. & Macey, B.M. 2016. Why grow *Ulva*? Its potential role in the future of aquaculture. *Perspect. Phycol.* 3:113–120.
Bolton, J.J., Robertson-Andersson, D.V., Shuuluka, D. & Kandjengo, L. 2009. Growing *Ulva* (Chlorophyta) in integrated systems as a commercial crop for abalone feed in South Africa: A SWOT analysis. *J. Appl. Phycol.* 21:575–583.
Bondoso, J., Balagué, V., Gasol, J.M. & Lage, O.M. 2014. Community composition of the *Planctomycetes* associated with different macroalgae. *FEMS Microbiol. Ecol.* 88:445–456.
Bondoso, J., Godoy-Vitorino, F., Balagué, V., Gasol, J.M., Harder, J. & Lage, O.M. 2017. Epiphytic *Planctomycetes* communities associated with three main groups of macroalgae. *FEMS Microbiol. Ecol.* 93:1–9.
Bonthond, G., Bayer, T., Krueger-Hadfield, S.A., Barboza, F.R., Nakaoka, M., Valero, M., Wang, G. et al. 2020. How do microbiota associated with an invasive seaweed vary across scales? *Mol. Ecol.* 29:2094–2108.
Bonthond, G., Bayer, T., Krueger-Hadfield, S.A., Stärck, N., Wang, G., Nakaoka, M., Künzel, S. et al. 2021. The role of host promiscuity in the invasion process of a seaweed holobiont. *ISME J.* 15:1668–1679.
Bordenstein, S.R. & Theis, K.R. 2015. Host biology in light of the microbiome: Ten principles of holobionts and hologenomes. *PLoS Biol.* 13:1–23.
Boulton, A.J., Marmonier, P. & Sarriquet, P.-E.X. 2007. Hyporheic invertebrate community composition in streams of varying salinity in south-western Australia: diversity peaks at intermediate thresholds. *River Res. Appl.* 23:579–594.
Bray, J. & Curtis, J. 1957. An ordination of the upland forest communities of southern Wisconsin. *Ecol. Monogr.* 27:325–349.
Brock, T.D. & Clyne, J. 1984. Significance of algal excretory products for growth of epilimnetic bacteria. *Appl. Environ. Microbiol.* 47:731–734.
Brodie, J., Williamson, C., Barker, G.L., Walker, R.H., Briscoe, A. & Yallop, M. 2016. Characterising the microbiome of *Corallina officinalis*, a dominant calcified intertidal red alga. *FEMS Microbiol. Ecol.* 92:1–12.
Brum, J.R., Schenck, R.O. & Sullivan, M.B. 2013. Global morphological analysis of marine viruses shows minimal regional variation and dominance of non-tailed viruses. *ISME J.* 7:1738–1751.
Brussaard, C.P.D. 2004. Viral control of phytoplankton populations - a review. *J. Eukaryot. Microbiol.* 51:125–138.
Buchfink, B., Xie, C. & Huson, D.H. 2014. Fast and sensitive protein alignment using DIAMOND. *Nat. Methods*. 12:59–60.
Buchholz, C.M., Krause, G. & Buck, B.H. 2012. Seaweed and Man. *In* Wiencke, C. & Bischof, K. [Eds.] *Seaweed Biology*. Springer Berlin Heidelberg, Berlin, Heidelberg, pp. 471–493.
Buck, B.H. & Shpigel, M. 2023. ULVA: Tomorrow's "Wheat of the sea", a model for an innovative mariculture. *J. Appl. Phycol.* 35:1067–1970.
Burgunter-Delamare, B., Boyen, C. & Dittami, S.M. 2021. Effect of essential oil- and iodine treatments on the bacterial microbiota of the brown alga *Ectocarpus siliculosus*. *J. Appl. Phycol.* 33:459–470.
Burgunter-Delamare, B., KleinJan, H., Frioux, C., Fremy, E., Wagner, M., Corre, E., Le Salver, A. et al. 2020. Metabolic complementarity between a brown alga and associated cultivable bacteria provide indications of beneficial interactions. *Front. Mar. Sci.* 7:10.3389/fmars.2020.00085.
Burgunter-Delamare, B., Rousvoal, S., Legeay, E., Tanguy, G., Fredriksen, S., Boyen, C. & Dittami, S.M. 2023. The *Saccharina latissima* microbiome: Effects of region, season, and physiology. *Front. Microbiol.* 13:1050939.
Burke, C., Steinberg, P., Rusch, D., Kjelleberg, S. & Thomas, T. 2011a. Bacterial community assembly based on functional genes rather than species. *Proc. Natl. Acad. Sci. U.S.A.* 108:14288–14293.
Burke, C., Thomas, T., Lewis, M., Steinberg, P. & Kjelleberg, S. 2011b. Composition, uniqueness and variability of the epiphytic bacterial community of the green alga *Ulva australis*. *ISME J.* 5:590–600.
Bushnell, B. 2019. BBTools https://sourceforge.net/projects/bbmap/.
Buytaers, F.E., Saltykova, A., Denayer, S., Verhaegen, B., Vanneste, K., Roosens, N.H.C., Piérard, D. et al. 2021. Towards real-time and affordable strain-level metagenomics-based foodborne outbreak investigations using Oxford

Nanopore sequencing technologies. *Front. Microbiol.* 12:738284.
Cai, J., Lovatelli, A., Gamarro, E.G., Geehan, J., Lucente, D., Mair, G., Miao, W. et al. 2021. Seaweeds and microalgae: an overview for unlocking their potential in global aquaculture development. FAO Fisheries and Aquaculture Circular.
Calegario, G., Freitas, L., Appolinario, L.R., Venas, T., Arruda, T., Otsuki, K., Masi, B. et al. 2020. Conserved rhodolith microbiomes across environmental gradients of the Great Amazon Reef. *Sci. Total Environ.* 760:143411.
Califano, G., Kwantes, M., Abreu, M.H., Costa, R. & Wichard, T. 2020. Cultivating the macroalgal holobiont: Effects of Integrated Multi-Trophic Aquaculture on the microbiome of *Ulva rigida* (Chlorophyta). *Front. Mar. Sci.* 7: 10.3389.
Califano, G. & Wichard, T. 2018. Preparation of axenic cultures in *Ulva* (Chlorophyta). *In Protocols for Macroalgae Research*. Taylor & Francis, Boca Raton, Florida.
Cantarel, B.L., Coutinho, P.M., Rancurel, C., Bernard, T., Lombard, V. & Henrissat, B. 2009. The Carbohydrate-Active EnZymes database (CAZy): An expert resource for Glycogenomics. *Nucleic Acids Res.* 37:D233–8.
Capella-Gutiérrez, S., Silla-Martínez, J.M. & Gabaldón, T. 2009. trimAl: A tool for automated alignment trimming in large-scale phylogenetic analyses. *Bioinformatics*. 25:1972–1973.
Cardoso, I., Meißner, A., Sawicki, A., Bartsch, I., Valentin, K.-U., Steinhagen, S., Buck, B.H. et al. 2023. Salinity as a tool for strain selection in recirculating land-based production of *Ulva* spp. from germlings to adults. *J. Appl. Phycol* 35:1971–1986.
Carl, C., De Nys, R. & Paul, N.A. 2014. The seeding and cultivation of a tropical species of filamentous *Ulva* for algal biomass production. *PLoS ONE*. 9:e98700.
Carradec, Q., Poulain, J., Boissin, E., Hume, B.C.C., Voolstra, C.R., Ziegler, M., Engelen, S. et al. 2020. A framework for in situ molecular characterization of coral holobionts using Nanopore sequencing. *Sci. Rep.* 10:1–10.
Carrolo, M., Frias, M.J., Pinto, F.R., Melo-Cristino, J. & Ramirez, M. 2010. Prophage spontaneous activation promotes dna release enhancing biofilm formation in *Streptococcus pneumoniae*. *PLoS ONE*. 5:e15678.
Carugati, L., Corinaldesi, C., Dell'Anno, A. & Danovaro, R. 2015. Metagenetic tools for the census of marine meiofaunal biodiversity: An overview. *Mar. Genomics*. 24:11–20.
Cavalcanti, G.S., Shukla, P., Morris, M., Ribeiro, B., Foley, M., Doane, M.P., Thompson, C.C. et al. 2018. Rhodoliths holobionts in a changing ocean: Host-microbes interactions mediate coralline algae resilience under ocean acidification. *BMC Genomics*. 19:1–13.
Celepli, N., Sundh, J., Ekman, M., Dupont, C.L., Yooseph, S., Bergman, B. & Ininbergs, K. 2017. Meta-omic analyses of Baltic Sea cyanobacteria: diversity, community structure and salt acclimation. *Environ. Microbiol.* 19:673–686.
Charlier, R.H., Morand, P. & Finkl, C.W. 2008. How Brittany and Florida coasts cope with green tides. *Int. J. Environ. Stud.* 65:191–208.
Charlier, R.H., Morand, P., Finkl, C.W. & Thys, A. 2007. Green tides on the Brittany coasts. *Environ. Res. Eng. Manag.* 3:52–59.
Charon, J., Marcelino, V.R., Wetherbee, R., Verbruggen, H. & Holmes, E.C. 2020. Meta-transcriptomic detection of diverse and divergent RNA viruses in green and chlorarachniophyte algae. *Viruses*. 12:1180.
Charon, J., Murray, S. & Holmes, E.C. 2021. Revealing RNA virus diversity and evolution in unicellular algae transcriptomes. *Virus Evol.* 7:1–18.
Chen, L., Feng, J. & Xie, S. 2015. *Ulva shanxiensis* (Ulvaceae), a new species from Shanxi, China. *Novon J. Bot. Nomencl.* 23:397–405.
Chen, X., Hai, D., Li, J., Tan, J., Huang, S., Zhang, H., Chen, H. et al. 2021. Complete genome sequence of a novel mitovirus associated with *Lagenaria siceraria*. *Arch. Virol.* 166:3427–3431.
Chen, Z., Jin, W., Hoover, A., Chao, Y. & Ma, Y. 2023. Decoding the microbiome: Advances in genetic manipulation for gut bacteria. *Trends Microbiol.* 31:1143–1161.
Chen, Z., Liu, M., Yang, Y., Bi, M., Li, M. & Liu, W. 2022. Environmental and economic impacts of different disposal options for *Ulva prolifera* green tide in the Yellow Sea, China. *ACS Sustain. Chem. Eng.* 10:11483–11492.
Chevallereau, A., Pons, B.J., Van Houte, S. & Westra, E.R. 2022. Interactions between bacterial and phage communities in natural environments. *Nat. Rev. Microbiol.* 20:49–62.
Chiba, S., Castón, J.R., Ghabrial, S.A. & Suzuki, N. 2018. ICTV virus taxonomy profile: Quadriviridae. *J. Gen. Virol.* 99:1480–1481.
Chiba, Y., Tomaru, Y., Shimabukuro, H., Kimura, K., Hirai, M., Takaki, Y., Hagiwara, D. et al. 2020. Viral RNA genomes identified from marine macroalgae and a diatom. *Microbes Environ.* 35:ME20016.
Chopin, T. & Tacon, A.G.J. 2021. Importance of seaweeds and extractive species in global aquaculture production. *Rev. Fish. Sci. Aquac.* 29:139–148.
Clifford, E.L., Varela, M.M., De Corte, D., Bode, A., Ortiz, V., Herndl, G.J. & Sintes, E. 2019. Taurine is a major carbon and energy source for marine prokaryotes in the North Atlantic ocean off the Iberian peninsula. *Microb. Ecol.* 78:299–312.
Clokie, M.R.J., Millard, A.D., Letarov, A.V. & Heaphy, S. 2011. Phages in nature. *Bacteriophage*. 1:31–45.
Cobbin, J.C., Charon, J., Harvey, E., Holmes, E.C. & Mahar, J.E. 2021. Current challenges to virus discovery by meta-transcriptomics. *Curr. Opin. Virol.* 51:48–55.
Cole, J.J. 1982. Interactions between bacteria and algae in aquatic ecosystems. *Annu. Rev. Ecol. Syst.* 13:291–314.
Collins, F.S., Morgan, M. & Patrinos, A. 2003. The Human Genome Project: Lessons from large-scale biology. *Science*. 300:286–290.
Comba González, N.B., Niño Corredor, A.N., López Kleine, L. & Montoya Castaño, D. 2021. Temporal changes of the epiphytic bacteria community from the marine macroalga *Ulva lactuca* (Santa Marta, Colombian-Caribbean). *Curr. Microbiol.* 78:534–543.
Conceição-Neto, N., Zeller, M., Lefrère, H., De Bruyn, P., Beller, L., Deboutte, W., Yinda, C.K. et al. 2015. Modular approach to customise sample preparation procedures for viral metagenomics: A reproducible protocol for virome analysis. *Sci. Rep.* 5:1–14.
Copertino, M.D.S., Tormena, T. & Seeliger, U. 2009. Biofiltering efficiency, uptake and assimilation rates of *Ulva clathrata*

(Roth) J. Agardh (Clorophyceae) cultivated in shrimp aquaculture waste water. *J. Appl. Phycol.* 21:31–45.
Cotas, J., Gomes, L., Pacheco, D. & Pereira, L. 2023. Ecosystem services provided by seaweeds. *Hydrobiology*. 2:75–96.
Cottier-Cook, E.J., Cabarubias, J.P., Brakel, J., Brodie, J., Buschmann, A.H., Campbell, I., Critchley, A.T. et al. 2022. A new progressive management pathway for improving seaweed biosecurity. *Nat. Commun.* 13:7401.
Coyte, K.Z., Rao, C., Rakoff-Nahoum, S. & Foster, K.R. 2021. Ecological rules for the assembly of microbiome communities. *PLOS Biol.* 19:e3001116.
Coyte, K.Z., Schluter, J. & Foster, K.R. 2015. The ecology of the microbiome: Networks, competition, and stability. *Science*. 350:663–666.
Croft, M.T., Lawrence, A.D., Raux-Deery, E., Warren, M.J. & Smith, A.G. 2005. Algae acquire vitamin B_{12} through a symbiotic relationship with bacteria. *Nature*. 438:90–93.
Croft, M.T., Warren, M.J. & Smith, A.G. 2006. Algae need their vitamins. *Eukaryot. Cell*. 5:1175–1183.
Cubit, J. 1975. Interaction of seasonally changing physical factors and grazing affecting high intertidal communities on a rocky shore. PhD thesis. University of Oregon, Oregon.
Cumsille, A., Durán, R.E., Rodríguez-Delherbe, A., Saona-Urmeneta, V., Cámara, B., Seeger, M., Araya, M. et al. 2023. GenoVi, an open-source automated circular genome visualizer for bacteria and archaea. *PLOS Comput. Biol.* 19:e1010998.
Curren, E., Yoshida, T., Kuwahara, V.S. & Leong, S.C.Y. 2019. Rapid profiling of tropical marine cyanobacterial communities. *Reg. Stud. Mar. Sci.* 25:100485.
Dai, C. & Wang, S. 2022. The structure and function of the *Sargassum fusiforme* microbiome under different conditions. *J. Mar. Sci. Eng.* 10:1401.
Davis, K.M., Zeinert, L., Byrne, A., Davis, J., Roemer, C., Wright, M. & Parfrey, L.W. 2023. Successional dynamics of the cultivated kelp microbiome. *J. Phycol.* 59:538–551.
De Clerck, O., Kao, S.M., Bogaert, K.A., Blomme, J., Foflonker, F., Kwantes, M., Vancaester, E. et al. 2018. Insights into the evolution of multicellularity from the sea lettuce genome. *Curr. Biol.* 28:2921-2933.
De Coster, W., D'Hert, S., Schultz, D.T., Cruts, M. & Van Broeckhoven, C. 2018. NanoPack: Visualizing and processing long-read sequencing data. *Bioinformatics*. 34:2666–2669.
De Fouw, J., Govers, L.L., Van De Koppel, J., Van Belzen, J., Dorigo, W., Sidi Cheikh, M.A., Christianen, M.J.A. et al. 2016. Drought, mutualism breakdown, and landscape-scale degradation of seagrass beds. *Curr. Biol.* 26:1051–1056.
De Meulenaere, K., Cuypers, W.L., Gauglitz, J.M., Guetens, P., Rosanas-Urgell, A., Laukens, K. & Cuypers, B. 2023. Selective whole-genome sequencing of *Plasmodium* parasites directly from blood samples by nanopore adaptive sampling. *mBio*. e01967-23.
De Roy, K., Clement, L., Thas, O., Wang, Y. & Boon, N. 2012. Flow cytometry for fast microbial community fingerprinting. *Water Res.* 46:907–919.
Deamer, D., Akeson, M. & Branton, D. 2016. Three decades of Nanopore sequencing. *Nat. Publ. Group*. 34:518–524.
Debray, R., Herbert, R.A., Jaffe, A.L., Crits-Christoph, A., Power, M.E. & Koskella, B. 2022. Priority effects in microbiome assembly. *Nat. Rev. Microbiol.* 20:109–121.
del Campo, E., Ramazanov, Z., Garcia-Reina, G. & Müller, D.G. 1997. Photosynthetic responses and growth performance of virus-infected and noninfected *Ectocarpus siliculosus* (Phaeophyceae). *Phycologia*. 36:186–189.
Deng, Z. & Delwart, E. 2021. ContigExtender: a new approach to improving de novo sequence assembly for viral metagenomics data. *BMC Bioinformatics*. 22:119.
Derelle, E., Ferraz, C., Escande, M.-L., Eychenié, S., Cooke, R., Piganeau, G., Desdevises, Y. et al. 2008. Life-cycle and genome of OtV5, a large DND virus of the pelagic marine unicellular green alga *Ostreococcus tauri*. *PLoS ONE*. 3:e2250.
DeSantis, T.Z., Hugenholtz, P., Larsen, N., Rojas, M., Brodie, E.L., Keller, K., Huber, T. et al. 2006. Greengenes, a chimera-checked 16S rRNA gene database and workbench compatible with ARB. *Appl. Environ. Microbiol.* 72:5069–5072.
Deutsch, Y., Gur, L., Berman Frank, I. & Ezra, D. 2021. Endophytes from algae, a potential source for new biologically active metabolites for disease management in aquaculture. *Front. Mar. Sci.* 8:636636.
Deutsch, Y., Ofek-Lalzar, M., Borenstein, M., Berman-Frank, I. & Ezra, D. 2023. Re-introduction of a bioactive bacterial endophyte back to its seaweed (*Ulva* sp.) host, influences the host's microbiome. *Front. Mar. Sci.* 10:1099478.
Dhiman, S., Ulrich, J.F., Wienecke, P., Wichard, T. & Arndt, H. 2022. Stereoselective total synthesis of (−)-thallusin for bioactivity profiling. *Angew. Chem. Int. Ed.* 61:e202206746.
Dittami, S.M., Duboscq-Bidot, L., Perennou, M., Gobet, A., Corre, E., Boyen, C. & Tonon, T. 2016. Host-microbe interactions as a driver of acclimation to salinity gradients in brown algal cultures. *ISME J.* 10:51–63.
Dittami, S.M., Gravot, A., Renault, D., Goulitquer, S., Eggert, A., Bouchereau, A., Boyen, C. et al. 2011. Integrative analysis of metabolite and transcript abundance during the short-term response to saline and oxidative stress in the brown alga *Ectocarpus siliculosus*. *Plant Cell Environ.* 34:629–42.
Doorenspleet, K., Jansen, L., Oosterbroek, S., Kamermans, P., Bos, O., Wurz, E., Murk, A. et al. 2021. The long and the short of it: Nanopore based eDNA metabarcoding of marine vertebrates works; sensitivity and specificity depend on amplicon lengths. preprint. https://doi.org/10.1101/2021.11.26.470087
Droop, M.R. 1957. Vitamin B_{12} in marine ecology. *Nature*. 180:1041–1042.
Du, X., Li, X., Cheng, K., Zhao, W., Cai, Z., Chen, G. & Zhou, J. 2023. Virome reveals effect of *Ulva prolifera* green tide on the structural and functional profiles of virus communities in coastal environments. *Sci. Total Environ.* 883:163609.
Duarte, C.M., Bruhn, A. & Krause-Jensen, D. 2021. A seaweed aquaculture imperative to meet global sustainability targets. *Nat. Sustain.* 5:185–193.
Duckworth, D.H. 1976. Who discovered bacteriophage? *Bacteriol. Rev.* 40:793–802.
Dupont, C.L., Larsson, J., Yooseph, S., Ininbergs, K., Goll, J., Asplund-Samuelsson, J., McCrow, J.P. et al. 2014. Functional tradeoffs underpin salinity-driven divergence in microbial community composition. *PLoS ONE*. 9: e89549.
Düsedau, L., Ren, Y., Hou, M., Wahl, M., Hu, Z.-M., Wang, G. & Weinberger, F. 2023. Elevated temperature-induced epimicrobiome shifts in an invasive seaweed *Gracilaria vermiculophylla*. *Microorganisms*. 11:599.

Edwards, A., Debbonaire, A., Nicholls, S., Rassner, S., Sattler, B., Cook, J., Davy, T. et al. 2016. In-field metagenome and 16S rRNA gene amplicon nanopore sequencing robustly characterize glacier microbiota. preprint https://doi.org/10.1101/073965

Egan, S., Fernandes, N.D., Kumar, V., Gardiner, M. & Thomas, T. 2014. Bacterial pathogens, virulence mechanism and host defence in marine macroalgae. *Environ. Microbiol.* 16:925–938.

Egan, S. & Gardiner, M. 2016. Microbial dysbiosis: Rethinking disease in marine ecosystems. *Front. Microbiol.* 7:1–8.

Egan, S., Harder, T., Burke, C., Steinberg, P., Kjelleberg, S. & Thomas, T. 2013. The seaweed holobiont: Understanding seaweed-bacteria interactions. *FEMS Microbiol. Rev.* 37:462–476.

Faarghl, A.A. 2012. Thiamine and pyridoxine alleviate oxidative damage by copper stress in green alga *Chlorella vulgaris*. *Egypt. J. Microbiol.* 47:97–110.

FAO 2020. The State of World Fisheries and Aquaculture 2020. Sustainability in action. https://doi.org/10.4060/ca9229en.

Fenchel, T., King, G.M. & Blackburn, T.H. 2012. Chapter 7. Aquatic Sediments. *In Bacterial Biogeochemistry*. Elsevier, pp. 121–142.

Fern, L.L., Abidin, A.A.Z. & Yusof, Z.N.B. 2017. Upregulation of thiamine (vitamin B_1) biosynthesis gene upon stress application in *Anabaena* sp. and *Nannochloropsis oculata*. *J. Plant Biotechnol.* 44:462–471.

Fernandes, D.R.P., Yokoya, N.S. & Yoneshigue-Valentin, Y. 2011. Protocol for seaweed decontamination to isolate unialgal cultures. *Braz. J. Pharmacogn.* 21:313–316.

Fernández, L., Rodríguez, A. & García, P. 2018. Phage or foe: An insight into the impact of viral predation on microbial communities. *ISME J.* 12:1171–1179.

Ferrier-Pagès, C., Martinez, S., Grover, R., Cybulski, J., Shemesh, E. & Tchernov, D. 2021. Tracing the trophic plasticity of the coral–dinoflagellate symbiosis using amino acid compound-specific stable isotope analysis. *Microorganisms*. 9:182.

Fjeld, A. 1972. Genetic control of cellular differentiation in *Ulva mutabilis*. Gene effects in early development. *Dev. Biol.* 28:326–343.

Fletcher, R.L. 1996. The Occurrence of "Green Tides"— a Review. *In* Schramm, W. & Nienhuis, P. H. [Eds.] *Marine Benthic Vegetation*. Springer Berlin Heidelberg, Berlin, Heidelberg, pp. 7–43.

Flynn, K.J. & Wright, C.R.N. 1986. The simultaneous assimilation of ammonium and l-arginine by the marine diatom *Phaeodactylum tricornutum* Bohlin. *J. Exp. Mar. Biol. Ecol.* 95:257–269.

Foster, Z.S.L., Sharpton, T.J. & Grünwald, N.J. 2017. Metacoder: An R package for visualization and manipulation of community taxonomic diversity data. *PLoS Comput. Biol.* 13:1–15.

Fries, L. 1973. Requirements for organic substances in seaweeds. *Bot. Mar.* 16:19–31.

Frigstad, H., Kaste, Ø., Deininger, A., Kvalsund, K., Christensen, G., Bellerby, R.G.J., Sørensen, K. et al. 2020. Influence of riverine input on norwegian coastal systems. 7:1–14.

Fuhrman, J.A. 1999. Marine viruses and their biogeochemical and ecological effects. *Nature*. 399:541–548.

Gachon, C.M.M., Sime-Ngando, T., Strittmatter, M., Chambouvet, A. & Kim, G.H. 2010. Algal diseases: Spotlight on a black box. *Trends Plant Sci.* 15:633–640.

Ganesh, A. E., Sunita-Das, K., Chandrasekar, G., Arun, G. & Balamurugan, S. 2010. Monitoring of total heterotrophic bacteria and *Vibrio* spp. in an aquaculture pond. *Curr. Res. J. Biol. Sci.* 2:48–52.

Gao, G., Clare, A.S., Rose, C. & Caldwell, G.S. 2017. Intrinsic and extrinsic control of reproduction in the green tide-forming alga, Ulva rigida. *Environ. Exp. Bot.* 139:14–22.

Gao, G., Zhong, Z., Zhou, X. & Xu, J. 2016. Changes in morphological plasticity of *Ulva prolifera* under different environmental conditions: A laboratory experiment. *Harmful Algae*. 59:51–58.

García-Caparrós, P., Hasanuzzaman, M. & Lao, M.T. 2019. Oxidative stress and antioxidant defense in plants under salinity. *In* Hasanuzzaman, M., Fotopoulos, V., Nahar, K. & Fujita, M. [Eds.] *Reactive Oxygen, Nitrogen and Sulfur Species in Plants*. 1st ed. Wiley, pp. 291–309.

Geiger, O., López-Lara, I.M. & Sohlenkamp, C. 2013. Phosphatidylcholine biosynthesis and function in bacteria. *Biochim. Biophys. Acta BBA - Mol. Cell Biol. Lipids*. 1831:503–513.

Gemin, M., Peña-Rodríguez, A., Quiroz-Guzmán, E., Magallón-Servín, P., Barajas-Sandoval, D. & Elizondo-González, R. 2019. Growth-promoting bacteria for the green seaweed *Ulva clathrata*. *Aquac. Res.* 50:3741–3748.

Georgiades, K. & Raoult, D. 2011. Defining pathogenic bacterial species in the genomic era. *Front. Microbiol.* 10.3389/fmicb.2010.00151.

Germaine, K., Keogh, E., Garcia-Cabellos, G., Borremans, B., Lelie, D., Barac, T., Oeyen, L. et al. 2004. Colonisation of poplar trees by gfp expressing bacterial endophytes. *FEMS Microbiol. Ecol.* 48:109–118.

Ghabrial, S.A., Ochoa, W.F. & Baker, T.S. 2008. Partitiviruses : General Features. *In Encyclopedia of Virology*. pp. 68–75.

Ghaderiardakani, F., Califano, G., Mohr, J., Abreu, M., Coates, J. & Wichard, T. 2019. Analysis of algal growth- and morphogenesis- promoting factors in an integrated multi-trophic aquaculture system for farming *Ulva* spp. *Aquac. Environ. Interact.* 11:375–91.

Ghaderiardakani, F., Coates, J.C. & Wichard, T. 2017. Bacteria-induced morphogenesis of *Ulva intestinalis* and *Ulva mutabilis* (Chlorophyta): a contribution to the lottery theory. *FEMS Microbiol. Ecol.* 93:1–12.

Ghaderiardakani, F., Langhans, L., Kurbel, V.B., Fenizia, S. & Wichard, T. 2022. Metabolite profiling reveals insights into the species-dependent cold stress response of the green seaweed holobiont *Ulva* (Chlorophyta). *Environ. Exp. Bot.* 200:104913.

Gherna, R.L. & Reddy, C.A. 2014. Culture Preservation. *In* Reddy, C. A., Beveridge, T. J., Breznak, J. A., Marzluf, G. A., Schmidt, T. M. & Snyder, L. R. [Eds.] *Methods for General and Molecular Microbiology*. ASM Press, Washington, DC, USA, pp. 1019–1033.

Gibb, R., Albery, G.F., Becker, D.J., Brierley, L., Connor, R., Dallas, T.A., Eskew, E.A. et al. 2021. Data proliferation, reconciliation, and synthesis in viral ecology. *BioScience*. 71:1148–1156.

Gilbert, J.A. & Lynch, S.V. 2019. Community ecology as a framework for human microbiome research. *Nat. Med.* 25:884–889.

Glasl, B., Haskell, J.B., Aires, T., Serrão, E.A., Bourne, D.G., Webster, N.S. & Frade, P.R. 2021. Microbial surface biofilm responds to the growth-reproduction-senescence cycle of the dominant coral reef macroalgae *Sargassum* spp. *Life*. 11:1199.
Gloor, G.B., Macklaim, J.M., Pawlowsky-Glahn, V. & Egozcue, J.J. 2017. Microbiome datasets are compositional: and this is not optional. *Front. Microbiol.* 8:2224.
Gödeke, J., Paul, K., Lassak, J. & Thormann, K.M. 2011. Phage-induced lysis enhances biofilm formation in *Shewanella oneidensis* MR-1. *ISME J.* 5:613–626.
Goecke, F., Labes, A., Wiese, J. & Imhoff, J.F. 2010. Review chemical interactions between marine macroalgae and bacteria. *Mar. Ecol. Prog. Ser.* 409:267–300.
Goldfine, H. 1984. Bacterial membranes and lipid packing theory. *J. Lipid Res.* 25:1501–1507.
Gonçalves, M.F.M., Esteves, A.C. & Alves, A. 2020. Revealing the hidden diversity of marine fungi in Portugal with the description of two novel species, *Neoascochyta fuci* sp. nov. and *Paraconiothyrium salinum* sp. nov. *Int. J. Syst. Evol. Microbiol.* 70:5337–5354.
Gonçalves, M.F.M., Vicente, T.F.L., Esteves, A.C. & Alves, A. 2019. *Neptunomyces aureus* gen. et sp. nov. (Didymosphaeriaceae, Pleosporales) isolated from algae in Ria de Aveiro, Portugal. *MycoKeys*. 60:31–44.
Green, J.L., Bohannan, B.J.M. & Whitaker, R.J. 2008. Microbial biogeography: from taxonomy to traits. *Science*. 320:1039–1043.
Green, L. & Fong, P. 2016. The good, the bad and the *Ulva*: the density dependent role of macroalgal subsidies in influencing diversity and trophic structure of an estuarine community. *Oikos*. 125:988–1000.
Gregory, G.J. & Boyd, E.F. 2021. Stressed out: Bacterial response to high salinity using compatible solute biosynthesis and uptake systems, lessons from *Vibrionaceae*. *Comput. Struct. Biotechnol. J.* 19:1014–1027.
Grinter, R. & Greening, C. 2021. Cofactor F_{420}: an expanded view of its distribution, biosynthesis and roles in bacteria and archaea. *FEMS Microbiol. Rev.* 45:fuab021.
Grueneberg, J., Engelen, A.H., Costa, R. & Wichard, T. 2016. Macroalgal morphogenesis induced by waterborne compounds and bacteria in coastal seawater. *PLoS ONE*. 11:1–22.
Guiry, M.D. & Guiry, G.M. 2023. AlgaeBase. Available At: https://www.algaebase.org (last accessed September 18, 2023).
Guo, J.-H., Qi, H.-Y., Guo, Y.-H., Ge, H.-L., Gong, L.-Y., Zhang, L.-X. & Sun, P.-H. 2004. Biocontrol of tomato wilt by plant growth-promoting rhizobacteria. *Biol. Control*. 29:66–72.
Gurumurthy, M., Rao, M., Mukherjee, T., Rao, S.P.S., Boshoff, H.I., Dick, T., Barry, C.E. et al. 2013. A novel F_{420}-dependent antioxidant mechanism protects *Mycobacterium tuberculosis* against oxidative stress and bactericidal agents. *Mol. Microbiol.* 87:744–755.
Haider, A., Ringer, M., Kotroczó, Z., Mohácsi-Farkas, C. & Kocsis, T. 2023. The current level of MALDI-TOF MS applications in the detection of microorganisms: a short review of benefits and limitations. *Microbiol. Res.* 14:80–90.
Hairston, N.G., Ellner, S.P., Geber, M.A., Yoshida, T. & Fox, J.A. 2005. Rapid evolution and the convergence of ecological and evolutionary time. *Ecol. Lett.* 8:1114–1127.
Hamady, M. & Knight, R. 2009. Microbial community profiling for human microbiome projects: Tools, techniques, and challenges. *Genome Res.* 19:1141–1152.
Hamner, S., Brown, B.L., Hasan, N.A., Franklin, M.J., Doyle, J., Eggers, M.J., Colwell, R.R. et al. 2019. Metagenomic profiling of microbial pathogens in the Little Bighorn River, Montana. *Int. J. Environ. Res. Public. Health*. 16:1097.
Han, L., Yang, G.-P., Liu, C.-Y., Jin, Y.-M. & Liu, T. 2021. Emissions of biogenic sulfur compounds and their regulation by nutrients during an *Ulva prolifera* bloom in the Yellow Sea. *Mar. Pollut. Bull.* 162:111885.
Han, Q., Zhang, X., Chang, L., Xiao, L., Ahmad, R., Saha, M., Wu, H. et al. 2021. Dynamic shift of the epibacterial communities on commercially cultivated *Saccharina japonica* from mature sporophytes to sporelings and juvenile sporophytes. *J. Appl. Phycol.* 33:1171–1179.
Harsha Mohan, E., Madhusudan, S. & Baskaran, R. 2023. The sea lettuce *Ulva sensu lato*: Future food with health-promoting bioactives. *Algal Res.* 71:103069.
Harvey, J.B.J. & Goff, L.J. 2010. Genetic covariation of the marine fungal symbiont *Haloguignardia irritans* (Ascomycota, Pezizomycotina) with its algal hosts *Cystoseira* and *Halidrys* (Phaeophyceae, Fucales) along the west coast of North America. *Fungal Biol.* 114:82–95.
Hattab, Z.N.A., Al-Ajeel, S.A. & Kaaby, E.A.E. 2015. Effect of salinity stress on *Capsicum annuum* callus growth, regeneration and callus content of capsaicin, phenylalanine, proline and ascorbic acid. *J. Life Sci.* 10: :10.17265.
Haxo, F.T. & Clendenning, K.A. 1953. Photosynthesis and phototaxis in *Ulva lactuca* gametes. *Biol. Bull.* 105:103–114.
Hayden, H.S., Blomster, J., Maggs, C.A., Silva, P.C., Stanhope, M.J. & Waaland, J.R. 2003. Linnaeus was right all along: *Ulva* and *Enteromorpha* are not distinct genera. *Eur. J. Phycol.* 38:277–294.
Hengst, M.B., Andrade, S., González, B. & Correa, J.A. 2010. Changes in epiphytic bacterial communities of intertidal seaweeds modulated by host, temporality, and copper enrichment. *Microb. Ecol.* 60:282–290.
Herlemann, D.P.R., Labrenz, M., Jürgens, K., Bertilsson, S., Waniek, J.J. & Andersson, A.F. 2011. Transitions in bacterial communities along the 2000 km salinity gradient of the Baltic Sea. *ISME J.* 5:1571–1579.
Herlemann, D.P.R., Lundin, D., Andersson, A.F., Labrenz, M. & Jürgens, K. 2016. Phylogenetic signals of salinity and season in bacterial community composition across the salinity gradient of the Baltic Sea. *Front. Microbiol.* 7:1–13.
Herrero, M.-L., Brurberg, M.B., Ojeda, D.I. & Roleda, M.Y. 2020. Occurrence and pathogenicity of *Pythium* (Oomycota) on *Ulva* species (Chlorophyta) at different salinities. *ALGAE*. 35:79–89.
Hiraoka, M. & Oka, N. 2008. Tank cultivation of *Ulva prolifera* in deep seawater using a new "germling cluster" method. *J. Appl. Phycol.* 20:97–102.
Ho, Y.B. 1981. Mineral element content in *Ulva lactuca* L. with reference to eutrophication in Hong Kong coastal waters. *Hydrobiologia*. 77:43–47.
Hoffman, G.E. & Roussos, P. 2021. Dream: Powerful differential expression analysis for repeated measures designs. *Bioinformatics*. 37:192–201.

Hoffman, G.E. & Schadt, E.E. 2016. variancePartition: Interpreting drivers of variation in complex gene expression studies. *BMC Bioinformatics*. 17:17–22.
Hollants, J., Leliaert, F., De Clerck, O. & Willems, A. 2013a. What we can learn from sushi: A review on seaweed-bacterial associations. *FEMS Microbiol. Ecol.* 83:1–16.
Hollants, J., Leliaert, F., Verbruggen, H., Willems, A. & De Clerck, O. 2013b. Permanent residents or temporary lodgers: Characterizing intracellular bacterial communities in the siphonous green alga *Bryopsis*. *Proc. R. Soc. B Biol. Sci.* 280:1–8.
Hollants, J., Leroux, O., Leliaert, F., Decleyre, H., de Clerck, O. & Willems, A. 2011. Who is in there? Exploration of endophytic bacteria within the siphonous green seaweed *Bryopsis* (Bryopsidales, Chlorophyta). *PLoS ONE*. 6: e26458.
Hu, X., Li, D., Qiao, Y., Song, Q., Guan, Z., Qiu, K., Cao, J. et al. 2020. Salt tolerance mechanism of a hydrocarbon-degrading strain: Salt tolerance mediated by accumulated betaine in cells. *J. Hazard. Mater.* 392:122326.
Hu, Y.O.O., Karlson, B., Charvet, S. & Andersson, A.F. 2016. Diversity of pico- to mesoplankton along the 2000 km salinity gradient of the Baltic Sea. *Front. Microbiol.* 7:1–17.
Hudson, J., Kumar, V. & Egan, S. 2019. Comparative genome analysis provides novel insight into the interaction of *Aquimarina* sp. AD1, BL5 and AD10 with their macroalgal host. *Mar. Genomics*. 46:8–15.
Huerta-Cepas, J., Forslund, K., Coelho, L.P., Szklarczyk, D., Jensen, L.J., Von Mering, C. & Bork, P. 2017. Fast genome-wide functional annotation through orthology assignment by eggNOG-mapper. *Mol. Biol. Evol.* 34:2115–2122.
Hughey, J.R., Gabrielson, P.W., Maggs, C.A. & Mineur, F. 2021. Genomic analysis of the lectotype specimens of European *Ulva rigida* and *Ulva lacinulata* (Ulvaceae, Chlorophyta) reveals the ongoing misapplication of names. *Eur. J. Phycol.* 57:1–11.
Hughey, J.R., Gabrielson, P.W., Maggs, C.A., Mineur, F. & Miller, K.A. 2020. Taxonomic revisions based on genetic analysis of type specimens of *Ulva conglobata*, *U. laetevirens*, *U. pertusa* and *U. spathulata* (Ulvales, Chlorophyta). *Phycol. Res.* 69:148–153.
Hughey, J.R., Maggs, C.A., Mineur, F., Jarvis, C., Miller, K.A., Shabaka, S.H. & Gabrielson, P.W. 2019. Genetic analysis of the Linnaean *Ulva lactuca* (Ulvales, Chlorophyta) holotype and related type specimens reveals name misapplications, unexpected origins, and new synonymies. *J. Phycol.* 55:503–508.
Hurd, C.L., Law, C.S., Bach, L.T., Britton, D., Hovenden, M., Paine, E.R., Raven, J.A. et al. 2022. Forensic carbon accounting: Assessing the role of seaweeds for carbon sequestration. *J. Phycol.* 58:347–363.
Hussain, Sajid, Huang, J., Zhu, C., Zhu, L., Cao, X., Hussain, Saddam, Ashraf, M. et al. 2020. Pyridoxal 5′-phosphate enhances the growth and morpho-physiological characteristics of rice cultivars by mitigating the ethylene accumulation under salinity stress. *Plant Physiol. Biochem.* 154:782–795.
Hyatt, D., Chen, G.-L., LoCascio, P.F., Land, M.L., Larimer, F.W. & Hauser, L.J. 2010. Prodigal: prokaryotic gene recognition and translation initiation site identification. *BMC Bioinformatics*. 11:119.
Ichihara, K., Arai, S., Uchimura, M., Fay, E.J., Ebata, H., Hiraoka, M. & Shimada, S. 2009. New species of freshwater *Ulva*, *Ulva limnetica* (Ulvales, Ulvophyceae) from the Ryukyu Islands, Japan. *Phycol. Res.* 57:94–103.
Ichihara, K., Mineur, F. & Shimada, S. 2011. Isolation and temporal expression analysis of freshwater-induced genes in *Ulva limnetica* (Ulvales, Chlorophyta): Freshwater-induced genes fron *Ulva*. *J. Phycol.* 47:584–90.
Ichihara, K., Miyaji, K. & Shimada, S. 2013. Comparing the low-salinity tolerance of *Ulva* species distributed in different environments: Low-salinity tolerance of *Ulva* spp. *Phycol. Res.* 61:52–57.
Ihua, M.W., FitzGerald, J.A., Guiheneuf, F., Jackson, S.A., Claesson, M.J., Stengel, D.B. & Dobson, A.D.W. 2020. Diversity of bacteria populations associated with different thallus regions of the brown alga *Laminaria digitata*. *PLoS ONE*. 15: e0242675.
Infante-Villamil, S., Huerlimann, R. & Jerry, D.R. 2021. Microbiome diversity and dysbiosis in aquaculture. *Rev. Aquac.* 13:1077–1096.
Jahnke, L.S. & White, A.L. 2003. Long-term hyposaline and hypersaline stresses produce distinct antioxidant responses in the marine alga *Dunaliella tertiolecta*. *J. Plant Physiol.* 160:1193–1202.
Jain, M., Olsen, H.E., Paten, B. & Akeson, M. 2016. The Oxford Nanopore MinION: Delivery of Nanopore sequencing to the genomics community. *Genome Biol.* 17:239.
Jansen, H.M., Bernard, M.S., Nederlof, M.A.J., Van Der Meer, I.M. & Van Der Werf, A. 2022. Seasonal variation in productivity, chemical composition and nutrient uptake of *Ulva* spp. (Chlorophyta) strains. *J. Appl. Phycol.* 34:1649–1660.
Johannesson, K., Le Moan, A., Perini, S. & André, C. 2020. A darwinian laboratory of multiple contact zones. *Trends Ecol. Evol.* 35:1021–1036.
Johnson, J.S., Spakowicz, D.J., Hong, B.Y., Petersen, L.M., Demkowicz, P., Chen, L., Leopold, S.R. et al. 2019. Evaluation of 16S rRNA gene sequencing for species and strain-level microbiome analysis. *Nat. Commun.* 10:1–11.
Joint, I., Callow, M.E., Callow, J.A. & Clarke, K.R. 2000. The attachment of *Enteromorpha* zoospores to a bacterial biofilm assemblage. *Biofouling*. 16:151–158.
Joint, I., Tait, K., Callow, M.E., Callow, J.A., Milton, D., Williams, P. & Cámara, M. 2002. Cell-to-cell communication across the prokaryote-eukaryote boundary. *Science*. 298:1207.
Jost, L. 2007. Partitioning diversity into independent alpha and beta components. *Ecol. Soc. Am.* 88:2427–2439.
Juhmani, A.-S., Vezzi, A., Wahsha, M., Buosi, A., Pascale, F.D., Schiavon, R. & Sfriso, A. 2020. Diversity and dynamics of seaweed associated microbial communities inhabiting the lagoon of Venice. *Microorganisms*. 8:1657.
Jung, A., Metzner, M. & Ryll, M. 2017. Comparison of pathogenic and non-pathogenic *Enterococcus cecorum* strains from different animal species. *BMC Microbiol.* 17:33.
Kabiri, R., Naghizadeh, M. & Hatami, A. 2016. Protective role of arginine against oxidative damage induced by osmotic stress in Ajwain (*Trachyspermum ammi*) seedlings under hydroponic culture. *Journal of Plant Physiology and Breeding* 6:13–22.
Kakinuma, M., Coury, D.A., Kuno, Y., Itoh, S., Kozawa, Y., Inagaki, E., Yoshiura, Y. et al. 2006. Physiological and biochemical responses to thermal and salinity stresses in a sterile mutant of *Ulva pertusa* (Ulvales, Chlorophyta). *Mar. Biol.*

149:97–106.
Kalita, T.L. & Tytlianov, E.A. 2003. Effect of temperature and illumination on growth and reproduction of the green alga *Ulva fenestrata*. *Russian Journal of Marine Biology* 29:316–322.
Kallscheuer, N., Jogler, M., Wiegand, S., Peeters, S.H., Heuer, A., Boedeker, C., Jetten, M.S.M. et al. 2020. Three novel *Rubripirellula* species isolated from plastic particles submerged in the Baltic Sea and the estuary of the river Warnow in northern Germany. *Antonie Van Leeuwenhoek Int. J. Gen. Mol. Microbiol.* 113:1767–1778.
Kanehisa, M., Araki, M., Goto, S., Hattori, M., Hirakawa, M., Itoh, M., Katayama, T. et al. 2008. KEGG for linking genomes to life and the environment. *Nucleic Acids Res.* 36:480–484.
Kanehisa, M. & Goto, S. 2000. KEGG: Kyoto Encyclopedia of Genes and Genomes. *Nucleic Acids Res.* 28:27–30.
Kang, D.D., Li, F., Kirton, E., Thomas, A., Egan, R., An, H. & Wang, Z. 2019. MetaBAT 2: An adaptive binning algorithm for robust and efficient genome reconstruction from metagenome assemblies. *PeerJ*. 7:e7359.
Kang, S.-M., Radhakrishnan, R., You, Y.-H., Khan, A.L., Park, J.-M., Lee, S.-M. & Lee, I.-J. 2015. Cucumber performance is improved by inoculation with plant growth-promoting microorganisms. *Acta Agric. Scand. Sect. B — Soil Plant Sci.* 65:36–44.
Karst, S.M., Ziels, R.M., Kirkegaard, R.H., Sørensen, E.A., McDonald, D., Zhu, Q., Knight, R. et al. 2021. High-accuracy long-read amplicon sequences using unique molecular identifiers with Nanopore or PacBio sequencing. *Nat. Methods*. 18:165–169.
Katoh, K., Misawa, K., Kuma, K.I. & Miyata, T. 2002. MAFFT: A novel method for rapid multiple sequence alignment based on fast Fourier transform. *Nucleic Acids Res.* 30:3059–3066.
Ke, J., Wang, B. & Yoshikuni, Y. 2021. Microbiome engineering: Synthetic biology of plant-associated microbiomes in sustainable agriculture. *Trends Biotechnol.* 39:244–261.
Kerkhof, L. 2021. Is Oxford Nanopore sequencing ready for analyzing complex microbiomes? *FEMS*. 97:fiab001.
Kessler, R.W., Weiss, A., Kuegler, S., Hermes, C. & Wichard, T. 2018. Macroalgal–bacterial interactions: Role of dimethylsulfoniopropionate in microbial gardening by *Ulva* (Chlorophyta). *Mol. Ecol.* 27:1808–1819.
Khan, T., Song, W., Nappi, J., Marzinelli, E.M., Egan, S. & Thomas, T. 2023. Functional guilds and drivers of diversity in seaweed-associated bacteria. *FEMS Microbes*. 5:xtad023.
Kidgell, J.T., Magnusson, M., de Nys, R. & Glasson, C.R.K. 2019. Ulvan: A systematic review of extraction, composition and function. *Algal Res.* 39:101422.
Kieser, S., Brown, J., Zdobnov, E.M., Trajkovski, M. & McCue, L.A. 2020. ATLAS: A Snakemake workflow for assembly, annotation, and genomic binning of metagenome sequence data. *BMC Bioinformatics*. 21:257.
Kim, D., Song, L., Breitwieser, F.P. & Salzberg, S.L. 2016. Centrifuge: Rapid and sensitive classification of metagenomic sequences. *Genome Res.* 26:1721–1729.
Kim, G.H., Klochkova, T.A., Lee, D.J. & Im, S.H. 2016. Chloroplast virus causes green-spot disease in cultivated *Pyropia* of Korea. *Algal Res.* 17:293–9.
Kim, J.-H., Kang, E.J., Park, M.G., Lee, B.-G. & Kim, K.Y. 2011. Effects of temperature and irradiance on photosynthesis and growth of a green-tide-forming species (*Ulva linza*) in the Yellow Sea. *J. Appl. Phycol.* 23:421–432.
King, A.M.Q., Adams, M.J., Carstens, E.B. & Lefkowitz, E.J. 2012a. Tombusviridae. *In* King, A. M. Q., Adams, M. J., Carstens, E. B. & Lefkowitz, E. J. [Eds.] *Virus Taxonomy*. pp. 1111–1138.
King, A.M.Q., Adams, M.J., Carstens, E.B. & Lefkowitz, E.J. 2012b. Picornavirales. *In Virus Taxonomy*. pp. 835–839.
Kirst, G.O. 1989. Salinity tolerance of eukaryotic marine algae. *Annu. Rev. Plant Physiol. Plant Mol. Biol.* 40:21–53.
Klier, J., Dellwig, O., Leipe, T., Jürgens, K. & Herlemann, D.P.R. 2018. Benthic bacterial community composition in the oligohaline-marine transition of surface sediments in the Baltic Sea based on rRNA analysis. *Front. Microbiol.* 9:1–12.
Koga, R., Fukuhara, T. & Nitta, T. 1998. Molecular characterization of a single mitochondria-associated double-stranded RNA in the green alga *Bryopsis*. *Plant Mol. Biol.* 36:717–724.
Koga, R., Horiuchi, H. & Fukuhara, T. 2003. Double-stranded RNA replicons associated with chloroplasts of a green alga, *Bryopsis cinicola*. *Plant Mol. Biol.* 51:991–999.
Kohlmeyer, J. & Volkmann-Kohlmeyer, B. 2003. Marine ascomycetes from algae and animal hosts. *Bot. Mar.* 46: BOT.2003.026.
Kolmogorov, M., Yuan, J., Lin, Y. & Pevzner, P.A. 2019. Assembly of long, error-prone reads using repeat graphs. *Nat. Biotechnol.* 37:540–546.
Korth, F., Deutsch, B., Liskow, I. & Voss, M. 2012. Uptake of dissolved organic nitrogen by size-fractionated plankton along a salinity gradient from the North Sea to the Baltic Sea. *Biogeochemistry*. 111:347–360.
Kotta, J., Raudsepp, U., Szava-Kovats, R., Aps, R., Armoskaite, A., Barda, I., Bergström, P. et al. 2022. Assessing the potential for sea-based macroalgae cultivation and its application for nutrient removal in the Baltic Sea. *Sci. Total Environ.* 839:156230.
Kotta-Loizou, I., Castón, J.R., Coutts, R.H.A., Hillman, B.I., Jiang, D., Kim, D.H., Moriyama, H. et al. 2020. ICTV virus taxonomy profile: Chrysoviridae. *J. Gen. Virol.* 101:143–144.
Kovaka, S., Fan, Y., Ni, B., Timp, W. & Schatz, M.C. 2020. Targeted nanopore sequencing by real-time mapping of raw electrical signal with UNCALLED. *Nat. Biotechnol.*
Krause, E., Wichels, A., Giménez, L., Lunau, M., Schilhabel, M.B. & Gerdts, G. 2012. Small changes in pH have direct effects on marine bacterial community composition: a microcosm approach. *PLoS ONE*. 7:e47035.
Krishnani, K.K., Kathiravan, V., Natarajan, M., Kailasam, M. & Pillai, S.M. 2010. Diversity of sulfur-oxidizing bacteria in green-water system of coastal aquaculture. *Appl. Biochem. Biotechnol.* 162:1225–1237.
Krupovic, M., Dolja, V.V. & Koonin, E.V. 2015. Plant viruses of the *Amalgaviridae* family evolved via recombination between viruses with double-stranded and negative-strand RNA genomes. *Biol. Direct*. 10:1–7.
Krupovic, M., Varsani, A., Kazlauskas, D., Breitbart, M., Delwart, E., Rosario, K., Yutin, N. et al. 2020. *Cressdnaviricota*: A virus phylum unifying seven families of Rep-encoding viruses with single-stranded, circular DNA genomes. *J. Virol.* 94: e00582-20.

Krupovic, M., Varsani, A., Kuhn, J.H. & Kazlauskas, D. 2019. Create 1 new phylum (*Cressdnaviricota*) including 2 classes and 6 orders for classification of CRESS-DNA viruses. 10.13140/RG.2.2.25267.37923

Kumar, V., Zozaya-Valdes, E., Kjelleberg, S., Thomas, T. & Egan, S. 2016. Multiple opportunistic pathogens can cause a bleaching disease in the red seaweed Delisea pulchra. *Environ. Microbiol.* 18:3962–3975.

Lachnit, T., Blümel, M., Imhoff, J.F. & Wahl, M. 2009. Specific epibacterial communities on macroalgae: Phylogeny matters more than habitat. *Aquat. Biol.* 5:181–186.

Lachnit, T., Meske, D., Wahl, M., Harder, T. & Schmitz, R. 2011. Epibacterial community patterns on marine macroalgae are host-specific but temporally variable. *Environ. Microbiol.* 13:655–665.

Lachnit, T., Thomas, T. & Steinberg, P. 2016. Expanding our understanding of the seaweed holobiont: RNA viruses of the red alga *Delisea pulchra*. *Front. Microbiol.* 6:1–12.

Lage, O.M. & Graça, A.P. 2016. Biofilms: An Extra Coat on Macroalgae. *IntechOpen* 10.5772/63053.

Lahti, L. & Shetty, S. 2017. Tools for microbiome analysis in R. Microbiome package version 1.15.1.

Land, M., Hauser, L., Jun, S.-R., Nookaew, I., Leuze, M.R., Ahn, T.-H., Karpinets, T. et al. 2015. Insights from 20 years of bacterial genome sequencing. *Funct. Integr. Genomics*. 15:141–161.

Lane, D. 1991. 16S/23S rRNA sequencing. *In Nucleic Acid Techniques in Bacterial Systematics*. Wiley, New York, pp. 115–175.

Lanka, S.T.J., Klein, M., Ramsperger, U., Müller, D.G. & Knippers, R. 1993. Genome structure of a virus infecting the marine brown alga *Ectocarpus siliculosus*. *Virology*. 193:802–811.

Lavery, P.S., Lukatelich, R.J. & McComb, A.J. 1991. Changes in the biomass and species composition of macroalgae in a eutrophic estuary. *Estuar. Coast. Shelf Sci.* 33:1–22.

Lawrence, A.D., Nemoto-Smith, E., Deery, E., Baker, J.A., Schroeder, S., Brown, D.G., Tullet, J.M.A. et al. 2018. Construction of fluorescent analogs to follow the uptake and distribution of cobalamin (vitamin B_{12}) in bacteria, worms, and plants. *Cell Chem. Biol.* 25:941-951.

Lawton, R.J., Mata, L., De Nys, R. & Paul, N.A. 2013. Algal bioremediation of waste waters from land-based aquaculture using *Ulva*: selecting target species and strains. *PLoS ONE*. 8:e77344.

Lawton, R.J., Sutherland, J.E., Glasson, C.R.K. & Magnusson, M.E. 2021. Selection of temperate *Ulva* species and cultivars for land-based cultivation and biomass applications. *Algal Res.* 56:102320.

Le Lay, C., Shi, M., Buček, A., Bourguignon, T., Lo, N. & Holmes, E.C. 2020. Unmapped RNA virus diversity in termites and their symbionts. *Viruses*. 12:1–21.

LeBlanc, J.G., Milani, C., De Giori, G.S., Sesma, F., Van Sinderen, D. & Ventura, M. 2013. Bacteria as vitamin suppliers to their host: a gut microbiota perspective. *Curr. Opin. Biotechnol.* 24:160–168.

Lemay, M., Chen, M.Y., Mazel, F., Hind, K.R., Starko, S., Keeling, P.J., Martone, P.T. et al. 2020. Morphological complexity affects the diversity and composition of marine microbiomes. *ISME J.* 15:1372–1386.

Lemay, M., Davis, K.M., Martone, P.T. & Wegener Parfrey, L. 2021. Kelp-associated microbiota are structured by host anatomy. *J Phyc*. 57:1119–1130.

Lemay, M.A., Martone, P.T., Keeling, P.J., Burt, J.M., Krumhansl, K.A., Sanders, R.D. & Wegener Parfrey, L. 2018. Sympatric kelp species share a large portion of their surface bacterial communities. *Environ. Microbiol.* 20:658–670.

Lencer 2011. Location of Zeeland province in the Netherlands. https://nl.wikipedia.org/wiki/Bestand:Zeeland_in_the_Netherlands.svg.

Leskinen, E., Alström-Rapaport, C. & Pamilo, P. 2004. Phylogeographical structure, distribution and genetic variation of the green algae *Ulva intestinalis* and *U. compressa* (Chlorophyta) in the Baltic Sea area. *Mol. Ecol.* 13:2257–2265.

Li, D., Gao, Z. & Song, D. 2021. Analysis of environmental factors affecting the large-scale long-term sequence of green tide outbreaks in the Yellow Sea. *Estuar. Coast. Shelf Sci.* 260:107504.

Li, D., Gao, Z. & Wang, Z. 2022. Analysis of the reasons for the outbreak of Yellow Sea green tide in 2021 based on long-term multi-source data. *Mar. Environ. Res.* 178:105649.

Li, D., Luo, R., Liu, C.-M., Leung, C.-M., Ting, H.-F., Sadakane, K., Yamashita, H. et al. 2016. MEGAHIT v1.0: A fast and scalable metagenome assembler driven by advanced methodologies and community practices. *Methods*. 102:3–11.

Li, H. 2018. Minimap2: Pairwise alignment for nucleotide sequences. *Bioinformatics*. 34:3094–3100.

Li, H., Zhang, Y., Chen, J., Zheng, X., Liu, F. & Jiao, N. 2019. Nitrogen uptake and assimilation preferences of the main green tide alga *Ulva prolifera* in the Yellow Sea, China. *J. Appl. Phycol.* 31:625–635.

Li, J., Majzoub, M.E., Marzinelli, E.M., Dai, Z., Thomas, T. & Egan, S. 2022a. Bacterial controlled mitigation of dysbiosis in a seaweed disease. *ISME J.* 16:378–387.

Li, J., Weinberger, F., De Nys, R., Thomas, T. & Egan, S. 2023. A pathway to improve seaweed aquaculture through microbiota manipulation. *Trends Biotechnol.* 41:545–556.

Li, J., Weinberger, F., Saha, M., Majzoub, M.E. & Egan, S. 2022b. Cross-host protection of marine bacteria against macroalgal disease. *Microb. Ecol.* 84:1288–1293.

Lin, H. 2021. SilentGene/Bio-py: Bio-py. http://doi.org/10.5281/zenodo.4954426. Zenodo.

Lin, T. 2023. Editorial: New techniques in microbiome research. *Front. Cell. Infect. Microbiol.* 13:1158392.

Linares, F. 2006. Effect of dissolved free amino acids (DFAA) on the biomass and production of microphytobenthic communities. *J. Exp. Mar. Biol. Ecol.* 330:469–481.

Lindh, M.V., Sjöstedt, J., Andersson, A.F., Baltar, F., Hugerth, L.W., Lundin, D., Muthusamy, S. et al. 2015. Disentangling seasonal bacterioplankton population dynamics by high-frequency sampling. *Environ. Microbiol.* 17:2459–2476.

Linnaeus, C. 1753. Species plantarum, exhibentes plantas rite cognitas, ad genera relatas, cum differentiis specificis, nominibus trivialibus, synonymis selectis, locis natalibus, secundum systema sexuale digestas. Holmiae [Stockholm].

Liu, R., Zhang, Q.N., Lu, J., Zhang, C.H., Zhang, L. & Wu, Y. 2019. The effects of exogenous pyridoxal-5-phosphate on seedling growth and development of wheat under salt stress. *Cereal Res. Commun.* 47:442–454.

Loffredo, M.R., Savini, F., Bobone, S., Casciaro, B., Franzyk, H., Mangoni, M.L. & Stella, L. 2021. Inoculum effect of antimicrobial peptides. *Proc. Natl. Acad. Sci.* 118:e2014364118.

Lommel, S.A., Sit, T.L. & Carolina 2008. Tombusviruses. *In Encyclopedia of Virology (Third Edition)*. pp. 145–151.
Longford, S.R., Tujula, N.A., Crocetti, G.R., Holmes, A.J., Holmström, C., Kjelleberg, S., Steinberg, P.D. et al. 2007. Comparisons of diversity of bacterial communities associated with three sessile marine eukaryotes. *Aquat. Microb. Ecol.* 48:217–229.
Loret, Elvenn, Lluesma, M., Cassien, A., Brinvillier, D. & Loret, Erwann 2020. A marine virus controls the green algae *Ulva lactuca* proliferation in the bay of Marseille. hal-03081997
Los, D.A. & Murata, N. 2004. Membrane fluidity and its roles in the perception of environmental signals. *Biochim. Biophys. Acta BBA - Biomembr.* 1666:142–157.
Love, M.I., Huber, W. & Anders, S. 2014. Moderated estimation of fold change and dispersion for RNA-seq data with DESeq2. *Genome Biol.* 15:1–21.
Løvlie, A. 1969. Cell size, nucleic acids, and synthetic efficiency in the wild type and a growth mutant of the multicellular alga *Ulva mutabilis* Føyn. *Dev. Biol.* 20:349–367.
Lozupone, C.A. & Knight, R. 2007. Global patterns in bacterial diversity. *Proc. Natl. Acad. Sci. U. S. A.* 104:11436–11440.
Lu, J. & Salzberg, S.L. 2020. Ultrafast and accurate 16S rRNA microbial community analysis using Kraken2. *Microbiome*. 8:1–11.
Lubsch, A. & Timmermans, K. 2018. Uptake kinetics and storage capacity of dissolved inorganic phosphorus and corresponding N:P dynamics in *Ulva lactuca* (Chlorophyta). *J. Phycol.* 54:215–223.
Luo, M.B. & Liu, F. 2011. Salinity-induced oxidative stress and regulation of antioxidant defense system in the marine macroalga *Ulva prolifera*. *J. Exp. Mar. Biol. Ecol.* 409:223–228.
Luo, M.B., Liu, F. & Xu, Z.L. 2012. Growth and nutrient uptake capacity of two co-occurring species, *Ulva prolifera* and *Ulva linza*. *Aquat. Bot.* 100:18–24.
Ma, M., Zhuang, Y., Chang, L., Xiao, L., Lin, Q., Qiu, Q., Chen, D. et al. 2023. Naturally occurring beneficial bacteria *Vibrio alginolyticus* X-2 protects seaweed from bleaching disease. *mBio*. e00065-23.
Mącik, M., Gryta, A. & Frąc, M. 2020. Biofertilizers in agriculture: An overview on concepts, strategies and effects on soil microorganisms. *In Advances in Agronomy*. Elsevier, pp. 31–87.
MacKenzie, M. & Argyropoulos, C. 2023. An introduction to Nanopore sequencing: Past, present, and future considerations. *Micromachines*. 14:459.
Maestre, F.T., Callaway, R.M., Valladares, F. & Lortie, C.J. 2009. Refining the stress-gradient hypothesis for competition and facilitation in plant communities. *J. Ecol.* 97:199–205.
Maghini, D.G., Moss, E.L., Vance, S.E. & Bhatt, A.S. 2021. Improved high-molecular-weight DNA extraction, Nanopore sequencing and metagenomic assembly from the human gut microbiome. *Nat. Protoc.* 16:458–471.
Mallick, H., Rahnavard, A., McIver, L.J., Ma, S., Zhang, Y., Nguyen, L.H., Tickle, T.L. et al. 2021. Multivariable association discovery in population-scale meta-omics studies. *PLOS Comput. Biol.* 17:e1009442.
Mangmang, J.S., Deaker, R. & Rogers, G. 2015. Optimal plant growth-promoting concentration of *Azospirillum brasilense* inoculated to cucumber, lettuce and tomato seeds varies between bacterial strains. *Isr. J. Plant Sci.* 62:145–152.
Manhart, J.R. 1994. Phylogenetic analysis of green plant *rbc*L sequences. *Mol. Phylogenet. Evol.* 3:114–127.
Mantri, V.A., Kazi, M.A., Balar, N.B., Gupta, V. & Gajaria, T. 2020. Concise review of green algal genus *Ulva* Linnaeus. *J. Appl. Phycol.* 32:2725–2741.
Marijon, P., Chikhi, R. & Varré, J.S. 2020. Yacrd and fpa: Upstream tools for long-read genome assembly. *Bioinformatics*. 36:3894–3896.
Markager, S. & Sand-Jensen, K. 1990. Heterotrophic growth of *Ulva lactuca* (Chlorophyceae). *J. Phycol.* 26:670–673.
Marshall, K., Joint, I., Callow, M.E. & Callow, J.A. 2006. Effect of marine bacterial isolates on the growth and morphology of axenic plantlets of the green alga *Ulva linza*. *Microb. Ecol.* 52:302–310.
Martinez Arbizu, P. 2020. pairwiseAdonis: Pairwise multilevel comparison using adonis. R package version 0.4. https://github.com/pmartinezarbizu/pairwiseAdonis.
Martiny, J.B.H., Bohannan, B.J.M., Brown, J.H., Colwell, R.K., Fuhrman, J.A., Green, J.L., Horner-Devine, M.C. et al. 2006. Microbial biogeography: Putting microorganisms on the map. *Nat. Rev. Microbiol.* 4:102–112.
Mata, L., Schuenhoff, A. & Santos, R. 2010. A direct comparison of the performance of the seaweed biofilters, *Asparagopsis armata* and *Ulva rigida*. *J. Appl. Phycol.* 22:639–644.
Matsuo, Y., Imagawa, H., Nishizawa, M. & Shizuri, Y. 2005. Isolation of an algal morphogenesis inducer from a marine bacterium. *Science*. 307:1598.
McFall-Ngai, M., Hadfield, M.G., Bosch, T.C.G., Carey, H.V., Domazet-Lošo, T., Douglas, A.E., Dubilier, N. et al. 2013. Animals in a bacterial world, a new imperative for the life sciences. *Proc. Natl. Acad. Sci. U. S. A.* 110:3229–3236.
McKeown, D.A., Schroeder, J.L., Stevens, K., Peters, A.F., Sáez, C.A., Park, J., Rothman, M.D. et al. 2018. Phaeoviral infections are present in *Macrocystis*, *Ecklonia* and *Undaria* (Laminariales) and are influenced by wave exposure in Ectocarpales. *Viruses*. 10:410.
McKeown, D.A., Stevens, K., Peters, A.F., Bond, P., Harper, G.M., Brownlee, C., Brown, M.T. et al. 2017. Phaeoviruses discovered in kelp (Laminariales). *ISME J.* 11:2869–2873.
McMurdie, P.J. & Holmes, S. 2013. Phyloseq: an R package for reproducible interactive analysis and graphics of microbiome census data. *PLoS ONE*. 8: e61217.
McParland, E.L., Alexander, H. & Johnson, W.M. 2021. The osmolyte ties that bind: Genomic insights into synthesis and breakdown of organic osmolytes in marine microbes. *Front. Mar. Sci.* 8:689306.
Md, V., Misra, S., Li, H. & Aluru, S. 2019. Efficient architecture-aware acceleration of BWA-MEM for multicore systems. *Proc. - 2019 IEEE 33rd Int. Parallel Distrib. Process. Symp. IPDPS 2019*. 314–324.
Menaa, F., Wijesinghe, P.A.U.I., Thiripuranathar, G., Uzair, B., Iqbal, H., Khan, B.A. & Menaa, B. 2020. Ecological and industrial implications of dynamic seaweed-associated microbiota interactions. *Mar. Drugs*. 18:1–25.
Mendes, M., Navalho, S., Ferreira, A., Paulino, C., Figueiredo, D., Silva, D., Gao, F. et al. 2022. Algae as food in Europe: An over-

view of species diversity and their application. *Foods*. 11:1871.
Menge, B.A. & Sutherland, J.P. 1987. Community regulation: Variation in disturbance, competition, and predation in relation to environmental stress and recruitment. *Am. Nat.* 130:730–757.
Mensch, B., Neulinger, S.C., Graiff, A., Pansch, A., Künzel, S., Fischer, M.A. & Schmitz, R.A. 2016. Restructuring of epibacterial communities on *Fucus vesiculosus* forma *mytili* in response to elevated pCO_2 and increased temperature levels. *Front. Microbiol.* 7:1–15.
Mensch, B., Neulinger, S.C., Künzel, S., Wahl, M. & Schmitz, R.A. 2020. Warming, but not acidification, restructures epibacterial communities of the baltic macroalga *Fucus vesiculosus* with seasonal variability. *Front. Microbiol.* 11: 10.3389.
Meusnier, I., Olsen, J.L., Stam, W.T., Destombe, C. & Valero, M. 2001. Phylogenetic analyses of *Caulerpa taxifolia* (Chlorophyta) and of its associated bacterial microflora provide clues to the origin of the Mediterranean introduction. *Mol. Ecol.* 10:931–946.
Middelboe, M. & Brussaard, C.P.D. 2017. Marine viruses: Key players in marine ecosystems. *Viruses*. 9:1–6.
Minich, J. & Dinsdale, E.A. 2015. Experimental metagenomics: Influence of pulses of carbon dioxide on kelp forest microbial ecology. *Encycl. Metagenomics*. 176–812.
Minich, J.J., Morris, M.M., Brown, M., Doane, M., Edwards, M.S., Michael, T.P. & Dinsdale, E.A. 2018. Elevated temperature drives kelp microbiome dysbiosis, while elevated carbon dioxide induces water microbiome disruption. *PLoS ONE*. 13:1–23.
Minton, K. 2023. Spatial resolution of host–microbiome interactions. *Nat. Rev. Genet.* 25:79.
Mishra, P., Mishra, J. & Arora, N.K. 2021. Plant growth promoting bacteria for combating salinity stress in plants – Recent developments and prospects: A review. *Microbiol. Res.* 252:126861.
Mitsuhashi, S., Kryukov, K., Nakagawa, S., Takeuchi, J.S., Shiraishi, Y., Asano, K. & Imanishi, T. 2017. A portable system for rapid bacterial composition analysis using a nanopore-based sequencer and laptop computer. *Sci. Rep.* 7:1–9.
Mohsen, A.F., Khaleafa, A.F., Hashem, M.A. & Metwalli, A. 1974. Effect of some vitamins on growth, reproduction, amino acid, fat and sugar contents in *Ulva fasciata* Delile. *Bot. Mar.* 17:208–212.
Mosavikia, A.A., Mosavi, S.G., Seghatoleslami, M. & Baradaran, R. 2020. Chitosan nanoparticle and pyridoxine seed priming improves tolerance to salinity in milk thistle seedling. *Not. Bot. Horti Agrobot. Cluj-Napoca*. 48:221–233.
Mück, I. & Heubel, K.U. 2018. Ecological variation along the salinity gradient in the Baltic Sea area and its consequences for reproduction in the common goby. *Curr. Zool.* 64:259–270.
Müller, D.G. 1996. Host-virus interactions in marine brown algae. *Hydrobiologia*. 21:21–28.
Müller, D.G., Kawai, H., Stache, B. & Lanka, S. 1990. A virus infection in the marine brown alga *Ectocarpus siliculosus* (Phaeophyceae). *Bot. Acta*. 103:72–82.
Murúa, P., Garvetto, A., Egan, S. & Gachon, C.M.M. 2023. The reemergence of phycopathology: When algal biology meets ecology and biosecurity. *Annu. Rev. Phytopathol.* 61:231–255.
Nappi, J., Goncalves, P., Khan, T., Majzoub, M.E., Sophia, A., Ezequiel, G., Thomas, T. et al. 2022. Differential priority effects impact taxonomy and functionality of host- associated microbiomes. *Mol. Eco.* 32:6278–6293.
Nasr, A.H. & Bekheet, I.A. 1969. The effect of some organic micronutrients on some marine algae from Alexandria. *Hydrobiologia*. 34:295–304.
Nayfach, S., Camargo, A.P., Schulz, F., Eloe-Fadrosh, E., Roux, S. & Kyrpides, N.C. 2021. CheckV assesses the quality and completeness of metagenome-assembled viral genomes. *Nat. Biotechnol.* 39:578–585.
Nederlof, M.A.J., Neori, A., Verdegem, M.C.J., Smaal, A.C. & Jansen, H.M. 2022. *Ulva* spp. performance and biomitigation potential under high nutrient concentrations: implications for recirculating IMTA systems. *J. Appl. Phycol.* 34:2157–2171.
Nelson, D.R., Hazzouri, K.M., Lauersen, K.J., Jaiswal, A., Chaiboonchoe, A., Mystikou, A., Fu, W. et al. 2021. Large-scale genome sequencing reveals the driving forces of viruses in microalgal evolution. *Cell Host Microbe*. 29:250-266.
Nemergut, D.R., Schmidt, S.K., Fukami, T., O'Neill, S.P., Bilinski, T.M., Stanish, L.F., Knelman, J.E. et al. 2013. Patterns and processes of microbial community assembly. *Microbiol. Mol. Biol. Rev.* 77:342–356.
Neori, A., Chopin, T., Troell, M., Buschmann, A.H., Kraemer, G.P., Halling, C., Shpigel, M. et al. 2004. Integrated aquaculture: Rationale, evolution and state of the art emphasizing seaweed biofiltration in modern mariculture. *Aquaculture*. 231:361–391.
Nguyen, L.T., Schmidt, H.A., Von Haeseler, A. & Minh, B.Q. 2015. IQ-TREE: A fast and effective stochastic algorithm for estimating maximum-likelihood phylogenies. *Mol. Biol. Evol.* 32:268–274.
Nissimov, J.I., Campbell, C.N., Probert, I. & Wilson, W.H. 2022. Aquatic virus culture collection: An absent (but necessary) safety net for environmental microbiologists. *Appl. Phycol.* 3:211–225.
Nunes, J., McCoy, S.J., Findlay, H.S., Hopkins, F.E., Kitidis, V., Queirós, A.M., Rayner, L. et al. 2016. Two intertidal, non-calcifying macroalgae (*Palmaria palmata* and *Saccharina latissima*) show complex and variable responses to short-term CO_2 acidification. *ICES J. Mar. Sci.* 73:887–896.
Nygaard, A.B., Tunsjø, H.S., Meisal, R. & Charnock, C. 2020. A preliminary study on the potential of Nanopore MinION and Illumina MiSeq 16S rRNA gene sequencing to characterize building-dust microbiomes. *Sci. Rep.* 10:3209.
Nylander, J.A.A. 2004. MrModeltest2. *Evol. Biol. Cent. Upps. Univ.* 2:1–2.
Nylund, G.M., Persson, F., Lindegarth, M., Cervin, G., Hermansson, M. & Pavia, H. 2010. The red alga *Bonnemaisonia asparagoides* regulates epiphytic bacterial abundance and community composition by chemical defence. *FEMS Microbiol. Ecol.* 71:84–93.
Ojaveer, H., Jaanus, A., Mackenzie, B.R., Martin, G., Olenin, S., Radziejewska, T., Telesh, I. et al. 2010. Status of biodiversity in the Baltic Sea. *PLoS ONE*. 5:1–19.
Oksanen, J., Blanchet, F.G., Friendly, M., Kindt, R., Legendre, P., McGlinn, D., Minchin, P.R. et al. 2020. Vegan: Community ecology package. R package version 2.5-7.
Olanrewaju, O.S., Glick, B.R. & Babalola, O.O. 2017. Mechanisms of action of plant growth promoting bacteria. *World J. Microbiol. Biotechnol.* 33:197.

Oliveira, L.S.D., Gregoracci, G.B., Gueiros, G., Silva, Z., Salgado, L.T., Filho, G.A., Alves-ferreira, M. et al. 2012. Transcriptomic analysis of the red seaweed *Laurencia dendroidea* (Florideophyceae, Rhodophyta) and its microbiome. *BMC Genomics*. 13:1–13.

Olm, M.R., Brown, C.T., Brooks, B. & Banfield, J.F. 2017. dRep: a tool for fast and accurate genomic comparisons that enables improved genome recovery from metagenomes through de-replication. *ISME J.* 11:2864–2868.

Olofsson, M., Hagan, J.G., Karlson, B. & Gamfeldt, L. 2020. Large seasonal and spatial variation in nano- and microphytoplankton diversity along a Baltic Sea—North Sea salinity gradient. *Sci. Rep.* 10:1–12.

Olsson, J., Raikova, S., Mayers, J.J., Steinhagen, S., Chuck, C.J., Nylund, G.M. & Albers, E. 2020a. Effects of geographical location on potentially valuable components in *Ulva intestinalis* sampled along the Swedish coast. *Appl. Phycol.* 1:80–92.

Olsson, J., Toth, G.B., Oerbekke, A., Cvijetinovic, S., Wahlström, N., Harrysson, H., Steinhagen, S. et al. 2020b. Cultivation conditions affect the monosaccharide composition in *Ulva fenestrata*. *J. Appl. Phycol.* 32:3255–3263.

Ondov, B.D., Bergman, N.H. & Phillippy, A.M. 2011. Interactive metagenomic visualization in a web browser. *BMC Bioinformatics*. 12:385.

Ortiz-Baez, A.S., Shi, M., Hoffmann, A.A. & Holmes, E.C. 2021. RNA virome diversity and *Wolbachia* infection in individual *Drosophila simulans* flies. *J. Gen. Virol.* 102:001639.

Oshone, R., Ngom, M., Chu, F., Mansour, S., Sy, M.O., Champion, A. & Tisa, L.S. 2017. Genomic, transcriptomic, and proteomic approaches towards understanding the molecular mechanisms of salt tolerance in *Frankia* strains isolated from Casuarina trees. *BMC Genomics*. 18:633.

Osterhage, C., Kaminsky, R., König, G.M. & Wright, A.D. 2000. Ascosalipyrrolidinone A, an antimicrobial alkaloid, from the obligate marine fungus *Ascochyta salicorniae*. *J. Org. Chem.* 65:6412–6417.

Oxford Nanopore Technologies 2021. Accuracy. Available At: https://nanoporetech.com/accuracy.

Oxford Nanopore Technologies 2018. Medaka: Sequence correction provided by ONT Research.

Paix, B., Carriot, N., Barry-martinet, R. & Greff, S. 2020. A multi-omics analysis suggests links between the differentiated surface metabolome and epiphytic microbiota along the thallus of a mediterranean seaweed holobiont. *Front. Microbiol.* 11:10.3389/fmicb.2020.00494.

Paix, B., Potin, P., Schires, G., Le Poupon, C., Misson, B., Leblanc, C., Culioli, G. et al. 2021. Synergistic effects of temperature and light affect the relationship between *Taonia atomaria* and its epibacterial community: A controlled conditions study. *Environ. Microbiol.* 23:6777–6797.

Park, C.S., Sakaguchi, K., Kakinuma, M. & Amano, H. 2000. Comparison of the morphological and physiological features of the red rot disease fungus *Pythium* sp. isolated from *Porphyra yezoensis* from Korea and Japan. *Fish. Sci.* 66:261–269.

Park, S.-C. & Won, S. 2018. Evaluation of 16S rRNA databases for taxonomic assignments using a mock community. *Genomics Inform.* 16:e24.

Parks, D.H., Chuvochina, M., Waite, D.W., Rinke, C., Skarshewski, A., Chaumeil, P.-A. & Hugenholtz, P. 2018. A standardized bacterial taxonomy based on genome phylogeny substantially revises the tree of life. *Nat. Biotechnol.* 36:996–1004.

Parks, D.H., Imelfort, M., Skennerton, C.T., Hugenholtz, P. & Tyson, G.W. 2015. CheckM: Assessing the quality of microbial genomes recovered from isolates, single cells, and metagenomes. *Genome Res.* 25:1043–1055.

Parthasarathy, R., Chandrika, M., Yashavantha Rao, H.C., Kamalraj, S., Jayabaskaran, C. & Pugazhendhi, A. 2020. Molecular profiling of marine endophytic fungi from green algae: Assessment of antibacterial and anticancer activities. *Process Biochem.* 96:11–20.

Patel, P., Callow, M.E., Joint, I. & Callow, J. a 2003. Specificity in the settlement–modifying response of bacterial biofilms towards zoospores of the marine alga *Enteromorpha*. *Environ. Microbiol.* 5:338–349.

Patyshakuliyeva, A., Falkoski, D.L., Wiebenga, A., Timmermans, K. & Vries, R.P.D. 2019. Macroalgae derived fungi have high abilities to degrade algal polymers. *Microorganisms*. 8:1–16.

Payne, A., Holmes, N., Clarke, T., Munro, R., Debebe, B. & Loose, M. 2020. Readfish enables targeted nanopore sequencing of gigabase-sized genomes. *Nat. Biotechnol.* 39:442–450.

Peixoto, R.S., Rosado, P.M., Leite, D.C. de A., Rosado, A.S. & Bourne, D.G. 2017. Beneficial microorganisms for corals (BMC): Proposed mechanisms for coral health and resilience. *Front. Microbiol.* 8:1–16.

Pervez, M.T., Hasnain, M.J.U., Abbas, S.H., Moustafa, M.F., Aslam, N. & Shah, S.S.M. 2022. A comprehensive review of performance of next-generation sequencing platforms. *BioMed Res. Int.* 2022:1–12.

Pessarrodona, A., Assis, J., Filbee-Dexter, K., Burrows, M.T., Gattuso, J.-P., Duarte, C.M., Krause-Jensen, D. et al. 2022. Global seaweed productivity. *Sci. Adv.* 8:eabn2465.

Piedade, G.J., Wesdorp, E.M., Montenegro-Borbolla, E., Maat, D.S. & Brussaard, C.P.D. 2018. Influence of irradiance and temperature on the virus MpoV-45T infecting the Arctic picophytoplankter *Micromonas polaris*. 10:676.

Pintado, J., Del Olmo, G., Guinebert, T., Ruiz, P., Nappi, J., Thomas, T., Egan, S. et al. 2023. Manipulating the *Ulva* holobiont: Co-culturing *Ulva ohnoi* with *Phaeobacter* bacteria as a strategy for disease control in fish-macroalgae IMTA-RAS aquaculture. *J. Appl. Phycol.* 35:2017–2029.

Pires, D.P., Melo, L.D.R. & Azeredo, J. 2021. Understanding the complex phage-host interactions in biofilm communities. *Annu. Rev. Virol.* 8:73–94.

Pita, L., Rix, L., Slaby, B.M., Franke, A. & Hentschel, U. 2018. The sponge holobiont in a changing ocean: From microbes to ecosystems. *Microbiome*. 6:46.

Polikovsky, M., Califano, G., Dunger, N., Wichard, T. & Golberg, A. 2020. Engineering bacteria-seaweed symbioses for modulating the photosynthate content of *Ulva* (Chlorophyta): Significant for the feedstock of bioethanol production. *Algal Res.* 49:101945.

Props, R., Monsieurs, P., Mysara, M., Clement, L. & Boon, N. 2016. Measuring the biodiversity of microbial communities by flow cytometry. *Methods Ecol. Evol.* 7:1376–1385.

Provasoli, L. 1958. Effect of plant hormones on *Ulva*. *Biol. Bull.* 114:375–384.

Provasoli, L. 1968. Media and prospects for the cultivation of marine algae. *In Cultures and Collections of Algae*. Hakone, pp.

12–15.
Qiu, Z., Coleman, M.A., Provost, E., Campbell, A.H., Kelaher, B.P., Dalton, S.J., Thomas, T. et al. 2019a. Future climate change is predicted to affect the microbiome and condition of habitat-forming kelp. *Proc. R. Soc. B Biol. Sci.* 286: 10.1098.
Qiu, Z., Egidi, E., Liu, H., Kaur, S. & Singh, B.K. 2019b. New frontiers in agriculture productivity: Optimised microbial inoculants and in situ microbiome engineering. *Biotechnol. Adv.* 37:107371.
Qu, T., Zhao, X., Hao, Y., Zhong, Y., Guan, C., Hou, C., Tang, X. et al. 2020. Ecological effects of *Ulva prolifera* green tide on bacterial community structure in Qingdao offshore environment. *Chemosphere*. 244:125477.
Quast, C., Pruesse, E., Yilmaz, P., Gerken, J., Schweer, T., Yarza, P., Peplies, J. et al. 2013. The SILVA ribosomal RNA gene database project: Improved data processing and web-based tools. *Nucleic Acids Res.* 41:590–596.
R Core Team 2020. R: A language and environment for statistical computing. R Foundation for Statistical Computing. Vienna, Austria.
Rahaweman, A.C., Pamungkas, J., Madduppa, H., Thoms, C. & Tarman, K. 2016. Screening of endophytic fungi from chlorophyta and phaeophyta for antibacterial activity. *IOP Conf. Ser. Earth Environ. Sci.* 31:012026.
Rajeev, R., Adithya, K.K., Kiran, G.S. & Selvin, J. 2021. Healthy microbiome: a key to successful and sustainable shrimp aquaculture. *Rev. Aquac.* 13:238–258.
Ramírez-Puebla, S.T., Weigel, B.L., Jack, L., Schlundt, C., Pfister, C.A. & Mark Welch, J.L. 2022. Spatial organization of the kelp microbiome at micron scales. *Microbiome*. 10:1–20.
Rapala-Kozik, M., Wolak, N., Kujda, M. & Banas, A.K. 2012. The upregulation of thiamine (vitamin B_1) biosynthesis in *Arabidopsis thaliana* seedlings under salt and osmotic stress conditions is mediated by abscisic acid at the early stages of this stress response. *BMC Plant Biol.* 12:2.
Rath, K.M., Fierer, N., Murphy, D.V. & Rousk, J. 2019. Linking bacterial community composition to soil salinity along environmental gradients. *ISME J.* 13:836–846.
Ratzke, C., Barrere, J. & Gore, J. 2020. Strength of species interactions determines biodiversity and stability in microbial communities. *Nat. Ecol. Evol.* 4:376–383.
Reisky, L., Préchoux, A., Zühlke, M.K., Bäumgen, M., Robb, C.S., Gerlach, N., Roret, T. et al. 2019. A marine bacterial enzymatic cascade degrades the algal polysaccharide ulvan. *Nat. Chem. Biol.* 15:803–812.
Reisky, L., Stanetty, C., Mihovilovic, M.D., Schweder, T., Hehemann, J.H. & Bornscheuer, U.T. 2018. Biochemical characterization of an ulvan lyase from the marine flavobacterium *Formosa agariphila* KMM 3901T. *Appl. Microbiol. Biotechnol.* 102:6987–6996.
Remus-Emsermann, M.N.P., Lücker, S., Müller, D.B., Potthoff, E., Daims, H. & Vorholt, J.A. 2014. Spatial distribution analyses of natural phyllosphere-colonizing bacteria on *Arabidopsis thaliana* revealed by fluorescence *in situ* hybridization. *Environ. Microbiol.* 16:2329–2340.
Ren, C.-G., Liu, Z.-Y., Zhong, Z.-H., Wang, X.-L. & Qin, S. 2022. Integrated biotechnology to mitigate green tides. *Environ. Pollut.* 309:119764.
Reusch, T.B.H., Dierking, J., Andersson, H.C., Bonsdorff, E., Carstensen, J., Casini, M., Czajkowski, M. et al. 2018. The Baltic Sea as a time machine for the future coastal ocean. *Sci. Adv.* 4:eaar8195.
Riquelme, C., Rojas, A., Flores, V. & Correa, J.A. 1997. Epiphytic bacteria in a copper-enriched environment in northern Chile. *Mar. Pollut. Bull.* 34:816–820.
Risely, A. 2020. Applying the core microbiome to understand host–microbe systems. *J. Anim. Ecol.* 89:1549–1558.
Robledo, D.R., Sosa, P.A., Carcia-Reina, G. & Muller, D.G. 1994. Photosynthetic performance of healthy and virus-infected *Feldmannia irregularis* and *F. simplex* (Phaeophyceae). *Eur. J. Phycol.* 29:247–251.
Rodríguez-Verdugo, A., Buckley, J. & Stapley, J. 2017. The genomic basis of eco-evolutionary dynamics. *Mol. Ecol.* 26:1456–1464.
Roleda, M.Y. & Hurd, C.L. 2019. Seaweed nutrient physiology: application of concepts to aquaculture and bioremediation. *Phycologia*. 58:552–562.
Rosario, K., Breitbart, M., Harrach, B., Segalés, J., Delwart, E., Biagini, P. & Varsani, A. 2017. Revisiting the taxonomy of the family *Circoviridae*: establishment of the genus *Cyclovirus* and removal of the genus *Gyrovirus*. *Arch. Virol.* 162:1447–1463.
Rosenberg, E. & Zilber-Rosenberg, I. 2016. Microbes drive evolution of animals and plants: The hologenome concept. *mBio*. 7:1–8.
Roth-Schulze, A.J., Pintado, J., Zozaya-Valdés, E., Cremades, J., Ruiz, P., Kjelleberg, S. & Thomas, T. 2018. Functional biogeography and host specificity of bacterial communities associated with the marine green alga *Ulva* spp. *Mol. Ecol.* 27:1952–1965.
Roth-Schulze, A.J., Zozaya-Valdés, E., Steinberg, P.D. & Thomas, T. 2016. Partitioning of functional and taxonomic diversity in surface-associated microbial communities. *Environ. Microbiol.* 18:4391–4402.
Rowe, O.F., Dinasquet, J., Paczkowska, J., Figueroa, D., Riemann, L. & Andersson, A. 2018. Major differences in dissolved organic matter characteristics and bacterial processing over an extensive brackish water gradient, the Baltic Sea. *Mar. Chem.* 202:27–36.
Ruiz-Perez, C.A., Conrad, R.E. & Konstantinidis, K.T. 2021. MicrobeAnnotator: a user-friendly, comprehensive functional annotation pipeline for microbial genomes. *BMC Bioinformatics*. 22:11.
Ryback, B., Bortfeld-Miller, M. & Vorholt, J.A. 2022. Metabolic adaptation to vitamin auxotrophy by leaf-associated bacteria. *ISME J.* 16:2712–2724.
Rybak, A.S. 2018. Species of *Ulva* (Ulvophyceae, Chlorophyta) as indicators of salinity. *Ecol. Indic.* 85:253–261.
Sabanadzovic, S., Nibert, M.L., Krupovic, M., Tzanetakis, I.E. & Valverde, R.A. 2018. Reorganization of the family *Amalgaviridae* by recognizing five new species in the genus *Amalgavirus* and creating a new genus *Zybavirus*. ICTV proposal 2018.032P.
Saha, M., Dove, S. & Weinberger, F. 2020a. Chemically mediated microbial "gardening" capacity of a seaweed holobiont is

dynamic. *Microorganisms*. 8:1893.
Saha, M., Ferguson, R.M.W., Dove, S., Künzel, S., Meichssner, R., Neulinger, S.C., Petersen, F.O. et al. 2020b. Salinity and time can alter epibacterial communities of an invasive seaweed. *Front. Microbiol.* 10:1–16.
Saha, M., Rempt, M., Stratil, S.B., Wahl, M., Pohnert, G. & Weinberger, F. 2014. Defence chemistry modulation by light and temperature shifts and the resulting effects on associated epibacteria of *Fucus vesiculosus*. *PLoS ONE*. 9: e105333.
Saha, M. & Weinberger, F. 2019. Microbial "gardening" by a seaweed holobiont: Surface metabolites attract protective and deter pathogenic epibacterial settlement. *J. Ecol.* 107:2255–2265.
Šajbidor, J. 1997. Effect of some environmental factors on the content and composition of microbial membrane lipids. *Crit. Rev. Biotechnol.* 17:87–103.
Salles, J.F., Poly, F., Schmid, B., Roux, X.L., Poly, F., Schmid, B. & Roux, X.L. 2009. Community niche predicts the functioning of denitrifying bacterial assemblages. 90:3324–3332.
Sand-Jensen, K. 1988. Minimum light requirements for growth in *Ulva lactuca*. *Mar. Ecol. Prog. Ser.* 50:187–193.
Santos, A., van Aerle, R., Barrientos, L. & Martinez-Urtaza, J. 2020. Computational methods for 16S metabarcoding studies using Nanopore sequencing data. *Comput. Struct. Biotechnol. J.* 18:296–305.
Sato, Y., Miyazaki, N., Kanematsu, S., Xie, J., Ghabrial, S.A., Hillman, B.I. & Suzuki, N. 2019. ICTV virus taxonomy profile: *Megabirnaviridae*. *J. Gen. Virol.* 100:1269–1270.
Sauvage, T., Schmidt, W.E., Yoon, H.S., Paul, V.J. & Fredericq, S. 2019. Promising prospects of nanopore sequencing for algal hologenomics and structural variation discovery. *BMC Genomics*. 20:1–17.
Schneider, C.A., Rasband, W.S. & Eliceiri, K.W. 2012. NIH Image to ImageJ: 25 years of image analysis. *Nat. Methods*. 9:671–675.
Scholz, S., Serif, M., Schleheck, D., Sayer, M.D.J., Cook, A.M. & Küpper, F.C. 2021. Sulfoquinovose metabolism in marine algae. *Bot. Mar.* 64:301–212.
Sebök, S., Herppich, W.B. & Hanelt, D. 2019. Outdoor cultivation of *Ulva lactuca* in a recently developed ring-shaped photobioreactor: effects of elevated CO_2 concentration on growth and photosynthetic performance. *Bot. Mar.* 62:179–190.
Seemann, T. 2014. Prokka: rapid prokaryotic genome annotation. *Bioinformatics*. 30:2068–2069.
Seidel, M., Manecki, M., Herlemann, D.P.R., Deutsch, B., Schulz-Bull, D., Jürgens, K. & Dittmar, T. 2017. Composition and transformation of dissolved organic matter in the Baltic Sea. *Front. Earth Sci.* 5:1–20.
Sévin, D.C. & Sauer, U. 2014. Ubiquinone accumulation improves osmotic-stress tolerance in *Escherichia coli*. *Nat. Chem. Biol.* 10:266–272.
Sévin, D.C., Stählin, J.N., Pollak, G.R., Kuehne, A. & Sauer, U. 2016. Global metabolic responses to salt stress in fifteen species. *PLOS ONE*. 11:e0148888.
Shade, A. & Handelsman, J. 2012. Beyond the Venn diagram: The hunt for a core microbiome. *Environ. Microbiol.* 14:4–12.
Shade, A. & Stopnisek, N. 2019. Abundance-occupancy distributions to prioritize plant core microbiome membership. *Curr. Opin. Microbiol.* 49:50–58.
Sharma, P.V. & Thaiss, C.A. 2020. Host-microbiome interactions in the era of single-cell biology. *Front. Cell. Infect. Microbiol.* 10:569070.
Shi, H., Shi, Q., Grodner, B., Lenz, J.S., Zipfel, W.R., Brito, I.L. & De Vlaminck, I. 2020. Highly multiplexed spatial mapping of microbial communities. *Nature*. 588:676–681.
Shin, J., Lee, S., Go, M.J., Lee, S.Y., Kim, S.C., Lee, C.H. & Cho, B.K. 2016. Analysis of the mouse gut microbiome using full-length 16S rRNA amplicon sequencing. *Sci. Rep.* 6:1–10.
Shishlyannikov, S.M., Zakharova, Y.R., Volokitina, N.A., Mikhailov, I.S., Petrova, D.P. & Likhoshway, Y.V. 2011. A procedure for establishing an axenic culture of the diatom *Synedra acus* subsp. *radians* (Kütz.) Skabibitsch. from Lake Baikal. *Limnol. Oceanogr. Methods*. 9:478–484.
Sieber, C.M.K., Probst, A.J., Sharrar, A., Thomas, B.C., Hess, M., Tringe, S.G. & Banfield, J.F. 2018. Recovery of genomes from metagenomes via a dereplication, aggregation and scoring strategy. *Nat. Microbiol.* 3:836–843.
Simon, J.-C., Marchesi, J.R., Mougel, C. & Selosse, M.-A. 2019. Host-microbiota interactions: from holobiont theory to analysis. *Microbiome*. 7:5.
Singh, R.P., Mantri, V.A., Reddy, C.R.K. & Jha, B. 2011. Isolation of seaweed-associated bacteria and their morphogenesis-inducing capability in axenic cultures of the green alga *Ulva fasciata*. *Aquat. Biol.* 12:13–21.
Skrodenytė-Arbačiauskienė, V., Virbickas, T., Lukša, J., Servienė, E., Blažytė-Čereškienė, L. & Kesminas, V. 2021. Gut microbiome of wild Baltic salmon (*Salmo salar* L.) Parr. *Microb. Ecol.* 84:1294–1298.
Sleator, R.D. & Hill, C. 2002. Bacterial osmoadaptation: The role of osmolytes in bacterial stress and virulence. *FEMS Microbiol. Rev.* 26:49–71.
Smetacek, V. & Zingone, A. 2013. Green and golden seaweed tides on the rise. *Nature*. 504:84–88.
Snoeijs, P. 1999. Chapter 12 Marine and brackish waters. *In Swedish Plant Geography*. Uppsala, pp. 187–212.
Sohn, B.K., Kim, K.Y., Chung, S.J., Kim, W.S., Park, S.M., Kang, J.G., Rim, Y.S. et al. 2003. Effect of the different timing of AMF inoculation on plant growth and flower quality of chrysanthemum. *Sci. Hortic.* 98:173–183.
Song, W., Zhang, S., Majzoub, M.E., Egan, S., Kjelleberg, S. & Thomas, T. 2023. The impact of interspecific competition on the genomic evolution of *Phaeobacter inhibens* and *Pseudoalteromonas tunicata* during biofilm growth. *Environ. Microbiol.* 1462-2920.16553.
Spalding, H.L., Conklin, K.Y., Smith, C.M., O'Kelly, C.J. & Sherwood, A.R. 2016. New Ulvaceae (Ulvophyceae, Chlorophyta) from mesophotic ecosystems across the Hawaiian Archipelago. *J. Phycol.* 52:40–53.
Spoerner, M., Wichard, T., Bachhuber, T., Stratmann, J. & Oertel, W. 2012. Growth and thallus morphogenesis of *Ulva mutabilis* (Chlorophyta) depends on a combination of two bacterial species excreting regulatory factors. *J. Phycol.* 48:1433–1447.
Stamatakis, A. 2014. RAxML version 8: A tool for phylogenetic analysis and post-analysis of large phylogenies. *Bioinformat-*

ics. 30:1312–1313.
Stedt, K., Steinhagen, S., Trigo, J.P., Kollander, B., Undeland, I., Toth, G.B., Wendin, K. et al. 2022. Post-harvest cultivation with seafood process waters improves protein levels of *Ulva fenestrata* while retaining important food sensory attributes. *Front. Mar. Sci.* 9:991359.
Steinegger, M. & Söding, J. 2018. Clustering huge protein sequence sets in linear time. *Nat. Commun.* 9:2542.
Steinhagen, S., Düsedau, L. & Weinberger, F. 2021a. DNA barcoding of the German green supralittoral zone indicates the distribution and phenotypic plasticity of Blidingia species and reveals Blidingia cornuta sp. nov. *Taxon*. 70:1–17.
Steinhagen, S., Enge, S., Cervin, G., Larsson, K., Edlund, U., Schmidt, A.E.M., Wahlström, N. et al. 2022a. Harvest time can affect the optimal yield and quality of sea lettuce (*Ulva fenestrata*) in a sustainable sea-based cultivation. *Front. Mar. Sci.* 9:816890.
Steinhagen, S., Enge, S., Larsson, K., Olsson, J., Nylund, G.M., Albers, E., Pavia, H. et al. 2021b. Sustainable large-scale aquaculture of the northern hemisphere sea lettuce, *Ulva fenestrata*, in an off-shore seafarm. *J. Mar. Sci. Eng.* 9:615.
Steinhagen, S., Hoffmann, S., Pavia, H. & Toth, G.B. 2023. Molecular identification of the ubiquitous green algae *Ulva* reveals high biodiversity, crypticity, and invasive species in the Atlantic-Baltic Sea region. *Algal Res.* 73:103132.
Steinhagen, S., Karez, R. & Weinberger, F. 2019a. Cryptic, alien and lost species: molecular diversity of *Ulva* sensu lato along the German coasts of the North and Baltic Seas. *Eur. J. Phycol.* 54:466–83.
Steinhagen, S., Larsson, K., Olsson, J., Albers, E., Undeland, I., Pavia, H. & Toth, G.B. 2022b. Closed life-cycle aquaculture of sea lettuce (*Ulva fenestrata*): Performance and biochemical profile differ in early developmental stages. *Front. Mar. Sci.* 9:942679.
Steinhagen, S., Weinberger, F. & Karez, R. 2019b. Molecular analysis of *Ulva compressa* (Chlorophyta, Ulvales) reveals its morphological plasticity, distribution and potential invasiveness on German North Sea and Baltic Sea coasts. *Eur. J. Phycol.* 54:102–114.
Stepanauskas, R., JØrgensen, N.O.G., Eigaard, O.R., Žvikas, A., Tranvik, L.J. & Leonardson, L. 2002. Summer inputs of riverine nutrients to the Baltic Sea: bioavailability and eutrophication relevance. *Ecol. Monogr.* 72:579–597.
Stewart, G.R. & Larher, F. 1980. Accumulation of amino acids and related compounds in relation to environmental stress. *In Amino Acids and Derivatives*. Elsevier, pp. 609–635.
Stiger-Pouvreau, V. & Zubia, M. 2020. Macroalgal diversity for sustainable biotechnological development in French tropical overseas territories. *Bot. Mar.* 63:17–41.
Storero, L.P., Avaca, M.S. & Roche, A. 2022. Living under *Ulva* canopy: The case of the scavenger snail *Buccinastrum deforme* in a eutrophic macrotidal bay in Patagonia (Argentina). *Mar. Ecol.* 43:e12718.
Stratil, S.B., Neulinger, S.C., Knecht, H., Friedrichs, A.K. & Wahl, M. 2014. Salinity affects compositional traits of epibacterial communities on the brown macroalga *Fucus vesiculosus*. *FEMS Microbiol. Ecol.* 88:272–279.
Stratmann, J., Paputsoglu, G. & Oertel, W. 1996. Differentiation of *Ulva mutabilis* (Chlorophyta) gametangia and gamete release are controlled by extracellular inhibitors. *J. Phycol.* 32:1009–1021.
Sung, M.-S., Hsu, Yi-Ting, Hsu, Yuan-Ting, Wu, T.-M. & Lee, T.-M. 2009. Hypersalinity and hydrogen peroxide upregulation of gene expression of antioxidant enzymes in *Ulva fasciata* against oxidative stress. *Mar. Biotechnol.* 11:199–209.
Suttle, C.A. 2007. Marine viruses — major players in the global ecosystem. *Nat. Rev. Microbiol.* 5:801–812.
Svoboda, P., Lindström, E.S., Ahmed Osman, O. & Langenheder, S. 2018. Dispersal timing determines the importance of priority effects in bacterial communities. *ISME J.* 12:644–646.
Syukur, S., Richmond, J., Majzoub, M.E., Nappi, J., Egan, S. & Thomas, T. 2023. Not all parents are the same: Diverse strategies of symbiont transmission in seaweeds. *Environ. Microbiol.* 1462-2920.16564.
Tang, T., Cao, S., Zhu, B. & Li, Q. 2021. Ulvan polysaccharide-degrading enzymes: An updated and comprehensive review of sources category, property, structure, and applications of ulvan lyases. *Algal Res.* 60:102477.
Telesh, I.V. & Khlebovich, V.V. 2010. Principal processes within the estuarine salinity gradient: A review. *Mar. Pollut. Bull.* 61:149–155.
Thekke-Veetil, T., Lagos-Kutz, D., McCoppin, N.K., Hartman, G.L., Ju, H.K., Lim, H.S. & Domier, L.L. 2020. Soybean thrips (Thysanoptera: Thripidae) harbor highly diverse populations of arthropod, fungal and plant viruses. *Viruses*. 12:1376.
Thomas, F., Dittami, S.M., Brunet, M., Le Duff, N., Tanguy, G., Leblanc, C. & Gobet, A. 2019. Evaluation of a new primer combination to minimize plastid contamination in 16S rDNA metabarcoding analyses of alga-associated bacterial communities. *Environ. Microbiol. Rep.* 12:30–37.
Timmusk, S., Behers, L., Muthoni, J., Muraya, A. & Aronsson, A.C. 2017. Perspectives and challenges of microbial application for crop improvement. *Front. Plant Sci.* 8:1–10.
Toth, G.B., Harrysson, H., Wahlström, N., Olsson, J., Oerbekke, A., Steinhagen, S., Kinnby, A. et al. 2020. Effects of irradiance, temperature, nutrients, and pCO_2 on the growth and biochemical composition of cultivated *Ulva fenestrata*. *J. Appl. Phycol.* 32:3243–3254.
Tóth, T.N., Chukhutsina, V., Domonkos, I., Knoppová, J., Komenda, J., Kis, M., Lénárt, Z. et al. 2015. Carotenoids are essential for the assembly of cyanobacterial photosynthetic complexes. *Biochim. Biophys. Acta BBA - Bioenerg.* 1847:1153–1165.
Tran, L.-A.T., Vieira, C., Steinhagen, S., Maggs, C.A., Hiraoka, M., Shimada, S., Van Nguyen, T. et al. 2022. An appraisal of *Ulva* (Ulvophyceae, Chlorophyta) taxonomy. *J. Appl. Phycol.* 34:2689–2703.
Trigo, J.P., Engström, N., Steinhagen, S., Juul, L., Harrysson, H., Toth, G.B., Pavia, H. et al. 2021. In vitro digestibility and Caco-2 cell bioavailability of sea lettuce (*Ulva fenestrata*) proteins extracted using pH-shift processing. *Food Chem.* 356:129683.
Tujula, N.A., Crocetti, G.R., Burke, C., Thomas, T., Holmström, C. & Kjelleberg, S. 2010. Variability and abundance of the epiphytic bacterial community associated with a green marine Ulvacean alga. *ISME J.* 4:301–311.
Turnbaugh, P.J., Ley, R.E., Hamady, M., Fraser-Liggett, C.M., Knight, R. & Gordon, J.I. 2007. The Human Microbiome Project. *Nature*. 449:804–810.
Tuya, F., Wernberg, T. & Thomsen, M.S. 2008. The spatial arrangement of reefs alters the ecological patterns of fauna between

interspersed algal habitats. *Estuar. Coast. Shelf Sci.* 78:774–782.
Tyler, A.C., McGlathery, K.J. & Anderson, I.C. 2003. Benthic algae control sediment-water column fluxes of organic and inorganic nitrogen compounds in a temperate lagoon. *Limnol. Oceanogr.* 48:2125–2137.
Tyler, A.C., McGlathery, K.J. & Macko, S.A. 2005. Uptake of urea and amino acids by the macroalgae *Ulva lactuca* (Chlorophyta) and *Gracilaria vermiculophylla* (Rhodophyta). *Mar. Ecol. Prog. Ser.* 294:161–172.
Van Alstyne, K.L., Koellermeier, L. & Nelson, T.A. 2007. Spatial variation in dimethylsulfoniopropionate (DMSP) production in *Ulva lactuca* (Chlorophyta) from the Northeast Pacific. *Mar. Biol.* 150:1127–1135.
van der Loos, L.M., De Coninck, L., Zell, R., Lequime, S., Willems, A., De Clerck, O. & Matthijnssens, J. 2023. Highly divergent CRESS DNA and picorna-like viruses associated with bleached thalli of the green seaweed *Ulva*. *Microbiol. Spectr.* 11:5 e00255-23.
van der Loos, L.M., De Wilde, C., Willems, A., De Clerck. O. & Steinhagen, S. (2024) The cultivated sea lettuce (*Ulva*) microbiome: Successional and seasonal dynamics. *Aquaculture* 585: 740692
van der Loos, L.M., D'hondt, S., Engelen, A.H., Pavia, H., Toth, G.B., Willems, A., Weinberger, F. et al. 2022. Salinity and host drive *Ulva* associated bacterial communities across the Atlantic-Baltic Sea gradient. *Mol. Ecol.* 10.1111/mec.16462.
van der Loos, L.M., D'hondt, S., Willems, A. & De Clerck, O. 2021. Characterizing algal microbiomes using long-read nanopore sequencing. *Algal Res.* 59:102456.
van der Loos, L.M., Eriksson, B.K. & Falcão Salles, J. 2019. The macroalgal holobiont in a changing sea. *Trends Microbiol.* 27:635–650.
Van Etten, J.L., Graves, M.V., Müller, D.G., Boland, W. & Delaroque, N. 2002. *Phycodnaviridae* - Large DNA algal viruses. *Arch. Virol.* 147:1479–1516.
Vardi, A., Haramaty, L., Van Mooy, B.A.S., Fredricks, H.F., Kimmance, S.A., Larsen, A. & Bidle, K.D. 2012. Host–virus dynamics and subcellular controls of cell fate in a natural coccolithophore population. *Proc. Natl. Acad. Sci.* 109:19327–19332.
Vaser, R., Sović, I., Nagarajan, N. & Šikić, M. 2017. Fast and accurate de novo genome assembly from long uncorrected reads. *Genome Res.* 27:737–746.
Vergani, L., Patania, J., Riva, V., Nerva, L., Nuzzo, F., Gambino, G., Borin, S. et al. 2024. Deciphering the interaction of bacteria inoculants with the recipient endophytic community in grapevine micropropagated plants. *Appl. Environ. Microbiol.* 90:e02078-23.
Vermaat, J.E. & Sand-Jensen, K. 1987. Survival, metabolism and growth of *Ulva lactuca* under winter conditions: A laboratory study of bottlenecks in the life cycle. *Mar. Biol.* 95:55–61.
Vesty, E.F., Kessler, R.W., Wichard, T. & Coates, J.C. 2015. Regulation of gametogenesis and zoosporogenesis in *Ulva linza* (Chlorophyta): Comparison with *Ulva mutabilis* and potential for laboratory culture. *Front. Plant Sci.* 6:1–8.
Vieira, H.H., Bagatini, I.L., Guinart, C.M. & Vieira, A.A.H. 2016. *tuf*A gene as molecular marker for freshwater Chlorophyceae. *ALGAE*. 31:155–165.
Vierstraete, A.R. & Braeckman, B.P. 2022. Amplicon_sorter: A tool for reference-free amplicon sorting based on sequence similarity and for building consensus sequences. *Ecol. Evol.* 12:1–17.
Villnäs, A. & Norkko, A. 2011. Benthic diversity gradients and shifting baselines: Implications for assessing environmental status. *Ecol. Appl.* 21:2172–2186.
Vlok, M., Lang, A.S. & Suttle, C.A. 2019. Marine RNA virus quasispecies are distributed throughout the oceans. *mSphere*. 4: e00157.
Wahl, M., Goecke, F., Labes, A., Dobretsov, S. & Weinberger, F. 2012. The second skin: Ecological role of epibiotic biofilms on marine organisms. *Front. Microbiol.* 3:1–21.
Wahl, M., ShahnazL., Dobretsov, S., Saha, M., Symanowski, F., DavidK., Lachnit, T. et al. 2010. Ecology of antifouling resistance in the bladder wrack *Fucus vesiculosus*: Patterns of microfouling and antimicrobial protection. *Mar. Ecol. Prog. Ser.* 411:33–48.
Wahlström, N., Nylander, F., Malmhäll-Bah, E., Sjövold, K., Edlund, U., Westman, G. & Albers, E. 2020a. Composition and structure of cell wall ulvans recovered from *Ulva* spp. along the Swedish west coast. *Carbohydr. Polym.* 233:115852.
Wahlström, N., Steinhagen, S., Toth, G., Pavia, H. & Edlund, U. 2020b. Ulvan dialdehyde-gelatin hydrogels for removal of heavy metals and methylene blue from aqueous solution. *Carbohydr. Polym.* 249:116841.
Wan, A.H.L., Wilkes, R.J., Heesch, S., Bermejo, R., Johnson, M.P. & Morrison, L. 2017. Assessment and characterisation of Ireland's green tides (*Ulva* species). *PLoS ONE*. 12:e0169049.
Wang, H., Elyamine, A.M., Liu, Y., Liu, W., Chen, Q., Xu, Y., Peng, T. et al. 2022. *Hyunsoonleella* sp. HU1-3 increased the biomass of *Ulva fasciata*. *Front. Microbiol.* 12:788709.
Wang, J., Tang, X., Mo, Z. & Mao, Y. 2022. Metagenome-assembled genomes from *Pyropia haitanensis* microbiome provide insights into the potential metabolic functions to the seaweed. *Front. Microbiol.* 13:1–14.
Wang, K., Zhang, S., Zhou, X., Yang, X., Li, X., Wang, Y., Fan, P. et al. 2023. Unambiguous discrimination of all 20 proteinogenic amino acids and their modifications by nanopore. *Nat. Methods*. 21:92–101.
Wang, Yunhao, Zhao, Y., Bollas, A., Wang, Yuru & Au, K.F. 2021. Nanopore sequencing technology, bioinformatics and applications. *Nat. Biotechnol.* 39:1348–1365.
Ward, G.M., Faisan, J.P., Cottier-Cook, E.J., Gachon, C., Hurtado, A.Q., Lim, P.E., Matoju, I. et al. 2020. A review of reported seaweed diseases and pests in aquaculture in Asia. *J. World Aquac. Soc.* 51:815–828.
Webster, N.S., Soo, R., Cobb, R. & Negri, A.P. 2011. Elevated seawater temperature causes a microbial shift on crustose coralline algae with implications for the recruitment of coral larvae. *ISME J.* 5:759–770.
Wegner, C.E., Richter-Heitmann, T., Klindworth, A., Klockow, C., Richter, M., Achstetter, T., Glöckner, F.O. et al. 2013. Expression of sulfatases in *Rhodopirellula baltica* and the diversity of sulfatases in the genus *Rhodopirellula*. *Mar. Genomics*. 9:51–61.
Weigel, B.L., Miranda, K.K., Fogarty, E.C., Watson, A.R. & Pfister, C.A. 2022. Functional insights into the kelp microbiome from

metagenome-assembled genomes. *mSystems*. 7:e01422-21.
Weigel, B.L. & Pfister, C.A. 2019. Successional dynamics and seascape-level patterns of microbial communities on the canopy-forming kelps *Nereocystis luetkeana* and *Macrocystis pyrifera*. *Front. Microbiol.* 10:10.3389/fmicb.2019.00346.
Weilguny, L., De Maio, N., Munro, R., Manser, C., Birney, E., Loose, M. & Goldman, N. 2023. Dynamic, adaptive sampling during nanopore sequencing using Bayesian experimental design. *Nat. Biotechnol.* 41:1018–1025.
Weinberger, F., Beltran, J., Correa, J.A., Lion, U., Pohnert, G., Kumar, N., Steinberg, P. et al. 2007. Spore release in *Acrochaetium* sp. (Rhodophyta) is bacterially controlled. *J. Phycol.* 43:235–241.
Weiss, A., Costa, R. & Wichard, T. 2017. Morphogenesis of *Ulva mutabilis* (Chlorophyta) induced by *Maribacter* species (Bacteroidetes, Flavobacteriaceae). *Bot. Mar.* 60:197–206.
Wendling, C. 2023. Prophage mediated control of higher order interactions - insights from systems approaches. 10.32942/X2ZK52
Weng, P., Yang, H., Mo, Z., Zhang, W., Yan, Y., Rong, X. & Li, J. 2024. Application and evaluation of probiotics against red rot disease in *Pyropia*. *Aquaculture*. 578:740050.
Whittington, J. & Smith, F.A. 1992. Salinity-induced malate accumulation in *Chara*. *J. Exp. Bot.* 43:837–842.
Wichard, T. 2015. Exploring bacteria-induced growth and morphogenesis in the green macroalga order Ulvales (Chlorophyta). *Front. Plant Sci.* 6:1–19.
Wichard, T. 2023. From model organism to application: Bacteria-induced growth and development of the green seaweed *Ulva* and the potential of microbe leveraging in algal aquaculture. *Semin. Cell Dev. Biol.* 134:69–78.
Wichard, T., Charrier, B., Mineur, F., Bothwell, J.H., De Clerck, O. & Coates, J.C. 2015. The green seaweed *Ulva*: A model system to study morphogenesis. *Front. Plant Sci.* 6:1–8.
Wichard, T. & Oertel, W. 2010. Gametogenesis and gamete release of *Ulva mutabilis* and *Ulva lactuca* (Chlorophyta): Regulatory effects and chemical characterization of the "swarming inhibitor." *J. Phycol.* 46:248–259.
Wickham, H. 2016. ggplot2: Elegant graphics for data analysis. https://ggplot2.tidyverse.org. Springer-Verlag New York.
Wiegand, S., Rast, P., Kallscheuer, N., Jogler, M., Heuer, A., Boedeker, C., Jeske, O. et al. 2021. Analysis of bacterial communities on North Sea macroalgae and characterization of the isolated Planctomycetes *Adhaeretor mobilis* gen. nov., sp. nov., *Roseimaritima multifibrata* sp. nov., *Rosistilla ulvae* sp. nov. and *Rubripirellula lacrimiformis* sp. nov. *Microorganisms*. 9:1–34.
Wijgerde, T., van Ballegooijen, M., Nijland, R., van der Loos, L.M., Kwadijk, C., Osinga, R., Murk, A. et al. 2020. Adding insult to injury: Effects of chronic oxybenzone exposure and elevated temperature on two reef-building corals. *Sci. Total Environ.* 733:139030.
Willis, A.D. 2019. Rarefaction, alpha diversity, and statistics. *Front. Microbiol.* 10:10.3389/fmicb.2019.02407.
Witherden, E.A., Moyes, D.L., Bruce, K.D., Ehrlich, S.D. & Shoaie, S. 2017. Using systems biology approaches to elucidate cause and effect in host–microbiome interactions. *Curr. Opin. Syst. Biol.* 3:141–146.
Wu, Y.-W., Simmons, B.A. & Singer, S.W. 2016. MaxBin 2.0: an automated binning algorithm to recover genomes from multiple metagenomic datasets. *Bioinformatics*. 32:605–607.
Xiao, J., Zhang, Xiaohong, Gao, C., Jiang, M., Li, R., Wang, Z., Li, Y. et al. 2016. Effect of temperature, salinity and irradiance on growth and photosynthesis of *Ulva prolifera*. *Acta Oceanol. Sin.* 35:114–121.
Xing, Q., Bi, G., Cao, M., Belcour, A., Aite, M., Mo, Z. & Mao, Y. 2021. Comparative transcriptome analysis provides insights into response of *Ulva compressa* to fluctuating salinity conditions. *J. Phycol.* 57:1295–1308.
Xing, Q., Tosi, L., Braga, F., Gao, X. & Gao, M. 2015. Interpreting the progressive eutrophication behind the world's largest macroalgal blooms with water quality and ocean color data. *Nat. Hazards*. 78:7–21.
Xiong, Y., Yang, R., Sun, X., Yang, H. & Chen, H. 2018. Effect of the epiphytic bacterium *Bacillus* sp. WPySW2 on the metabolism of *Pyropia haitanensis*. *J. Appl. Phycol.* 30:1225–1237.
Yaakop, A.S., Chan, K.-G., Ee, R., Lim, Y.L., Lee, S.-K., Manan, F.A. & Goh, K.M. 2016. Characterization of the mechanism of prolonged adaptation to osmotic stress of *Jeotgalibacillus malaysiensis* via genome and transcriptome sequencing analyses. *Sci. Rep.* 6:33660.
Yang, Y., Zhang, M., Alalawy, A.I., Almutairi, F.M., Al-Duais, M.A., Wang, J. & Salama, E.-S. 2021. Identification and characterization of marine seaweeds for biocompounds production. *Environ. Technol. Innov.* 24:101848.
Yau, S. & Seth-Pasricha, M. 2019. Viruses of polar aquatic environments. *Viruses*. 11:1–15.
Ye, N. hao, Zhang, X. wen, Mao, Y. ze, Liang, C. wei, Xu, D., Zou, J., Zhuang, Z. meng et al. 2011. "Green tides" are overwhelming the coastline of our blue planet: Taking the world's largest example. *Ecol. Res.* 26:477–485.
Yoon, S.-H., Ha, S.-M., Kwon, S., Lim, J., Kim, Y., Seo, H. & Chun, J. 2017. Introducing EzBioCloud: A taxonomically united database of 16S rRNA gene sequences and whole-genome assemblies. *Int. J. Syst. Evol. Microbiol.* 67:1613–1617.
Zahra, N., Raza, Z.A. & Mahmood, S. 2020. Effect of salinity stress on various growth and physiological attributes of two contrasting maize genotypes. *Braz. Arch. Biol. Technol.* 63:e20200072.
Zell, R., Groth, M., Selinka, L. & Selinka, H.-C. 2022. Picorna-like viruses of the Havel river, Germany. *Front. Microbiol.* 13:865287.
Zhang, L., Liao, W., Huang, Y., Wen, Y., Chu, Y. & Zhao, C. 2022. Global seaweed farming and processing in the past 20 years. *Food Prod. Process. Nutr.* 4:23.
Zhang, X., Song, Y., Liu, D., Keesing, J.K. & Gong, J. 2015. Macroalgal blooms favor heterotrophic diazotrophic bacteria in nitrogen-rich and phosphorus-limited coastal surface waters in the Yellow Sea. *Estuar. Coast. Shelf Sci.* 163:75–81.
Zhou, H., He, K., Chen, J. & Zhang, X. 2022. LinDA: linear models for differential abundance analysis of microbiome compositional data. *Genome Biol.* 23:95.

Summary

Seaweeds live together in symbiosis with numerous microorganisms, including bacteria, fungi, and viruses. These microorganisms are essential to the life and functioning of seaweeds. In this PhD thesis, we studied green seaweeds of the genus *Ulva*, who depend on their bacterial symbionts for normal morphological development and growth. The general objective was to investigate how the *Ulva* holobiont — a collective entity of host and associated microbes — reacts to environmental change. We focused in particular on salinity as key environmental parameter in the Baltic Sea area in northern Europe, where more than 15 *Ulva* species occur in sympatry along a natural salinity gradient. In six research chapters, we explored the dynamics of microbial communities associated with *Ulva* in both natural populations and aquaculture facilities.

Chapter 2 introduces a long-read Oxford Nanopore sequencing workflow to analyse bacterial communities based on full-length 16S rRNA gene sequences. *Ulva*-associated bacterial communities were distinctly different from the communities found in seawater and sediment. In addition, the *Ulva* microbiome exhibited higher variability across the various sites compared to environmental samples. Samples associated with cultivated *Ulva* in particular demonstrated high relative abundances of known growth-promoting bacteria. The workflow implemented in our study enables the generation of results within 24 hours and is a promising tool for rapid microbial surveys in aquaculture applications.

Chapter 3 delves further into the comparison of bacterial communities associated with cultivated *Ulva* and natural *Ulva* populations. We monitored seasonal and successional fluctuations over an eleven-month period in land-based tanks and offshore seafarms, covering all aquaculture stages from the nursery phase through outplanting in the field up to the harvest. Our findings revealed a highly dynamic *Ulva* microbiome, with bacterial composition undergoing rapid transformation following outplanting, showing significant differences from nursery samples within just seven days. During the *Ulva* hatchling phase, the microbiome composition was more influenced by nursery conditions than host specificity, indicating the crucial role of the nursery environment as a microbial source pool. This suggests that *Ulva* hatchlings are susceptible to newly introduced microbes, emphasizing the potential for microbiota manipulation during nursery conditions.

Chapter 4 presents a comprehensive taxonomic characterization of bacterial communities spanning 15 *Ulva* species along a 2,000 km environmental gradient in the Baltic Sea, encompassing a total of 481 samples. Salinity was the main driver of bacterial community composition, with the most significant shift occurring in the horohalinicum (the transition zone from freshwater to marine conditions). Additionally, we observed secondary host-specific effects. Collectively, salinity and host factors accounted for between 34% and 91% of the variation in the abundance of the different bacterial genera. Our results contradict earlier statements that *Ulva*-associated bacterial communities are largely stochastically defined.

Chapter 5 expands our focus beyond taxonomic composition to encompass the functional potential of *Ulva*-associated bacterial communities along the Atlantic–Baltic Sea salinity gradient. Through the analysis of 639 metagenome-assembled genomes, we uncovered a widespread potential for carbon, sulphur, nitrogen, and vitamin metabolism, including the biosynthesis of amino acids and vitamin B. While the taxonomic turnover within bacterial communities was substantial, functional turnover was comparatively lower, indicating functional stability. However, we also identified changes in the functional profile across the environmental gradient that likely contribute to oxidative stress mitigation, cellular osmotic homeostasis, and membrane stabilization in response to salinity variations. We therefore hypothesised that characteristic bacterial communities associated with distinct salinity regions may facilitate the host's acclimation across the environmental gradient.

Chapter 6 investigates the effect of introducing bacterial inoculants, originating from either low or high salinity areas, on the growth of *Ulva fenestrata* under two different salinity treatments (low versus high salinity). Our results showed that *Ulva* growth increased 74–120% with the addition of an *Aquipuribacter* strain (originally isolated from low salinity), a *Maribacter*, or a *Zobellia* strain (both isolated from high salinity), in comparison to the effects observed with the other 21 tested strains. Importantly, this growth-enhancing effect was specific to germling cultures under low salinity conditions. These findings highlight the significance of life-history phases and environmental conditions in comprehending the dynamics of the seaweed holobiont.

Chapter 7 provides the first characterisation of *Ulva*-associated viral communities. We identified 20 putative novel viruses that were highly divergent, belonging to the Circular Rep-Encoding Single-Stranded (CRESS) DNA viruses, *Durnavirales* (double-stranded RNA viruses), *Ghabrivirales* (dsRNA), *Mitoviridae* (single-stranded RNA), *Tombusviridae* (ssRNA), and *Picornavirales* (ssRNA). The CRESS DNA viruses and picorna-like viruses were particularly abundant in bleached *Ulva* specimens and nearly absent from healthy individuals. While these viruses could be implicated in the bleaching of *Ulva*, it is also plausible that the bleaching may result from stress, thereby facilitating the proliferation of viruses. This study underscores the gaps in our understanding of the diversity and ecology of seaweed viruses, particularly within the context of algal diseases.

Altogether, our findings indicate that (i) the *Ulva* microbiome is highly dynamic and harbours a largely unexplored biodiversity, (ii) the bacterial community composition is primarily determined by the environment and secondarily by host, and (iii) although bacteria can facilitate *Ulva*'s acclimation to the environment, the environment itself determines their ability to affect host performance. In summary, our studies underscore the intricate interplay between the *Ulva* microbiome, environmental factors, and host dynamics, shedding light on the complex relationships that govern the acclimation and performance of *Ulva* in an ecological context.

Samenvatting

Zeewieren leven samen in symbiose met talloze micro-organismen, waaronder bacteriën, schimmels en virussen. Deze micro-organismen zijn essentieel voor het leven en functioneren van zeewieren. In dit proefschrift bestudeerden we groene zeewieren van het geslacht *Ulva*. Deze zeewieren zijn afhankelijk van hun bacteriële symbionten voor normale morfologische ontwikkeling en groei. Het doel van dit proefschrift was om te onderzoeken hoe het *Ulva* holobiont — een collectieve entiteit van gastheer en geassocieerde microben — reageert op veranderingen in het milieu. We richtten ons met name op het zoutgehalte als een belangrijke omgevingsparameter in het Oostzeegebied in Noord-Europa, waar meer dan 15 *Ulva*-soorten samen voorkomen langs een natuurlijke saliniteitsgradiënt. In zes onderzoeks-hoofdstukken onderzochten we de dynamiek van microbiële gemeenschappen geassocieerd met *Ulva*, zowel in natuurlijke populaties als in aquacultuurfaciliteiten.

Hoofdstuk 2 introduceert een Oxford Nanopore sequencing-workflow om bacteriële gemeenschappen te analyseren op basis van volledige 16S rRNA-gensequenties. *Ulva*-geassocieerde bacteriële gemeenschappen verschilden duidelijk van de gemeenschappen in zeewater en sediment. Bovendien vertoonden de gemeenschappen op *Ulva* hogere variabiliteit tussen de verschillende locaties in vergelijking met omgevingsmonsters. Met name monsters van gekweekte *Ulva* bevatten groeibevorderende bacteriën in hoge dichtheden. De workflow toegepast in onze studie maakt het generen van resultaten binnen 24 uur mogelijk en is een veelbelovende techniek voor snelle microbiële inventarisatie in aquacultuurtoepassingen.

Hoofdstuk 3 duikt dieper in op de vergelijking van bacteriële gemeenschappen geassocieerd met gekweekte en natuurlijke *Ulva*-populaties. We volgden seizoens- en successiefluctuaties gedurende een periode van elf maanden in onshore en offshore kwekerijen. Deze periode omvatte de gehele aquacultuurcyclus, van de 'kraamkamerfase' en het uitplanten in het veld tot aan de oogst. De resultaten toonden dat het *Ulva* microbioom zeer dynamisch is; de bacteriële samenstelling van de kiemplantjes veranderde na het uitplanten in het veld significant binnen slechts zeven dagen. Tijdens de kraamkamerfase werd de microbiële samenstelling meer beïnvloed door omstandigheden tijdens de kweek dan door de specifieke soort van de gastheer. Dit suggereert dat *Ulva* kiemplantjes met name tijdens de kraamkamerfase nog vatbaar zijn voor nieuw geïntroduceerde microben, waardoor de kraamkamer een ideale gelegenheid biedt voor het manipuleren van het microbioom.

Hoofdstuk 4 geeft een uitgebreide taxonomische karakterisering van bacteriële gemeenschappen in 481 monsters, verzameld op 15 *Ulva*-soorten langs een 2,000 km milieu-gradiënt in de Oostzee. Het zoutgehalte was de belangrijkste bepalende factor in de samenstelling van bacteriële gemeenschappen. De meest significante verschuiving vond plaats in het horohalinicum (de overgangszone van zoetwater naar mariene omstandigheden). Daarnaast observeerden we gastheer-specifieke effecten. Gezamenlijk verklaarden zoutgehalte en gastheer-factoren tussen de 34% en 91% van de variatie in de abundantie van de bacteriële genera. Onze resultaten spreken eerdere beweringen tegen dat *Ulva*-geassocieerde bacteriële gemeenschappen grotendeels stochastisch zijn gedefinieerd.

Hoofdstuk 5 verbreedt de focus van taxonomische samenstelling naar het functionele potentieel van *Ulva*-geassocieerde bacteriële gemeenschappen langs de Oostzee saliniteitsgradiënt. Een analyse van 639 metagenoom-geassembleerde bacteriële genomen toonde een wijdverbreid potentieel voor koolstof-, zwavel-, stikstof-, en vitamine metabolisme, inclusief de biosynthese van aminozuren en vitamine B. Hoewel de taxonomische samenstelling van bacteriële gemeenschappen snel veranderde over de saliniteitsgradiënt, was er een hoge mate van functionele stabiliteit. Desondanks identificeerden we veranderingen in het functionele profiel langs de omgevingsgradiënt die bijdragen aan de verlichting van oxidatieve stress, cellulaire osmotische

homeostase, en membraanstabilisatie als reactie op zoutgehaltevariaties. Wij hypothetiseerden daarom dat kenmerkende bacteriële gemeenschappen geassocieerd met specifieke zoutgehaltegebieden de acclimatisatie van de gastheer aan de omgeving kunnen faciliteren.

Hoofdstuk 6 onderzoekt het effect van het introduceren van bacteriële inoculanten, afkomstig uit gebieden met lage versus hoge zoutgehaltes, op de groei van *Ulva fenestrata* onder twee verschillende zoutgehaltes (lage versus hoge saliniteit). Onze resultaten toonden aan dat *Ulva*-groei met 74–120% toenam na toevoeging van een *Aquipuribacter* stam (oorspronkelijk geïsoleerd uit een gebied met laag zoutgehalte), een *Maribacter*, of een *Zobellia* stam (beide geïsoleerd uit hoog zoutgehalte), vergeleken met de effecten van de andere 21 geteste stammen. Belangrijk was dat dit groeibevorderende effect enkel waargenomen werd in de juveniele fase onder lage saliniteitcondities. Deze bevindingen benadrukken dat het belangrijk is om rekening te houden met levensfase en omgevingsparameters als we de dynamiek van het zeewier-holobiont willen begrijpen.

Hoofdstuk 7 presenteert de eerste karakterisering van *Ulva*-geassocieerde virale gemeenschappen. We identificeerden 20 potentieel nieuwe en zeer verschillende virussen die behoren tot de Circular Rep-Encoding Single-Stranded (CRESS) DNA-virussen, *Durnavirales* (dubbelstrengs RNA-virussen), *Ghabrivirales* (dsRNA), *Mitoviridae* (enkelstrengs RNA-virussen), *Tombusviridae* (ssRNA), en *Picornavirales* (ssRNA). De CRESS DNA-virussen en picorna-achtige virussen waren met name talrijk aanwezig in verbleekte *Ulva* thalli en vrijwel afwezig in gezonde individuen. Hoewel deze virussen betrokken zouden kunnen zijn bij het verbleken van *Ulva*, is het ook plausibel dat het verbleken het gevolg kan zijn van stress, waardoor virussen de kans krijgen sterk te prolifereren. Deze studie benadrukt het kennis-gat in ons begrip van de diversiteit en ecologie van zeewier-virussen, met name in de context van algenziekten.

De resultaten in dit proefschrift tonen aan dat (i) het *Ulva* microbioom zeer dynamisch is en een nog grotendeels onontdekte biodiversiteit herbergt, (ii) de samenstelling van de bacteriële gemeenschap primair wordt bepaald door het milieu en secundair door de gastheer, en (iii) hoewel bacteriën de acclimatisatie van *Ulva* aan de omgeving kunnen faciliteren, de omgeving zelf ook grote impact heeft op het vermogen van bacteriën om de fysiologie van de gastheer te beïnvloeden. Samengevat benadrukt ons onderzoek de gecompliceerde wisselwerking tussen de *Ulva* gastheer, geassocieerde microbiota, en omgevingsfactoren, en dragen onze resultaten bij aan het begrip van de complexe relaties die de acclimatisatie en prestaties van *Ulva* beïnvloeden in een ecologische context.

About the author

Luna van der Loos got acquainted with seaweeds early in life, spending countless hours in tide pools and snorkelling the Atlantic Ocean. Luna completed her Bachelor of Science (cum laude, 2012–2015) with a specialization in Marine Biology at the University of Groningen, the Netherlands. She continued with her Master of Science (summa cum laude, 2015–2018) in Groningen to explore the various aspects of seaweed research. Her studies included a research project with the Naturalis Biodiversity Center in the Caribbean to investigate tropical seaweed diversity and phylogeny, and a thesis project with Catriona Hurd (UTAS, Australia) to study the effects of ocean acidification on fleshy seaweeds in the temperature ecosystems of Tasmania's beautiful coastline. After completing her MSc degree, Luna worked for a year as a research associate with the ANEMOON Foundation and as a junior scientist at Wageningen University. Here, she was introduced to Nanopore sequencing and its uses in microbiome research. In the meantime, she wrote a project proposal for an FWO PhD fellowship together with Olivier De Clerck, Anne Willems, and Frederik Leliaert at Ghent University, Belgium. Luna started her PhD in Ghent in January 2020 at the Phycology Research Group. During her PhD, she was awarded the VLIZ Brilliant Marine Research Idea grant for her work on algal viruses (2020) and the Best Oral Presentation award at the European Phycological Conference (2023). Luna has co-authored 13 peer-reviewed publications between 2016 and 2024, ten of which as first author. She also wrote a field guide to the seaweeds of the Netherlands when the pandemic made working in the lab impossible and worked on various side projects during her PhD involving seaweed biodiversity in Belgium and the Netherlands. After her PhD, Luna will continue exploring European *Ulva* biodiversity within the EULVA (European *Ulva* Taxonomy Initiative) project and work on assembling an *Ulva* pan-genome.

Contact
Luna van der Loos
Email: luna.vanderloos@ugent.be
ORCiD: https://orcid.org/0000-0002-8421-2881
ResearchGate: https://www.researchgate.net/profile/Luna-Van-Der-Loos
LinkedIn: https://www.linkedin.com/in/luna-van-der-loos-105838111/

List of publications

Publications included in this thesis

van der Loos, L.M., Eriksson, B.K. & Falcão Salles, J. (2019) The macroalgal holobiont in a changing sea. *Trends in Microbiology* 27:635–650. [adapted for Chapter 1]

van der Loos, L.M., D'hondt, S., Willems, A. & De Clerck, O. (2021) Characterizing algal microbiomes using long-read Nanopore sequencing. *Algal Research* 59:102456. [Chapter 2]

van der Loos, L.M., De Wilde, C., Willems, A., De Clerck. O. & Steinhagen, S. (2024) The cultivated sea lettuce (*Ulva*) microbiome: Successional and seasonal dynamics. *Aquaculture* 585:740692. [Chapter 3]

van der Loos, L.M., D'hondt, S., Engelen, A.H., Pavia, H., Toth, G.B., Willems, A., Weinberger, F., De Clerck, O. & Steinhagen, S. (2022) Salinity and host drive *Ulva* associated bacterial communities across the Atlantic–Baltic Sea gradient. *Molecular Ecology* 10.1111/mec.16462. [Chapter 4]

van der Loos, L.M., De Coninck, L., Zell, R., Lequime, S., Willems, A., De Clerck, O. & Matthijnssens, J. (2023) Highly divergent CRESS DNA and picorna-like viruses associated with bleached thalli of the green seaweed *Ulva*. *Microbiology Spectrum* 11:5 e00255-23. [Chapter 7]

Other publications during candidature

van der Loos, L.M. & Nijland, R. (2020) Biases in bulk: DNA metabarcoding of marine communities and the methodology involved. *Molecular Ecology* 10.1111/mec.15592.

De Clerck, O. & van der Loos, L.M. (2020) Chapter 1 Algen en wieren. In: Verleye, T.J., De Raedemaecker, F., Vandepitte, L., Fockedey, N., Lescrauwaet, A.-K., De Pooter, D. & Mees, J. (Eds.) Niet-inheemse soorten in het Belgisch deel van de Noordzee en aanpalende estuaria anno 2020. VLIZ. Oostende, Belgium. 623 pages. ISBN: 9789464206005.

Wijgerde, T., van Ballegooijen, M., Nijland, R., van der Loos, L.M., Kwadijk, C., Osinga, R., Murk, A. & Slijkerman, D. (2020) Adding insult to injury: Effects of chronic oxybenzone exposure and elevated temperature on two reef-building corals. *Science of the Total Environment* 733:139030.

van der Loos, L.M., Karremans, M. & Perk, F. (2021) Veldgids Zeewieren (Fieldguide to the seaweeds of the Netherlands). KNNV Uitgeverij. Zeist, Nederland. 288 pages. ISBN: 9789050118019.

Hoeksema, B.W., van der Loos, L.M. & van Moorsel, G.W.N.M. (2022) Coral diversity matches marine park zonation but not economic value of coral reef sites at St. Eustatius, eastern Caribbean. *Journal of Environmental Management* 320:115829.

van der Loos, L.M. et al. (2023) Non-indigenous seaweeds in the Northeast Atlantic Ocean, the Mediterranean Sea and Macaronesia: A critical synthesis of diversity, spatial and temporal patterns. *European Journal of Phycology* DOI: 10.1080/09670262.2023.2256828.

Selection of public outreach

TV interviews, radio interviews, and podcasts

- Radio interview with Vroege Vogels, 7 March 2021 at radio NPO1, "Waarom zeewieren bijzonder nuttig en belangrijk zijn"
  www.nporadio1.nl/nieuws/binnenland/2d930ede-b44e-4c6e-a2cc-ac2b2bc09115/waarom-wieren-bijzonder-nuttig-en-belangrijk-zijn

- Podcast "Verstrengeld" in an episode about *Ulva*, 1 October 2022
  www.platformdis.nl/podcast-verstrengeld/

- TV interview with Vroege Vogels, 18 November 2022 at NPO2, in an episode about the Kop van Schouwen (Zeeland)
  www.bnnvara.nl/vroegevogels/artikelen/kustbescherming-als-leefgebied-voor-talloze-zeewieren

- Radio interview with Vroege Vogels, 20 August 2023 at radio NPO1, "Grevelingenmeer kleurt minder rozerood dan vorig jaar"
  www.bnnvara.nl/vroegevogels/artikelen/grevelingenmeer-kleurt-minder-rozerood-dan-vorig-jaar

A selection of articles in the magazine Het Zeepaard of the Dutch Strandwerkgemeenschap

- van der Loos, L.M., Karremans, M. & Perk, F. (2021) *Ceramium sungminbooi* — een cryptische roodwiersoort in Nederland. *Het Zeepaard* 81(2): 67-72

- Perk, F., van der Loos, L.M. & Karremans, M. (2021) Heeft *Antithamnion cruciatum* zich eindelijk gevestigd in Nederland? *Het Zeepaard* 81(5): 271-284

- Karremans, M., van der Loos, L.M. & Perk, F. (2022) Fijnvertakt geleiwier *Gelidium spinosum*: een nieuwe roodwiersoort in Nederland. *Het Zeepaard* 82(3): 93-102

- van der Loos, L.M., Perk, F. & Karremans, M. (2022) *Radicilingua mediterranea*: een nieuwe roodwiersoort in Nederland. *Het Zeepaard* 82(4/5): 147-157

A selection of news articles at the website NatureToday

- Steeds meer zeewiersoorten in Nederland (2-MEI-2021)
  www.naturetoday.com/intl/nl/naturereports/message/?msg=27633

- Zeeland drie roodwieren rijker (1-MEI-2022)
  www.naturetoday.com/intl/nl/nature-reports/message/?msg=29118

- Nieuw roodwier maakt Grevelingenmeer wollig (5-FEB-2023)
  www.naturetoday.com/intl/nl/nature-reports/message/?msg=30349

Newspaper interviews

- "Zeeleven is gevarieerder dan het landleven", *Haarlems Dagblad*, 3 April 2021, by Hein Flach
- "Veldgids voor zeewier moet de leek enthousiasmeren", *Friesch Dagblad*, 10 April 2021, by Wouter Hoving
- "Is zeewier het nieuwe goud? Het potentieel als vervanger van vlees, plastic en…asbest", *Volkskrant*, 16 July 2021, by Jean-Pierre Geelen

A selection of popular-scientific articles in magazines

- "De kracht van data" Onderwatersport #3 2020, pages 40-45 [about citizen science]
- "Stijgers en dalers in het Zeeuwse water" Onderwatersport #4 2020, pages 42-47 [about citizen science]
- "Samen sterk!" Onderwatersport #6 2020, pages 42-45 [about symbiosis]
- "Gulle gevers" Onderwatersport #1 2021, pages 42-45 [about microbiomes]
- "Een snelcursus zeewieren" Hippocampus #2 2021, pages 44-47 [about seaweeds]
- "Zeewieren in Nederland — zoek de verschillen" Onderwatersport #2 2021, pages 40-45 [about seaweeds]

A day spent capturing footage for an episode of Vroege Vogels (11 October 2022)

" 'K wou nog iets zeggen
Maar ik weet niet meer
Dan was het zeker niks"

– Spinvis, in: Ik wil alleen maar zwemmen